The control of plant defense responses and seedling growth during interactions with beneficial and non-beneficial organisms

Dissertation

zur Erlangung des akademischen Grades *doctor rerum naturalium*

(Dr. rer. nat.)

vorgelegt dem Rat der Biologisch-Pharmazeutischen Fakultät der

Friedrich-Schiller-Universität Jena

von Stefan Schuck (Diplom-Biologe)

geboren am 27.08.1982 in Sulzbach am Main

Gutachter:

1. **Prof. Dr. Ian Baldwin**

   Max-Planck-Institut für chemische Ökologie

   Hans-Knöll-Str. 8

   07745 Jena

2. **PD Dr. Axel Mithöfer**

   Max-Planck-Institut für chemische Ökologie

   Hans-Knöll-Str. 8

   07745 Jena

3. **Prof. Dr. Karl-Heinz Kogel**

   Justus-Liebig-Universität Giessen

   Heinrich-Buff-Ring 26-32

   35392 Giessen

Datum der öffentlichen Verteidigung: 27. August 2013

Table of contents:

Chapter 1: General Introduction

The wild tobacco species *Nicotiana attenuata* Torrey ex S. Watson 1871 is an annual desert model plant germinating from long-lived seed banks in monoculture-like populations after wildfires (Preston & Baldwin, 1999). As a consequence of growing in that post-fire environment, these *N. attenuata* monocultures then have to face a variety of herbivores and pathogens which also need to re-establish in the burnt habitat, a circumstance (amongst others) that makes it hard for this plant species to anticipate the occurrence of its natural enemies (Bossart & Gage, 1990; Baldwin & Ohnmeiss, 1993; Baldwin *et al*., 1994; Baldwin, 2001; Rayapuram *et al*., 2008). These hostile organisms require adequate defense responses of *N. attenuata* to either tolerate damage/losses caused by the attackers (by compensatory mechanisms) or to resist the attackers (by reducing the attacker´s performance) (Strauss & Agrawal, 1999; Diezel *et al*., 2009; Medzhitov *et al*., 2012). It appears that selection favors the evolution of a mixed strategy of defense allocation to both resistance and tolerance mechanisms and that plants trade off between those (Strauss & Agrawal, 1999; Nunez-Farfan *et al*., 2007). Tolerance allows for a compensatory regrowth with only relatively low Darwinian fitness costs compared to an undamaged state and might be mediated by special protection or reactivation of meristem tissue, resource bunkering into storage organs (*e.g*. roots) or an increase in photosynthetic capacity, the reconfiguration of primary metabolism and nutrient uptake (Kessler & Baldwin, 2002; Schwachtje *et al*., 2006; Schwachtje & Baldwin, 2008). For example, in *N. attenuata* the regulatory subunit (GAL83) of a heterotrimeric kinase complex (SnRK1; sucrose non-fermenting-1-related protein kinase 1) mediates tolerance to insect herbivory by regulating the carbon allocation to the roots (Schwachtje *et al*., 2006). Besides tolerance mechanisms, plants possess also a huge arsenal of resistance mechanisms being distinguished in constitutive and inducible ones (Kempel *et al*., 2011). Constitutive resistance mechanisms of *N. attenuata* against herbivores include trichomes and the chemical compounds contained therein (Weinhold & Baldwin, 2011; Weinhold *et al*., 2011), and a relatively thick cuticle helps this plant species to protect itself from pathogen attack (Dominguez *et al*., 2011; Hettenhausen *et al*., 2012). In order to minimize defense-associated fitness costs and most efficiently tailor defense responses to specific attackers, *N. attenuata* has evolved an enormous set of inducible resistance mechanisms,

too (Baldwin *et al*., 1998; van Dam *et al*., 2000; Kessler & Baldwin, 2002; Hui *et al*., 2003). Inducibility of defense responses allows for adaptive phenotypic plasticity as an evolutionary favored mechanism enabling a plant to cope with changes in its environment (Agrawal, 1999; Baldwin, 1999). Plant resistance increases Darwinian fitness in case of pathogen/herbivore attack, but at the same time it is also costly because the production of defense metabolites consumes limited nutrient resources that could have been used for growth and reproduction instead and some defense compounds might even exhibit autotoxicity potential (Baldwin & Callahan, 1993; Baldwin, 1998; Baldwin *et al*., 1998; van Dam & Baldwin, 2001). The consequences of fitness costs associated with plant resistance are even more pronounced if competition is involved, and intraspecific competition in monoculture-like populations as formed by *N. attenuata* in post-fire environments is typically one-sided/asymmetric, therefore causing huge differences in Darwinian fitness between conspecifics (Weiner & Thomas, 1986; Preston & Baldwin, 1999; Meldau *et al*., 2012). Besides resource consumption and autotoxicity, also other factors contribute to plant resistance being costly, for example negative side effects on mutualistic interactions like pollination (Kessler & Baldwin, 2002; Kessler & Baldwin, 2007). For instance, the *N. attenuata* herbivore species *Manduca sexta* specialized on solanaceous host plants is a serious threat in form of its nearly insatiable larvae and at the same time an important pollinator (Yamamoto & Fraenkel, 1960; Euler & Baldwin, 1996; Kessler & Baldwin, 2007; Kessler *et al*., 2010). Thus, *N. attenuata* plants need to trade off evading herbivory against being pollinated by this lepidopteran species, leading to a herbivore pressure-regulated shift in the ratio of two types of flowers differing in opening time and emission of the pollinator-attracting flower volatile benzyl acetone (Kessler *et al*., 2010). In addition, *N. attenuata* copes with this herbivory-pollination dilemma by increasing nectar levels of the defense metabolite nicotine in case of herbivory or mechanical damage independently from the benzyl acetone emission pattern, while the regulation of nectar nicotine levels and benzyl acetone emission are otherwise coordinated in a diurnal way to synchronize with the nocturnal pollination activity of *M. sexta* moths to maximize flower advertisement and minimize pollinator deterrence (Euler & Baldwin, 1996). *Vice versa* to the disruption of mutualism by activation of resistance mechanisms, mutualistic interactions can also negatively affect a plant's ability to defend itself, as demonstrated for the reduced defensive power of *N. attenuata* against *M. sexta* herbivory after being colonized by the

two closely related plant growth promoting root endophytic fungi *Piriformospora indica* and *Sebacina vermifera* (Barazani *et al*., 2005).

N. attenuata's defense responses comprise direct as well as indirect strategies (Keinanen *et al*., 2001; Kessler & Baldwin, 2001; van Dam *et al*., 2001; Kessler & Baldwin, 2002; Rayapuram *et al*., 2008). Direct defenses comprise mechanical structures like above mentioned trichomes as well as chemical compounds with toxic or antinutritive function, whereas indirect defenses protect the plant by the aid of the attacker´s natural enemies (War *et al*., 2012). Nicotine and 17-hydroxygeranyllinalool diterpene glycosides are probably the best examples for inducible toxic defense metabolites (Steppuhn *et al*., 2004; Steppuhn & Baldwin, 2007; Heiling *et al*., 2010), while trypsine proteinase inhibitors are exemplary for inducible antinutritive compounds (van Dam & Baldwin, 2003; Zavala *et al*., 2004). And a pathogen-inducible PR-13/thionin protein protects *N. attenuata* from infection by phytopathogenic bacteria of the genus *Pseudomonas* (Rayapuram *et al*., 2008). Certain phenolic compounds (*e.g*. chlorogenic acid and rutin) are thought to be broad-spectrum plant defense metabolites and some of those are inducible by insect herbivory (*i.e*. chlorogenic acid and its polyamine conjugates), however the extent to which they are really toxic to the herbivore seems to heavily depend on the tested herbivore species (Isman & Duffey, 1982; Bi *et al*., 1997; Keinänen *et al*., 2001; Steppuhn *et al*., 2004; Rayapuram & Baldwin, 2008). Well-known examples for induced indirect defenses of *N. attenuata* against insect herbivores are "green leaf volatiles", as well as mono- and sesquiterpenoid volatiles and branched-chain aliphatic acids emitted and attracting the herbivor's predators, either by the damaged plant itself or the feeding herbivore after metabolization of plant-derived precursors (Kessler & Baldwin, 2001; Allmann & Baldwin, 2010; Stork *et al*., 2011).

Inducibility of defenses is typically not found to be homogenous across all plant parts, but rather highly variable depending on the respective plant organ or tissue examined, and the relative value of the Darwinian fitness thereof ("optimal defense theory") (Ohnmeiss & Baldwin, 2000; McCall & Fordyce, 2010; Diezel *et al*., 2011; Meldau *et al*., 2012). Young metabolic sink tissues and reproductive organs are generally better defended than senescing metabolic source leaves, as demonstrated by the correlation between basal and inducible levels of defensive compounds in a certain plant part with the fitness value thereof (Meldau *et al*., 2012).

Even though they might provide in general good protection against generalist herbivores, certain defense metabolites might be ineffective against a specialist herbivore, as it is the case with the nicotine-tolerant specialist *M. sexta* (van Dam *et al*., 2000; Steppuhn *et al*., 2004; Govind *et al*., 2010). The occurrence of such host specialists is generally favored in monoculture-like populations as typically formed by *N. attenuata* (Preston & Baldwin, 1999; Fried *et al*., 2010). In case of being attacked by an adapted specialist herbivore, plant counteractions might be even exploited by the attackers for their better performance, *e.g*. by sequestration of defense metabolites toxic to potential predators and parasitoids or by using such metabolites as oviposition and host plant location cues (Thorpe & Barbosa, 1986; Bentz & Barbosa, 1992; Kahl *et al*., 2000; del Campo *et al*., 2001). However, plants do not only need to distinguish specialists from generalist herbivores, but also between different feeding behaviors (chewing *vs.* phloem-feeding) (Heidel & Baldwin, 2004; Ali & Agrawal, 2012). Chewing insects typically cause extensive tissue damage and induce rather the defense-related phytohormones jasmonic acid (JA) and ethylene (ET), whereas phloem-feeders typically cause only minor tissue damage with a preferential induction of another defense-related phytohormone, salicylic acid (SA) (Ali & Agrawal, 2012). A good example for this specific plant signaling mechanisms is provided by the *N. attenuata*-*M. sexta* interaction. Distinct elicitors occuring in the oral secretion (OS) of *M. sexta* larvae such as the fatty acid-amino acid conjugate (FAC) N-linolenoyl-L-glutamate (18:3-Glu) induce a plant reaction in form of a rapid and transient burst of JA and ET and changes in plant secondary metabolism mediated by the signaling of these phytohormones (Halitschke *et al*., 2001; Voelckel & Baldwin, 2004; Diezel *et al*., 2009). After perception of *M. sexta* presence, JA biosynthesis is initialized within only few minutes in *N. attenuata* by the release of linolenic acid out of chloroplast membrane lipids catalyzed by one major glycerolipase A1, GLA1 (Kallenbach *et al*., 2010). Since *M. sexta* is already adapted to nicotine which is much more effective against non-adapted generalist herbivores, its inducibility by JA is attenuated by ET, a mechanism to avoid wasting energy and costly resources for the production of defensive compounds that would be anyway rather ineffective against *M. sexta* (Lynds & Baldwin, 1998; Kahl *et al*., 2000; Winz & Baldwin, 2001). In contrast to nicotine, other JA-inducible secondary metabolites, such as trypsine proteinase inhibitors, 17-hydroxygeranyllinalool diterpene glycosides and terpenoid plant volatiles retain their JA-inducibility after *M. sexta* OS elicitation (Kahl *et al*., 2000; Keinänen *et al*., 2001; van Dam *et al*., 2001; Lou & Baldwin, 2003).

Similar to their importance in defense against herbivorous insects, JA, ET and SA also play a crucial role in pathogen defense signaling. If plants are attacked by biotrophic and hemibiotrophic pathogens, they typically react by activation of the SA signaling pathway and a localized cell death (hypersensitive reaction) to restrict pathogen spread, while necrotrophic pathogens that could potentially even benefit from a hypersensitive cell death rather activate the JA signaling pathway (Glazebrook, 2005; Takemoto *et al*., 2005; Kliebenstein & Rowe, 2008). The activation of the SA signaling pathway after pathogen attack is involved in the establishment of systemic acquired resistance (SAR), a mechanism that mediates long-lasting and broad-spectrum protection of distal uninfected plant parts after a local infection event (Pieterse *et al*., 2012). In contrast, another form of systemic resistance (induced systemic resistance, ISR) induced by the interaction with plant-growth-promoting organisms such as rhizobacteria and *P. indica* is SA-independent and leads to the priming of JA-dependent defenses (Waller *et al*., 2006; Molitor & Kogel, 2009).

However, these signaling pathways implicated in plant defense responses can be exploited by certain pathogens to even promote disease progression, by herbivores to suppress host defense responses, and by mutualists to facilitate early host colonization (Zhao *et al*., 2003; Diezel *et al*., 2009; Thatcher *et al*., 2009; Jacobs *et al*., 2011; Pieterse *et al*., 2012). For example, the plant growth-promoting fungus *P. indica* suppresses plant innate immunity via the JA signaling pathway during early root colonization, a mechanism probably contributing to the abilty of this fungus to colonize plants of a very large host-range (Jacobs et al., 2011). However, plants are able to control the extent of *P. indica* colonization and thereby ensure the beneficial outcome of the interaction via ET signaling and by indole-3-acetaldoxime-derived products (Camehl *et al*., 2010; Nongbri *et al*., 2012). An example for manipulation of host phytohormone signaling is the interaction of *N. attenuata* with the generalist herbivore *Spodoptera exigua* (Diezel *et al*., 2009). Although being – like *M. sexta* – a chewing lepidopteran herbivore known to typically induce a JA and ET response in the attacked plant, *S. exigua* contains enhanced glucose oxidase (GOX) activity in its oral excretion compared to *M. sexta* and therefore elicits a relatively high SA burst, at the same time attenuating JA and ET levels (Diezel *et al*., 2009; Ali & Agrawal, 2012). Since SA signaling antagonizes JA signaling, this can be interpreted as the attempt of a generalist which is less adapted to host plant-specific defenses to suppress those inducible by JA signaling (Ali & Agrawal, 2012). Numerous examples for phytohormones and

effectors produced by phytopathogens to manipulate host plant defense are known from literature (Jones & Dangl, 2006; Tsavkelova *et al*., 2006; de Jonge *et al*., 2011; Schmidt & Panstruga, 2011; Cheng *et al*., 2012; Nowicki *et al*., 2012). For instance, *Phytophthora capsici* elicitor treatment of transgenic *Arabidopsis* plants ectopically expressing the *Phytophthora sojae* effector Avh331 revealed a role of this protein in suppressing the defense-related mitogen-activated protein kinase signaling pathway (Cheng *et al*., 2012).

Phytopathogen effectors have evolved as virulence factors typically as consequence of an arms race between pathogens and host plants, a process leading to selection pressure on the pathogen side towards host specialization (van der Does & Rep, 2007; Ellis *et al*., 2009; Stergiopoulos & de Wit, 2009; Antonovics *et al*., 2013). These effectors are produced to counter basal plant resistance mediated by the recognition of pathogen/microbe-associated molecular patterns (PAMPs/MAMPs) which results in the activation of plant defense responses (PAMP-triggered immunity, PTI) (Dangl & Jones, 2001; Jones & Dangl, 2006). The so-called "elicitins" form a special effector class probably restricted to the oomycetes *Phytophthora* and *Pythium* (Panabieres *et al*., 1995; Panabieres *et al*., 1997; Avrova *et al*., 2004; Jiang *et al*., 2006; Kamoun, 2006). However, plants can evolve the ability to recognize pathogen effectors, not only directly by plant resistance (R) proteins encoded by the respective *R* genes, but according to the "guard hypothesis" also indirectly via complexes formed by pathogen effectors with their plant protein targets (Dangl & Jones, 2001; Jones & Dangl, 2006). R protein activation then leads to effector-triggered immunity (ETI) of the plant and specific resistance (Dangl & Jones, 2001; Jones & Dangl, 2006; Murray *et al*., 2007). ETI is a stronger and accelerated version of PTI and therefore both, basal and specific resistance mechanisms, share certain pathway components (Dangl & Jones, 2001; Jones & Dangl, 2006; Murray *et al*., 2007). During evolution, pathogens can overcome ETI by developing either novel effectors to regain host susceptibility (effector-triggered susceptibility) or by down-regulation of expression/the loss of effector-encoding genes (Rouxel & Balesdent, 2010). For example, the tobacco-specialized pathogen *Phytophthora parasitica* var. *nicotianae* (Ppn) down-regulates *in planta* the expression of the elicitin parasiticein to evade host recognition and therefore rather prevents than manipulates the elicitation of plant defense responses (Colas *et al*., 2001).

In analogy to pathogen recognition via PAMPs/MAMPs and the resulting PTI, researchers proposed similar plant perception mechanisms also with respect to herbivore attack, *i.e.* the recognition of herbivore-associated molecular patterns (HAMPs) such as FACs and GOX leading to the activation of according plant defense responses and HAMP-triggered immunity (Truitt *et al*., 2004; Mithofer & Boland, 2008; Hogenhout & Bos, 2011). PAMP/MAMP and HAMP perception is complemented by the recognition of damage-associated molecular patterns (DAMPs) providing the plant with information on cell integrity (Boller & Felix, 2009; Heil, 2009).

A special protein without known catalytic function, $Hs1^{pro-1}$ from the wild beet *Beta procumbens* is supposed to be a member of a novel, atypical class of R proteins contributing to resistance against the plant pathogenic nematodes *Heterodera schachtii* in sugar beet and *Heterodera glycines* in soybean (Cai *et al*., 1997; Ellis & Jones, 1998; Thurau *et al*., 2003; Schulte *et al*., 2006; McLean *et al*., 2007). While $Hs1^{pro-1}$ plays a role in specific nematode resistance, an *Arabidopsis* ortholog of this protein, HSPRO2, was demonstrated to be involved in basal resistance against *Pseudomonas syringae* pv. *tomato* (Murray *et al*., 2007). For *Arabidopsis* it was further shown that HSPRO2 and its paralog HSPRO1 are able to interact with a regulatory subunit of plant SnRK1 complexes *in vitro* and *in planta* (Gissot *et al*., 2006). Plant SnRK1 enzymes are central regulators of energy metabolism, development, growth and stress tolerance, including plant tolerance to herbivory (Schwachtje *et al*., 2006; Baena-Gonzalez *et al*., 2007; Cho *et al*., 2012). Thus, in addition to basal and *R* gene-mediated resistance, a role in plant growth and development as well as plant tolerance to herbivores has to be considered for those $Hs1^{pro-1}$ homologs, too. In view of these differences in function, it is tempting to speculate that $Hs1^{pro-1}$and its homologs either underwent a process of drastic functional diversification during speciation events, or – which is even more plausible – play a very basic role in the overlapping part of basal and specific resistance pathways, maybe functioning even in a junction point between resistance and tolerance.

Taken all this informations on *N. attenuata*'s arsenal of different responses to herbivore and pathogen attack together, this plant species needs to possess a very smart and complex signaling system to a) perceive the individual attackers, b) integrate and trade off this information input against other factors relevant to the plant's Darwinian fitness, c) initialize an

adequate and well-orchestrated response tailored to the particular attacker and d) minimize response-associated fitness costs and negative side effects for plant mutualists. During this thesis, I focused mainly on the function of two genes, *GLA1* and *HSPRO*, in these complex plant signaling and trade-off processes.

In manuscripts 1 and 2, I analyzed in detail the role of the *N. attenuata* lipase GLA1 in oxylipin-mediated signaling processes occurring during *M. sexta* herbivory and infection by phytopathogenic microorganisms, in particular *Phytophthora parasitica* var. *nicotianae.* I demonstrated a central yet distinct role in the biogenesis of oxylipins during insect attack and pathogen infection.

In manuscripts 3 and 4, I demonstrated that HSPRO, the *N. attenuata* homolog of *Beta procumbens* Hs1^{pro-1}, controls seedling growth promotion during the mutualistic interaction between *P. indica* and *N. attenuata.* I proposed that HSPRO acts via SnRK1 signaling, a mechanism that could help integrating HSPRO in the tolerance responses to *M. sexta* herbivory in *N. attenuata* plants.

Objectives of this thesis:

1) Understand the biochemical mechanisms underlying the activation of oxylipin biogenesis in plants during insect attack. Particular emphasis was put on the study of the interaction between *N. attenuata* plants and *M. sexta* larvae.

2) Understand the biochemical mechanisms underlying the activation of oxylipin biogenesis during infection of plants by fungi and oomycete pathogens. Particular emphasis was put on the study of the interaction between *Phytophthora parasitica* var. *nicotianae* and *N. attenuata* plants.

3) Understand the role of the insect-induced *HSPRO* gene in the interaction of *N. attenuata* plants with insect herbivores and beneficial and pathogenic microorganisms. Particular emphasis was put on the study of the interaction of *N. attenuata* plants with *M. sexta* and the broad host-range mutualistic fungus *P. indica*.

Chaper 2: Manuscript overview

Manuscript 1:

Revealing complexity and specificity in the activation of lipase-mediated oxylipin biosynthesis: A specific role of the *Nicotiana attenuata* GLA1 lipase in the activation of jasmonic acid biosynthesis in leaves and roots

Gustavo Bonaventure, Stefan Schuck and Ian T. Baldwin

Published in Plant, Cell & Environment, Vol. 34, No. 9, pp. 1507-1520 (2011)

In manuscript 1, I demonstrated that NaGLA1 is the major lipase specifically supplying substrate (linolenic acid) for the biosynthesis of the phytohormone jasmonic acid (JA). Therefore I performed experiments with transgenic *Nicotiana attenuata* genotypes stably silenced in the expression of Na*GLA1* by inverted-repeat technique. In those experiments I analyzed the production of JA and other oxylipins produced from different biosynthetic pathways as well as the accumulation pattern of lysolipids in response to various stimuli inducing either Na*GLA1* expression [infection by phytopathogenic fungi such as *Phytophthora parasitica* var. *nicotianae* (Ppn)] or NaGLA1 activation [wounding and treatment with the *Manduca sexta* elicitor N-linolenoyl-L-glutamate (simulated insect herbivory)]. As a result, this study revealed that NaGLA1 is able to use multiple lipid classes as substrate and rather specifically feeds the JA biosynthetic pathway in response to wounding and N-linolenoyl-L-glutamate treatment in *N. attenuata* leaves. However, NaGLA1 also affects early divinyl ether production and the expression of divinyl ether biosynthetic enzymes upon Ppn attack.

Stefan Schuck and Dr. Gustavo Bonaventure planned and performed the experiments, analyzed the data and wrote the manuscript. Prof. Dr. Ian T. Baldwin participated in experimental design and writing of the manuscript.

Jena, 21.01.2013 ……

Prof. Dr. Ian T. Baldwin

Manuscript 2:

Analysis of the role of NaGLA1 in *Nicotiana attenuata* defense responses against the oomycete *Phytophthora parasitica* var. *nicotianae*

Stefan Schuck, Mario Kallenbach, Ian T. Baldwin and Gustavo Bonaventure

Will be submitted to Plant, Cell & Environment

In manuscript 2, I focused on NaGLA1's role during the infection of *Nicotiana attenuata* with *Phytophthora parasitica* var. *nicotianae* (Ppn) encouraged by the strong inducibility of its transcriptional expression during Ppn infection revealed in manuscript 1. The monitoring of disease progression (Ppn abundance and symptom strength), oxylipin and metabolic profiling, as well as lysolipid and microarray analysis comparing Ppn-infected *N. attenuta* wildtype and genotypes stably silenced in Na*GLA1* expression revealed that NaGLA1 is probably involved in the generation of some signaling compounds. This hypothesis is supported by the differential regulation of a huge number of stress responsive genes differentially regulated between wild-type and Na*GLA1*-silenced *N. attenuata* plants and the NaGLA1-dependent release of specific lysolipid species and oxylipins in response to Ppn infection.

Stefan Schuck and Dr. Gustavo Bonaventure planned and performed the experiments, analyzed the data and wrote the manuscript. Dr. Mario Kallenbach developed the method for extraction and analysis used for oxylipin profiling and participated in writing the manuscript. Prof. Dr. Ian T. Baldwin participated in experimental design and writing of the manuscript.

Jena, 21.01.2013 ……

Prof. Dr. Ian T. Baldwin

Manuscript 3:

HSPRO controls early *Nicotiana attenuata* seedling growth during interaction with the fungus *Piriformospora indica*

Stefan Schuck, Iris Camehl, Paola A. Gilardoni, Ralf Ölmüller, Ian T. Baldwin and Gustavo Bonaventure

Published in Plant Physiology, Vol. 160, No. 2, pp. 929–943 (2012)

In manuscript 3, I characterized NaHSPRO, the *Nicotiana attenuata* homolog to the putative nematode resistance protein $Hs1^{pro-1}$ from *Beta procumbens*. NaHSPRO was originally identified in a SuperSAGE transcriptomic analysis because it is differentially induced in leaves by treatment of *N. attenuata* with the elicitor N-linolenoyl-L-glutamate from the specialist insect herbivore *Manduca sexta*. In addition, I could show that its expression is also inducible by the phytopathogenic bacterium *Pseudomonas syringae* pv. *tomato* DC3000 in leaves and the mutualistic fungus *Piriformospora indica* in roots. These transcriptional expression results suggested an involvement of NaHSPRO in *N. attenuata*'s interaction with these organisms. To test hypotheses based on this assumption, transgenic *N. attenuata* plants had been generated stably silenced in Na*HSPRO* expression by inverted-repeat technique and were used together with wild-type *N. attenuata* plants for various experiments. No ecological relevance could be demonstrated for NaHSPRO in *N. attenuata*'s defense against *M. sexta* and *P. syringae*, however I found that it acts as negative regulator of *P. indica*-mediated plant growth promotion.

Stefan Schuck, Dr. Iris Camehl and Dr. Gustavo Bonaventure planned and performed the experiments, analyzed the data and wrote the manuscript. Dr. Paola A. Gilardoni participated in the identification of the full-length Na*HSPRO* cDNA sequence, was involved in generating the *N. attenuata* plants stably silenced in Na*HSPRO* expression and helped writing the manuscript. Prof. Dr. Ralf Ölmüller and Prof. Dr. Ian T. Baldwin participated in the design and coordination of experiments and writing of the manuscript.

Jena, 21.01.2013 ……

Prof. Dr. Ian T. Baldwin

Manuscript 4:

HSPRO acts via SnRK1-mediated signaling in the regulation of *Nicotiana attenuata* seedling growth promoted by *Piriformospora indica*

Stefan Schuck, Ian T. Baldwin and Gustavo Bonaventure

Published online (Vol. 34, No. 9; e23537) in Plant Signaling & Behavior on 18.01.2013

In manuscript 4, I followed up on the hypothesis emerging from manuscript 3 that NaHSPRO controls *Piriformospora indica*-mediated growth promotion in *Nicotiana attenuata* seedlings through SnRK1signaling. To test this hypothesis, transgenic *N. attenuata* plants stably silenced in Na*HSPRO* expression were crossed with those stably silenced in the expression of Na*GAL83*, a regulatory subunit of the SnRK1 kinase complex. By comparing seedling weight gain in presence of *P. indica* using those transgenic *N. attenuata* crosses and appropriate controls, I could show that NaGAL83 functions as much as a negative regulator of *P. indica*-mediated growth promotion as NaHSPRO, indicating that the observed effect might be indeed due to SnRK1 signaling.

Stefan Schuck and Dr. Gustavo Bonaventure planned the experiments and wrote the manuscript. Performance of the experiments and data analysis was done by Stefan Schuck. Prof. Dr. Ian T. Baldwin participated in experimental design and writing of the manuscript.

Jena, 21.01.2013 ……

Prof. Dr. Ian T. Baldwin

Chapter 3: Manuscript 1

Revealing complexity and specificity in the activation of lipase-mediated oxylipin biosynthesis: A specific role of the *Nicotiana attenuata* GLA1 lipase in the activation of JA biosynthesis in leaves and roots

Plant, Cell & Environment

Plant, Cell and Environment (2011) **34**, 1507–1520 doi: 10.1111/j.1365-3040.2011.02348.x

Revealing complexity and specificity in the activation of lipase-mediated oxylipin biosynthesis: a specific role of the *Nicotiana attenuata* GLA1 lipase in the activation of jasmonic acid biosynthesis in leaves and roots

GUSTAVO BONAVENTURE, STEFAN SCHUCK & IAN T. BALDWIN

Department of Molecular Ecology, Max Planck Institute of Chemical Ecology, Hans Knöll Str. 8, D-07745 Jena, Germany

ABSTRACT

The activation of enzymatic oxylipin biosynthesis upon wounding, herbivory and pathogen attack depends on the biochemical activation of lipases that make polyunsaturated fatty acids (PUFAs) available to lipoxygenases (LOXs). The identity and number of the lipases involved in this process remain controversial and they probably differ among plant species. Analysis of transgenic *Nicotiana attenuata* plants (ir-*gla1*) stably reduced in the expression of the Na*GLA1* gene showed that this plastidial glycerolipase is a major supplier of trienoic fatty acids for jasmonic acid (JA) biosynthesis in leaves and roots after wounding and simulated herbivory, but not during infection with the oomycete *Phytophthora parasitica* (var. *nicotianae*). NaGLA1 was not essential for the developmental control of JA biosynthesis in flowers and for the biosynthesis of C_6 volatiles by the hydroperoxide lyase (HPL) pathway; however, it affected the metabolism of divinyl ethers (DVEs) early during infection with *P. parasitica* (var. *nicotianae*) and the accumulation of Na*DES1* and Na*LOX1* mRNAs. Profiling of lysolipids by LC–MS/MS was consistent with a rapid activation of NaGLA1 and indicated that this lipase utilizes different lipid classes as substrates. The results revealed the complexity and specificity of the regulation of lipase-mediated oxylipin biosynthesis, highlighting the existence of pathway- and stimulus-specific lipases.

Key-words: fatty acids; insect herbivory; lysolipids; tobacco.

INTRODUCTION

In leaves, the rapid activation of jasmonic acid (JA) biosynthesis upon insect herbivory, pathogen infection or mechanical damage depends on the biochemical activation of constitutively expressed enzymes in the chloroplast. The first step in JA production is catalysed by a glycerolipase class A enzyme that deacylates glycerolipids from plastidial membranes to release free 9,12,15-octadecatrienoic acid (18:3) and 7,10,13-hexadecatrienoic acid (16:3) (Creelman & Mullet 1997; Weber, Vick & Farmer 1997; Ishiguro *et al*. 2001; Ellinger *et al*. 2010; Kallenbach *et al*. 2010). These free trienoic fatty acids are rapidly dioxygenated by 13-lipoxygenases (13-LOXs) to generate 13*S*-hydroperoxydated derivatives which are converted into (9*S*,13*S*)-12-oxo-phytodienoic acid (OPDA) by the sequential action of allene oxide synthase (AOS) and allene oxide cyclase (AOC) in the chloroplast (Vick & Zimmerman 1983, 1984). OPDA is then exported from this organelle and imported into the peroxisome where (+)-7-*iso*-JA is produced (Vick & Zimmerman 1984). JA can be conjugated to isoleucine (Ile) by JAR1 in *Arabidopsis thaliana* (Suza & Staswick 2008) or its homologs in other plant species (Wang *et al*. 2008; Suza *et al*. 2010; VanDoorn *et al*. 2011) to form the bioactive molecule jasmonyl-L-isoleucine ((+)-7-iso-JA-Ile) (Suza & Staswick 2008). In *Arabidopsis* leaves, acylated OPDA accumulates to high levels in glycerolipids (Stelmach *et al*. 2001), and this JA precursor may be freed by lipases to supply the JA biosynthesis pathway (Ellinger *et al*. 2010). In *Nicotiana attenuata* leaves, lipid-esterified OPDA is not detected before or after wounding or simulated herbivory (Kallenbach *et al*. 2010), and the accumulation of these molecules in leaves has thus far been restricted to *Arabidopsis* (Böttcher & Weiler 2007).

The lipase-catalysed step involved in the activation of JA biosynthesis has been a matter of debate in the last years. The first lipase reported to mediate JA production in flowers was the *Arabidopsis* DEFECTIVE IN ANTHER DEHISCENCE 1 (DAD1) (Ishiguro *et al*. 2001), and later the *Arabidopsis* DONGLE (DGL) and AtPLAI were identified as lipases involved in the wound-induced and basal biosynthesis of JA, respectively (Yang *et al*. 2007; Hyun *et al*. 2008). In a recent study, Ellinger *et al*. (2010) have revisited the participation of these three and other lipases in the supply of substrates for JA biosynthesis in *Arabidopsis* leaves, and shown that DAD1 and DGL are not essential for the early (within 60 min) accumulation of JA after wounding. However, the *dad1* mutant accumulates 50% of wild-type (WT) levels of JA in leaves after 60 min of this stimulus, and PLA-Iγ1-deficient plants accumulate 50% of

Correspondence: G. Bonaventure. Fax: +49 3641 571102; e-mail: gbonaventure@ice.mpg.de

WT levels of JA at 30 min after wounding, but not before or after this stimulus (Ellinger *et al.* 2010). Additional lipases had partial effects on basal or wound-induced JA accumulation, demonstrating that in *Arabidopsis* leaves, the accumulation of JA is determined by multiple lipases probably acting at different stages of the wound response (Ellinger *et al.* 2010).

In *N. attenuata*, the transient silencing of the *GLYCEROLIPASE A1* gene (NaGLA1; a close homolog of DAD1 and DGL) by virus-induced gene silencing (VIGS) showed that this lipase is an important supplier of substrates for JA biosynthesis in leaves after wounding and simulated herbivory (Kallenbach *et al.* 2010). Similar to DAD1, DGL and PLA-Iγ1, NaGLA1 belongs to the phospholipase-A_1 class I (PLA_1-I) family of phospholipases, which is characterized by the presence of an N-terminal chloroplast transit peptide and a conserved lipase-3 domain with the catalytic triad Ser-Asp-His (Ryu 2004). NaGLA1 has *in vitro* activity towards different glycerolipids [i.e. phosphatidylcholine (PC), monogalactosyl diglyceride (MGDG) and triacylglyceride] and releases fatty acids preferentially from the *sn-1* position of PC (Kallenbach *et al.* 2010).

The kinetic of jasmonate accumulation after mechanical damage varies considerably between plant species and tissues. For example, after a single wound event, *Arabidopsis* leaves show a peak of JA accumulation after 90 min of the stimulus with levels remaining significantly higher than basal levels for at least 24 h (Glauser *et al.* 2008a). In wounded pea (*Pisum sativum* L.) leaves, JA accumulates in a biphasic manner with a rapid and transient burst at 1 h and a second burst at 48 h after the stimulus (Yang *et al.* 2009). In soybean (*Glycine max*), wounded hypocotyls show a peak in JA accumulation at 8 h after the stimulus, and the levels remain almost constant for 24 h (Creelman, Tierney & Mullet 1992). The *N. attenuata* wounded leaves show a burst of JA that lasts approximately 1 h and wanes after 2 h of the stimulus (Schittko, Preston & Baldwin 2000). Additionally, similar to maize (*Zea mays*), eggplant (*Solanum melongena*) and black nightshade (*Solanum nigrum*), *N. attenuata* plants amplify JA biosynthesis by two- to threefold upon perception of insect elicitors such as fatty acid–amino acid conjugates (FACs) (McCloud & Baldwin 1997; Schmelz *et al.* 2009; Kallenbach *et al.* 2010; VanDoorn *et al.* 2011). These differences in the pattern and amplitude of JA accumulation probably reflect differences in the regulatory mechanisms used by diverse plants to activate JA biosynthesis and therefore in the activation of the lipase(s) involved in the supply of trienoic fatty acids for this pathway. Importantly, the almost immediate accumulation of JA that follows the wound response (Glauser *et al.* 2008a) shows that the initial accumulation of this phytohormone depends on the initial (basal) levels of expression of the JA biosynthetic enzymes and it is independent of the transcriptional activation of these genes (positive feedback) that usually follows the JA burst (Reymond *et al.* 2000; Sasaki *et al.* 2001; Devoto *et al.* 2005; Bonaventure *et al.* 2007). *DAD*1 and *DGL* expression is induced by wounding (Hyun *et al.* 2008; Ellinger *et al.* 2010); however, Na*GLA1* transcript levels are repressed by this treatment within the first hour of the response (Kallenbach *et al.* 2010), suggesting a differential transcriptional regulation of JA biosynthesis-associated lipases in different plant species.

Two additional biosynthesis pathways that depend on the activation of lipases to release free polyunsaturated fatty acids (PUFAs) from membranes are those producing C_6 volatile aldehydes and their derivatives [green leaf volatiles (GLVs)], and divinyl ethers (DVEs). In the case of GLVs, 18:2 and 18:3 are dioxygenated by 13-LOXs to generate 13*S*-hydroperoxides, which are cleaved by hydroperoxide lyase (HPL) into C_6 and C_{12} products in the chloroplast. GLVs are immediately emitted by leaves upon different stresses, including mechanical damage, insect herbivory and pathogen attack (Croft, Juttner & Slusarenko 1993; Stowe *et al.* 1995; Allmann *et al.* 2010). DVE biosynthesis commonly starts with the dioxygenation of 18:2 and 18:3 by cytosolic 9-LOXs to generate 9*S*-hydroperoxydated derivatives, which are converted into ethers with three [colneleic acid (CA)] or four [colnelenic acid (CnA)] double bonds by DVE synthase (DES) (Gobel *et al.* 2001); however, some plant species can also produce DVE derivatives of 13*S*-hydroperoxides (Grechkin & Hamberg 1996). DVEs are strongly induced in tobacco and potato plants in response to pathogens, such as *Phytophthora parasitica* var. *nicotianae* and *Phytophthora infestans*, and the expression of *9-LOX* and *9-DES* genes are strongly induced by these pathogens (Weber *et al.* 1999; Gobel *et al.* 2002; Fammartino *et al.* 2007). It has been shown that DVEs have antimicrobial properties by, for example, inhibiting mycelial growth and spore germination of some *Phytophthora* species (Prost *et al.* 2005).

In this study, we demonstrated by the generation of *N. attenuata* plants stably reduced in the expression of NaGLA1 (ir-*gla1*) by RNAi-mediated gene silencing that this lipase is a specific supplier of trienoic fatty acids for JA biosynthesis in leaves and roots after wounding and simulated herbivory, and that it utilizes multiple glycerolipid substrates as a source of trienoic fatty acids. We also showed that additional lipases must participate in the supply of fatty acid substrates for JA biosynthesis during *P. parasitica* (var. *nicotianae*) infection, flower development and the biosynthesis of GLVs by the HPL pathway. Moreover, alternative functions for NaGLA1 were revealed by the analysis of the regulation of Na*DES1* and Na*LOX1* gene expression in ir-*gla1* plants during infection with *P. parasitica* (var. *nicotianae*) and *Fusarium oxysporum*, and by changes in the rate of accumulation of DVEs at early stages of *P. parasitica* (var. *nicotianae*) infection. We propose that distinct lipases (probably belonging to the PLA_1-I family) control the mentioned lipase-regulated biosynthesis processes and that each lipase is activated by distinct stimuli.

MATERIALS AND METHODS

Plant and fungus growth and treatments

Seeds of *N. attenuata* plants were germinated on agar plates containing Gamborg's B5 medium as previously described (Krügel *et al.* 2002). The plates were maintained in a growth chamber (Snijders Scientific, Tilburg, the Netherlands) at 26 °C/16 h (155 μmol s^{-1} m^{-2} light), 24 °C/8 h dark for 10 d. Ten-day-old seedlings were transferred to TEKU pots (Pöppelmann GmbH & Co. KG, Lohne, Germany) with Klasmann plug soil (Klasmann-Deilmann GmbH, Geesten, Germany). After 10 d, the seedlings were transferred to soil in 1 L pots and grown in the glasshouse under high-pressure sodium lamps (200–300 μmol s^{-1} m^{-2}) with a day/night ratio of 16 h (26–28 °C)/8 h (22–24 °C) and 45–55% humidity. *Phytophthora parasitica* (var. *nicotianae*) and *F. oxysporum* Schlechtendal: Fries f. sp. *tuberosi* cultures were obtained from the DSMZ (German Collection of Microorganisms and Cell Cultures) and were grown on potato dextrose agar (PDA) (Sigma, Taufkirchen, Germany).

Leaf wounding was performed by rolling three times a fabric pattern wheel on each side of the midvein of 40-day-old rosette-stage plants. For FAC treatment, the wounds were immediately supplied with 20 μL of synthetic *N*-linolenoyl-glutamic acid (18:3-Glu; 0.03 nmol μL^{-1}). Leaf tissue was collected at different times after the treatments and was frozen immediately in liquid nitrogen for subsequent analysis. For infection of *N. attenuata* plants with *P. parasitica* (var. *nicotianae*) and *F. oxysporum*, a sterile syringe needle was streaked once on plates with 2-week-old cultures of the pathogens and used to gently prick the hypocotyls of 20-day-old seedlings. For the control treatment, a sterile needle was streaked on an empty PDA plate and used to prick the hypocotyls. The infection zone was immediately covered with a moist cotton plug. At different times, leaf and root samples were harvested and immediately frozen in liquid nitrogen for subsequent analyses.

Generation of transgenic ir-*gla1* lines

Transgenic *N. attenuata* (ir-*gla1*) plants reduced in the expression of NaGLA1 were generated via leaf disc *Agrobacterium*-mediated transformation and seedling regeneration as previously described (Krügel *et al.* 2002). The binary vector used for plant transformation was pSOL8 (Bubner *et al.* 2006) engineered to carry a 293 bp fragment of Na*GLA1* cDNA (GenBank accession: FJ821553) subcloned in inverted repeat orientation (pSOL8PLA1). These fragments were generated by PCR using the primers listed in Supporting Information Table S1 and cDNA of NaGLA1 as template. T_1 transformed plants were analysed by quantification of JA levels in leaves after wounding and for T-DNA single insertion by Southern blot hybridization (see below). Segregation analysis of hygromycin resistance in T_2 seedlings was performed on agar plates supplemented with hygromycin (0.025 mg mL^{-1}). Two lines, ir-*gla1* A-09-848-2 (848) and A-09-849-2 (849) showed the lowest levels of JA accumulation after leaf wounding and had a single T-DNA insertion in their genomes. These lines were used for all experiments. Southern blot analysis was performed as previously described (Körner *et al.* 2009).

Analysis of phytohormones in leaves and roots

For analysis of JA, JA–Ile and OPDA, 0.2 g of frozen leaf or root tissues was homogenized to a fine powder in the presence of liquid nitrogen. One millilitre of ethyl acetate spiked with 200 ng [$^2H_2$]JA and 40 ng [$^{13}C_6$]JA–Ile was added to the samples, and after vortexing the samples were centrifuged for 15 min at 13 200 *g* (4 °C). The upper organic phase was transferred into a fresh tube and the leaf material was re-extracted with 0.5 mL ethyl acetate. The organic phases were pooled and evaporated to dryness. The dry residue was reconstituted in 0.4 mL of 70/30 (v/v) methanol/water for analysis with an LC–ESI–MS/MS instrument (Varian 1200 Triple-Quadrupole-LC-MS system; Varian, Palo Alto, CA, USA). Ten microlitres of the sample was injected in a ProntoSIL column (C18-ace-EPS, 50 × 2 mm, 5 μm, 120 Å; Bischoff, Leonberg, Germany) connected to a pre-column (C18, 4 × 2 mm; Phenomenex, Torrance, CA, USA). As mobile phases, 0.05% formic acid in water (solvent A) and methanol (solvent B) were used in a gradient mode with the following conditions: time/concentration (min/%) for B: 0.0/15; 2.5/15; 4.5/98; 10.5/98; 12.0/15; 15.0/15; time/flow (min/mL): 0.0/0.4; 1.5/0.2; 1.5/0.2; 10.5/0.4; 15.0/0.4. Compounds were detected in the ESI negative mode and multiple reaction monitoring (MRM) according to the parameters shown in Supporting Information Table S2. Quantification of endogenous OPDA was performed by external calibration with commercial OPDA (Cayman, Ann Arbor, MI, USA) and the [$^2H_2$]JA IS.

Analysis of lysolipids in leaves

Half a gram of frozen leaf tissue was transferred into 8 mL glass tubes (Corning, Schiphol-Rijk, the Netherlands) containing 2 mL of 2-propanol and incubated at 80 °C for 10 min to inactivate lipases. On cooling, 3.75 mL of 2/1 (v/v) methanol/chloroform containing internal standards (200 ng of Lyso PG-17:1 and 200 ng of Lyso PC-17:0 (Avanti Polar Lipids, Alabaster, AL, USA) were added and the samples were thoroughly ground. Then, 1.25 mL of chloroform and 1 mL of water were added, and after vortexing the samples were centrifuged for 25 min at 800 *g* (4 °C). The lower organic phase was transferred into a fresh glass tube and the aqueous phase/leaf material was re-extracted with 3 mL of chloroform. The organic phases were pooled and the samples were evaporated under a stream of nitrogen and reconstituted in 0.4 mL of 70/20/10 (v/v/v) methanol/water/chloroform. The samples were split in two (0.2 mL each). To one-half of the samples, 10 μL of a 1 M aqueous solution of sodium acetate was added (final concentration of 50 mM) and used for the analysis of lyso-PC (LPC), monogalactosyl monoglyceride (MGMG) and digalactosyl monoglyceride (DGMG). The second half of the samples was used for the analysis of lyso-PG (LPG).

Lysolipids were analysed with an LC–ESI–MS/MS instrument (Varian 1200 Triple-Quadrupole-LC-MS system). For LPC, MGMG and DGMG analyses, 10 μL of the sample was injected in a Gemini-NX column (C18; 3 μm, 50 × 2 mm, 110 Å Phenomenex) attached to a pre-column (C18, 4 × 2 mm; Phenomenex). As mobile phases, 0.05% formic acid in water (solvent A) and methanol (solvent B) were used in a gradient mode with the following conditions: time/concentration (min/%) for B: 0.0/15, 1.5/15, 5.0/98, 18.0/98, 22.0/15, 25.0/15; time/flow (min/mL): 0.0/0.1, 1.0/0.1, 1.5/0.2, 5.0/0.2, 18.0/0.2, 22.0/0.2, 25.0/0.1. To minimize contaminations, the solvent eluting from the column was injected into the mass spectrometer only between 1.5 and 18.5 min. Between 0 and 1.5 min, and 18.5 and 25 min, a mixture of 1/1 (v/v) methanol/water was injected to flush the MS/MS system. The MS was used in positive ion mode and ions were detected using MRM after CID with argon gas (Supporting Information Table S3). For LPG analysis, 10 μL of the sample was injected onto a C_{18} column (4 × 2 mm; Phenomenex). Similar mobile phases were used as described above with small changes: time/concentration (min/%) for B: 0.0/15, 1.5/15, 4.0/98, 15.0/98, 17.0/15, 20.0/15; time/flow (min/mL): 0.0/0.1, 1.0/0.1, 1.5/0.2, 4.0/0.2, 15.0/0.2, 17.0/0.2, 20.0/0.1. To minimize contaminations, the solvent eluting from the column was injected into the mass spectrometer only between 1.5 and 17 min. Between 0 and 1.5 min, and 1.5 and 17 and 20 min, a mixture of 1/1 (v/v) methanol/water was injected to flush the MS/MS system. The MS was used in negative ion mode and ions were detected using MRM (Supporting Information Table S3). For ionization, the needle was set at 5000 V and the drying gas (nitrogen) at 300 °C and 20 psi (housing 50 °C). The detector was set at 1800 V. Quantification of LPC and LPG species was made based on the peak areas of the internal standards added (Lyso PC-17:0 and Lyso PG-17:1, respectively), the ion transitions presented in Supporting Information Table S3 and standard curves generated by spiking the IS at increasing concentrations in a leaf matrix (i.e. leaf extract) to correct for suppression of ionization. In case of LPG, the quantification was based on the released fatty acid (Supporting Information Table S3), and differences in ionization efficiencies between different fatty acids may affect the absolute amounts of LPG presented in the figures corresponding to the analysis of lysolipids. MGMG and DGMG were quantified using the LPC-17:0 IS added, the ion transitions presented in Supporting Information Table S3 and the corresponding response curves generated by injecting different concentrations of the IS mixed with TLC-purified MGMG and MGDG generated from hydrogenated MGDG and digalactosyl diglyceride (DGDG) (Matreya, Pleasant Gap, PA, USA; see below). An estimated response factor of 900 was applied to the peak areas corresponding to MGMG and DGMG. MGMG and DGMG were generated *in vitro* as previously described (Murakami *et al.* 1991) using *Rhizopus arrhizus* and *Mucor javanicus* lipases (Sigma), and hydrogenated MGDG and DGDG (Matreya) as substrates.

Analysis of DVEs in roots and leaves

One hundred milligrams of frozen root or leaf material was homogenized to a fine powder in the presence of liquid nitrogen. Samples were extracted with 1 mL of ethyl acetate spiked with 500 ng of etherolenic acid (EnA) (Larodan, Malmö, Sweden) as the internal standard. After centrifugation at 4 °C for 10 min, the organic phase was transferred into a fresh tube and the leaf material was re-extracted with 0.5 mL of ethyl acetate. After centrifugation, the organic phases were combined, evaporated to dryness under a gentle stream of nitrogen and reconstituted in 0.2 mL of 70/25/5 (v/v/v) methanol/water/chloroform. DVEs were analysed with an LC-ESI-MS/MS instrument (Varian 1200 Triple-Quadrupole-LC-MS system) by injecting 10 μL of the sample in a ProntoSIL column (C18; 5 μm, 50 × 2 mm; Bischoff) attached to a pre-column (C18, 4 × 2 mm; Phenomenex). As mobile phases, 0.05% formic acid in water (solvent A) and methanol (solvent B) were used in a gradient mode with the following conditions: time/concentration (min/%) for B: 0.0/15, 1.5/15, 4.5/98, 19.5/98, 20.5/15, 25.0/15; time/flow (min/mL): 0.0/0.1, 1.0/0.1, 1.5/0.2, 4.5/0.2, 18.5/0.2, 19.5/0.2, 25/0.1. Samples were analysed in the ion negative mode and ions were detected using MRM after CID (Supporting Information Table S4). For ionization, the needle was set at 5000 V and the drying gas (nitrogen) at 300 °C and 20 psi (housing 50 °C). The detector was set at 1800 V. Quantification was made based on the internal standards added and standard curves. As standards for fragmentation and retention times, EnA and etheroleic acid (EA) were purchased from Larodan, and CA and CnA were obtained from peeled potato tubers (Galliard & Phillips 1972).

Collection and analysis of GLVs

Leaves from ir-*gla1* and WT plants were induced by wounding and immediately enclosed in volatile collection chambers. Volatiles were trapped on 20 mg of Super-Q absorbent (ARS, Philadelphia, PA, USA) for a period of 30 min [coincident with the peak of C_6 volatile emission (Allmann *et al.* 2010)] as previously described (Vandoorn *et al.* 2010).

Analysis of gene expression by quantitative real-time PCR (qPCR)

Total RNA extraction and qPCR were performed as previously described (Gilardoni *et al.* 2010) using the eukaryotic elongation factor 1A (NaeEF1A) mRNA as an internal standard and the primers listed in Supporting Information Table S1. All the reactions were performed with at least three biological replicates.

Accession numbers

NaGLA1 (FJ821553), NaLOX1 (AY254347), NaDES1 (HQ824835).

RESULTS

Stably reduced NaGLA1 expression does not affect growth and reproduction of *N. attenuata* plants

To study the role of NaGLA1 in oxylipin biosynthesis in *N. attenuata*, stably transformed plants with reduced levels of Na*GLA1* expression were generated by inverted repeat-mediated gene silencing. These lines were named ir-*gla1*, and two homozygous independently transformed lines (848 and 849) carrying a single T-DNA insertion were selected and used for all experiments in this study (see Materials and methods and Supporting Information Fig. S1). The efficiency of gene silencing in these lines was evaluated by the quantification of Na*GLA1* transcript levels by RT-qPCR, and these levels were reduced on average by 75% compared to WT plants in the different tissues (see below).

Under controlled growth conditions (i.e. glasshouse or chambers), the growth and morphology of ir-*gla1* plants were indistinguishable from those of WT plants at all stages of development (Supporting Information Fig. S2). Importantly, flower morphology and seed setting (number of seeds per capsule and number of capsules per plant) were also unaffected in ir-*gla1* plants compared to WT plants (Supporting Information Fig. S2) and (data not shown), respectively.

NaGLA1 supplies substrates for JA biosynthesis in leaves, but it is not essential for JA biosynthesis in flowers and C_6 volatile production in leaves

After wounding and FAC elicitation, *N. attenuata* leaves respond with a single burst of JA and JA–Ile that peaks approximately at 60 min and wanes to basal levels after 2 h (Schittko *et al.* 2000). The levels of JA and JA–Ile accumulation were first quantified in leaves of WT and ir-*gla1* plants at 0, 1, 2 and 4 h after wounding and FAC elicitation with synthetic 18:3-Glu as the single elicitor (Kallenbach *et al.* 2010). After these treatments and compared to WT plants, ir-*gla1* lines accumulated on average 36–40% of WT levels of JA (Fig. 1a,b), and 37–45% of WT levels of JA–Ile

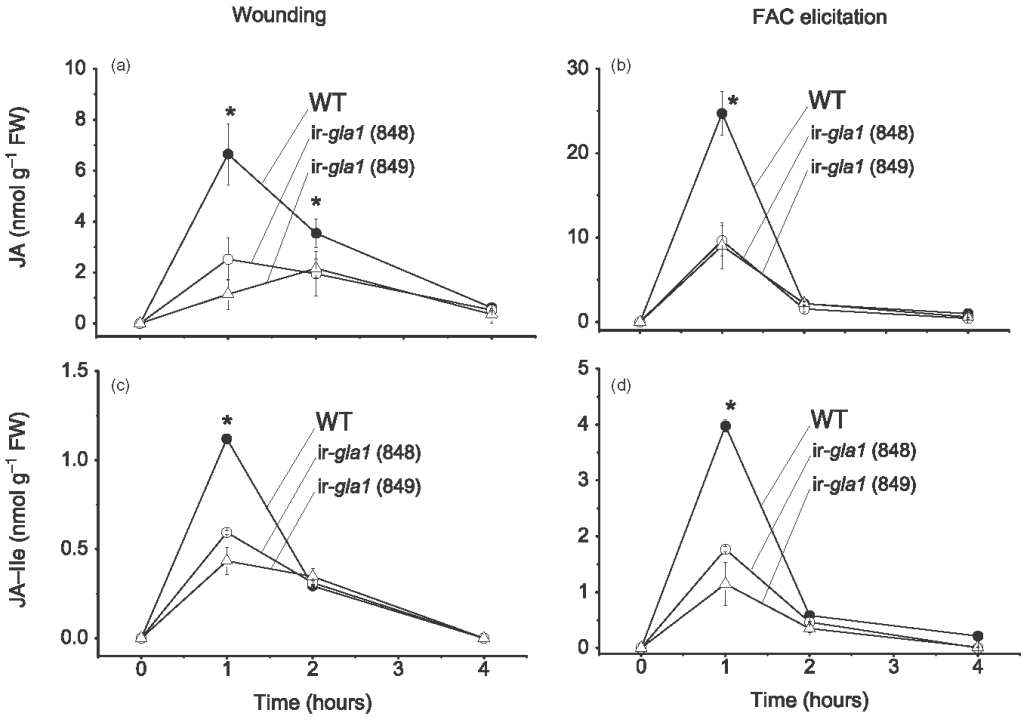

Figure 1. Accumulation of jasmonic acid (JA) and JA–isoleucine (Ile) in leaves of wild-type (WT) and ir-*gla1* plants after wounding and fatty acid–amino acid conjugate (FAC) elicitation. Leaves from WT and ir-*gla1* plants (lines 848 and 849) were either wounded with a fabric pattern wheel or wounded plus the addition of 18:3-Glu (FAC elicitation). Leaf samples were harvested at different times, extracted, and the amounts of JA and JA–Ile in wounded (a,c) and FAC-elicited (b,d) leaves were quantified by LC–MS/MS. *$P < 0.05$, Student's *t*-test (WT versus ir-*gla1* at same time point), $n = 4$, bars denote ± SE.

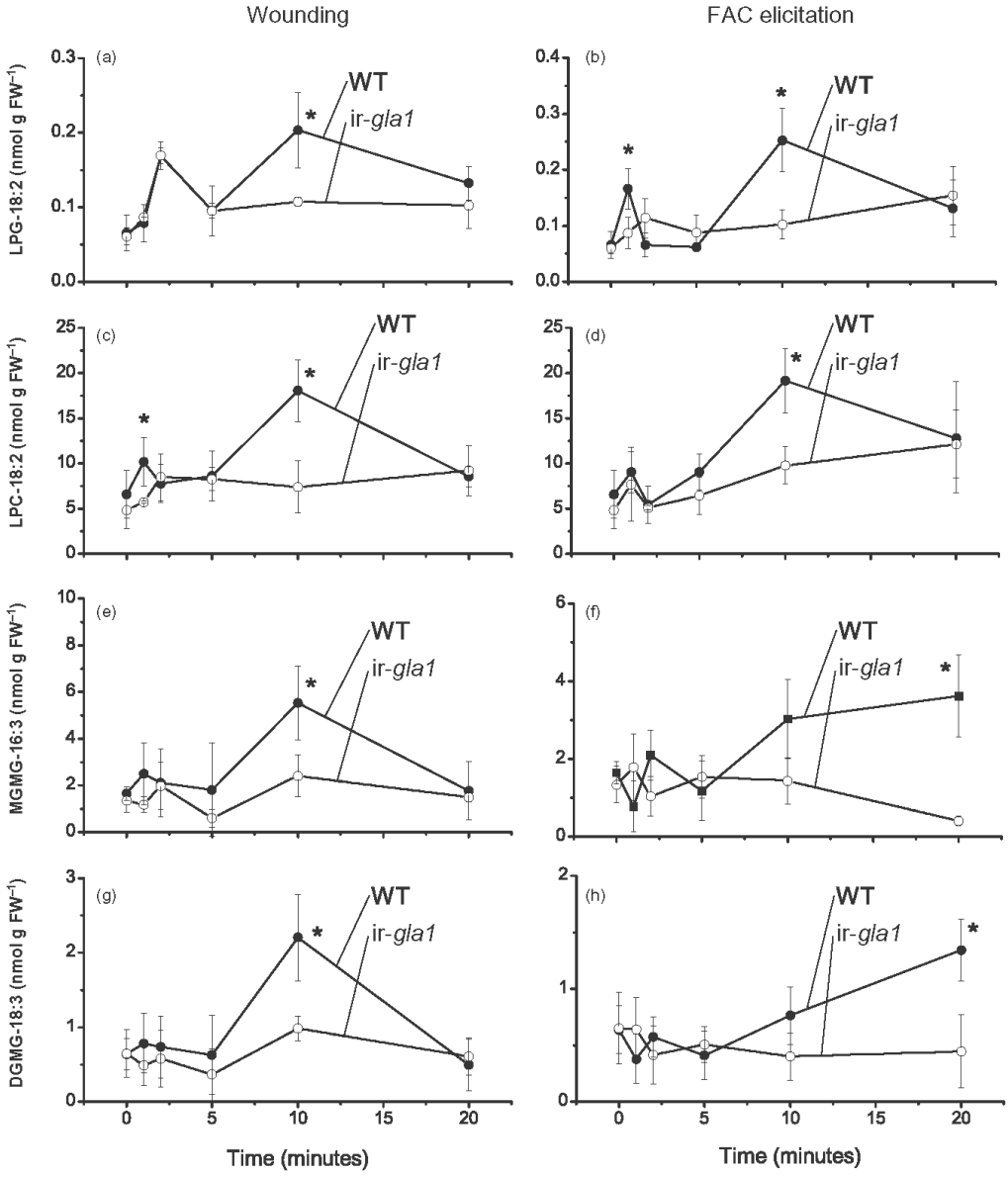

Figure 2. Accumulation of lysolipids in leaves of wild-type (WT) and ir-*gla1* plants after wounding and fatty acid–amino acid conjugate (FAC) elicitation. Leaves from WT and ir-*gla1* plants (only line 849 is shown) were either wounded with a fabric pattern wheel or wounded plus the addition of 18:3-Glu (FAC elicitation treatment). Leaf samples were harvested at different times, extracted, and the amounts of lyso-PC (LPC), lyso-PG (LPG), monogalactosyl monoglyceride (MGMG) and digalactosyl monoglyceride (DGMG) in wounded (a,c,e,g) and FAC-elicited (b,d,f,h) leaves were quantified by LC–MS/MS. The amounts of LPG-18:2, LPC-18:2, MGMG-16:3 and DGMG-18:3 are shown; the full data set is presented in Supporting Information Figs S6–S8. *$P < 0.05$, Student's *t*-test (WT versus ir-*gla1* at same time point), $n = 4$, bars denote ± SD.

(Fig. 1c,d). Although reduced in amplitude, the kinetic of JA and JA–Ile accumulation was similar between ir-*gla1* and WT plants.

Jasmonates are essential for flower development and fertility, and JA biosynthesis is developmentally controlled in flowers (Stintzi & Browse 2000; Ishiguro *et al.* 2001). Consistent with the normal flower development and fertility of ir-*gla1* plants, the levels of JA and JA–Ile at different stages of flower development were similar to WT (Supporting Information Fig. S3). The initial steps of C_6 aldehyde biosynthesis by the HPL pathway depend on the utilization of 18:2 and 18:3 to produce hexanal and (3*Z*)-hexenal, and take place in the chloroplast. To investigate whether Na*GLA1* supplies fatty acids for the burst of GLVs that occurs within 30 min after wounding in *N. attenuata* (Allmann *et al.* 2010), GLVs were quantified after this treatment in WT and ir-*gla1* plants. The amount of these volatiles produced did not differ between the plant types (Supporting Information Fig. S4).

NaGLA1 affects the accumulation of major lysolipids in leaves after wounding and FAC elicitation

Wounding and FAC elicitation in *N. attenuata* leaves cause a rapid and transient accumulation (within 20 min) of 13*S*-OOH-18:3 and OPDA, whereas the levels of free 18:3 do not change significantly (Kallenbach *et al.* 2010). It has been previously proposed that upon NaGLA1 activation, 18:3 is released rapidly from membranes and utilized by lipoxygenase 3 (NaLOX3) (Kallenbach *et al.* 2010). If this hypothesis is correct, it is expected to observe a rapid and transient accumulation of lysolipids generated by NaGLA1 activity. Thus, the levels of lysolipids derived from the major extraplastidial phospholipid PC, the major plastidial phospholipid phosphatidylglycerol (PG), and the plastidial galactolipids MGDG and DGDG were analysed within 20 min after leaf wounding and FAC elicitation in WT and ir-*gla1* plants. These lysolipids corresponded, respectively, to LPC, LPG, MGMG and DGMG. As a control, the levels of JA, JA–Ile and OPDA were also quantified within 20 min after the treatments, and the results (Supporting Information Fig. S5) were consistent with previously reported data obtained from plants silenced in Na*GLA1* expression by VIGS (Kallenbach *et al.* 2010).

The detectable molecular species of lysolipids corresponded to LPG-16:0, -16:1, -18:2, -18:3; LPC-16:0, -18:1, -18:2, -18:3; and MGMG-16:3, -18:3 and DGDG-18:3. For clarity, one example for each lysolipid molecular species is shown in Fig. 2, and all the molecular species are presented in Supporting Information Figs S6–S8. Additionally, because both ir-*gla1* lines showed similar results, only those corresponding to line 849 are shown.

For all LPG molecular species in WT leaves, an increase in their levels with a peak at 10 min (enhanced by FAC elicitation) and a decrease at 20 min after both wounding and FAC elicitation were detected (Fig. 2a,b; Supporting Information Fig. S6). In ir-*gla1* plants, a ~3-fold reduction in the levels of most LPG species was observed at 10 min after wounding and FAC elicitation (Fig. 2a; Supporting Information Fig. S6g,h). Interestingly, in WT leaves, FAC elicitation also induced a first smaller peak of LPG accumulation at 1 min that was not evident after wounding (except for LPG-18:2; Fig. 2a). This first peak was either abrogated or delayed in ir-*gla1* plants (Fig. 2b; Supporting Information Fig. S6).

The accumulation pattern of LPC in WT plants was largely similar to that of LPG: a peak of accumulation at 10 min after wounding and FAC elicitation followed by a decrease at 20 min (Fig. 2c,d; Supporting Information Fig. S7). The only exception was LPC-16:0, which kept accumulating after 10 min of FAC elicitation (Supporting Information Fig. S7b). A first smaller peak of accumulation at 1 min was also evident for LPC species particularly after wounding, and it was more prominent for LPC-16:0 and -18:1 species (Supporting Information Fig. S7a,g). In ir-*gla1* leaves, the levels of most LPC species were significantly reduced between two- and threefold (Fig. 2c,d; Supporting Information Fig. S7). Interestingly, and in contrast to LPG species, FAC elicitation did not increase LPC levels compared to wounding within 20 min after the treatments; however, as mentioned earlier, it affected the pattern of accumulation of LPC-16:0 (Supporting Information Fig. S7a,b).

Similar to LPG and LPC, the amounts of MGMG and DGMG increased after wounding in WT plants peaking at 10 min and decreasing at 20 min (Fig. 2e,g; Supporting Information Fig. S8a,c,e). Interestingly, FAC elicitation changed the pattern of accumulation of these lysolipids with a slower, but more constant, increase in the levels of MGMG and DGMG compared to wounding (Fig. 2f,h; Supporting Information Fig. S8b,d,f). In ir-*gla1* leaves, the levels of both MGMG and DGMG were significantly reduced between two- and threefold (Fig. 2e–h; Supporting Information Fig. S8).

NaGLA1 mRNA levels are affected by *P. parasitica* (var. *nicotianae*) and *F. oxysporum* infection, and NaGLA1 affects early JA accumulation in roots and DVE in leaves

A recent study has shown that during *Pseudomonas syringae* infection, accumulation of OPDA and JA was not affected in the *dgl* and *dad1 Arabidopsis* mutants, indicating that these lipases are not involved in *P. syringae*-triggered jasmonate biosynthesis (Ellinger *et al.* 2010). *Nicotiana attenuata* does not accumulate JA upon *P. syringae* pv. *tomato* DC3000 infection (Rayapuram *et al.* 2008); however, infection with *P. parasitica* (var. *nicotianae*) induces the accumulation of this phytohormone (see below). Moreover, infection with this pathogen also induces the synthesis of DVEs in *N. attenuata* leaves (see below). We also analysed plants infected with the fungus *F. oxysporum*, which does not stimulate the formation of JA and DVEs in *N. attenuata*; however, it affects Na*GLA1* gene expression (see below). Infection with these two pathogens was

performed by gently pricking the hypocotyls of early rosette-stage plants (20 d old) with a needle containing spores of the pathogens (or not: control treatment) and by covering the infection zone with a moist cotton plug.

Firstly, for quantification of JA and DVEs, root and leaf samples were analysed at early time points after infection [4 and 24 h post-infection (HPI) and later 96 HPI (when necrotic lesions, in the case of *P. parasitica* var. *nicotianae*, or chlorosis, in the case of *F. oxysporum*, covered c. 10% of the leaf area]. In roots of untreated WT and ir-*gla1* plants, CA and CnA accumulated to similar levels (22 and 3.5 nmol g^{-1} FW on average, respectively), and infection by the two pathogens did not affect their levels (Supporting Information Fig. S9 and data not shown for 96 HPI). JA accumulation in roots of WT and ir-*gla1* plants was not affected significantly after infection compared to the control treatment; however, the latter (i.e. hypocotyl wounding) induced JA accumulation at 4 h in roots of WT plants, and the levels were curtailed by 50% in ir-*gla1* plants (Fig. 3a).

In leaves of untreated plants, CA and CnA accumulated on average to 1 and 0.15 nmol g^{-1} FW, respectively, and after 96 HPI the levels increased on average to 18 and 15 nmol g^{-1} FW after *P. parasitica* (var. *nicotianae*) infection in both WT and ir-*gla1* plants (Supporting Information Fig. S10). Interestingly, although the accumulation of these DVEs was similar at 96 HPI, *P. parasitica* (var. *nicotianae*) infection reduced by more than fourfold the accumulation of CA and CnA in leaves at 4 and 24 HPI in ir-*gla1* plants, whereas only at 24 HPI in WT plants (Fig. 3b). Thus, although this effect was detected in both genotypes, it was accelerated in ir-*gla1* plants, suggesting that NaGLA1 affects the early metabolism of DVE accumulation in leaves. In contrast, *F. oxysporum* infection did not affect the accumulation of CA and CnA in leaves (Fig. 3b; Supporting Information Fig. S10). After *P. parasitica* (var. *nicotianae*) infection, JA accumulation in leaves did not change significantly during the first 24 h and it was induced at 96 HPI; however, the levels were similar between plant types (Supporting Information Fig. S11). *Fusarium oxysporum* infection did not affect JA levels compared to the control treatment (Supporting Information Fig. S11).

Gene expression analysis showed that both pathogens strongly reduced the levels of NaGLA1 mRNA in roots after 24 and 96 HPI (Fig. 4a), whereas they strongly (more than 20-fold) up-regulated the levels in leaves (albeit with different kinetics; Fig. 4g). In roots and leaves of ir-*gla1* plants, the accumulation of Na*GLA1* mRNA remained suppressed (Fig. 4b,h).

Infection of *N. tabacum* plants with *P. parasitica* (var. *nicotianae*) is known to induce the expression of Nt*DES1* and Nt*LOX1*, two genes involved in DVE biosynthesis in this plant species (Fammartino *et al.* 2007, 2010). The expression of the two homologs of these genes in *N. attenuata* (Na*DES1*and Na*LOX1*) was also analysed in infected WT and ir-*gla1* plants. In contrast to Na*GLA1* mRNA, the levels of Na*DES1* mRNA were strongly (more than 50-fold) induced by both pathogens in roots of both WT

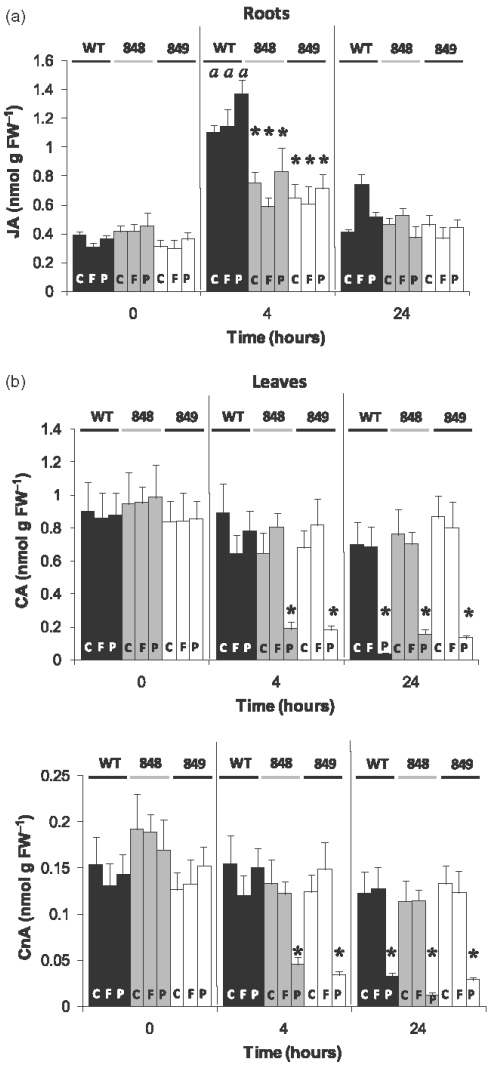

Figure 3. Quantification of jasmonic acid (JA) in roots and divinyl ether (DVE) in leaves of wild-type (WT) and ir-*gla1* plants within 24 h after pathogen infection. The hypocotyls of 20-day-old WT and ir-*gla1* (lines 848 and 849) seedlings were pricked with a needle (control treatment; c) or with a needle containing spores of *Fusarium oxysporum* (F) or *Phytophthora parasitica* (var. *nicotianae*) (P). After 4 and 24 h post-infection (HPI), roots and leaf samples were collected, and the levels of JA in roots (a) and colneleic acid (CA) and colnelenic acid (CnA) in leaves (b) were quantified by LC–MS/MS. $^{a}P < 0.05$, Student's *t*-test (treatment at 4 h in WT versus same treatment at 0 h in WT); $^{*}P < 0.05$, Student's *t*-test (treatment in ir-*gla1* versus treatment in WT at same time point); $n = 4$, bars denote ± SE.

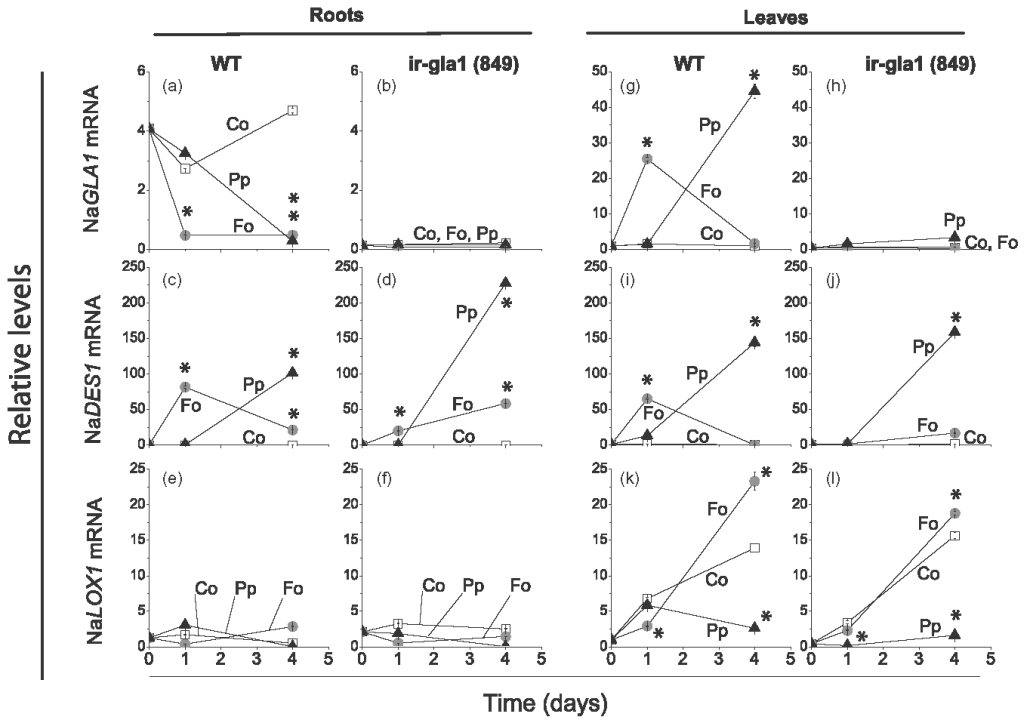

Figure 4. Expression levels of Na*GLA1*, Na*LOX1* and Na*DES1* mRNA in roots and leaves after pathogen infection. The hypocotyls of 20-day-old wild-type (WT) and ir-*gla1* (only line 849 is shown) seedlings were pricked with a sterile needle (control treatment; Co) or with a needle containing spores of *Fusarium oxysporum* (Fo) or *Phytophthora parasitica* (var. *nicotianae*; Pp). After 24 and 96 h post-infection (HPI), leaf and root samples were harvested, total RNA was extracted and used to quantify Na*GLA1*, Na*LOX1* and Na*DES1* transcript levels in roots or leaves by RT-qPCR (data are expressed as relative expression levels to a reference gene; see Materials and methods). $*P < 0.05$, Student's *t*-test (treatment versus control treatment at same time point), $n = 3$ (biological replicates), bars denote ± SE.

(Fig. 4c) and ir-*gla1* (Fig. 4d) plants albeit with different kinetics. In WT leaves, the levels of Na*DES1* mRNA were also strongly induced by infection with a similar pattern to that of Na*GLA1* mRNA (Fig. 4i); however, in ir-*gla1* leaves, the induction of Na*DES1* transcripts by *F. oxysporum* [but not *P. parasitica* (var. *nicotianae*)] was largely suppressed (Fig. 4j). The accumulation of Na*LOX1* transcripts in roots of infected plants showed no significant changes (Fig. 4e,f), but in leaves of WT and ir-*gla1* plants, it was induced by more than 15-fold by *F. oxysporum* and the control treatment (hypocotyl pricking) (Fig. 4k,l). *Phytophthora parasitica* (var. *nicotianae*) transiently induced this transcript's levels in WT leaves by fivefold (Fig. 4k), an effect largely suppressed in leaves of ir-*gla1* plants (Fig. 4l).

The time of lesion appearance in infected plants, the speed of lesion propagation (as quantified by the % of leaf area affected in time) and plant mortality (100% 1 week after infection) were similar between WT and ir-*gla1* plants (data not shown).

DISCUSSION

In *Arabidopsis*, the activation of JA biosynthesis depends on multiple lipases probably acting at different phases of the JA burst after wounding and *P. syringae* infection (Ellinger *et al.* 2010). Upon these treatments, *Arabidopsis* leaves accumulate OPDA to high levels either in free or acylated forms (Stelmach *et al.* 2001; Glauser *et al.* 2008b; Ellinger *et al.* 2010), and OPDA plays an important role as a signal molecule in this plant species (Stintzi *et al.* 2001; Taki *et al.* 2005). Lipases involved in JA biosynthesis have been therefore proposed to release not only trienoic fatty acids, but also OPDA from chloroplast membrane lipids (Ellinger *et al.* 2010). In contrast, other plant species, such as *N. attenuata*, accumulate low and transient levels of OPDA after wounding or simulated herbivory, and acylated forms of this oxylipin are not detectable (Kallenbach *et al.* 2010). These differences in lipid accumulation together with the number of lipases involved in the supply

of substrates for JA biosynthesis are probably responsible in part for the differences in the pattern of JA and JA–Ile accumulation between *Arabidopsis* and *N. attenuata* after wounding. In contrast to *Arabidopsis* where mutations of specific lipase genes affect JA accumulation only at specific periods after leaf wounding (Ellinger *et al.* 2010), the reduction in Na*GLA1* expression decreased jasmonate production in leaves throughout the duration of the JA burst (Fig. 1), suggesting that NaGLA1 supplies trienoic fatty acids during the entire duration of this process.

The production of jasmonates in ir-*gla1* plants was however not completely curtailed, and these plants accumulated 35–50% of WT levels of JA and JA–Ile in leaves after wounding and FAC elicitation. These remaining levels of jasmonates indicated that either residual NaGLA1 activity in ir-*gla1* plants was sufficient to partially supply trienoic acids to the JA biosynthesis pathway or that, similar to *Arabidopsis*, additional lipases are involved in this process. Similar conclusions can be drawn for the accumulation of JA in roots after hypocotyl wounding (Fig. 3a). WT levels of jasmonate accumulation at different stages of flower development in ir-*gla1* plants demonstrated that NaGLA1 is not essential for the developmental control of JA formation in this organ, and similarly, the WT levels of leaf C_6 volatile production in these plants indicated that this lipase is not essential to supply the HPL pathway. The accelerated reduction of DVE levels in leaves of ir-*gla1* plants at early stages of infection with *P. parasitica* (var. *nicotianae*) revealed that NaGLA1 affects (by still unknown mechanisms) early DVE metabolism in *N. attenuata* (Fig. 5).

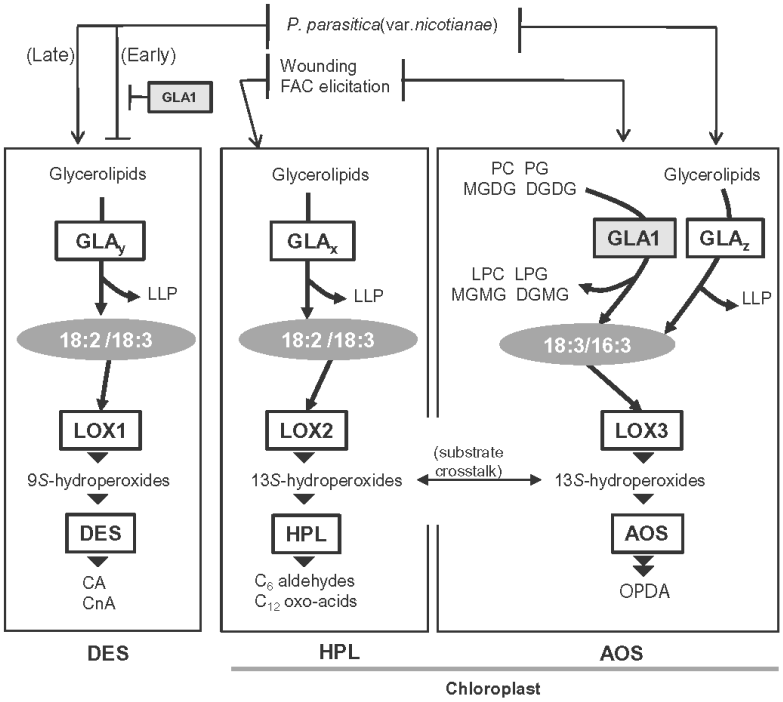

Figure 5. Schematic representation of the proposed lipase-mediated regulation of the allene oxide synthase (AOS), hydroperoxide lyase (HPL) and divinyl ether (DVE) synthase (DES) pathways in *Nicotiana attenuata* leaves. Upon wounding and fatty acid–amino acid conjugate (FAC) elicitation, NaGLA1 gets activated to release trienoic fatty acids (18:3/16:3) from different glycerolipid classes [phosphatidylcholine (PC), phosphatidylglycerol (PG), monogalactosyl diglyceride (MGDG), digalactosyl diglyceride (DGDG)] in the plastid and envelope, and to generate the lysolipids (LLPs): lyso-PC (LPC), lyso-PG (LPG), monogalactosyl monoglyceride (MGMG) and digalactosyl monoglyceride (DGMG). This NaGLA1-generated pool of 18:3/16:3 is used for jasmonic acid (JA) biosynthesis by the AOS pathway. Infection of plants by *Phytophthora parasitica* (var. *nicotianae*) induces JA formation in leaves via activation of an unknown glycerolipase (GLA_z). Formation of C_6 aldehydes and C_{12} oxo-acids by the HPL pathway, and colneleic acid (CA) and colnelenic acid (CnA) during advanced-stage infection by the DES pathway depends on the activation of additional glycerolipases (GLA_x and $_y$). *Phytophthora parasitica* (var. *nicotianae*) suppresses DVE accumulation during the early stage of infection, a process which is negatively affected by NaGLA1. C_{18} 13S-hydroperoxides may be exchangeable between the AOS and HPL pathways (substrate crosstalk; see text for references).

NaGLA1 and FAC perception affect the accumulation of different lysolipid classes after wounding

The accumulation of most of the lysolipids analysed after wounding and FAC elicitation was significantly decreased by two- to threefold in ir-*gla1* compared to WT plants, indicating that NaGLA1 is a major determinant of the production of these molecules after these treatments. The strict dependency of the formation of these lysolipids on NaGLA1 indicated that this formation was not a technical artefact brought about by the unspecific hydrolysis of membrane lipids after tissue disruption by wounding. Moreover, this conclusion was also substantiated by the specific changes induced by FAC elicitation on the pattern of lysolipid accumulation. Together, the results suggested that the 18:3 supplied by NaGLA1 for JA biosynthesis originates from different pools (lipid classes), and it is therefore not restricted to a specific lipid class in *N. attenuata* leaves. These results were in agreement with the *in vitro* activity of NaGLA1 towards different lipid substrates (Kallenbach *et al.* 2010).

The transient accumulation of most lysolipids was consistent with the rapid, transient and sequential accumulation of 13*S*-OOH-18:3 and OPDA after wounding and FAC elicitation (Kallenbach *et al.* 2010), and it was therefore also consistent with the rapid activation of NaGLA1 to provide 18:3 for JA biosynthesis. In the case of LPG, FAC elicitation induced an increased peak of accumulation at 1 and 10 min compared to wounding, whereas in the case of lyso-galactolipids, FAC elicitation promoted a slower, but more sustained, accumulation of MGMG and DGMG than wounding (Fig. 2; Supporting Information Figs S6–S8). The effect of FAC elicitation was, however, not so evident in the accumulation of LPC molecular species with the exception of LPC-16:0, whose levels remained high and did not decline after 10 min of the treatment (Supporting Information Fig. S7b). Together, these results revealed that the perception of FACs by leaves influences the activity of NaGLA1, which is reflected in the differential accumulation of lysolipids.

In vitro, NaGLA1 preferentially removed fatty acids from the *sn-1* position of PC. The formation of LPG species containing 16:0 and 16:1 indicated that *sn-1* lysolipids were formed from C_{18}/C_{16} (*sn-1/sn-2*) PG. Detection of LPC-16:0 species suggested however that *sn-2* lipase activity was also activated during wounding and FAC elicitation, removing C_{18} fatty acids from C_{16}/C_{18} (*sn-1/sn-2*) PC. Because the accumulation of these molecules was strongly dependent on NaGLA1 expression (Supporting Information Fig. S9), the results suggested that *in vivo* NaGLA1 also presents *sn-2* lipase activity. Alternatively, however, the possibility that the activity of other *sn-2* acylhydrolases is affected indirectly by reduced NaGLA1 activity cannot be ruled out.

The localization of plastidial enzymes involved in JA biosynthesis has been reported in different chloroplast compartments depending on the enzyme and the plant species. For example, AtLOX2 in *Arabidopsis* has been identified as an abundant protein in the stroma of the chloroplast (Peltier *et al.* 2006), while AtAOS has been detected in plastoglobules (Ytterberg, Peltier & van Wijk 2006), the inner chloroplast envelope (Froehlich *et al.* 2003) and thylakoid membranes (Peltier *et al.* 2004). In potato leaves (*Solanum tuberosum*), StLOX-H3 has been localized in both the stroma and thylakoid membranes, while StAOS localizes preferentially in thylakoid membranes (Farmaki *et al.* 2007). In maize (*Z. mays*), ZmAOC is a soluble choloroplast enzyme (Ziegler *et al.* 1997), and in potato StAOC is weakly associated to thylakoids and also present in the stroma (Farmaki *et al.* 2007). PC is a major constituent of the chloroplast envelope, but it is excluded from the plastid membrane and inner membrane systems (Browse *et al.* 1986). NaGLA1 localizes to the chloroplast (Kallenbach *et al.* 2010), and the NaGLA1-dependent formation of LPC suggested that this enzyme is either localized or has access to the chloroplast envelope, thereby utilizing PC, PG and galactolipids as substrates.

NaGLA1 participates in the activation of NaDES1 and NaLOX1 gene expression during *P. parasitica* (var. *nicotianae*) and *F. oxysporum* infection

Phytophthora parasitica (var. *nicotianae*) and *F. oxysporum* infection had a strong and opposite effect on Na*GLA1* expression in roots and leaves (Fig. 4), suggesting that different mechanisms for the regulation of Na*GLA1* expression are activated in these tissues. These strong effects on Na*GLA1* mRNA levels were, however, not reflected in changes in JA accumulation in roots or leaves after infection, suggesting that NaGLA1 may be playing additional roles during this process. One of these potential additional roles was the previously mentioned metabolism of DVE in leaves during the early stages of infection by *P. parasitica* (var. *nicotianae*). A second process involved the role of Na*GLA1* in the differential induction of Na*LOX1* and Na*DES1* mRNA levels after infection with *F. oxysporum* and *P. parasitica* (var. *nicotianae*). Although the underlying mechanisms are at present unknown, it was interesting to note that NaGLA1 was important to generate a signal induced by *F. oxysporum*, and targeting activation of Na*DES1* expression in both roots and leaves (Fig. 4c,d,i,j), whereas NaGLA1 was important for the induction of Na*LOX1* expression after *P. parasitica* (var. *nicotianae*) in leaves (Fig. 4k,l). Because wounding of the hypocotyls (control treatment) also induced Na*LOX1* transcript levels in leaves and this induction was unaffected in ir-*gla1* plants (Fig. 4k,l), the results indicated that the expression of the Na*LOX1* gene is induced by a signal induced by *P. parasitica* (var. *nicotianae*) and dependent on NaGLA1 activity, but independent of jasmonate accumulation.

Substrate crosstalk between the AOS and HPL pathways

A previous study has disclosed a metabolic crosstalk (exchange of substrates) between the HPL and AOS pathways in *N. attenuata*; plants with reduced expression of NaAOS emit higher amounts of GLVs and plants with reduced expression of NaHPL produce more JA after OS elicitation compared to WT plants (Halitschke *et al.* 2004). *Nicotiana attenuata* plants with reduced Na*LOX2* (a 13-LOX specific for GLV biosynthesis) expression do not produce more JA after OS elicitation than WT plants (Allmann *et al.* 2010), and because NaGLA1 does not participate in the supply of substrates for GLV biosynthesis, the results revealed that the metabolic crosstalk between the AOS and HPL pathways probably occurs at the level of 13-hydroperoxide accumulation (Halitschke *et al.* 2004) (Fig. 5).

CONCLUSIONS

The understanding of the mechanisms that activate NaGLA1 at the biochemical level may prove the key to understanding how JA biosynthesis is triggered after wounding, insect attack and pathogen infection. Moreover, the identification of lipases (probably belonging to the PLA_1-I family) involved in the supply of fatty acids to other oxylipin biosynthesis pathways (Fig. 5) would be important to understand how these pathways are biochemically activated. Finally, the elucidation of alternative functions of NaGLA1 during pathogen infection would also reveal new aspects of NaGLA1-mediated regulatory mechanisms.

ACKNOWLEDGMENT

The Max Planck Society is acknowledged for funding.

REFERENCES

Allmann S., Halitschke R., Schuurink R. & Baldwin I. (2010) Oxylipin channelling in *Nicotiana attenuata*: lipoxygenase 2 supplies substrates for green leaf volatile production. *Plant, Cell & Environment* **33,** 2028–2040.

Bonaventure G., Gfeller A., Proebsting W.M., Hortensteiner S., Chetelat A., Martinoia E. & Farmer E.E. (2007) A gain-of-function allele of TPC1 activates oxylipin biogenesis after leaf wounding in *Arabidopsis*. *The Plant Journal* **49,** 889–898.

Böttcher C. & Weiler E.W. (2007) Cyclo-oxylipin-galactolipids in plants: occurrence and dynamics. *Planta* **226,** 629–637.

Browse J., Warwick N., Somerville C.R. & Slack C.R. (1986) Fluxes through the prokaryotic and eukaryotic pathways of lipid synthesis in the '16:3' plant *Arabidopsis thaliana*. *Biochemical Journal* **235,** 25–31.

Bubner B., Gase K., Berger B., Link D. & Baldwin I.T. (2006) Occurrence of tetraploidy in *Nicotiana attenuata* plants after *Agrobacterium*-mediated transformation is genotype specific but independent of polysomaty of explant tissue. *Plant Cell Reports* **25,** 668–675.

Creelman R.A. & Mullet J.E. (1997) Biosynthesis and action of jasmonates in plants. *Annual Reviews in Plant Physiology and Plant Molecular Biology* **48,** 355–381.

Creelman R.A., Tierney M.L. & Mullet J.E. (1992) Jasmonic acid/methyl jasmonate accumulate in wounded soybean hypocotyls and modulate wound gene expression. *Proceedings of the National Academy of Sciences of the United States of America* **89,** 4938–4941.

Croft K., Juttner F. & Slusarenko A.J. (1993) Volatile products of the lipoxygenase pathway evolved from *Phaseolus vulgaris* (L.) leaves inoculated with *Pseudomonas syringae* pv *phaseolicola*. *Plant Physiology* **101,** 13–24.

Devoto A., Ellis C., Magusin A., Chang H.S., Chilcott C., Zhu T. & Turner J.G. (2005) Expression profiling reveals COI1 to be a key regulator of genes involved in wound- and methyl jasmonate-induced secondary metabolism, defence, and hormone interactions. *Plant Molecular Biology* **58,** 497–513.

Ellinger D., Stingl N., Kubigsteltig I.I., Bals T., Juenger M., Pollmann S., Berger S., Schuenemann D. & Mueller M.J. (2010) DONGLE and DEFECTIVE IN ANTHER DEHISCENCE1 lipases are not essential for wound- and pathogen-induced jasmonate biosynthesis: redundant lipases contribute to jasmonate formation. *Plant Physiology* **153,** 114–127.

Fammartino A., Cardinale F., Gobel C., Mene-Saffrane L., Fournier J., Feussner I. & Esquerre-Tugaye M.T. (2007) Characterization of a divinyl ether biosynthetic pathway specifically associated with pathogenesis in tobacco. *Plant Physiology* **143,** 378–388.

Fammartino A., Verdaguer B., Fournier J., Tamietti G., Carbonne F., Esquerre-Tugaye M.T. & Cardinale F. (2010) Coordinated transcriptional regulation of the divinyl ether biosynthetic genes in tobacco by signal molecules related to defense. *Plant Physiology and Biochemistry* **48,** 225–231.

Farmaki T., Sanmartin M., Jimenez P., Paneque M., Sanz C., Vancanneyt G., Leon J. & Sanchez-Serrano J.J. (2007) Differential distribution of the lipoxygenase pathway enzymes within potato chloroplasts. *Journal of Experimental Botany* **58,** 555–568.

Froehlich J.E., Wilkerson C.G., Ray W.K., McAndrew R.S., Osteryoung K.W., Gage D.A. & Phinney B.S. (2003) Proteomic study of the *Arabidopsis thaliana* chloroplastic envelope membrane utilizing alternatives to traditional two-dimensional electrophoresis. *Journal of Proteome Research* **2,** 413–425.

Galliard T. & Phillips D.R. (1972) The enzymic conversion of linoleic acid into 9-(nona-1',3'-dienoxy)non-8-enoic acid, a novel unsaturated ether derivative isolated from homogenates of *Solanum tuberosum* tubers. *Biochemical Journal* **129,** 743–753.

Gilardoni P., Schuck S., Jüngling R., Rotter B., Baldwin I. & Bonaventure G. (2010) SuperSAGE analysis of the *Nicotiana attenuata* transcriptome after fatty acid–amino acid elicitation (FAC): identification of early mediators of insect responses. *BMC Plant Biology* **10,** 66.

Glauser G., Grata E., Dubugnon L., Rudaz S., Farmer E.E. & Wolfender J.L. (2008a) Spatial and temporal dynamics of jasmonate synthesis and accumulation in *Arabidopsis* in response to wounding. *Journal of Biological Chemistry* **283,** 16400–16407.

Glauser G., Grata E., Rudaz S. & Wolfender J.L. (2008b) High-resolution profiling of oxylipin-containing galactolipids in *Arabidopsis* extracts by ultra-performance liquid chromatography/time-of-flight mass spectrometry. *Rapid Communications in Mass Spectrometry* **22,** 3154–3160.

Gobel C., Feussner I., Schmidt A., Scheel D., Sanchez-Serrano J., Hamberg M. & Rosahl S. (2001) Oxylipin profiling reveals the preferential stimulation of the 9-lipoxygenase pathway in elicitor-treated potato cells. *Journal of Biological Chemistry* **276,** 6267–6273.

Gobel C., Feussner I., Hamberg M. & Rosahl S. (2002) Oxylipin profiling in pathogen-infected potato leaves. *Biochimica et Biophysica Acta* **1584,** 55–64.

Grechkin A.N. & Hamberg M. (1996) Divinyl ether synthase from garlic (*Allium sativum* L.) bulbs: sub-cellular localization and substrate regio- and stereospecificity. *FEBS Letters* **388,** 112–114.

Halitschke R., Ziegler J., Keinanen M. & Baldwin I.T. (2004) Silencing of hydroperoxide lyase and allene oxide synthase reveals substrate and defense signaling crosstalk in *Nicotiana attenuata*. *The Plant Journal* **40,** 35–46.

Hyun Y., Choi S., Hwang H.J., *et al.* (2008) Cooperation and functional diversification of two closely related galactolipase genes for jasmonate biosynthesis. *Developmental Cell* **14,** 183–192.

Ishiguro S., Kawai-Oda A., Ueda J., Nishida I. & Okada K. (2001) The *DEFECTIVE IN ANTHER DEHISCENCE* gene encodes a novel phospholipase A1 catalyzing the initial step of jasmonic acid biosynthesis, which synchronizes pollen maturation, anther dehiscence, and flower opening in *Arabidopsis*. *The Plant Cell* **13,** 2191–2209.

Kallenbach M., Alagna F., Baldwin I.T. & Bonaventure G. (2010) *Nicotiana attenuata* SIPK, WIPK, NPR1, and fatty acid–amino acid conjugates participate in the induction of jasmonic acid biosynthesis by affecting early enzymatic steps in the pathway. *Plant Physiology* **152,** 96–106.

Körner E., von Dahl C., Bonaventure G. & Baldwin I.T. (2009) Pectin methylesterase NaPME1 contributes to the emission of methanol during insect herbivory and to the elicitation of defence responses in *Nicotiana attenuata*. *Journal of Experimental Botany* **60,** 2631–2640.

Krügel T., Lim M., Gase K., Halitschke R. & Baldwin I.T. (2002) *Agrobacterium*-mediated transformation of *Nicotiana attenuata*, a model ecological expression system. *Chemoecology* **12,** 177–183.

McCloud E.S. & Baldwin I.T. (1997) Herbivory and caterpillar regurgitants amplify the wound-induced increases in jasmonic acid but not nicotine in *Nicotiana sylvestris*. *Planta* **203,** 430–435.

Murakami N., Imamura H., Morimoto T., Ueda T., Nagai S., Sakakibara J. & Yamada N. (1991) Selective preparation of sn-1 and sn-2 lysogalactolipids by enzymatic hydrolysis using lipase (from *Rhizopus arrhizus*). *Tetrahedron Letters* **32,** 1331–1334.

Peltier J.B., Ytterberg A.J., Sun Q. & van Wijk K.J. (2004) New functions of the thylakoid membrane proteome of *Arabidopsis thaliana* revealed by a simple, fast, and versatile fractionation strategy. *Journal of Biological Chemistry* **279,** 49367–49383.

Peltier J.B., Cai Y., Sun Q., Zabrouskov V., Giacomelli L., Rudella A., Ytterberg A.J., Rutschow H. & van Wijk K.J. (2006) The oligomeric stromal proteome of *Arabidopsis thaliana* chloroplasts. *Molecular & Cellular Proteomics* **5,** 114–133.

Prost I., Dhondt S., Rothe G., *et al.* (2005) Evaluation of the antimicrobial activities of plant oxylipins supports their involvement in defense against pathogens. *Plant Physiology* **139,** 1902–1913.

Rayapuram C., Wu J., Haas C. & Baldwin I.T. (2008) PR-13/thionin but not PR-1 mediates bacterial resistance in *Nicotiana attenuata* in nature, and neither influences herbivore resistance. *Molecular Plant–Microbe Interactions* **21,** 988–1000.

Reymond P., Weber H., Damond M. & Farmer E.E. (2000) Differential gene expression in response to mechanical wounding and insect feeding in *Arabidopsis*. *The Plant Cell* **12,** 707–719.

Ryu S.B. (2004) Phospholipid-derived signaling mediated by phospholipase A in plants. *Trends in Plant Science* **9,** 229–235.

Sasaki Y., Asamizu E., Shibata D., *et al.* (2001) Monitoring of methyl jasmonate-responsive genes in *Arabidopsis* by cDNA macroarray: self-activation of jasmonic acid biosynthesis and crosstalk with other phytohormone signaling pathways. *DNA Research* **8,** 153–161.

Schittko U., Preston C.A. & Baldwin I.T. (2000) Eating the evidence? *Manduca sexta* larvae can not disrupt specific jasmonate induction in *Nicotiana attenuata* by rapid consumption. *Planta* **210,** 343–346.

Schmelz E.A., Engelberth J., Alborn H.T., Tumlinson J.H. & Teal P.E.A. (2009) Phytohormone-based activity mapping of insect herbivore-produced elicitors. *Proceedings of the National Academy of Sciences of the United States of America* **106,** 653–657.

Stelmach B., Müller A., Hennig P., Gebhardt S., Schubert-Zsilavecz M. & Weiler E. (2001) A novel class of oxylipins, sn1-*O*-(12-oxophytodienoyl)-sn2-*O*-(hexadecatrienoyl)-monogalactosyl diglyceride, from *Arabidopsis thaliana*. *Journal of Biological Chemistry* **276,** 12832–12838.

Stintzi A. & Browse J. (2000) The *Arabidopsis* male-sterile mutant, opr3, lacks the 12-oxophytodienoic acid reductase required for jasmonate synthesis. *Proceedings of the National Academy of Sciences of the United States of America* **97,** 10625–10630.

Stintzi A., Weber H., Reymond P., Browse J. & Farmer E.E. (2001) Plant defense in the absence of jasmonic acid: the role of cyclopentenones. *Proceedings of the National Academy of Sciences of the United States of America* **98,** 12837–12842.

Stowe M.K., Turlings T.C., Loughrin J.H., Lewis W.J. & Tumlinson J.H. (1995) The chemistry of eavesdropping, alarm, and deceit. *Proceedings of the National Academy of Sciences of the United States of America* **92,** 23–28.

Suza W.P. & Staswick P.E. (2008) The role of JAR1 in jasmonoyl-L: -isoleucine production during *Arabidopsis* wound response. *Planta* **227,** 1221–1232.

Suza W.P., Rowe M.L., Hamberg M. & Staswick P.E. (2010) A tomato enzyme synthesizes (+)-7-iso-jasmonoyl-L-isoleucine in wounded leaves. *Planta* **231,** 717–728.

Taki N., Sasaki-Sekimoto Y., Obayashi T., *et al.* (2005) 12-Oxo-phytodienoic acid triggers expression of a distinct set of genes and plays a role in wound-induced gene expression in *Arabidopsis*. *Plant Physiology* **139,** 1268–1283.

Vandoorn A., Kallenbach M., Borquez A.A., Baldwin I.T. & Bonaventure G. (2010) Rapid modification of the insect elicitor *N*-linolenoyl-glutamate via a lipoxygenase-mediated mechanism on *Nicotiana attenuata* leaves. *BMC Plant Biology* **10,** 164.

VanDoorn A., Bonaventure G., Schmidt D. & Baldwin I.T. (2011) Regulation of jasmonate metabolism and activation of systemic signaling in *Solanum nigrum*: COI1 and JAR4 play overlapping yet distinct roles. *New Phytologist* **190,** 640–652.

Vick B.A. & Zimmerman D.C. (1983) The biosynthesis of jasmonic acid: a physiological role for plant lipoxygenase. *Biochemical and Biophysical Research Communications* **111,** 470–477.

Vick B.A. & Zimmerman D.C. (1984) Biosynthesis of jasmonic acid by several plant species. *Plant Physiology* **75,** 458–461.

Wang L., Allmann S., Wu J. & Baldwin I.T. (2008) Comparisons of LIPOXYGENASE3- and JASMONATE-RESISTANT4/6-silenced plants reveal that jasmonic acid and jasmonic acid–amino acid conjugates play different roles in herbivore resistance of *Nicotiana attenuata*. *Plant Physiology* **146,** 904–915.

Weber H., Vick B.A. & Farmer E.E. (1997) Dinor-oxo-phytodienoic acid: a new hexadecanoid signal in the jasmonate family. *Proceedings of the National Academy of Sciences of the United States of America* **94,** 10473–10478.

Weber H., Chetelat A., Caldelari D. & Farmer E.E. (1999) Divinyl ether fatty acid synthesis in late blight-diseased potato leaves. *The Plant Cell* **11,** 485–493.

Yang H.R., Tang K., Liu H.T., Pan Q.H. & Huang W.D. (2009) Jasmonic acid is induced in a biphasic manner in response of pea seedlings to wounding. *Journal of Integrative Plant Biology* **51,** 562–573.

Yang W., Devaiah P., Pan X., Isaac G., Welti R. & Wang X. (2007) AtPLA1 is an acyl hydrolase involved in basal jasmonic acid production and *Arabidopsis* resistance to *Botrytis cinerea*. *Journal of Biological Chemistry* **282,** 18116–18128.

Ytterberg A.J., Peltier J.B. & van Wijk K.J. (2006) Protein profiling of plastoglobules in chloroplasts and chromoplasts. A surprising site for differential accumulation of metabolic enzymes. *Plant Physiology* **140,** 984–997.

Ziegler J., Hamberg M., Miersch O. & Parthier B. (1997) Purification and characterization of allene oxide cyclase from dry corn seeds. *Plant Physiology* **114,** 565–573.

Received 17 February 2011; received in revised form 30 March 2011; accepted for publication 9 April 2011

SUPPORTING INFORMATION

Additional Supporting Information may be found in the online version of this article:

Figure S1. Southern blot analysis of ir-*gla1* plants.
Figure S2. Growth and morphology of ir-*gla1* plants.
Figure S3. Accumulation of jasmonic acid (JA) and JA–isoleucine (Ile) at different stages of flower development in wild-type (WT) and ir-*gla1* plants.
Figure S4. Analysis of green leaf volatiles (GLVs) in wild-type (WT) and ir-*gla1* plants after wounding.
Figure S5. Accumulation of jasmonic acid (JA), JA–isoleucine (Ile) and (9*S*,13*S*)-12-oxo-phytodienoic acid (OPDA) in leaves of wild-type (WT) and ir-*gla1* plants within 20 min after wounding and fatty acid–amino acid conjugate (FAC) elicitation.
Figure S6. Lyso-PG (LPG) levels in leaves of wild-type (WT) and ir-*gla1* plants after wounding and fatty acid–amino acid conjugate (FAC) elicitation.
Figure S7. Lyso-PC (LPC) levels in leaves of wild-type (WT) and ir-*gla1* plants after wounding and fatty acid–amino acid conjugate (FAC) elicitation.
Figure S8. Monogalactosyl monoglyceride (MGMG) and digalactosyl monoglyceride (DGMG) levels in leaves of wild-type (WT) and ir-*gla1* plants after wounding and fatty acid–amino acid conjugate (FAC) elicitation.
Figure S9. Accumulation of colneleic acid (CA) and colnelenic acid (CnA) in roots of wild-type (WT) and ir-*gla1* plants after 4 and 24 h of pathogen infection.
Figure S10. Accumulation of colneleic acid (CA) and colnelenic acid (CnA) in leaves of wild-type (WT) and ir-*gla1* plants after 96 h of pathogen infection.
Figure S11. Accumulation of jasmonic acid (JA) in leaves of wild-type (WT) and ir-*gla1* plants after pathogen infection.
Table S1. Primer sequences.
Table S2. Parameters used for the analysis of phytohormones by LC–MS/MS.
Table S3. Parameters used for the analysis of lysolipids in leaves by LC–MS/MS.
Table S4. Parameters used for the analysis of divinyl ethers (DVEs) in roots and leaves by LC–MS/MS.

Please note: Wiley-Blackwell are not responsible for the content or functionality of any supporting materials supplied by the authors. Any queries (other than missing material) should be directed to the corresponding author for the article.

Table SI. Primer sequences

Primers for RT-qPCR		
Gene name	Forward	Reverse
NaLOX1	AATACAAGTCGGACCGCATC	CACCTTGGTCAGGATCACCT
NaGLA1	AGTAGCAGATGATGTTAGTACATGTA	ACATGTGAATATGCCCATGGCATACT
NaDES1	CCTACTCTACACGCTCGACTTGCT	ATCCAACGACGAACTGCCCTTTCT
Primers for the construction of the pSOL8PLA1 vector		
LIP13-32	GCGGCGCTGCAGACAGGACATAGTCTTGGTGC	
LIP14-32	GCGGCGGTCGACGCCCATGGCATACTATTGTC	
LIP15-32	GCGGCGGAGCTCACAGGACATAGTCTTGGTGC	
LIP16-32	GCGGCGCTCGAGGCCCATGGCATACTATTGTC	

Table SII. Parameters used for the analysis of phytohormones by LC-MS/MS

Phytohormone	Capillary E (V)	M1 (m/z)	M2 (m/z)	Collision E (V)	Rt (min)
SA	35	137	93	15	6
$^{2}H_4$-SA	35	141	97	15	6
JA	35	209	59	12	5.9
$^{2}H_2$-JA	35	213	59	12	6.6
ABA	35	263	153	9	5.6
$^{2}H_6$-ABA	35	269	159	9	5.6
JA-Ile	45	322	130	19	7.3
JA-$^{13}C_6$-Ile	45	328	136	19	7.3

Additional parameters
Collision Gas: 2.1mTorr
API Drying Gas : 19 psi, 300°C
API Nebulizing Gas : 60 psi
Needle : 4500 V
Shield : 600V
Detector : 1800V

Table SIII. Parameters used for the analysis of lysolipids in leaves by LC-MS/MS

Lysolipid	Ion detected	FA composition	M1 (m/z)	M2 (m/z)	Collision E (V)	Capillary CID	Column
LPC	[M+H]+	16:0	496	184(1)	10	35	Gemini NX
LPC	[M+H]+	17:0	510	184(1)	10	35	Gemini NX
LPC	[M+H]+	18:0	524	184(1)	10	35	Gemini NX
LPC	[M+H]+	18:1	522	184(1)	10	35	Gemini NX
LPC	[M+H]+	18:2	520	184(1)	10	35	Gemini NX
LPC	[M+H]+	18:3	518	184(1)	10	35	Gemini NX
MGMG	[M+Na]+	16:0	515	185(2)	26	45	Gemini NX
MGMG	[M+Na]+	18:0	543	185(2)	26	45	Gemini NX
MGMG	[M+Na]+	16:3	509	185(2)	26	45	Gemini NX
MGMG	[M+Na]+	18:3	537	185(2)	26	45	Gemini NX
DGMG	[M+Na]+	16:0	678	515(3)	40	35	Gemini NX
DGMG	[M+Na]+	18:0	705	543(3)	40	35	Gemini NX
DGMG	[M+Na]+	16:3	672	509(3)	40	35	Gemini NX
DGMG	[M+Na]+	18:3	699	537(3)	40	35	Gemini NX
LPG	[M-H]-	16:0	483	255(4)	24	35	precolumn C18
LPG	[M-H]-	16:1	481	253(4)	24	35	precolumn C18
LPG	[M-H]-	18:0	511	283(4)	24	35	precolumn C18
LPG	[M-H]-	18:1	509	281(4)	24	35	precolumn C18
LPG	[M-H]-	18:2	507	279(4)	24	35	precolumn C18
LPG	[M-H]-	18:3	505	277(4)	24	35	precolumn C18
LPG	[M-H]-	17:1	495	267(4)	24	35	precolumn C18

(1) Ion detected corresponds to head group rearrangement (Al-Saad et al., 2003)
(2) Ion detected corresponds to the released galactose moiety (Kim et al., 1999)
(3) Ion detected corresponds to the loss of one galactose moiety (this study)
(4) Ion detected corresponds to the released free fatty acid (this study)

References

Al-Saad KA, Zabrouskov V, Siems WF, Knowles NR, Hannan RM, Hill HH, Jr. (2003) Matrix-assisted laser desorption/ionization time-of-flight mass spectrometry of lipids: ionization and prompt fragmentation patterns. Rapid Commun Mass Spectrom 17: 87-96

Kim YH, Choi JS, Hong J, Yoo JS, Kim MS (1999) Identification of acylated glycoglycerolipids from a cyanobacterium, Synechocystis sp., by tandem mass spectrometry. Lipids 34: 847-853

Table SIV. Parameters used for the analysis of DVEs in roots and leaves by LC-MS/MS

DVE	Ion detected	M1 (m/z)	M2 (m/z)	Collision E (V)	Capillary CID
Etheroleic acid (EA)	[M+H]-	293	210	12.5	35
Etherolenic acid (EnA)	[M+H]-	291	210	12.5	35
Colneleic acid (CA)	[M+H]-	293	170	12.5	35
Colnelenic acid (CnA)	[M+H]-	291	170	12.5	35

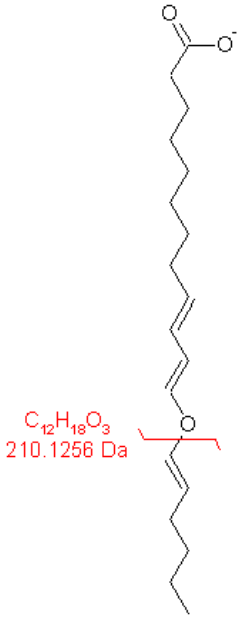

Formula Weight = 293.4216086

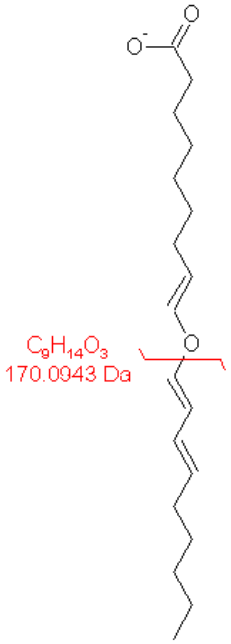

Formula Weight = 293.4216086

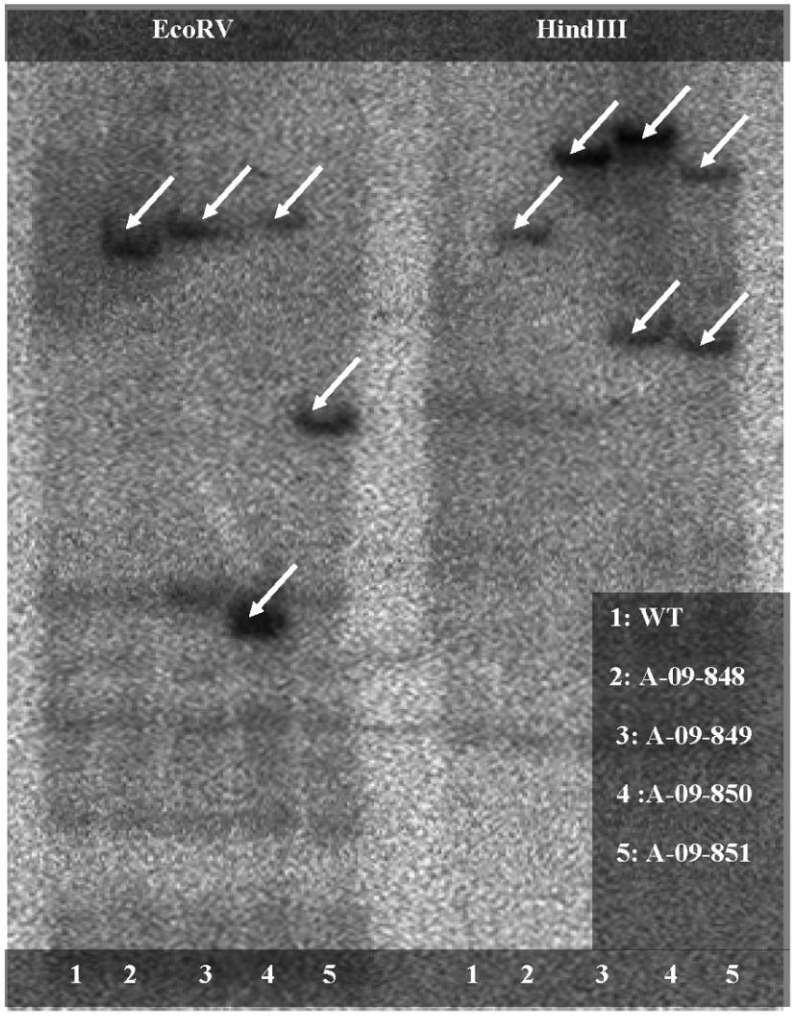

Figure S1. Southern blot analysis of ir-*gla1* plants
Genomic DNA from four independent ir-*gla1* lines (A-09-848, A-09-849, A-09-850, A-09-851) and WT was digested with either EcoRV or HindIII and resolved by agarose gel electrophoresis. A ^{32}P-labeled PCR product from the hygromycin resistance gene (*nptII*) was used as a probe. The white arrows point to individual T-DNA insertions. Numbers refer to WT and independent ir-gla1 lines (see inset).

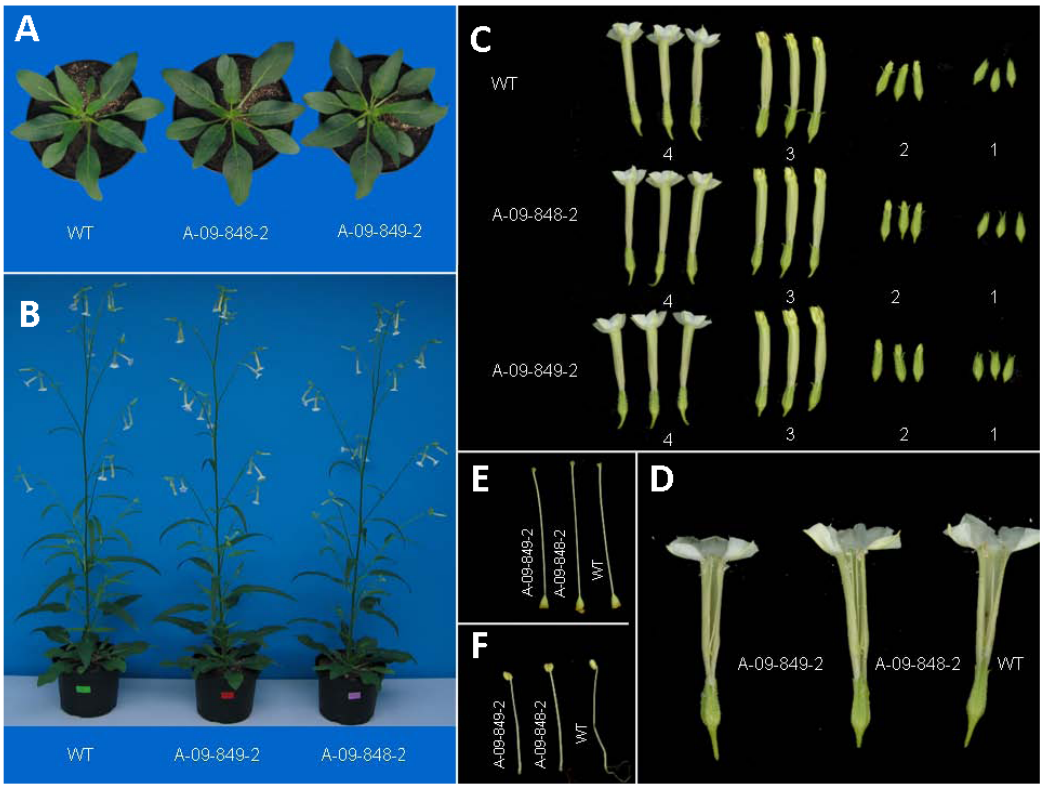

Figure S2: Growth and morphology of ir-*gla1* plants
(**A**) Rossette stage WT and ir-*gla1* (lines A-09-848-2 (848) and A-09-849-2 (849)) *N. attenuata* plants. (**B**) Flowering stage WT and ir-gla1 plants. (**C**) Flowers of WT and ir-gla1 plants at different stages of development (1: closed bud; 2: opened bud; 3: fully elongated corolla; 4: opened corolla). (**D,E,F**) Detail of an opened corolla flower showing pistils (**E**) and stamens (**F**).

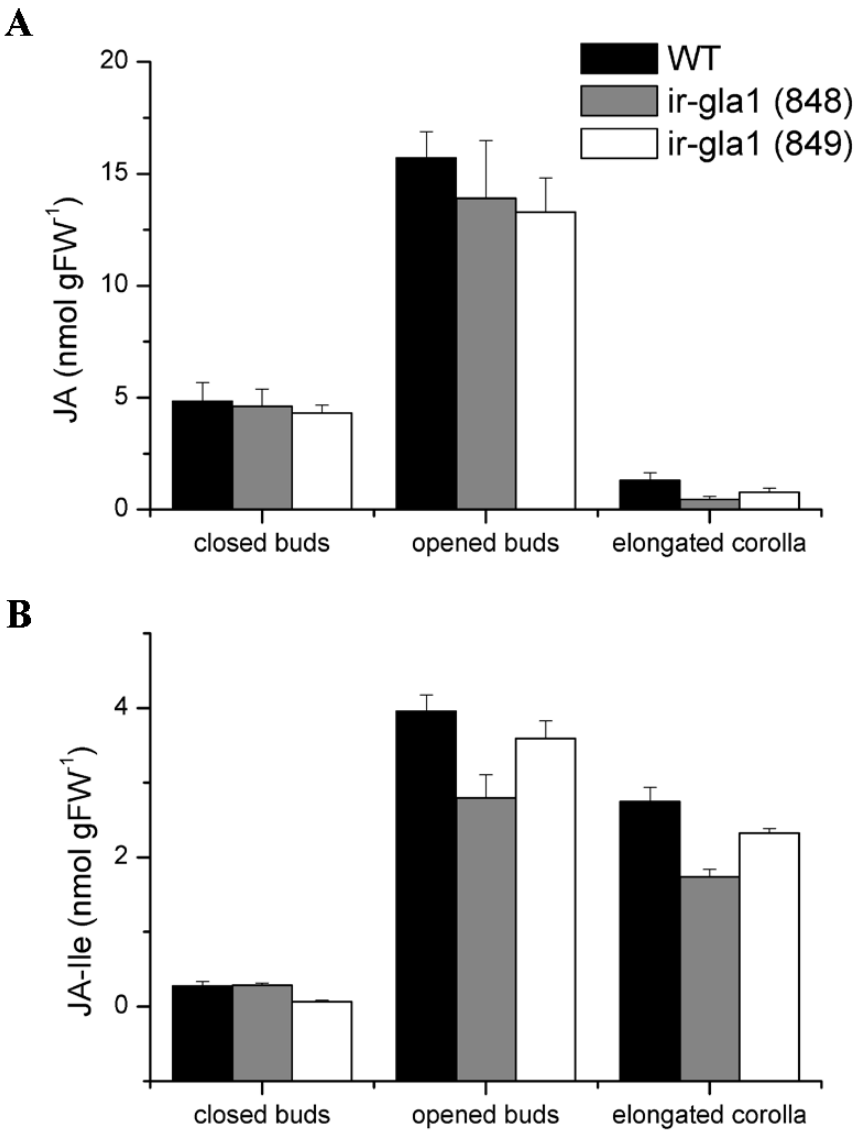

Figure S3. Accumulation of JA and JA-Ile at different stages of flower development in WT and ir-*gla1* plants

Developing flowers from WT and ir-*gla1* (lines 848 and 849) plants were harvested at different stages and JA (**A**) nd JA-Ile (**B**) were quantified by LC-MS/MS (*n*=3, bars denote +/- SE).

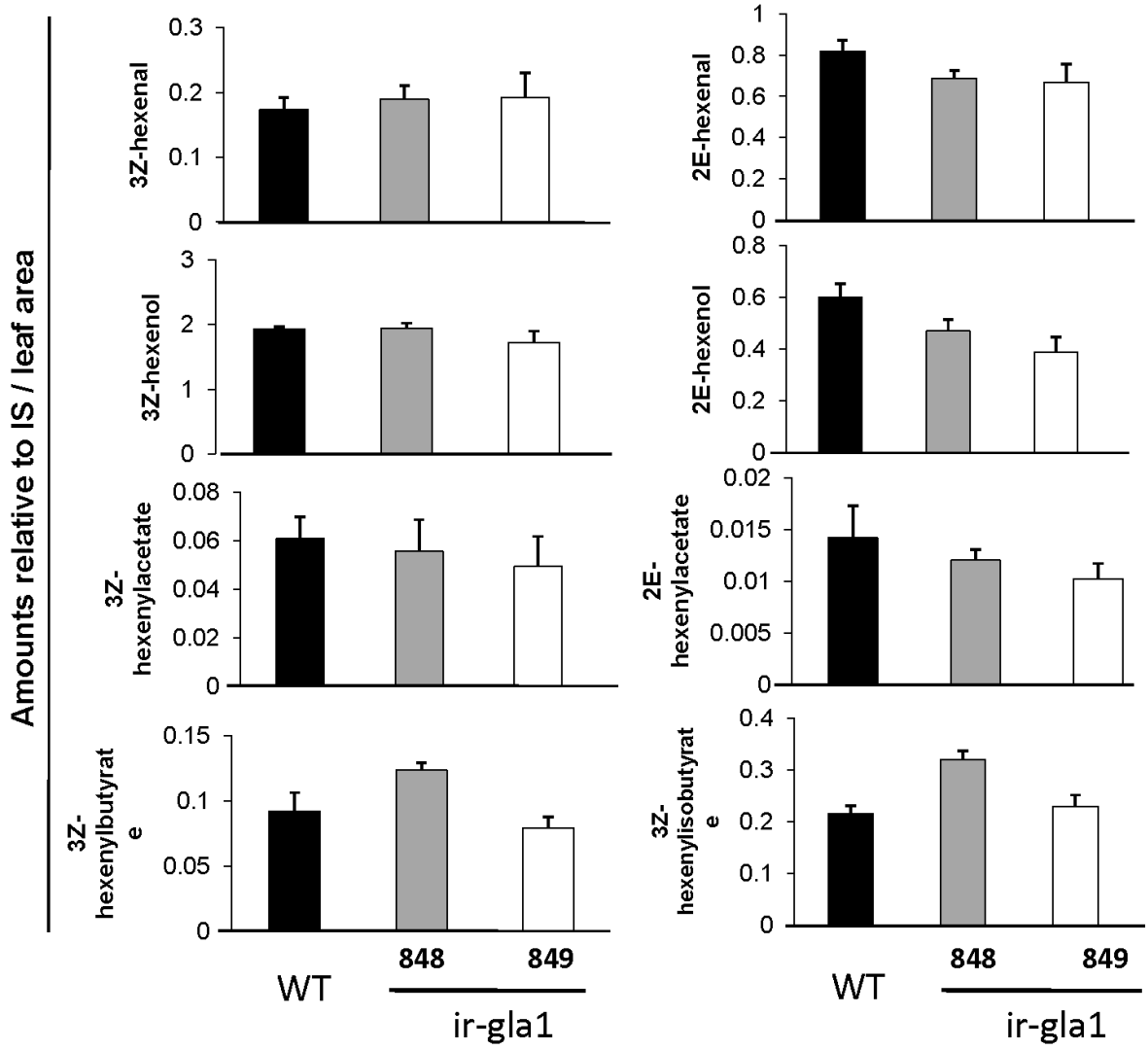

Figure S4. Analysis of GLVs in WT and ir-*gla1* plants after wounding

Leaves from ir-*gla1* and WT plants were wounded with a fabric pattern wheel and immediately enclosed in volatile collection chambers. Volatiles were trapped for a period of 30 min and analyzed by GC-MS (*n*=5, bars denote +/- SE).

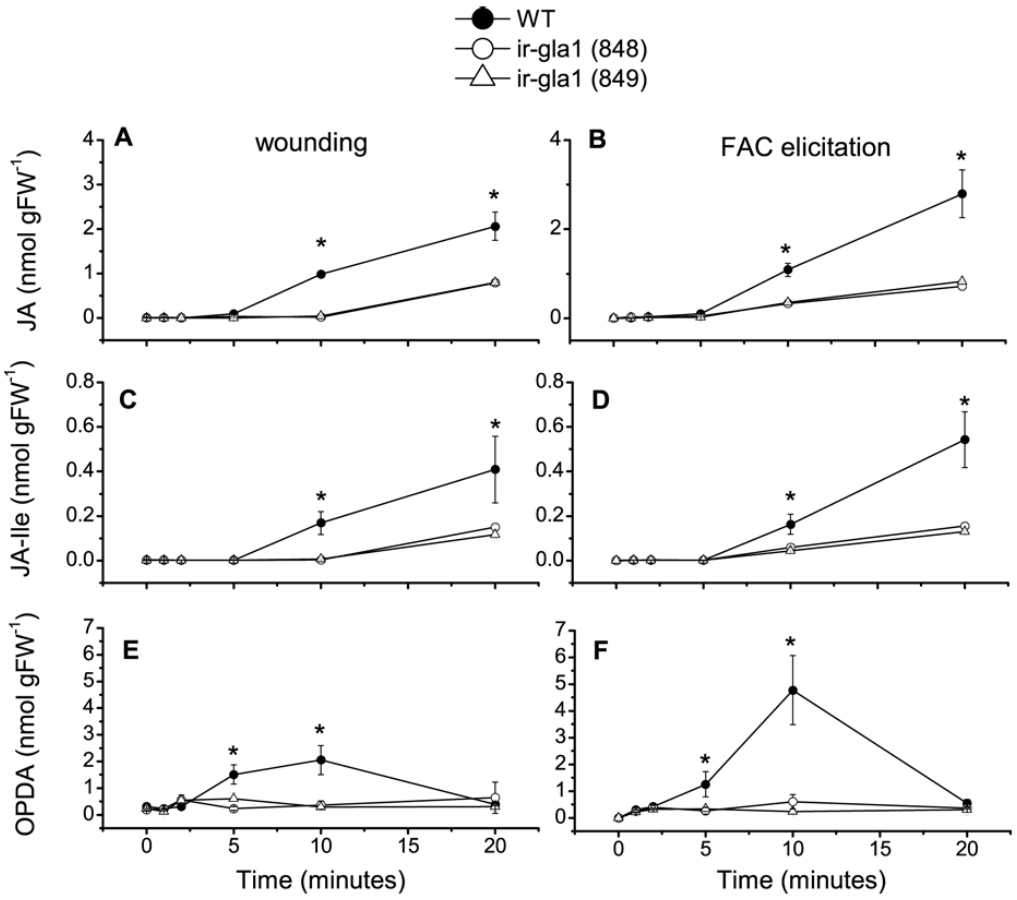

Figure S5. Accumulation of JA, JA-Ile and OPDA in leaves of WT and ir-*gla1* plants within 20 min after wounding and FAC elicitation

Leaves of 40-day-old WT and ir-*gla1* (lines 848 and 849) plants were wounded with a fabric pattern wheel or elicited with 18:3-Glu (FAC). After different times, leaf samples were harvested and JA (**A,B**), JA-Ile (**C,D**) and OPDA (**E,F**) were quantified by LC-MS/MS. *: $P < 0.05$, Students t-test (ir-*gla1* vs WT at same time point), n=4, bars denote +/- SD.

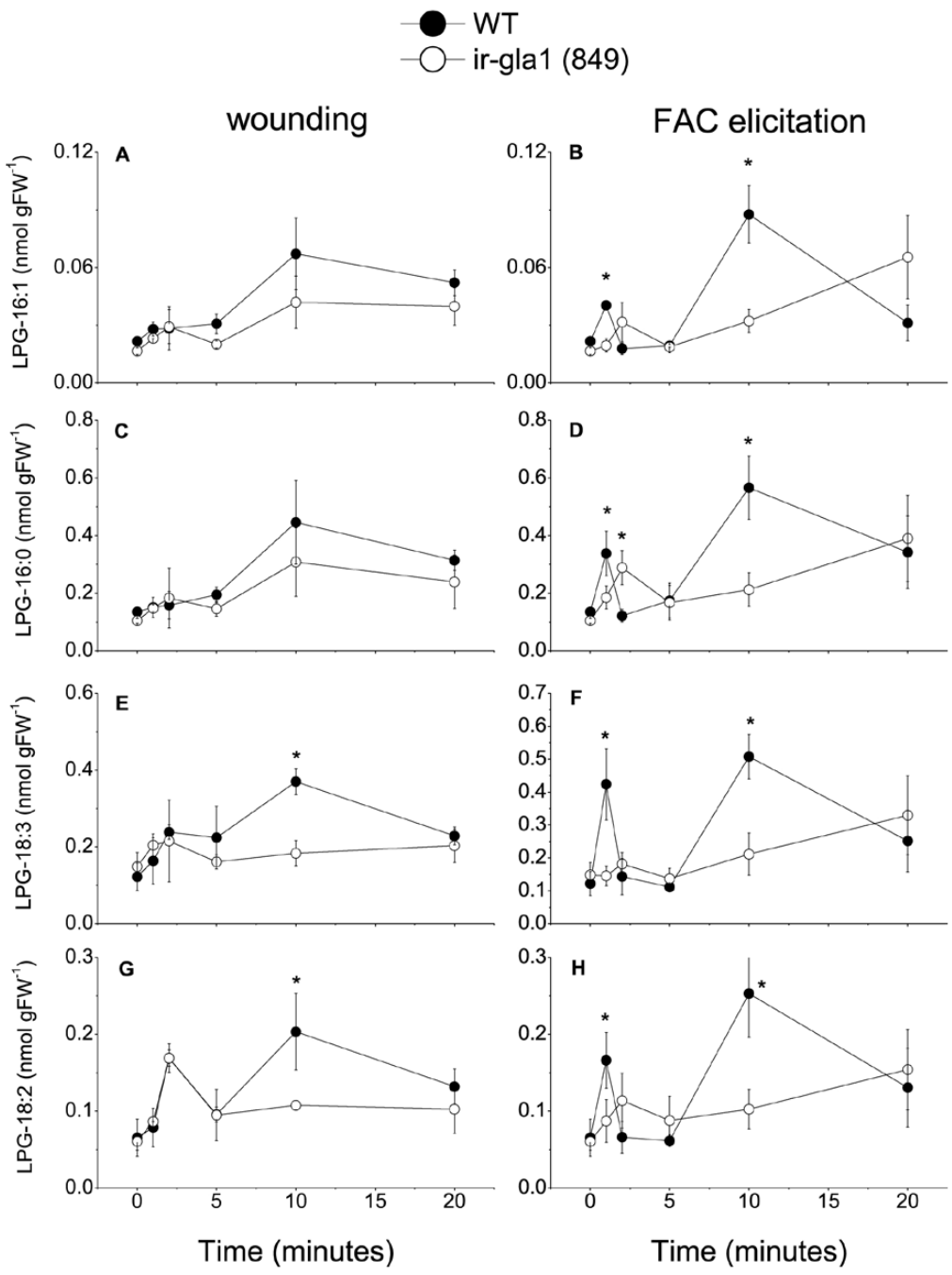

Figure S6. LPG levels in leaves of WT and ir-*gla1* plants after wounding and FAC elicitation
Leaves of 40-day-old WT and ir-*gla1* (line 849) plants were wounded with a fabric pattern wheel or elicited with 18:3-Glu (FAC). After different times, leaf samples were harvested and LPG molecular species in wounded (**A,C,E,G**) and FAC elicited (**B,D,F,H**) leaves were quantified by LC-MS/MS. *: $P < 0.05$, Students t-test (ir-*gla1* vs WT at same time point), n=4, bars denote +/- SD.

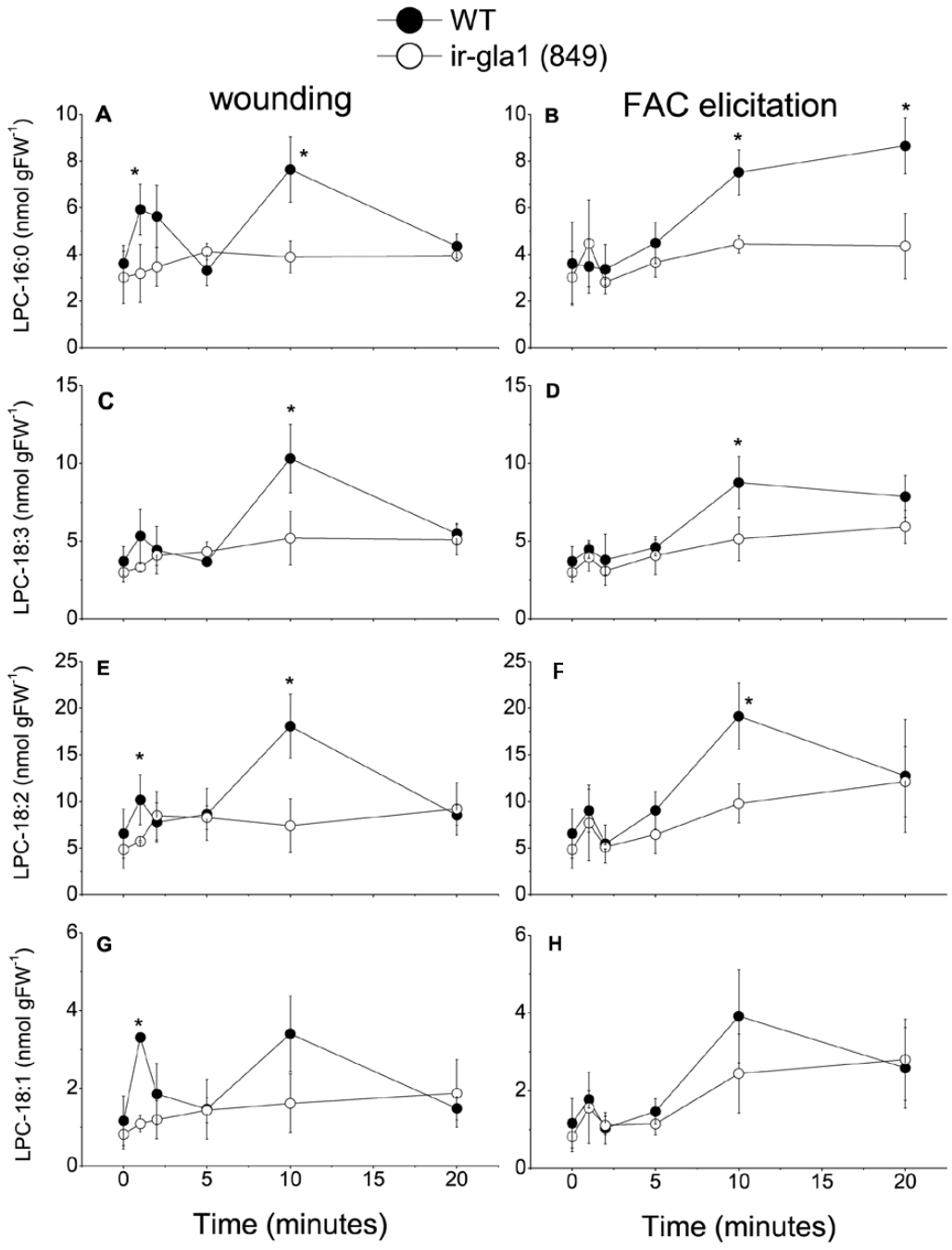

Figure S7. LPC levels in leaves of WT and ir-*gla1* plants after wounding and FAC elicitation
Leaves of 40-day-old WT and ir-*gla1* (line 849) plants were wounded with a fabric pattern wheel or elicited with 18:3-Glu (FAC). After different times, leaf samples were harvested and LPC molecular species in wounded (**A,C,E,G**) and FAC elicited (**B,D,F,H**) leaves were quantified by LC-MS/MS. *: $P < 0.05$, Students t-test (ir-*gla1* vs WT at same time point), n=4, bars denote +/- SD.

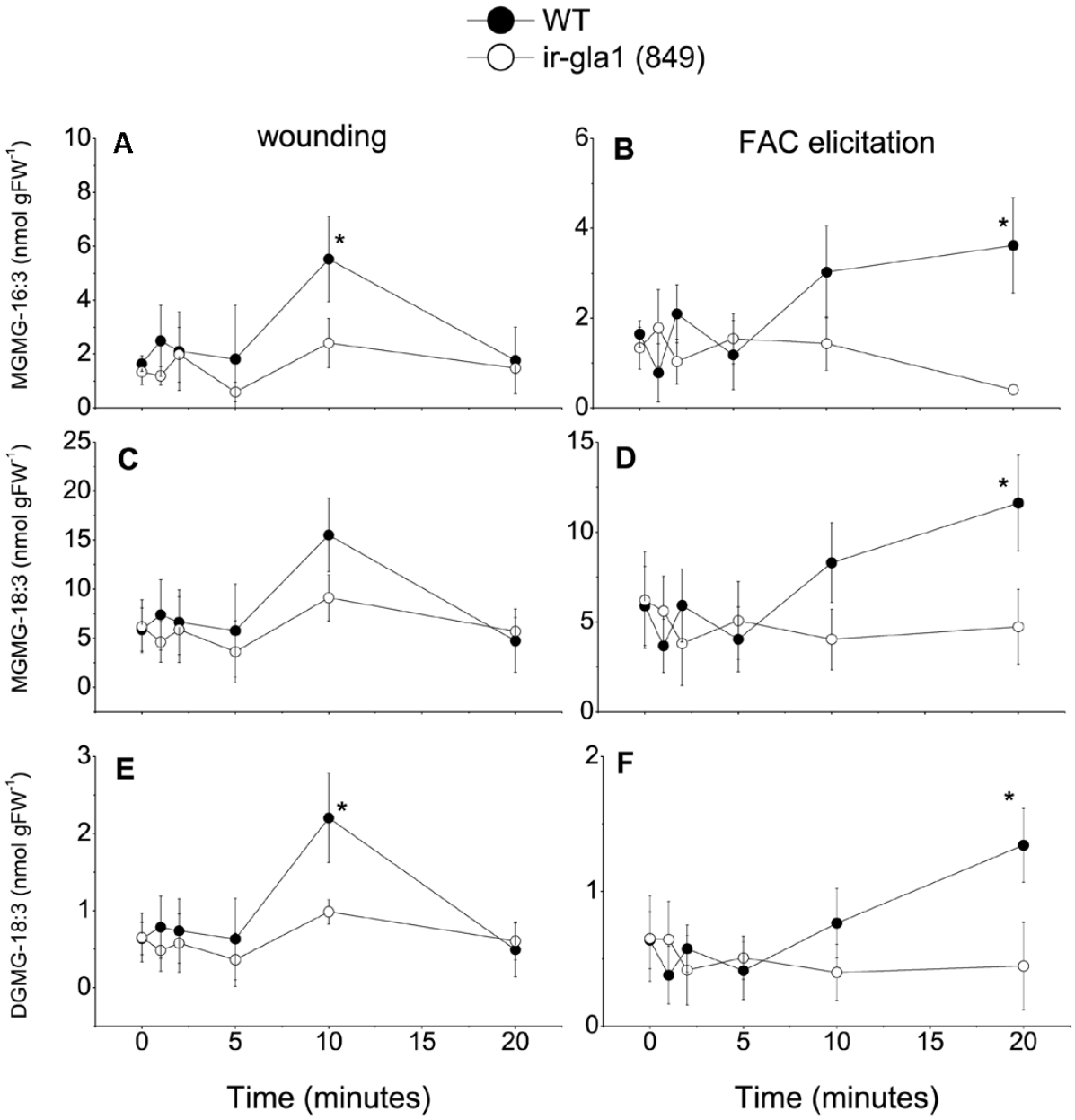

Figure S8. MGMG and DGMG levels in leaves of WT and ir-*gla1* plants after wounding and FAC elicitation

Leaves of 40-day-old WT and ir-*gla1* (line 849) plants were wounded with a fabric pattern wheel or elicited with 18:3-Glu (FAC). After different times, leaf samples were harvested and MGMG and DGMG molecular species in wounded (**A,C,E,G**) and FAC elicited (**B,D,F,H**) leaves were quantified by LC-MS/MS. *: $P < 0.05$, Students t-test (ir-gla1 vs WT at same time point), n=4, bars denote +/- SD.

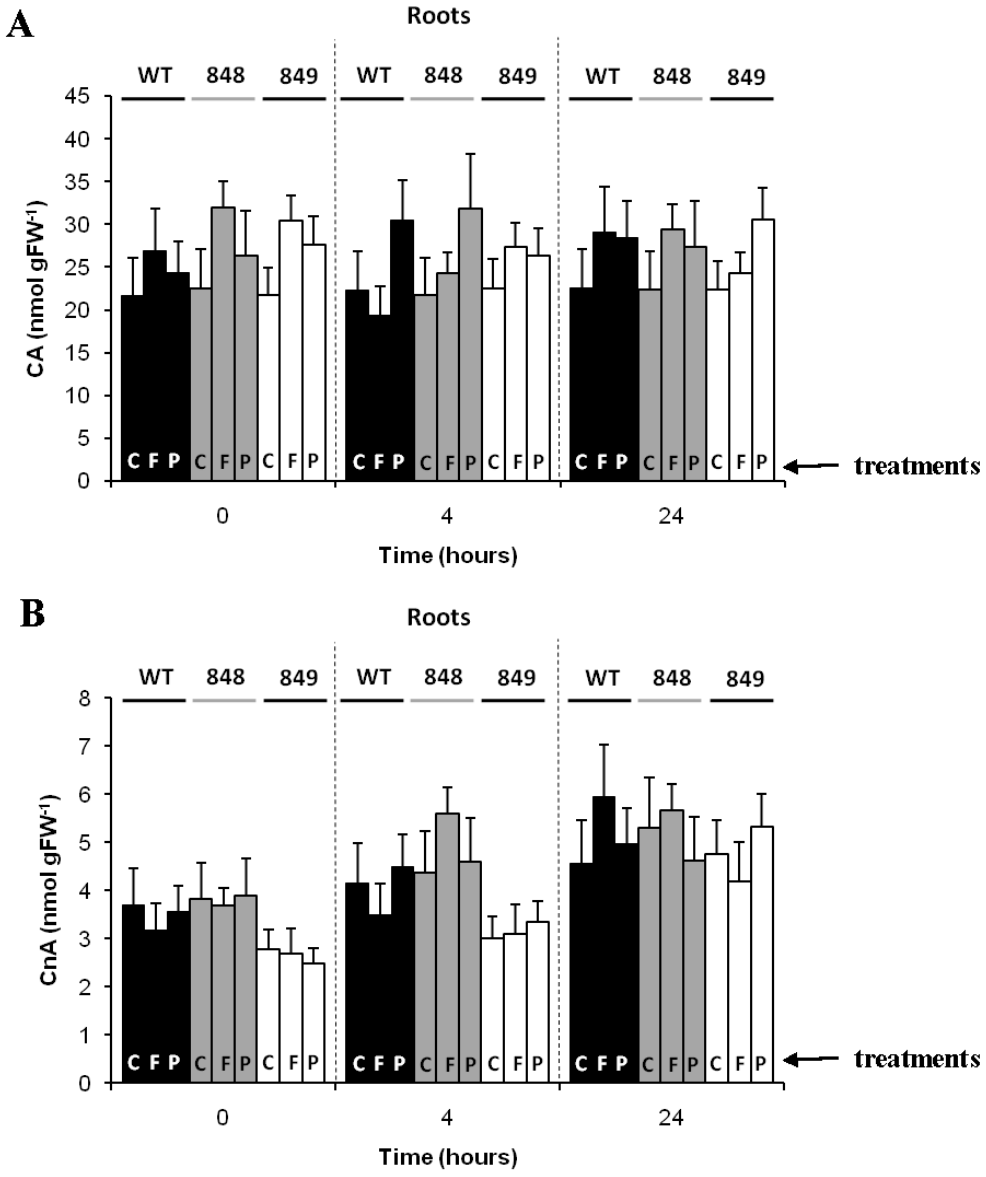

Figure S9. Accumulation of CA and CnA in roots of WT and ir-*gla1* plants after 4 and 24 h of pathogen infection

The hypocotyls of 20-day-old WT and ir-*gla1* (lines 848 and 849) seedlings were pricked with a sterile needle (control treatment; C) or with a needle containing spores of *F. oxysporum* (F) or *P. parasitica* (var. *nicotianae*) (P). After 4 and 24 h post-infection, root samples were collected and CA (**A**) and CnA (**B**) were quantified by LC-MS/MS (n=4, bars denote +/- SE).

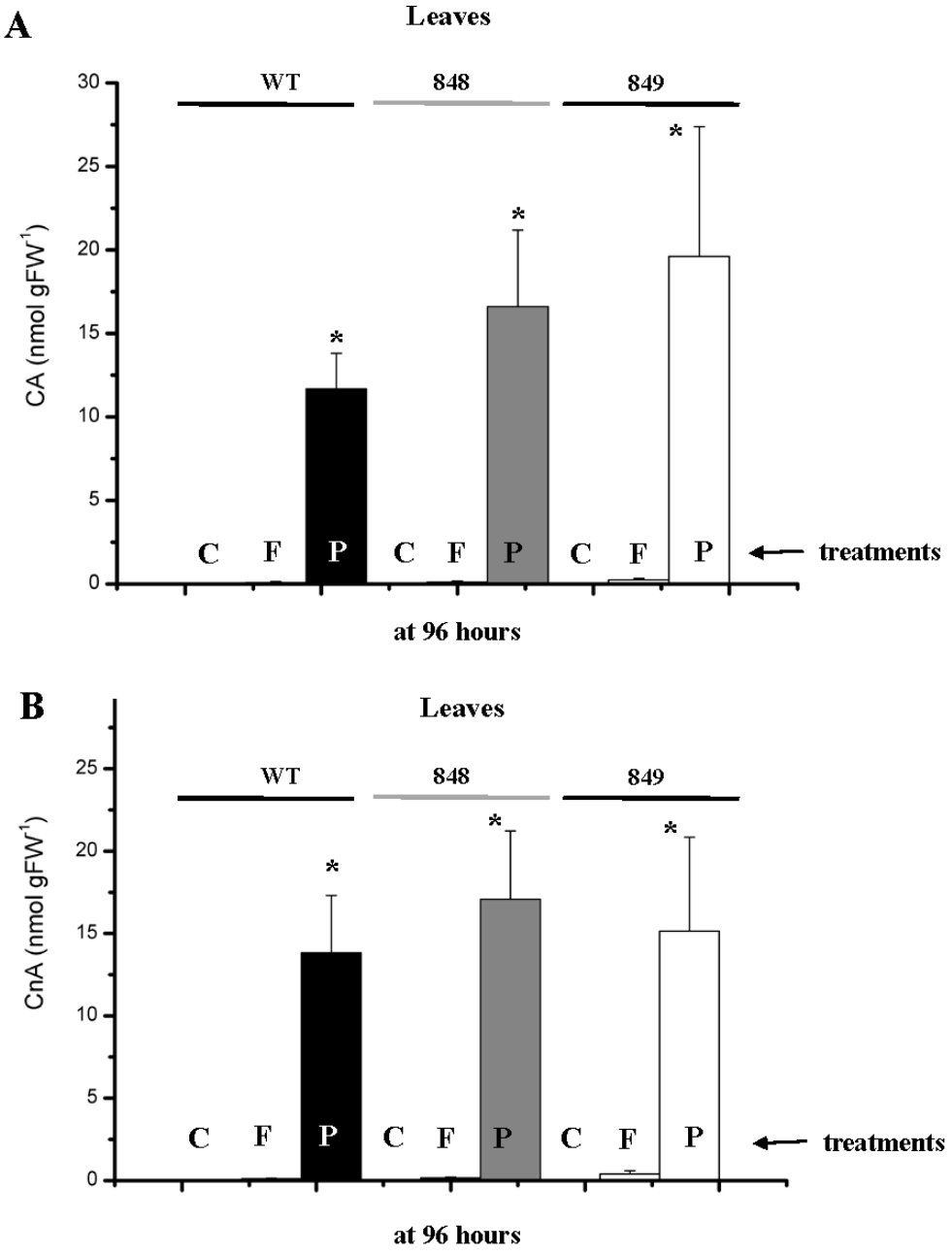

Figure S10. Accumulation of CA and CnA in leaves of WT and ir-*gla1* plants after 96 h of pathogen infection

The hypocotyls of 20-day-old WT and ir-*gla1* (lines 848 and 849) seedlings were pricked with a sterile needle (control treatment; C) or with a needle containing spores of *F. oxysporum* (F) or *P. parasitica* (var. *nicotianae*) (P). After 96 h post-infection, leaf samples were collected and CA (**A**) and CnA (**B**) were quantified by LC-MS/MS. *: $P < 0.05$, Students t-test (P treatment vs C treatment), n=4 for **A**, n=8 for **B**, bars denote +/- SE.

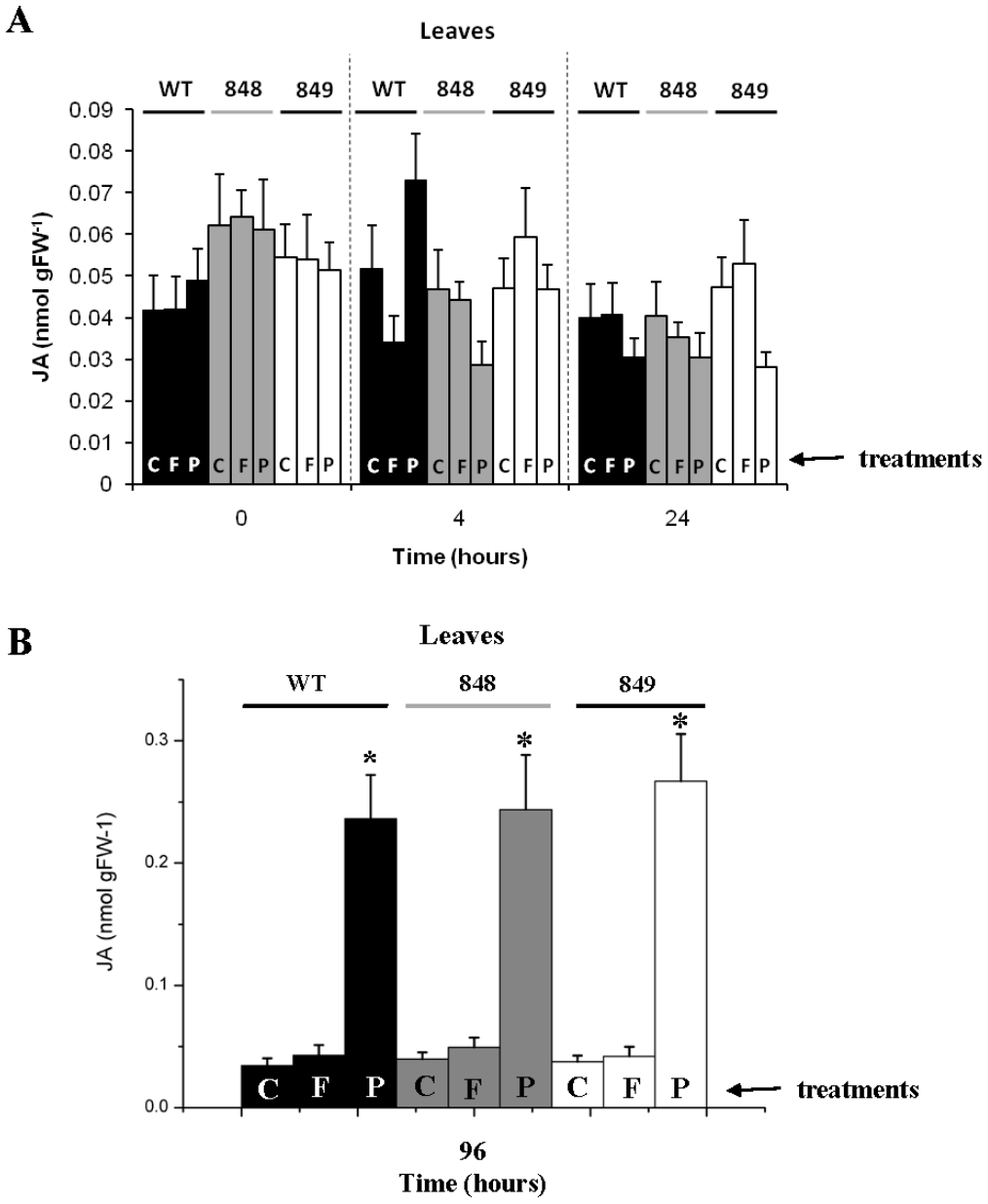

Figure S11. Accumulation of JA in leaves of WT and ir-*gla1* plants after pathogen infection
The hypocotyls of 20-day-old WT and ir-*gla1* (lines 848 and 849) seedlings were pricked with a sterile needle (control treatment; C) or with a needle containing spores of *F. oxysporum* (F) or *P. parasitica* (var. *nicotianae*) (P). After 4 and 24 h (**A**) and 96 h (**B**) post-infection, leaf samples were collected and JA was quantified by LC-MS/MS. *: $P < 0.05$, Students t-test (P treatment vs C treatment), n=4 for **A**, n=8 for **B**, bars denote +/- SE.

Chapter 4:

Analysis of the role of NaGLA1 in *Nicotiana attenuata* defense responses against the oomycete *Phytophthora parasitica* var. *nicotianae*

Title: Analysis of the role of NaGLA1 in *Nicotiana attenuata* defense responses against the oomycete *Phytophthora parasitica* var. *nicotianae*

Running title: NaGLA1´s role in *Nicotiana attenuata´*s defense against *Phytophthora parasitica*

Authors: Stefan Schuck, Mario Kallenbach, Ian T. Baldwin and Gustavo Bonaventure

Affiliation: Max Planck Institute for Chemical Ecology, Department of Molecular Ecology, Hans Knöll Str. 8, Jena 07745, Germany.

Corresponding author: Gustavo Bonaventure

Max Planck Institute for Chemical Ecology

Department of Molecular Ecology

Hans Knöll Str. 8, Jena 07745, Germany

Email address: gbonaventure@ice.mpg.de

Tel: +49 (0)3641 571118, Fax: +49 (0)3641 571102

Chapter 4: Manuscript 2

Analysis of the role of NaGLA1 in *Nicotiana attenuata* defense responses against the oomycete *Phytophthora parasitica* var. *nicotianae*

Abstract

The expression of the *Nicotiana attenuata GLYCEROLIPASE A1* (*NaGLA1*) gene was shown to be drastically induced during infection with the phytopathogenic oomycete *Phytophthora parasitica* var. *nicotianae* (Ppn) (Bonaventure, Schuck & Baldwin 2011). *Na*GLA1 catalyzes the initial step in the biosynthesis of the phytohormone jasmonic acid (JA) as a response to insect herbivory and wounding. In contrast, Ppn-inducible JA production does not depend on *Na*GLA1 expression, suggesting a different role for *Na*GLA1 during Ppn infection (Bonaventure *et al.* 2011). To assess whether *Na*GLA1 significantly contributes to the Ppn-inducible increase in total lipase A activity occurring during the infection process, leaf samples from *N. attenuata* wild-type (WT) and transgenic plants stably silenced in the expression of *NaGLA1* (ir-*gla1*) were subjected to a lipase activity assay with radiolabeled phosphatidyl-choline as substrate. The results showed that *Na*GLA1 did not contribute significantly to total lipase A activity. However, we showed that this enzyme participates in the specific formation of lysolipids derived from phosphatidylglycerol, phosphatidylcholine and galactolipids and in the release of oleic, linoleic and linolenic acids. Moreover, the formation of 9-hydroxy-linoleic acid and three additional oxylipins was reduced in Ppn-infected leaves of ir-*gla1* plants. Gene expression profiling of leaves revealed that 4192 genes were differentially affected in their expression in infected ir-*gla1* plants compared to WT. Metabolic profiling of infected leaves demonstrated that these changes in metabolic gene expression were strongly reflected in changes in the accumulation of several secondary metabolites, including phenylpropanoids, polyamines, and terpenoids.

Keyword index

Nicotiana attenuata, *Phytophthora parasitica* var. *nicotianae*, lipase, oxylipin, signaling

Abbreviations:

HPLC: high performance liquid chromatography

LC: liquid chromatography

MS: mass spectrometer

n: sample size (number of biological replicates)

SD: standard deviation

SE: standard error

TLC: thin-layer chromatography

ToF: time-of-flight detector

UPLC: ultraperformance liquid chromatography

Fatty acid moieties are abbreviated as follows: (number of carbon atoms:number of carbon-carbon double bonds in the molecule); *e.g.* (18:3) stands for linolenic acid because the molecule contains 18 carbon atoms, of which six are connected by three double bonds.

Introduction

Land plants and their pathogens share a long history of common evolution proven by fossil evidence of plant defense against fungal endophytes dated back to 400 million years ago (Kemen & Jones 2012; Krings *et al.* 2007). Despite a preservation potential considered as very low, fossil records exist suggesting that a considerable number of plant endophytic oomycetes existed at least by the Carboniferous (Krings, Taylor & Dotzler 2011). Among those, the majority were probably rather saprotrophic. The first oomycete fossil with haustoria indicative for plant parasitism stems from *Combresomyces williamsonii* found in the cortical tissue of a seed fern species (*Lyginopteris oldhamia*) and is approximately 315 million years old (Krings *et al.* 2011; Strullu-Derrien *et al.* 2011). Since that geological period, oomycetes and land plants had plenty time to coevolve following the "zigzag" model proposed by Jones & Dangl (2006) (Burdon & Thrall 2009; Jones & Dangl 2006). According to that model, plants perceive microbe-associated molecular patterns (MAMPs) which elicit a defense response (pathogen-triggered immunity, PTI). In order to avoid this PTI, pathogenic (virulent) microbes produce effectors to regain susceptibility of their host plant (pathogen-triggered susceptibility, PTS). However, these effectors might become recognizable by the plant via receptor proteins mediating resistance (*R*-gene products) and then induce defense responses again (effector-triggered immunity, ETI). In this case, the effectors are called avirulence (Avr) proteins which are encoded by corresponding *Avr* genes. During evolution pathogens can develop effectors targeting this *R*-gene-mediated host recognition and these novel effectors can then become recognizable by the plant by new

receptors in a "gene-for-gene resistance" manner, a mechanism leading to an evolutionary arms race between pathogens and their host plants (Keen 1990; Van der Biezen & Jones 1998). A typical example for gene-for-gene resistance is the tomato Cf-9 receptor which recognizes the Avr9 peptide from the fungal pathogen *Cladosporium fulvum* (Rowland *et al.* 2005). Gene-for-gene resistance explains also the observed differences in resistance of various tobacco cultivars to specific races of the oomycete *Phytophthora parasitica* var. *nicotianae* (Ppn), the causal agent of black shank disease and huge economic losses, and the variable resistance of several *Nicotiana rustica* accessions to Ppn race 0 (Nifong *et al.* 2011; van Jaarsveld, Wingfield & Drenth 2002). Already several years ago, a resistance gene from the tobacco cultivar Coker 371-Gold designated "*Ph*" was identified which confers resistance to Ppn race 0 (Carlson *et al.* 1997). As additional mechanism to the production of novel effectors in order to maintain virulence, certain Ppn strains down-regulate *in planta* the expression of parasiticein, a small secretory protein belonging to the so-called "elicitin" family, to avoid host recognition of these fungal proteins and, as a consequence, the elicitation of plant defense responses (Colas *et al.* 2001). In case of a hemibiotrophic phytopathogen like Ppn, these plant responses typically comprise a hypersensitive response to spatially restrict pathogen growth (Takemoto, Hardham & Jones 2005). This hypersensitive response is in susceptible ("compatible" interaction) tobacco preceded by a biphasic reactive oxygen species (ROS) and ethylene burst after Ppn infection (Wi, Ji & Park 2012). Two different NADPH oxidase isoforms mediate this biphasic ROS burst, the first one being transient and weak and the second one being rather massively (Wi *et al.* 2012). Studies using tobacco cell culture treated with cryptogein, a proteinaceous elicitor from *Phytophthora cryptogea*, and ergosterol, a typical fungal sterol, revealed further that these

oomycete elicitors are able to induce plant cell acidification and the production of ROS, as well as signaling processes in which Calcium ion release from internal reservoirs, phospholipase C and phospholipase A2 are involved, ultimately leading to an increased production of the sesquiterpenoid phytoalexin capsidiol and the stimulation of the biosynthesis of phenylpropanoid-derived cell wall constituents (Amelot *et al.* 2012; Kasparovsky, Blein & Mikes 2004; Kasparovsky *et al.* 2003; Lebrun-Garcia *et al.* 2002). Furthermore, signaling processes mediated by mitogen activated kinases seem to be involved in tobacco defense response to *Phytophthora sp*. (Liu *et al.* 2003; Takemoto *et al.* 2005; Zhang & Klessig 2000). After treatment of cultured potato cells with elicitors from *Phytophthora infestans*, the transcriptional expression and enzymatic activity of a 9-lipoxygenase (9-LOX) is induced accompanied by an increase in phospholipase A activity, leading to the release of polyunsaturated fatty acids from membrane lipids as substrates for the formation of oxidized fatty acid products (oxylipins) such as the divinyl ethers (DVEs) colneleic and colnelenic acid (Gobel *et al.* 2001). A study in *Arabidopsis* suggests that oxylipins derived from the 9-LOX pathway (including colneleic and colnelenic acid) play a role in cell wall modification essential for lateral root development and pathogen arrest (Vellosillo *et al.* 2007). Supporting an involvement in plant defense against pathogens (including *Phytophthora sp*.), several oxylipins were shown to possess antimicrobial activities *in vitro*, including the above mentioned DVEs (Fammartino *et al.* 2007; Prost *et al.* 2005; Weber *et al.* 1999). Even though the transcriptional expression of a 13-LOX is also induced in potato cells after *Phytophthora infestans*-elicitor treatment, levels of products derived from this pathway, *e.g*. jasmonic acid (JA), remained only

very low, suggesting that those play only minor roles (if at all) during the potato-*Phytophthora* interaction (Gobel *et al.* 2001).

In order to tailor their response to specific pathogens most efficiently, plants use a very complex signaling network including various phytohormones such as the already mentioned ethylene and JA, but also salicylic acid, to regulate the expression of defense-related genes accordingly (Kunkel & Brooks 2002). Ppn, as well as another phytopathogenic fungus, *Fusarium oxysporum*, are known to strongly induce transcript levels of a gene encoding for a glycerolipase A1 (GLA1) in leaves of the wild tobacco *Nicotiana attenuata* (Bonaventure *et al.* 2011). In this plant species, GLA1 was originally identified to be the major lipase activated after wounding and insect herbivory and to initialize the biosynthesis of JA by the release of linolenic acid out of chloroplast membrane lipids within only few minutes (Bonaventure *et al.* 2011; Kallenbach *et al.* 2010). Most interestingly and despite the strong inducibility of *GLA1* expression upon Ppn infection, it does not affect JA levels during the infection process in *N. attenuata* leaves. Even though no changes in the final levels of another group of oxylipins - the Ppn-inducible DVEs - could be demonstrated in this previous study, transcript levels encoding for the two enzymes catalyzing DVE production from polyunsaturated fatty acids, *N. attenuata* lipoxygenase 1 and DVE synthase, were altered in a GLA1-regulated manner during Ppn infection. Therefore it was hypothesized that GLA1 is involved in the generation of a signal after Ppn infection leading to the observed transcriptional changes (Bonaventure *et al.* 2011). However, the nature of this signal remained mysterious and therefore it was the objective of this study to unravel the role of GLA1 during this plant-oomycete interaction in more detail.

Material and Methods

Plant growth

Seeds of the 31st inbred generation of *Nicotiana attenuata* Torrey ex S. Watson 1871, derived from seeds originally collected in 1988 from a native population in Washington County, Utah, were used for all experiments as wild-type genotype (WT). In addition to WT, two genetically independent transgenic *N. attenuata* plant lines stably reduced in the expression of Na*GLA1* by inverted-repeat silencing technique (ir-*gla1*) were used (Bonaventure *et al.* 2011). *N. attenuata seeds* were germinated on Gamborg's B5 medium (Duchefa, Haarlem, the Netherlands) as previously described in Krugel *et al.* (2002) and maintained in growth chambers (Snijders Scientific, Tilburg, the Netherlands) at a day/night cycle of 16 h light (155 µmol s^{-1} m^{-2}) at 26°C and 8 h darkness at 24°C. 10 days after germination seedlings were transferred to TEKU pots (Pöppelmann GmbH & Co. KG, Lohne, Germany) containing sand and grown in the glasshouse for 14 days under high-pressure sodium lamps (Philips, Eindhoven, the Netherlands, 200-300 µmol s^{-1} m^{-2} light) with a day/night cycle of 16 h (26-28°C)/8 h (22-24°C) and 45 to 55% relative humidity. After 10 days in TEKU pots, plantlets were transferred to 400 mL-pots filled with sand and transferred for experiments to a growth chamber with a day/night cycle of 16 h (22°C)/8 h (22°C) and 65% relative humidity, in which the experiments were performed after giving the plantlets 4 days to adjust to the new environment.

Plant inoculation with Phytophthora parasitica nicotianae

Phytophthora parasitica Dastur 1913 var. *nicotianae* (van Breda de Haan 1896) Tucker 1931 (Ppn) was obtained from the DSMZ (German Collection of Microorganisms and Cell Cultures, Braunschweig, Germany) and grown on potato dextrose agar (PDA) (Sigma, Taufkirchen, Germany) at 26°C in the dark. Inoculation of 24 days old *N. attenuata* plants (early rosette stage with ~ 4-5 leaves) with Ppn was performed by putting a PDA plug (5 mm diameter) containing a two weeks old Ppn culture onto a wounding site generated by pricking with a sterile needle into the hypocotyl. To facilitate infection, a high humidity environment was generated by covering the wounding site and the agar plug with a wet piece of cotton and the trays were covered with a plastic lid for one day. As a control, a similar procedure was done with a pure PDA plug, except for the microarray experiment where untreated plants served as control. At different time points, shoots were harvested and immediately frozen in liquid nitrogen for subsequent analyses. Recording of disease progression based on morphological changes was done by taking photographs from Ppn-infected and control plants at 0, 2.5 and 4 days after inoculation (dai).

Quantitative real-time PCR

For quantification of Ppn infection rates, DNA was extracted from Ppn-infected (n=14-19) and non-infected (n=3) *N. attenuata* shoots (WT and two ir-*gla1* lines) at 2.5 and 4 dai by the CTAB method (Schuck *et al.* 2012). Quantitative real-time PCR (qPCR) was performed with a Mx3005P Multiplex qPCR system (Stratagene, La Jolla, CA) and the qPCR Core kit for SYBR® Green I (Eurogentec, Liege, Belgium) with 20 ng of isolated DNA as template. The copy number

of the Ppn *TRANSLATION ELONGATION FACTOR 1 ALPHA* (*PpnEF1A*) gene relative to the 20 ng of total sample DNA was used to quantify colonization rates of Ppn by Ct-value comparison. For quantification, the primers Ppn_EF1a_fwd 5´-GGCGGTATTGGCACGGTA-3´ and Ppn_EF1a_rev 5´-GCCGACGTTGTCACCAGG-3´ were used. Those were designed based on *EF1A* sequence specificities of Ppn compared to *N. attenuata* and *N. tabacum* (Supplemental Figure S1 A) and amplification specificity to *PpnEF1A* was tested against *N. attenuata EF1A* using standard PCR with similar reaction conditions as in the qPCR (Supplemental Figure S1 B). All reactions were performed using the following qPCR conditions: initial denaturation step of 95°C for 30 s, followed by 40 cycles each of 95°C for 30 s and 60°C for 1 min, with a final extension step of 95°C for 30 s and 60°C for 1 min.

Abscisic acid and salicylic acid quantification

Shoots from Ppn-infected and control plants (WT and two ir-*gla1* lines) were harvested at 0 (n=6-7), 4 (n=3-4), 24 (n=3-4) and 96 (n=5-8) hours after inoculation and immediately frozen in liquid nitrogen. 200 mg of each shoot were homogenized to a fine powder with a Geno/Grinder 2000 (BTC and OPS Diagnostics, Bridgewater, USA) in the presence of liquid nitrogen. One mL of ethyl acetate spiked with 40 ng of each [$^2H_6$]-ABA and [$^2H_4$]-SA as internal standard was used for extraction. After centrifugation for 15 min at 12,000*g* (4°C), the upper organic phase was transferred into a fresh 2 mL tube and the residual phase was re-extracted with 0.5 mL ethyl acetate, thereafter both organic phases were pooled. Then samples were evaporated to dryness under reduced pressure. The dry residue was reconstituted in 0.2 mL of 70/30 (v/v) methanol/water for analysis by LC-MS (liquid chromatography-mass spectrometry; Varian 1200

Triple-Quadrupole-LC-MS system; Varian, Palo Alto, California, USA). From each sample, ten microlitres were injected onto a ProntoSIL column (C18-ace-EPS, 50 x 2 mm, 5 mm, 120 Å; Bischoff, Leonberg, Germany) connected to a pre-column (C18, 4 x 2 mm; Phenomenex, Torrance, California, USA). As mobile phases, 0.05% formic acid in water (solvent A) and methanol (solvent B) were used in a gradient mode with the following conditions: time/concentration (min/%) for B: 0.0/15; 2.5/15; 4.5/98; 10.5/98; 12.0/15; 15.0/15; time/flow (min/mL): 0.0/0.4; 1.5/0.2; 1.5/0.2; 10.5/0.4; 15.0/0.4. Compounds were detected in the ESI negative mode and multiple reaction monitoring (MRM) according to the parameters described in Bonaventure *et al.* (2011). Quantification was made based on peak area comparison with the internal standards.

Lysolipid analysis

Four days after inoculation, shoots from Ppn-infected and control plants (WT and two ir-*gla1* lines; n=3-5) were harvested and immediately frozen in liquid nitrogen. Approximately 500 mg of frozen sample was transferred into ice-cold 8 mL glass tubes (Corning, Schiphol-Rijk, Netherlands) filled with 2 mL 2-propanol and incubated at 80 °C for 10 minutes to inactivate lipases. While cooling on ice, 3.75 mL of 2/1 (v/v) methanol/chloroform containing internal standards [200 ng of each, lysophosphatidylglycerol-17:1 (LPG-17:1), lysophosphatidyl-ethanolamine-14:0 (LPE-14:0), lysophospatidic acid-17:0 (LPA-17:0), lysophosphatidylinositol-13:0 (LPI-13:0) and lysophosphatidylcholine-17:0 (LPC-17:0) (Avanti Polar Lipids, Alabaster, Alabama, USA)] were added. After adding 1.25 mL of chloroform and 1 mL of water and mixing thoroughly, the samples were centrifuged for 25 min at 800*g* (4°C). The lower organic

phase was transferred into a fresh glass tube and the remaining material re-extracted with 3 mL chloroform. The organic phases were pooled and evaporated under a stream of nitrogen. The dried residual was reconstituted in 0.4 mL of methanol/water/chloroform 70/20/10 (v/v/v). Lysolipids were analyzed by LC–MS^3 (Varian 1200 Triple-Quadrupole-LC-MS system). 10 µL of the sample were injected onto a ProntoSIL C8 column (C8 ace EPS; 5 µm, 50 x 2 mm, 120 Å, Bischoff). As mobile phases, 0.05% formic acid in water (solvent A) and methanol (solvent B) were used in gradient mode with the following conditions: time/concentration (min/%) for B: 0.0/15, 1.5/15, 5.0/98, 18.0/98, 22.0/15, 25.0/15; time/flow (min/mL): 0.0/0.4, 1.0/0.4, 1.5/0.2, 22.0/0.2, 22.5/0.4, 25.0/0.4. Lysolipids were detected using MRM after CID with argon gas. For ionization, the needle was set at 5000 V and the drying gas (nitrogen) at 300°C and 20 psi (housing 50°C). The detector was set at 1800 V. Lysolipids were analyzed in positive and negative ionization mode (see Supplemental Table S2 for details). Quantification of LPC, LPG, LPA, LPI and LPE species was made according to the description in Bonaventure *et al.* (2011) based on the peak areas of the internal standards added. DGMG was quantified using the LPC-17:0 added and an estimated response factor of 900 applied to the peak area corresponding to DGMG.

Oxylipin analysis

Shoots from Ppn-infected and control plants (WT and ir-*gla1* line 1; five biological replicates per genotype and treatment) were harvested at 4 dai, immediately frozen in liquid nitrogen and thoroughly ground to fine powder. About 500 mg of this frozen sample was transferred into ice-cold 8 mL glass tubes filled with 5 mL of an extraction solvent (2-

propanol/chloroform 1/1 (v/v) containing 0.0025% 2-butyl-6-hydroxy toluene and as internal standards 250 ng [$^2H_2$]-dihydro-jasmonic acid, 50 ng [$^2H_4$]-salicylic acid, 50 ng [$^2H_6$]-abscisic acid and 50 ng isoleucyl-[$^{13}C_6$]-jasmonic acid). After intensive mixing for 30 seconds, samples were centrifuged at 4 °C and 720*g* for 10 minutes and the supernatant transferred into a fresh pre-cooled glass tube with a Pasteur pipette. Then the sample volume was reduced under a gentle nitrogen stream and samples were transferred with a Pasteur pipette on Supelclean LC-NH2 solid phase extraction columns (Supelco, Sigma-Aldrich, Munich, Germany) preconditioned with ice-cold 2-propanol/chloroform (1/1; v/v). After loading the sample, columns were first washed with two column volumes (~ 2 mL) 2-propanol/chloroform (1/1; v/v) and eluted with three volumes (~3 mL) methanol/acetic acid (98/2; v/v) into a 4 mL-glass vial. The eluent was dried under a gentle nitrogen stream and samples re-dissolved in 0.2 mL methanol. Oxylipins were separated and analyzed on an UPLC system (Dionex) connected to a Micro-ToF-Q mass spectrometer (Bruker Daltonics). Two microliters of extract were injected onto a C8 column (Kinetex C8; 2.6 µm, 50 x 2.1 mm, 100 Å, Phenomenex). As mobile phases, 0.1% (v/v) acetonitrile and 0.05% (v/v) formic acid in water (solvent A) and 0.05% (v/v) formic acid in acetonitrile (solvent B) were used in gradient mode with the following conditions: time/concentration (min/%) for B: -5/20, 0/20, 20/98, 25/98 using a constant flow of 0.4 min mL^{-1}. The MS detection was performed in negative ionization mode with the following instrument settings: capillary voltage 4500 V, nebulizer gas pressure 1.4 bar, dry gas temperature 180°C; dry gas flow 10 L min^{-1}, mass range 50-1000 m/z. For MS/MS spectra collection, the instrument was run in MS²-Auto mode collecting MS-MS spectra from the 3 most abundant precursor ions at each retention time using a collision energy of 35V. Sodium formate clusters [a 10 mM solution of NaOH in 50/50% (v/v)

2-propanol/water containing 0.2% formic acid] were used for internal mass calibration. Sum formulas were calculated using the SumFormula tool integrated in the Data-Analysis software (Bruker Daltonics) with respect to isotopic patterns and logical fragmentations. If standards were available, oxylipins were identified by comparing their retention times and mass spectra with the according standard.

Quantification of PLA activity in leaf extracts

Phospholipase A activity in leaf extracts was determined by thoroughly grinding with a plastic pestle 0.8-mm-leaf discs (weighed with a microbalance) from control and Ppn-infected WT and ir-*gla1 N. attenuata* plants (4 dai) in 1.7 mL plastic tubes containing 50 µL reaction buffer (50 mM aqueous K-phosphate [pH=6.5], 0.2% (v/v) Triton X-100/water). After centrifugation at 16,000*g* for 5 min at 4ºC, 50 µL of the supernatant were transferred into 4 mL glass vials containing 1.2 mL of reaction buffer and 0.3 µCi of [^{14}C-1]-L-α-dipalmitoyl-phosphatidylcholine (114 µCi µmol^{-1}; Perkin Elmer, Rodgau, Germany). Two biological replicates per plant genotype and per treatment were used. The reactions were carried out at room temperature. 0.2 mL aliquots were taken at 0, 15, 30, 60 and 120 min and immediately mixed with 1 mL 2/1 (v/v) chloroform/methanol in 2 mL screw-cap glass vials. After phase separation, the upper aqueous phase was removed and the organic phase evaporated under a stream of argon. The samples were reconstituted in 0.1 mL of 2/1 (v/v) chloroform/methanol and loaded on Partisil® K6 silica plates (Whatman, Dassel, Germany) which were 1/3, 2/3 and fully developed with 25/10/1 (v/v/v) chloroform/methanol/water. After air drying, the TLC plates were exposed to radioactivity sensitive screens for different times and the screens were scanned

with a FLA-3000 scanner (Fujifilm, Duesseldorf, Germany). Band intensities corresponding to radiolabeled free palmitic acid, lyso-PC and PC were quantified (as percentage of total activity) with the Aida Image Analyzer v3.11 software (Fujifilm).

Microarray analysis

Shoots from Ppn-infected and non-infected ir-*gla1* 1 and WT *N. attenuata* plants were harvested at 2.5 dai and used for microarray analysis (3 biological replicates per genotype and treatment and six arrays in total; see Accession numbers in Material and Method section). This time point was chosen as a compromise to cover genes expressed in both Ppn infection stages (the early as well as the late phase), *i.e*. before the first visible disease symptoms started to appear (~3-4 days after inoculation) but when GLA1 expression was already highly induced (Bonaventure *et al.* 2011). Total RNA was extracted using the method described by Kistner & Matamoros (2005) and RNA quality was checked by spectrophotometry (NanoDrop, Wilmington, DE). Genomic DNA contaminations were removed by DNAse treatment following commercial instructions (Turbo DNase; Ambion, Europe) and the resulting RNA was cleaned up with RNeasy MinElute columns (Qiagen, Hilden, Germany). Afterwards RNA quality was checked with the RNA 6000 Nano kit (Agilent, Santa Clara, CA) using an Agilent 2100 Bioanalyzer. Labeled cRNA was generated from total RNA with the Quick Amp labeling kit (Agilent) following commercial specifications and the cRNA yield was determined spectrophotometrically (NanoDrop). Hybridization of the labeled cRNA was done using the Gene Expression Hybridization kit (Agilent) following commercial instructions onto a 44K custom designed 60mer *N. attenuata* Agilent microarray as previously described (Kallenbach *et*

al. 2011). Hybridization, washing and analysis were performed according to Kallenbach *et al.* (2011). Data was extracted using the Agilent Feature Extraction software (version 9.5) and analyzed with the SAM (Significance Analysis of Microarrays) software from Multiexperiment Viewer (MeV v4.8) (http://mev.tm4.org/) (Tusher, Tibshirani & Chu 2001). The *q*-values for each gene corresponded to a computed false discovery rate (FDR) of less than 5%. Changes in gene expression were considered to be significant when the $\log_2$ of the fold change in signal intensity (ir-*gla1*1 vs. WT) was greater than 1 or smaller than -1. Gene annotation was done with Blast2Go software (http://www.blast2go.com/ b2glaunch).

Metabolic profiling of Ppn-infected shoots

Shoots from Ppn-infected and ir-*gla1* 1 and WT *N. attenuata* plants were collected at 2.5 dai for metabolic profiling (5 biological replicates per genotype and treatment). Shoot tissue was ground with a Geno/Grinder 2000 in the presence of liquid nitrogen and extracted with 1 mL of 40% (v/v) methanol/50 mM aqueous sodium acetate buffer (pH=4.8) per 100 mg of shoot tissue by thoroughly mixing. Samples were centrifuged at 12,000*g* for 20 min at 4°C and their supernatant was transferred into fresh 1.5 mL tubes. To ensure removal of all residual particles, samples were centrifuged again at 12,000*g* for 20 min at 4°C. 200 µL of the supernatant were transferred into 2 mL glass vials with insert for analysis by UPLC-ToF-MS (ultra-pressure-liquid-chromatography time-of-flight mass spectrometry) similar to the method previously described (Gilardoni *et al.* 2011). Two microliters of extract was injected onto a C18 Acclaim column (Dionex, 2.2 µm particle size, 150 × 2.1 mm inner diameter) and separated using an RSLC system (Dionex). Solvent A was 0.1% (v/v) acetonitrile (Baker, HPLC grade) and 0.05%

(v/v) formic acid in deionized water and solvent B was acetonitrile and 0.05% (v/v) formic acid. The following gradient conditions were used [time/concentration (min/%) for B]: -3/10, 0/10, 0.5/80, 6.5/80 with a flow rate kept at 400 µL min^{-1}. Ions generated from eluting compounds with an electrospray ionization source in positive and negative ion mode were detected with a MicroToF mass spectrometer (Bruker Daltonics). The following instrument settings were used: capillary voltage, 4500 V; capillary exit 130 V; dry gas temperature 200°C; dry gas flow, 8 liters min^{-1}. Sodium formate clusters [10 mM solution of NaOH in 50/50% (v/v) 2-propanol/water containing 0.2% formic acid] were used for mass calibration. Data sets were analyzed within a retention time range from 125 to 550 s and a mass (m/z) range from 90 to 1400. As previously described by (Gaquerel, Heiling, Schoettner, Zurek & Baldwin 2010) raw data files were converted to netCDF format using the export function of the Data Analysis version 4.0 software (Bruker Daltonics) and processed using the R (www.r-project.org) packages XCMS (Tautenhahn, Bottcher & Neumann 2008) and CAMERA (http://www.bioconductor.org/biocLite.R). For peak detection by centWave method (Tautenhahn *et al.* 2008) the following parameter settings were used in XCMS: ppm = 20, snthresh = 10, peak width = 5 to 20 s. Parameter settings used for retention time correction were minfrac = 1, bw = 60 s, mzwid = 0.1D, span = 1, and missing = extra = 0 (Gaquerel *et al.* 2010).

Multiple sequence alignment

DNA and protein sequences were aligned using the Geneious 5.5.7 software (Biomatters, Auckland, New Zealand) with default parameters. For alignment of nucleotide sequences from *TRANSLATION ELONGATION FACTOR 1 ALPHA* (*EF1A*), three different NCBI database

entries were used for Ppn (EF418929, GU191189 and EU080678), one for *N. attenuata* (sequence will be submitted to NCBI) as well as one from *N. tabacum* (D63396). For protein alignment of *N. attenuata* GLA1 (ACZ57767) with its full-length homolog from *N. tabacum*, *Nt*ACRE14 (AAV92888), a previous alignment with genome sequences of tobacco obtained from the solgenomics website (http://solgenomics.net/tools/blast/index.pl) became necessary because the original *Nt*ACRE14 sequence was available at the NCBI database only in a truncated version. Therefore it was blasted (blastn) against two databases ("*N. tabacum* Methylation Filtered Genome TGI:v.1 Contigs" and "*N. tabacum* Methylation Filtered Genome TGI:v1 Processed Reads") available on the solgenomics website and the best hits were used for alignment and full-length protein sequence retrieval of *Nt*ACRE14 (Supplemental Figure S3).

Statistical analysis

Microarray data was analyzed using MeV v4.8 (http://www.tm4.org/mev/), oxylipin and metabolic profiling data was analyzed using Metaboanalyst 2.0 online software (http://www.metaboanalyst.ca/MetaboAnalyst/faces/Home.jsp). One-way analysis of variance (ANOVA) and mean value comparison by the Tukey post-hoc test were calculated using the SPSS Statistics software version 17.0 (SPSS, Chicago, Illinois, USA).

Accession numbers

Data from this article can be found under the following accession numbers: *NaEF1a* (will be submitted to NCBI), Agilent Chip platform (GPL13527; NCBI GEO database), microarray data (will be submitted to NCBI GEO database).

Results

NaGLA1 has no impact on black shank disease progression

To test whether GLA1 directly affects *N. attenuata* defense against Ppn, disease symptom progression (darkish discoloration and beginning necrosis) was monitored and documented photographically in *N. attenuata* wildtype (WT) and two ir-*gla1* lines (stably silenced in *GLA1* expression). In addition, the relative abundance of Ppn *TRANSLATION ELONGATION FACTOR 1 ALPHA* genomic DNA in infected and non-infected *N. attenuata* WT and ir-*gla1* (two lines) plants was quantified by qPCR to assess Ppn growth rates in these genotypes, considering the possibility that symptom development does not necessarily have to correlate with pathogen abundance. GLA1 did not influence disease progression in *N. attenuata* plants infected with Ppn, neither morphologically as documented in Figure 1 since the first visible disease symptoms occurred simultaneously in WT and ir-*gla1* genotypes at 4 dai, nor in form of fungal performance, since qPCR quantification of Ppn abundance at 2.5 and 4 dai did not show any difference between WT and ir-*gla1* lines (Supplemental Figure S4).

GLA1-mediated changes after Ppn infection associated directly to its lipase function

A previous publication focused on the influence of GLA1 on the production of the phytohormone jasmonic acid (JA) and the divinyl ethers colneleic and colnelenic acid during Ppn infection, revealing no impact of GLA1 at the final levels of these oxylipins at 4 days of Ppn

infection (Bonaventure *et al.* 2011). Therefore a less biased approach was taken focusing on GLA1´s enzymatic function as a glycerolipase A1 (Bonaventure *et al.* 2011; Kallenbach *et al.* 2010). Because it is known that Ppn increases lipase A activity (Roy *et al.* 1995; Scherer *et al.* 2002), a lipase activity assay with Ppn-infected *N. attenuata* WT and ir-*gla1* (2 lines) leaf tissue was performed at 4 dai to assess a potential GLA1 contribution to total lipase A activity increased by Ppn. As shown in Figure 2 A, total lipase A activity is not influenced in a GLA1-dependent manner. In agreement to the literature, total lipase A activity was induced by Ppn compared to controls about 4-5 fold, however no difference between WT and ir-*gla1* lines could be observed. To further investigate GLA1´s role as a lipase and whether it could be involved in the production of distinct lysolipids in response to Ppn that possess potential signaling function (Canonne *et al.* 2011; Munnik & Testerink 2009), lipids were extracted from Ppn-infected shoots of WT and two ir-*gla1* lines and various lysolipid species were quantified by LC-MS. Several of those were increased upon Ppn infection at 4 dai (DGMG-18:3, LPC-16:0, LPC-18:0, LPC-18:2, LPC-18:3, LPE-16:0, LPE-18:2, LPI-16:0, LPI-18:2, LPI:18:3, LPG-16:0, LPA:18:2), however without significant differences between WT and both ir-*gla1* lines (Supplemental Figure S5). The only lysolipid species inducible by Ppn (~4-fold in WT) and the induction of which specifically relied on *GLA1* expression (almost no difference in ir-*gla1* plants after Ppn infection compared to controls) turned out to be palmitoleoyl-physphatidylglycerol (LPG-16:1) (Figure 2 B). A strong trend for a GLA1-mediated reduction in levels of Ppn-inducible lysolipids could be also observed for several phosphatidylcholine-derived lysolipids (LPC-16:0, LPC-18:2 and LPC-18:3), as well as monolinolenoyl-digalactosylglycerol (DGMG-18:3), at least for one of the two tested Ppn-infected ir-*gla1 N. attenuata* lines compared to WT (Supplemental Figure S5).

GLA1-dependent changes in oxylipin levels upon Ppn infection

To assess whether Ppn induced the production of oxylipin species different from JA and DVE (Bonaventure *et al.* 2011), another untargeted approach was used to analyze molecules carrying a free carboxyl group. Shoot extracts from Ppn-infected WT and ir-*gla1* plants (4 dai) were enriched in carboxyl-group containing molecules and analyzed by UPLC-qTOF-MS/MS. Already the chromatograms of samples from both genotypes revealed the presence of various ions inducible by Ppn and specifically regulated in a GLA1-dependent manner, including three ions that represent unsaturated C18-fatty acids (oleic acid, linoleic acid and linolenic acid), one ion representing 9-hydroxy-linoleic acid and three other ions likely representing additional oxylipins (Figure 3). Characterization and identification of those compounds was done based on MS/MS-data and by help of commercial standards (Figure 4).

GLA1 has drastic effect on gene expression during Ppn infection

To further explore the role of GLA1 during the infection response to Ppn, a microarray analysis was performed at 2.5 dai using shoot tissue of one *N. attenuata* ir-*gla1* line and WT. Gene expression changes were evaluated with an Agilent custom-array containing 43,533 *N. attenuata* probes and representing approximately 70 to 80% of the *N. attenuata* transcriptome (Gase & Baldwin 2012; Gilardoni *et al.* 2011). When $\log_2$[fold-change (FC) in normalized signal intensity of ir-*gla1* vs. WT probe] was larger or equal to 1, or smaller or equal to -1, respectively, and the *q*-value was lower than 0.05 (corresponding to a false discovery rate (FDR) less than 5%), the respective gene was considered as differentially regulated. The microarray data analysis

revealed that constitutive gene expression between non-infected WT and ir-*gla1* differed only very little (54 genes differentially regulated) with 47 genes up- and 7 down-regulated (Figure 5 A). This difference is however by orders of magnitude smaller compared to that observed during Ppn infection (4192 differentially regulated genes between WT and ir-*gla1*) (Figure 5 B). The majority of those genes (2497) were down- and 1695 genes were up-regulated in ir-*gla1* compared to WT. Only six genes (one encoding for vacuolar processing enzyme 1, another encoding for a NBS-LRR type of disease resistance protein, and four more genes that could not be annotated) were in both treatments differentially up-regulated in *N. attenuata* ir-*gla1* vs. WT shoots. Additional six genes (encoding for senescence-associated protein 13, a NAC domain protein, a beta-1,3-glucanase, a homogentisate-dioxygenase, a tropinone reductase homolog and another gene that could not be annotated) were differentially up-regulated in untreated controls and down-regulated in ir-*gla1* vs. WT during Ppn infection (Figure 5 C). Classified based on Gene Ontology numbers encoding for biological processes in which those genes are involved (Figure 5 D), a major portion of genes differentially regulated after Ppn infection turned out to be implicated in response to stimuli and signaling (22.5%), and another 2% were involved in the regulation of transcription, supporting the hypothesis of a potential signaling role of GLA1 products. While analyzing the microarray data (Supplemental Excel File and Supplemental Tables S6 and S7) in more detail, several genes involved in phytohormone biosynthesis, perception and response were found to be differentially regulated between ir-*gla1* and WT during Ppn infection (Supplemental Table S6), *e.g*. auxin-inducible genes were up-regulated as well as a gene encoding for an auxin-influx transporter, while those that are repressed by auxin, or encode for proteins which remove auxin out of the cell (auxin efflux facilitator) or inactivate

auxin by conjugation to amino acids were down-regulated. In addition, ethylene biosynthesis genes and ethylene-responsive genes were down-regulated in ir-*gla1* compared to WT during Ppn infection, as it could be found also for gibberellin biosynthesis and responsive genes. Genes involved in SA, JA and ABA signaling were affected after Ppn infection in a GLA1-dependent manner, too. Also many genes supposed to be involved in defense response to Ppn and other fungal phytopathogens were differentially regulated between Ppn-infected WT and ir-*gla1 N. attenuata* plants (Supplemental Table S7), such as genes playing a role in cell acidification (Lebrun-Garcia *et al.* 2002; Mathieu *et al.* 1996), mitogen activated protein kinase signaling (Lebrun-Garcia *et al.* 2002; Liu *et al.* 2003; Zhang & Klessig 2000), peroxidation processes and reactive oxygen species production (Able, Guest & Sutherland 2000; Groten & Barz 2000; Lherminier *et al.* 2009; Simon-Plas, Elmayan & Blein 2002; Yoshioka *et al.* 2003), regulation of defense-related secondary metabolism such as phytoalexin production (Bohlmann *et al.* 2002; Yu 1995), cell wall fortification (Day & Graham 2007; La Camera *et al.* 2004), direct antifungal defense (*e.g.* chitinases) (Lan *et al.* 2000; Liu, Ekramoddoullah & Zamani 2005) and genes known to be elicited in the Avr9/Cf-9 system (Rowland *et al.* 2005). In general, such defense-related genes were rather down-regulated in Ppn-infected ir-*gla1* compared to WT, providing a good argument for higher susceptibility of ir-*gla1* plants to Ppn compared to WT which was not confirmed by disease progression monitoring (Figure 1 and Supplemental Figure S4). Interestingly, the expression of several photosynthesis-related genes (Supplemental Excel File) is differentially up-regulated in Ppn-infected ir-*gla1* compared to WT which can be interpreted as higher WT susceptibility to Ppn compared to ir-*gla1*, since it is known for *Phytophthora infestans* that it negatively effects the expression of photosynthetic genes (Gyetvai *et al.* 2012;

Koch, Noga & Strittmatter 1994; Restrepo *et al.* 2005; Schnabel, Strittmatter & Noga 1998) and for *Phytophthora ramorum* that it reduces photosynthetic capacity (Manter, Kelsey & Karchesy 2007).

Abscisic and salicylic acid induction upon Ppn is GLA1-independent

A previous publication focused on the influence of GLA1 on the production of the phytohormone jasmonic acid (JA) and the divinyl ethers colneleic and colnelenic acid during Ppn infection, revealing no impact of GLA1 at the final levels of these oxylipins at 4 days of Ppn infection (Bonaventure *et al.* 2011). Consistent with those previous measurements and in order to extend the knowledge gained from them, and because several genes involved in abscisic (ABA) and salicylic acid (SA) signaling were found to be differentially regulated by GLA1 after Ppn infection (Supplemental Table S6), the influence of GLA1 on the levels of these phytohormones was also studied in a Ppn infection experiment comparing WT and two ir-*gla1* lines. As shown in Supplemental Figure S8, levels of ABA and SA are induced by Ppn at 4 dai. In non-inoculated plants and in early Ppn infection stage (4 and 24 hours after inoculation) levels of both phytohormones were close to the detection limit. Only at 4 dai ABA levels increased up to ~4 nmol per gram fresh weight (gFW^{-1}) and that of SA up to ~10 nmol gFW^{-1} in Ppn-infected plants. However, the levels observed in WT do not differ from those of ir-*gla1* lines, demonstrating that the levels of those phytohormones are not altered in a GLA1-dependent manner.

GLA1 affects secondary metabolites produced after Ppn infection

To check whether the changes in gene expression observed in the microarray analysis (Supplemental Exel File and Supplemental Tables S6 and S7) are translated into changes of polar secondary metabolite levels, a metabolic profiling approach was chosen to quantify differentially (WT versus ir-*gla1* line 1) regulated ions at 2.5 days of Ppn infection using UPLC-microTOF-MS. The time point of 2.5 dai was chosen in consistency to the microarray experiment to allow direct comparison between transcriptomic and metabolomic differences between ir-*gla1* 1 and WT. After separation by retention time via UPLC, metabolites eluting from the column between 125 and 550 seconds and having a mass-to-charge (m/z) ratio between 90 and 1400 were ionized by electrospray ionization (ESI) and analyzed in negative and positive detection modes (see Materials and Methods for a more detailed description). For data processing, ions were considered as differentially regulated when their abundance differed significantly (t-test; $p<0.05$) between sample sets (n=5) from Ppn-infected WT and ir-*gla1* 1 *N. attenuata* shoots and this fold-change (FC) in ion abundance (ir-*gla1* 1 vs. WT) was either equal or greater than 2 or equal or smaller than 0.5 (see Vulcano plots in Figure 6 C and D). As a result, 81 ions were found to be differentially regulated, of which 39 were up- ($2.42<FC<12.44$) and 42 down-regulated ($0.05<FC<0.32$) in ir-*gla1* 1 compared to WT (Figure 6 A-D and Supplemental Table S9). Approximately half of the GLA1-regulated ions could not be annotated by m/z value (considering the potential error in accuracy as ± 0.02) and retention time comparison with entries from public and custom databases (Gaquerel *et al.* 2010). The other half of GLA1-regulated ions could be assigned to the categories lipid derivatives, diterpene glycosides, flavonoids, phytohormones and their derivatives, polyamines and their derivatives, alkaloids, amino acids,

and two categories (phenolic compounds and organic acids) comprising the residual compounds not assignable to other categories (see Figure 6 A and B and Supplemental Table S9). As an overall pattern, dimalonylated diterpene glycosides were found to be down-regulated in ir-*gla1* vs. WT, as well as the majority of polyamine derivatives, whereas flavonoids were up-regulated (Supplemental Table S9).

Discussion

Impact of GLA1 on Ppn performance on N. attenuata

As shown in Bonaventure *et al.* (2011), *NaGLA1* transcription is induced by the phytopathogens *Fusarium oxysporum* and Ppn. During analysis of NCBI blastx results, *Na*GLA1 turned out to be highly homolog to the *Nt*ACRE14 (*Nicotiana tabacum* Avr9/Cf-9 rapidly elicited protein 14) sequence, the transcription of which was previously shown to be rapidly elicited in transgenic tobacco Bright Yellow-2 cells expressing the tomato Cf-9 receptor capable of perceiving the Avr9 peptide from the phytopathogenic fungus *Cladosporium fulvum* (Supplemental Figure S10) (Rowland *et al.* 2005). Thus it was tempting to hypothesize for GLA1 a rather general role in plant defense against fungal pathogens. To get a first impression on whether GLA1 really plays a major role in *N. attenuata´*s interaction with Ppn, symptomatic disease progression was compared between *N. attenuata* WT and ir-*gla1* plants (Figure 1), resulting in no difference between both genotypes. This simultaneous symptom development could have been caused by similar growth rates of Ppn in infected WT and ir-*gla1* plants. Therefore Ppn abundance was quantified by qPCR to test whether this assumption applies or not (Supplemental Figure S4). Indeed Ppn growth rate was similar between WT and ir-*gla1*. However, a biological relevance of GLA1 in *N. attenuata´*s interaction with Ppn or other phytopathogenic fungi cannot be ruled out. As described in the method section, a rather harsh "needle-prick" method was chosen to inoculate *N. attenuata* with actively growing Ppn culture, almost forcing the pathogen to enter the plant and causing it to die within only a few (5-7) days.

This artificial experimental setup did not reflect nature at all, where *Phytophthora* spores are usually disseminated by wind or water (Granke *et al.* 2009) and need to overcome tough physical plant barriers (Judelson & Blanco 2005). Besides, such moist and cool growth conditions are not that common in desert environments like the natural habitat of *N. attenuata* during its growing season. Unfortunately, no appropriate pathosystem exploitable for experiments with phytopathogenic fungi and *N. attenuata* had been established so far. Pilot experiments also with other phytopathogenic fungi (*Fusarium oxysporum*, *Botrytis cinerea*, *Alternaria brassicicola*, *Alternaria alternata* and a *Phoma sp*.) and other inoculation methods (spore suspension instead of actively growing mycelium; different plant developmental stages; application by dipping roots or spraying plantlets with spore suspension) turned out to be even less suitable, hinting to a great basal or a quite early occurring age-related resistance of *N. attenuata* similar to that observed with *Phytophthora infestans*-attacked *Nicotiana benthiamana* (Shibata, Kawakita & Takemoto 2010), at least regarding the fungal pathogens tested (personal observations). Therefore and despite its disadvantages, the use of Ppn and the "needle-prick" method appeared still most appropriate for the experiments performed in this study. Besides, a recent study on metabolite production during early Ppn infection (1 hour and 2 days after inoculation) of tobacco used a similar inoculation method (Ppn plug directly on plant) and similar plant developmental stage (shoots having 4-5 leaves) for their experiment (Cho *et al.* 2012). The establishment of a proper *N. attenuata* pathosystem using native fungal pathogens suitable for lab experiments was subject of another study in which also *N. attenuata* ir-*gla1* genotype was compared to WT, revealing that GLA1 indeed has big impact on disease progression of certain phytopathogens (data not shown; manuscript in preparation). A lot of defense-related genes could be observed to

be down-regulated in Ppn-infected *N. attenuata* ir-*gla1* compared to WT plants (Supplemental Table S7), meaning that their transcription relies on *GLA1* expression induced by Ppn. These differentially down-regulated genes are known to be either directly involved in biotic stress-mediated signaling processes (including also mitogen activated protein kinases and WRKY transcription factors) (Dellagi *et al.* 2000; Skibbe *et al.* 2008; Zhang & Klessig 2000), active plant defense against fungal pathogens (*e.g.* genes encoding chitinases) (Lan *et al.* 2000) or rather passive defense mechanisms (*e.g.* genes involved in phenylpropanoid biosynthesis pathway necessary for lignification or participating in cutin biosynthesis, thereby leading to cell wall enforcement) (Cho *et al.* 2012; La Camera *et al.* 2004). These changes in gene expression were partly reflected in secondary metabolism (Figure 6 and Supplemental Table S9). For instance, ions assigned to the phenolic compound sinapoyl malate as well as the majority of ions representing phenylpropanoid-derived polyamine conjugates (phenolamides) were found to be differentially down-regulated in Ppn-infected ir-*gla1* plants compared to WT. However, ions assigned to shikimic acid as metabolic precursor for phenylalanine biosynthesis [and therefore lignin components produced via the phenylalanine ammonia-lyase (PAL) pathway] were differentially up-regulated in ir-*gla1* compared to WT, as well as flavonoids which are not implicated in cell wall enforcement (Saedler & Baldwin 2004), indicating that GLA1 controls rather specifically the up-regulation of genes and secondary metabolites involved in lignifications after Ppn attack. In other words, silencing *GLA1* expression results after Ppn attack in the accumulation of initial amino acid precursers that could have been used for the biosynthesis of lignin and phenolamides and which are now better available for flavonoid biosynthesis. The differential down-regulation of ions representing phenolamides in Ppn-infected

ir-*gla1* plants compared to *N. attenuata* WT suggests an enhanced pathogen susceptibility of ir-*gla1* not only because of a potentially reduced cell wall fortification, but also because of a potential lack of direct fungitoxic effects caused by some of these compounds (Bassard *et al* 2010). Besides, conjugation to phenylpropanoid-derived moieties can alter the polyamine homeostasis by removal of free polyamines, and also the ratio between individual polyamines (*e.g*. spermidine, spermidine and putrescine) (Bassard *et al.* 2010). The ratio of spermine together with spermidine compared to putrescine is critical for the decision on cell fate during pathogen attack (undergoing programmed cell death in form of hypersensitive response or starting a rescue attempt by activation of other defense responses) (Bassard *et al.* 2010). Spermine and Spermidine catabolism produces H_2O_2 and triggers hypersensitive response by significant contribution to the second phase of an oxidative burst, a process antagonized by putrescine (Bassard *et al.* 2010). In comparison to free polyamines, phenolamides possess also by far higher reactive oxygen species scavenging capabilities leading to cell protection (Edreva, Velikova & Tsonev 2007). As shown in Supplemental Table S9, the majority of phenolamides differentially down-regulated in Ppn-infected *N. attenuata* ir-*gla1* vs. WT could be annotated to spermidine conjugates, while free putrescine was differentially up-regulated, therefore it would be tempting to speculate that ir-*gla1* plants tend more to the activation of alternative defense responses and less to hypersensitive cell death, an idea that could not be confirmed by morphological observations following symptomatic disease progression (Figure 1). In addition, the metabolic profiling after Ppn infection revealed dimalonylated 17-hydroxygeranyllinalool diterpene glycosides (HGL-DTGs) as differentially down-regulated in ir-*gla1* plants after Ppn infection. The malonylation of these anti-herbivore defensive metabolites was shown to depend

on jasmonate and a hydroxyprolin-rich systemin glycopeptide (ppHS) in *N. attenuata* (Heiling *et al.* 2010). Since jasmonic acid (JA) levels are known not to differ during Ppn infection in *N. attenuata* ir-*gla1* and WT lines (Bonaventure *et al.* 2011), it might be possible that GLA1 influences the activation of ppHS or other processes involved in HGL-DTG malonylation independently from JA. Nothing is published on a potential antimicrobial role of HGL-DTGs so far, therefore it can be only speculated about a possible defensive function in *N. attenuata* against Ppn or other phytopathogens.

Influence of GLA1 on phytohormone balance during Ppn infection

Previous studies demonstrated a role of GLA1 in the production of jasmonic acid upon herbivory and wounding, however not during Ppn infection (Bonaventure *et al.* 2011; Kallenbach *et al.* 2010). This could be explained either by compensation due to high activity of residual GLA1 enzyme levels in *GLA1*-silenced *N. attenuata* plants, or by the action of redundant lipases activated during Ppn infection, similarly as already described for GLA1-related lipases from *Arabidopsis* in response to the bacterial pathogen *Pseudomonas syringae* pv. *tomato* DC3000 (Ellinger, Stingl, Kubigsteltig, Bals, Juenger, Pollmann, Berger, Schuenemann & Mueller 2010). There was also no GLA1-mediated difference detectable in abscisic (ABA) and salicylic acid (SA) levels during Ppn infection (Supplemental Figure S8). However, genes involved in either the biosynthesis of or the response to those phytohormones (JA, ABA and SA) were differentially regulated at 2.5 days after Ppn infection between *N. attenuata* WT and ir-*gla1* (Supplemental Table S6), indicating that there may exist differences in the levels of those

phytohormones at least in this time gap (between 1 and 4 days after Ppn infection) which was not covered by the phytohormone analysis. Regarding expression of genes involved in ABA, SA and JA biosynthesis it is also necessary to consider that not all changes in transcription translate to changes in protein and metabolism. And regarding the responsiveness of genes induced by those phytohormones it has to be taken also into account that the expression of many stress responsive genes is regulated by multiple different stimuli (Atkinson & Urwin 2012; Walley *et al.* 2007; Xiong, Schumaker & Zhu 2002). The microarray analysis revealed also differences in gene expression between Ppn-infected ir-*gla1* and WT pointing to reduced ethylene and gibberellin and increased auxin levels in ir-*gla1* vs. WT. Unfortunately those had not been quantified during Ppn infection and therefore it can be only speculated whether those change in a GLA1-dependent manner.

GLA1-specific changes in oxylipin and lysolipid production during Ppn infection

Focusing more on GLA1´s known enzymatic function (Bonaventure *et al.* 2011; Kallenbach *et al.* 2010), it was hypothesized that it could be an important lipase A contributing to the described increase in activity for this lipase type detected after *Phytophthora* infection (Roy *et al.* 1995; Scherer *et al.* 2002). This study demonstrated that this is not the case (Figure 2 A). Furthermore a potentially important role of GLA1 in lipid recycling during plant autophagy-like processes which would have most likely lead to substantial changes in lipase activity in Ppn-infected ir-*gla1* and WT *N. attenuata* plants can be also ruled out (Hong *et al.* 2000; Moreau 1987; Munnik & Testerink 2009; Talbot & Kershaw 2009). A GLA1-dependent impact on

chloroplast membrane fluidity and lipid composition during *N. attenuata´*s defense against Ppn important for proper chloroplast function has to be considered, too (Yamamoto, Ford & Barber 1981). In this case the changes could be rather minute but specific and therefore barely detectable in the total lipase A activity analysis in which other lipases, *i.e.* patatin-like lipases, are likely to be the dominant contributors to total lipase A activity (La Camera *et al.* 2005; La Camera *et al.* 2004). Indeed GLA1 appears to regulate quite specifically the release of very distinct lysolipids as demonstrated for palmitoleoyl-lysophosphatidylglycerol (LPG-16:1) (Figure 2 B), probably extendable to several lysophosphatidylcholine species (LPC-16:0, LPC-18:2 and LPC-18:3) as well as monolinolenoyl-digalactosylglycerol (DGMG-18:3) (Supplemental Figure S5), and maybe including also lysolipid species that had not been quantified. This is especially interesting regarding the relative abundance and distribution of phoshphatidylcholine and galactolipids in the chloroplast as the compartment to which GLA1 is localized (Kallenbach *et al.* 2010). The galactolipids digalactosyl-diacylglycerol (DGDG) and monogalactosyl-diacylglycerol (MGDG) constitute up to 80% of all chloroplast lipids, emphasizing the potential of GLA1 by being able to generate detectable differences in DGMG-18:3 levels from these highly abundant lipid species as substrate (Nakamura *et al.* 2003). In contrast to galactolipids, phosphatidylcholine is restricted to the outer surface of the chloroplast envelope membrane (Dorne *et al.* 1985). The lysolipid data (Supplemental Figure S5) therefore suggests that GLA1 has either direct access to the chloroplast envelope membrane or indirectly leads to the production of lysophosphatidylcholine, *e.g*. by controlling other lipases. Lysophosphatidylcholines are known to be important signaling molecules in plants leading to cytoplasmic acidification upon elicitor-activation of a phospholipase A2 (Viehweger, Dordschbal

& Roos 2002), a process occurring also during the tobacco response to *Phytophthora* elicitation (Kasparovsky *et al.* 2004). In a previous study on GLA1's influence on lysolipid levels in leaves during early JA biosynthesis after wounding and simulated insect herbivory, substrates for GLA1 were found to be recruited mainly from the same lipid classes mentioned also as potential GLA1 substrates in this study, *i.e*. galactolipids, phosphatidylglycerol and phosphatidylcholine (Bonaventure *et al.* 2011). That pevious study showed also that occurrence of distinct lysolipid products associated with the early JA burst allowing for conclusions on *sn*-1 or *sn*-2 lipase specificity of GLA1 (Bonaventure *et al.* 2011). The obtained data gave rise to the hypothesis that GLA1 possesses – despite its *in vitro* demonstrated *sn*-1 specificity (Kallenbach *et al.* 2010) – either both, *sn*-1 and *sn*-2 lipase activities *in planta* and has access to the chloroplast envelope membrane, or indirectly changes the activity of other lipases with *sn*-2 activity, therefore suggesting that these alternative scenarios might apply also for GLA1's role during the *N. attenuata*-Ppn interaction (Bonaventure *et al.* 2011).

Apart from the production of lysolipids, GLA1 participates in the release of oleic, linoleic and linolenic acid, as well as the biogenesis of 9-hydroxy-linoleic acid (Figures 3 and 4), compounds known to be inducible in plants by *Phytophthora* elicitors (Cho *et al.* 2012; Gobel *et al.* 2002; Kachroo & Kachroo 2009; Shah 2005). Depending on the tested pathogen and the used concentration those compounds exhibit antifungal activity *in vitro* (Cantrell *et al.* 2008; Walters *et al.* 2004), however at least linoleic and linolenic acid seem to be – in contrast to 9-hydroxy-linoleic acid – ineffective against Ppn (Prost *et al.* 2005). And *in vitro* observed inhibition of mycelial growth and spore germination not necessarily reflect the *in planta* situation (Fauconnier *et al.* 2008). Besides the ability of linoleic and linolenic acid to inhibit mycelial growth of several

fungal phytopathogens *in vitro*, the exogenous application of those is known to induce systemic resistance in potato against *Phytophthora infestans* as additional defense mechanism against phytopathogenic fungi (Cohen, Gisi & Mosinger 1991). Although the mechanism is unclear, systemic resistance is induced probably not by the fatty acids themselves, but possibly via signaling compounds produced by the plant in response to the interaction of the fatty acids with the plasma membrane (Cohen *et al.* 1991).

Taken together, the unsaturated C18-fatty acids, the oxylipin species and the lysolipids differentially regulated between Ppn-infected WT and ir-*gla1 N. attenuata* plants (or other second messengers induced thereof) could have a signaling function, explaining also the large number of genes differentially regulated between *N. attenuata* WT and ir-*gla1* after Ppn infection (Figures 5 and Supplemental Excel File) partly reflected in secondary metabolite changes (Figure 6 and Supplemental Table S9). This hypothesis is briefly summarized in the model illustrated in Figure 7. However, it has to be considered that the observed results could have been also caused not directly by GLA1 activity, but mediated also indirectly, *e.g.* by the action of other lipases stimulated by the release of free fatty acids by GLA1 and the products derived thereof (Kachroo & Kachroo 2009; Cohen *et al.* 1991). Referring back again to the observed increase of total lipase A activity after Ppn infection, it is noteworthy that at least two members of the dominating patatin class lipases in tobacco possess both, *sn*-1 and *sn*-2 lipid cleavage site activity (La Camera *et al.* 2004), whereas GLA1 exhibits – at least *in vitro* – *sn*-1 specificity (Kallenbach *et al.* 2010). This is important because Cho *et al.* (2012) found for Ppn-infected tobacco that oxidation of phospholipid-esterified fatty acids occurs preferentially at the *sn*-2 position and the authors further assumed based on their data that those oxidized fatty acids

are more likely to be hydrolyzed from phospholipids by lipases. If these findings from tobacco also apply to its wild relative *N. attenuata*, the *sn*-1 specific GLA1 would be less likely the lipase directly responsible for the production of 9-hydroxy-linoleic acid and other oxylipins, but more of a regulator of the activity from other lipases hydrolyzing lipids at the *sn*-2 position, suggesting once more a rather indirect role of GLA1 during *N. attenuata´*s defense signaling against Ppn.

Acknowledgements

We thank the Max Planck Society for financial support and Prof. Dr. Jianqiang Wu for providing the Ppn culture.

References

Able A.J., Guest D.I. & Sutherland M.W. (2000) Hydrogen peroxide yields during the incompatible interaction of tobacco suspension cells inoculated with *Phytophthora nicotianae*. *Plant Physiology*, **124**, 899-910.

Amelot N., de Borne F.D., Clemente H.S., Mazars C., Grima-Pettenati J. & Briere C. (2012) Transcriptome analysis of tobacco BY-2 cells elicited by cryptogein reveals new potential actors of calcium-dependent and calcium-independent plant defense pathways. *Cell Calcium*, **51**, 117-130.

Atkinson N.J. & Urwin P.E. (2012) The interaction of plant biotic and abiotic stresses: from genes to the field. *Journal of Experimental Botany*, **63**, 3523-3543.

Bassard J.E., Ullmann P., Bernier F. & Werck-Reichhart D. (2010) Phenolamides: bridging polyamines to the phenolic metabolism. *Phytochemistry*, **71**, 1808-1824.

Bohlmann J., Stauber E.J., Krock B., Oldham N.J., Gershenzon J. & Baldwin I.T. (2002) Gene expression of 5-epi-aristolochene synthase and formation of capsidiol in roots of *Nicotiana attenuata* and *N. sylvestris*. *Phytochemistry*, **60**, 109-116.

Bonaventure G., Schuck S. & Baldwin I.T. (2011) Revealing complexity and specificity in the activation of lipase-mediated oxylipin biosynthesis: a specific role of the *Nicotiana attenuata* GLA1 lipase in the activation of jasmonic acid biosynthesis in leaves and roots. *Plant Cell Environ*, **34**, 1507-1520.

Burdon J.J. & Thrall P.H. (2009) Coevolution of plants and their pathogens in natural habitats. *Science*, **324**, 755-756.

Canonne J., Froidure-Nicolas S. & Rivas S. (2011) Phospholipases in action during plant defense signaling. *Plant Signal Behav*, **6**, 13-18.

Cantrell C.L., Case B.P., Mena E.E., Kniffin T.M., Duke S.O. & Wedge D.E. (2008) Isolation and identification of antifungal fatty acids from the basidiomycete *Gomphus floccosus*. *J Agric Food Chem*, **56**, 5062-5068.

Carlson S.R., Wolff M.F., Shew H.D. & Wernsman E.A. (1997) Inheritance of resistance to race 0 of *Phytophthora parasitica* var. *nicotianae* from the flue-cured tobacco cultivar Coker 371-Gold. *Plant Disease*, **81**, 1269-1274.

Cho K., Kim Y., Wi S.J., Seo J.B., Kwon J., Chung J.H., Park K.Y. & Nam M.H. (2012) Non-targeted metabolite profiling in compatible pathogen-inoculated tobacco (*Nicotiana tabacum* L. cv Wisconsin 38) using UPLC-Q-TOF mass spectrometry. *J Agric Food Chem*, **60**, 11015-11028.

Cohen Y., Gisi U. & Mosinger E. (1991) Systemic resistance of potato plants against *Phytophthora infestans* induced by unsaturated fatty acids. *Physiological and Molecular Plant Pathology*, **38**, 255-263.

Colas V., Lacourt I., Ricci P., Vanlerberghe-Masutti F., Venard P., Poupet A. & Panabieres F. (1998) Diversity of virulence in *Phytophthora parasitica* on tobacco, as reflected by nuclear RFLPs. *Phytopathology*, **88**, 205-212.

Day B. & Graham T. (2007) The plant host pathogen interface: cell wall and membrane dynamics of pathogen-induced responses. *Ann N Y Acad Sci*, **1113**, 123-134.

Dellagi A., Heilbronn J., Avrova A.O., Montesano M., Palva E.T., Stewart H.E., Toth I.K., Cooke D.E.L., Lyon G.D. & Birch P.R.J. (2000) A potato gene encoding a WRKY-like

transcription factor is induced in interactions with *Erwinia carotovora* subsp *atroseptica* and *Phytophthora infestans* and is coregulated with class I endochitinase expression. *Molecular Plant-Microbe Interactions*, **13**, 1092-1101.

Dorne A.J., Joyard J., Block M.A. & Douce R. (1985) Localization of phosphatidylcholine in outer envelope membrane of spinach chloroplasts. *J Cell Biol*, **100**, 1690-1697.

Edreva A.M., Velikova V.B. & Tsonev T.D. (2007) Phenylamides in plants. *Russian Journal of Plant Physiology*, **54**, 287-301.

Ellinger D., Stingl N., Kubigsteltig, II, Bals T., Juenger M., Pollmann S., Berger S., Schuenemann D. & Mueller M.J. (2010) DONGLE and DEFECTIVE IN ANTHER DEHISCENCE1 lipases are not essential for wound- and pathogen-induced jasmonate biosynthesis: redundant lipases contribute to jasmonate formation. *Plant Physiology*, **153**, 114-127.

Fammartino A., Cardinale F., Gobel C., Mene-Saffrane L., Fournier J., Feussner I. & Esquerre-Tugaye M.T. (2007) Characterization of a divinyl ether biosynthetic pathway specifically associated with pathogenesis in tobacco. *Plant Physiology*, **143**, 378-388.

Fauconnier M.L., Rojas-Beltran J., Dupuis B., Delaplace P., Frettinger P., Gosset V. & du Jardin P. (2008) Changes in oxylipin synthesis after *Phytophthora infestans* infection of potato leaves do not correlate with resistance. *Plant Physiology and Biochemistry*, **46**, 823-831.

Gaquerel E., Heiling S., Schoettner M., Zurek G. & Baldwin I.T. (2010) Development and validation of a liquid chromatography-electrospray ionization-time-of-flight mass

spectrometry method for induced changes in *Nicotiana attenuata* leaves during simulated herbivory. *J Agric Food Chem*, **58**, 9418-9427.

Gase K. & Baldwin I.T. (2012) Transformational tools for next-generation plant ecology: manipulation of gene expression for the functional analysis of genes. *Plant Ecology and Diversity*, **5**, 485-490.

Gilardoni P.A., Hettenhausen C., Baldwin I.T. & Bonaventure G. (2011) *Nicotiana attenuata* LECTIN RECEPTOR KINASE1 suppresses the insect-mediated inhibition of induced defense responses during *Manduca sexta* herbivory. *Plant Cell*, **23**, 3512-3532.

Gobel C., Feussner I., Hamberg M. & Rosahl S. (2002) Oxylipin profiling in pathogen-infected potato leaves. *Biochim Biophys Acta*, **1584**, 55-64.

Gobel C., Feussner I., Schmidt A., Scheel D., Sanchez-Serrano J., Hamberg M. & Rosahl S. (2001) Oxylipin profiling reveals the preferential stimulation of the 9-lipoxygenase pathway in elicitor-treated potato cells. *J Biol Chem*, **276**, 6267-6273.

Granke L.L., Windstam S.T., Hoch H.C., Smart C.D. & Hausbeck M.K. (2009) Dispersal and movement mechanisms of *Phytophthora capsici* sporangia. *Phytopathology*, **99**, 1258-1264.

Groten K. & Barz W. (2000) Elicitor-induced defence reactions in cell suspension cultures of soybean cultivars. *Z Naturforsch C*, **55**, 718-730.

Gyetvai G., Sonderkaer M., Gobel U., Basekow R., Ballvora A., Imhoff M., Kersten B., Nielsen K.L. & Gebhardt C. (2012) The transcriptome of compatible and incompatible interactions of potato (*Solanum tuberosum*) with *Phytophthora infestans* revealed by DeepSAGE analysis. *Plos One*, **7**.

Heiling S., Schuman M.C., Schoettner M., Mukerjee P., Berger B., Schneider B., Jassbi A.R. & Baldwin I.T. (2010) Jasmonate and ppHsystemin regulate key malonylation steps in the biosynthesis of 17-hydroxygeranyllinalool diterpene glycosides, an abundant and effective direct defense against herbivores in *Nicotiana attenuata*. *Plant Cell*, **22**, 273-292.

Hong Y.W., Wang T.W., Hudak K.A., Schade F., Froese C.D. & Thompson J.E. (2000) An ethylene-induced cDNA encoding a lipase expressed at the onset of senescence. *Proceedings of the National Academy of Sciences of the United States of America*, **97**, 8717-8722.

Jones A.M., Chattopadhyay A., Shukla M., Zon J. & Saxena P.K. (2012) Inhibition of phenylpropanoid biosynthesis increases cell wall digestibility, protoplast isolation, and facilitates sustained cell division in American elm (*Ulmus americana*). *BMC Plant Biology*, **12**, 75.

Jones JD, Dangl JL (2006) The plant immune system. Nature **444,** 323-329

Judelson H.S. & Blanco F.A. (2005) The spores of *Phytophthora*: weapons of the plant destroyer. *Nat Rev Microbiol*, **3**, 47-58.

Kachroo A. & Kachroo P. (2009) Fatty acid-derived signals in plant defense. *Annual Review of Phytopathology*, **47**, 153-176.

Kallenbach M., Alagna F., Baldwin I.T. & Bonaventure G. (2010) *Nicotiana attenuata* SIPK, WIPK, NPR1, and fatty acid-amino acid conjugates participate in the induction of jasmonic acid biosynthesis by affecting early enzymatic steps in the pathway. *Plant Physiology*, **152**, 96-106.

Kallenbach M., Gilardoni P.A., Allmann S., Baldwin I.T. & Bonaventure G. (2011) C-12 derivatives of the hydroperoxide lyase pathway are produced by product recycling through lipoxygenase-2 in *Nicotiana attenuata* leaves. *New Phytologist*, **191**, 1054-1068.

Kasparovsky T., Blein J.P. & Mikes V. (2004) Ergosterol elicits oxidative burst in tobacco cells via phospholipase A2 and protein kinase C signal pathway. *Plant Physiology and Biochemistry*, **42**, 429-435.

Kasparovsky T., Milat M.L., Humbert C., Blein J.P., Havel L. & Mikes V. (2003) Elicitation of tobacco cells with ergosterol activates a signal pathway including mobilization of internal calcium. *Plant Physiology and Biochemistry*, **41**, 495-501.

Keen N.T. (1990) Gene-for-gene complementarity in plant-pathogen interactions. *Annu Rev Genet*, **24**, 447-463.

Kemen E. & Jones J.D.G. (2012) Obligate biotroph parasitism: can we link genomes to lifestyles? *Trends in Plant Science*, **17**, 448-457.

Kistner C. & Matamoros M. (2005) RNA isolation using phase extraction and LiCl precipitation. *AJ Marquez, Editorial Director. Lotus japonicus Handbook. Springer Verlag, Dordrecht, The Netherlands*, 123–124.

Koch C., Noga G. & Strittmatter G. (1994) Photosynthetic electron-transport is differentially affected during early stages of cultivar/race-specific interactions between potato and *Phytophthora infestans*. *Planta*, **193**, 551-557.

Krings M., Taylor T.N. & Dotzler N. (2011) The fossil record of the Peronosporomycetes (Oomycota). *Mycologia*, **103**, 455-457.

Krings M., Taylor T.N., Hass H., Kerp H., Dotzler N. & Hermsen E.J. (2007) Fungal endophytes in a 400-million-yr-old land plant: infection pathways, spatial distribution, and host responses. *New Phytologist*, **174**, 648-657.

Krugel T., Lim M., Gase K., Halitschke R. & Baldwin I.T. (2002) *Agrobacterium*-mediated transformation of *Nicotiana attenuata*, a model ecological expression system. *Chemoecology*, **12**, 177-183.

Kunkel B.N. & Brooks D.M. (2002) Cross talk between signaling pathways in pathogen defense. *Current Opinion in Plant Biology*, **5**, 325-331.

La Camera S., Geoffroy P., Samaha H., Ndiaye A., Rahim G., Legrand M. & Heitz T. (2005) A pathogen-inducible patatin-like lipid acyl hydrolase facilitates fungal and bacterial host colonization in *Arabidopsis*. *Plant Journal*, **44**, 810-825.

La Camera S., Gouzerh G., Dhondt S., Hoffmann L., Fritig B., Legrand M. & Heitz T. (2004) Metabolic reprogramming in plant innate immunity: the contributions of phenylpropanoid and oxylipin pathways. *Immunological Reviews*, **198**, 267-284.

Lan H.Y., Tian Y.C., Wang C.H., Liu G.Z., Zhang L.H., Wang L.L. & Chen Z.H. (2000) Studies of transgenic tobacco plants expressing beta-1,3-glucanase and chitinase genes and their potential for fungal resistance. *Yi Chuan Xue Bao*, **27**, 70-77.

Lebrun-Garcia A., Chiltz A., Gout E., Bligny R. & Pugin A. (2002) Questioning the role of salicylic acid and cytosolic acidification in mitogen-activated protein kinase activation induced by cryptogein in tobacco cells. *Planta*, **214**, 792-797.

Lherminier J., Elmayan T., Fromentin J., Elaraqui K.T., Vesa S., Morel J., Verrier J.L., Cailleteau B., Blein J.P. & Simon-Plas F. (2009) NADPH oxidase-mediated reactive

oxygen species production: subcellular localization and reassessment of its role in plant defense. *Molecular Plant-Microbe Interactions*, **22**, 868-881.

Liu J.J., Ekramoddoullah A.K. & Zamani A. (2005) A class IV chitinase is up-regulated by fungal infection and abiotic stresses and associated with slow-canker-growth resistance to *Cronartium ribicola* in western white pine (*Pinus monticol*a). *Phytopathology*, **95**, 284-291.

Liu Y.D., Jin H.L., Yang K.Y., Kim C.Y., Baker B. & Zhang S.Q. (2003) Interaction between two mitogen-activated protein kinases during tobacco defense signaling. *Plant Journal*, **34**, 149-160.

Manter D.K., Kelsey R.G. & Karchesy J.J. (2007) Photosynthetic declines in *Phytophthora ramorum*-infected plants develop prior to water stress and in response to exogenous application of elicitins. *Phytopathology*, **97**, 850-856.

Mathieu Y., Lapous D., Thomine S., Lauriere C. & Guern J. (1996) Cytoplasmic acidification as an early phosphorylation-dependent response of tobacco cells to elicitors. *Planta*, **199**, 416-424.

Moreau R.A. (1987) The involvement of membrane-degrading enzymes during infection of potato leaves by *Phytophthora infestans*. *ACS Symposium Series*, **325**, 343-354.

Munnik T. & Testerink C. (2009) Plant phospholipid signaling: "in a nutshell". *Journal of Lipid Research*, **50**, S260-S265.

Nakamura Y., Arimitsu H., Yamaryo Y., Awai K., Masuda T., Shimada H., Takamiya K. & Ohta H. (2003) Digalactosyldiacylglycerol is a major glycolipid in floral organs of *Petunia hybrida*. *Lipids*, **38**, 1107-1112.

Nifong J.M., Nicholson J.S., Shew H.D. & Lewis R.S. (2011) Variability for resistance to *Phytophthora nicotianae* within a collection of *Nicotiana rustica* accessions. *Plant Disease*, **95**, 1443-1447.

Prost I., Dhondt S., Rothe G., Vicente J., Rodriguez M.J., Kift N., Carbonne F., Griffiths G., Esquerre-Tugaye M.T., Rosahl S., Castresana C., Hamberg M. & Fournier J. (2005) Evaluation of the antimicrobial activities of plant oxylipins supports their involvement in defense against pathogens. *Plant Physiology*, **139**, 1902-1913.

Restrepo S., Myers K.L., del Pozo O., Martin G.B., Hart A.L., Buell C.R., Fry W.E. & Smart C.D. (2005) Gene profiling of a compatible interaction between *Phytophthora infestans* and *Solanum tuberosum* suggests a role for carbonic anhydrase. *Molecular Plant-Microbe Interactions*, **18**, 913-922.

Rowland O., Ludwig A.A., Merrick C.J., Baillieul F., Tracy F.E., Durrant W.E., Fritz-Laylin L., Nekrasov V., Sjolander K., Yoshioka H. & Jones J.D. (2005) Functional analysis of *Avr9/Cf-9 rapidly elicited* genes identifies a protein kinase, ACIK1, that is essential for full Cf-9-dependent disease resistance in tomato. *Plant Cell*, **17**, 295-310.

Roy S., Pouenat M.L., Caumont C., Cariven C., Prevost M.C. & Esquerretugaye M.T. (1995) Phospholipase-activity and phospholipid patterns in tobacco cells treated with fungal elicitor. *Plant Science*, **107**, 17-25.

Saedler R. & Baldwin I.T. (2004) Virus-induced gene silencing of jasmonate-induced direct defences, nicotine and trypsin proteinase-inhibitors in *Nicotiana attenuata*. *J Exp Bot*, **55**, 151-157.

Scherer G.F.E., Paul R.U., Holk A. & Martinec J. (2002) Down-regulation by elicitors of phosphatidylcholine-hydrolyzing phospholipase C and up-regulation of phospholipase A in plant cells. *Biochemical and Biophysical Research Communications*, **293**, 766-770.

Schnabel G., Strittmatter G. & Noga G. (1998) Changes in photosynthetic electron transport in potato cultivars with different field resistance after infection with *Phytophthora infestans*. *Journal of Phytopathology-Phytopathologische Zeitschrift*, **146**, 205-210.

Schuck S., Camehl I., Gilardoni P.A., Oelmueller R., Baldwin I.T. & Bonaventure G. (2012) HSPRO controls early *Nicotiana attenuata* seedling growth during interaction with the fungus *Piriformospora indica*. *Plant Physiology*, **160**, 929-943.

Shah J. (2005) Lipids, lipases, and lipid-modifying enzymes in plant disease resistance. *Annu Rev Phytopathol*, **43**, 229-260.

Shibata Y., Kawakita K. & Takemoto D. (2010) Age-related resistance of Nicotiana benthamiana against hemibiotrophic pathogen Phytophthora infestans requires both ethylene- and salicylic acid-mediated signaling pathways. *Molecular Plant-Microbe Interactions*, **23**, 1130-1142.

Simon-Plas F., Elmayan T. & Blein J.P. (2002) The plasma membrane oxidase NtrbohD is responsible for AOS production in elicited tobacco cells. *Plant Journal*, **31**, 137-147.

Skibbe M., Qu N., Galis I. & Baldwin I.T. (2008) Induced plant defenses in the natural environment: *Nicotiana attenuata* WRKY3 and WRKY6 coordinate responses to herbivory. *Plant Cell*, **20**, 1984-2000.

Strullu-Derrien C., Kenrick P., Rioult J.P. & Strullu D.G. (2011) Evidence of parasitic Oomycetes (Peronosporomycetes) infecting the stem cortex of the Carboniferous seed

fern *Lyginopteris oldhamia*. *Proceedings of the Royal Society B-Biological Sciences*, **278**, 675-680.

Takemoto D., Hardham A.R. & Jones D.A. (2005) Differences in cell death induction by *Phytophthora* elicitins are determined by signal components downstream of MAP kinase kinase in different species of *Nicotiana* and cultivars of *Brassica rapa* and *Raphanus sativus*. *Plant Physiology*, **138**, 1491-1504.

Talbot N.J. & Kershaw M.J. (2009) The emerging role of autophagy in plant pathogen attack and host defence. *Current Opinion in Plant Biology*, **12**, 444-450.

Tautenhahn R., Bottcher C. & Neumann S. (2008) Highly sensitive feature detection for high resolution LC/MS. *BMC Bioinformatics*, **9**, 504.

Tusher V.G., Tibshirani R. & Chu G. (2001) Significance analysis of microarrays applied to the ionizing radiation response (vol 98, pg 5116, 2001). *Proceedings of the National Academy of Sciences of the United States of America*, **98**, 10515-10515.

Van der Biezen E.A. & Jones J.D. (1998) Plant disease-resistance proteins and the gene-for-gene concept. *Trends Biochem Sci*, **23**, 454-456.

van Jaarsveld E., Wingfield M.J. & Drenth A. (2002) Evaluation of tobacco cultivars for resistance to races of *Phytophthora nicotianae* in South Africa. *Journal of Phytopathology*, **150**, 456-462.

Vellosillo T., Martinez M., Lopez M.A., Vicente J., Cascon T., Dolan L., Hamberg M. & Castresana C. (2007) Oxylipins produced by the 9-lipoxygenase pathway in *Arabidopsis* regulate lateral root development and defense responses through a specific signaling cascade. *Plant Cell*, **19**, 831-846.

Viehweger K., Dordschbal B. & Roos W. (2002) Elicitor-activated phospholipase A(2) generates lysophosphatidylcholines that mobilize the vacuolar H^+ pool for pH signaling via the activation of Na^+-dependent proton fluxes. *Plant Cell*, **14**, 1509-1525.

Walley J.W., Coughlan S., Hudson M.E., Covington M.F., Kaspi R., Banu G., Harmer S.L. & Dehesh K. (2007) Mechanical stress induces biotic and abiotic stress responses via a novel cis-element. *Plos Genetics*, **3**, 1800-1812.

Walters D., Raynor L., Mitchell A., Walker R. & Walker K. (2004) Antifungal activities of four fatty acids against plant pathogenic fungi. *Mycopathologia*, **157**, 87-90.

Weber H., Chetelat A., Caldelari D. & Farmer E.E. (1999) Divinyl ether fatty acid synthesis in late blight-diseased potato leaves. *Plant Cell*, **11**, 485-494.

Wi S.J., Ji N.R. & Park K.Y. (2012) Synergistic biosynthesis of biphasic ethylene and reactive oxygen species in response to hemibiotrophic *Phytophthora parasitica* in tobacco plants. *Plant Physiology*, **159**, 251-265.

Xiong L.M., Schumaker K.S. & Zhu J.K. (2002) Cell signaling during cold, drought, and salt stress. *Plant Cell*, **14**, S165-S183.

Yamamoto Y., Ford R.C. & Barber J. (1981) Relationship between thylakoid membrane fluidity and the functioning of pea-chloroplasts - effect of cholesteryl hemisuccinate. *Plant Physiology*, **67**, 1069-1072.

Yoshioka H., Numata N., Nakajima K., Katou S., Kawakita K., Rowland O., Jones J.D. & Doke N. (2003) *Nicotiana benthamiana* gp91phox homologs NbrbohA and NbrbohB participate in H_2O_2 accumulation and resistance to *Phytophthora infestans*. *Plant Cell*, **15**, 706-718.

Yu L.M. (1995) Elicitins from *Phytophthora* and basic resistance in tobacco. *Proceedings of the National Academy of Sciences of the United States of America*, **92**, 4088-4094.

Zhang S. & Klessig D.F. (2000) Pathogen-induced MAP kinases in tobacco. *Results Probl Cell Differ*, **27**, 65-84.

Tables

Supplemental Table S2. Applied detection parameters for lysolipid quantification.

ESI mode	Lysolipid species	Retention time (min)	Q1 (m/z)	Q3 (m/z)
Positive				
	DGMG-18:3	10.187	699	537
	LPE-14:0	10.508	448	405
	LPC-18:3	10.518	518	184
	LPE-18:3	10.752	498	455
	LPC-18:2	11.184	520	184
	LPE-18:2	11.291	500	457
	LPE-16:0	11.826	476	433
	LPC-16:0	11.857	496	184
	LPC-18:1	11.961	522	184
	LPC-17:0	12.348	510	184
	LPC-18:0	13.185	524	184
Negative				
	LPG-16:0	13.043	483	255
	LPG-16:1	12.525	481	253
	LPG-18:2	12.496	507	279
	LPG-18:3	11.587	505	277
	LPG-17:1	12.824	495	267
	LPA-16:0	13.458	409	152.5
	LPA-18:1	13.852	437	152.5
	LPA-17:0	14.285	423	152.5
	LPI-13:0	10.340	529	213
	LPI-16:0	12.953	571	255
	LPI-18:2	12.055	595	279
	LPI-18:3	11.248	593	277

Supplemental Table S6. List of selected genes involved in phytohormone signaling differentially regulated in Ppn-infected ir-*gla1* 1 vs. WT plants.

Gene ID	Annotation	Fold-change [a]	q-value (%)[a]	Accession No. [b]	E-value [b]
Auxin					
Na_06053	Auxin efflux facilitator SlPIN5	0.39	2.95	NP_001234192.1	5E-133
Na_04970	Auxin influx transport protein	3.01	3.10	ABN81351.1	0
Na_31254	Auxin-induced protein 6B	8.26	2.46	XP_002510511.1	6E-42
Na_28305	Auxin-induced protein 15A	6.18	4.69	XP_002270504.1	2E-43
Na_16486	Auxin-induced protein 5NG4	3.86	3.42	XP_002270961.1	8E-138
Na_26355	Auxin-induced protein 5ng4-like	3.57	4.80	XP_002280062.1	2E-58
Na_26447	Auxin-induced SAUR-like protein	5.03	4.34	AAM12778.1	5E-43
Na_13604	Auxin-repressed protein	0.01	1.97	AAS75891.1	2E-46
Na_15940	IAA-amino acid hydrolase 4	0.44	2.87	XP_002322806.1	3E-113
Na_17784	Indole-3-acetic acid-amido synthetase GH3.1	0.08	3.10	XP_002283886.1	6E-132
Na_07460	Indole-3-acetic acid-amido synthetase GH3.6	0.27	2.78	XP_002533739.1	0
Na_25231	Putative auxin growth promotor protein	2.77	4.91	AAK84479.1	3E-51
Na_23043	Putative auxin-induced SAUR-like protein	6.06	2.96	AAM12777.1	2E-42
Ethylene					
Na_10292	1-aminocyclopropane-1-carboxylate synthase	0.17	3.46	AER35095.1	1E-17
Na_01349	ACC oxidase ACO3	0.46	4.80	ABO32691.1	0
Na_11867	ACC oxidase	0.09	2.75	AAB05171.1	0
Na_02452	EIL4	0.28	3.19	AAP04000.1	0
Na_03087	EIL5	0.45	3.25	AAP04001.1	0
Na_09485	Ethylene receptor	0.35	4.69	ACC78614.1	0
Na_14761	Ethylene-responsive transcription factor 2	0.37	3.25	Q9LW50.1	2E-137
Na_18678	Ethylene-responsive transcription factor 4	0.20	2.80	Q9LW49.1	4E-125
Na_10937	Ethylene-responsive transcriptional coactivator	0.08	3.61	NP_001234468.1	3E-67
Gibberellin					
Na_07352	GAST-like protein	0.11	2.85	ACJ02356.1	6E-34
Na_11901	Gibberellin 2-oxidase 2	0.09	2.68	BAD17856.1	2E-149
Na_29056	Gibberellin 2-oxidase 5	0.45	2.80	ABO70986.1	9E-57
Na_05065	Gibberellin receptor GID1	0.22	3.07	XP_002518790.1	2E-120
Na_03457	GID1-like gibberellin receptor	0.30	2.92	NP_001234767.1	0
Na_41184	RGL2-2	0.39	3.14	AFN25702.1	1E-37
Salicylic acid					
Na_37835	Salicylic acid binding catalase	0.31	2.79	AAC48918.1	1E-17
Na_00040	Salicylic acid-binding protein	0.37	3.01	P49319.2	0
Na_19175	Salicylic acid-induced protein 19	0.05	2.66	AAQ75123.1	1E-98
Na_42358	S-adenosyl-L-methionine:benzoic acid/salicylic acid carboxyl methyltransferase	6.19	4.82	AFD28989.1	1E-21
Na_07568	Methyl salicylate esterase	0.16	2.94	Q6RYA0.1	3E-130
Na_12995	NPR1	0.47	2.87	ABH04326.1	5E-99
Jasmonic acid					
Na_01883	Jasmonate ZIM domain protein b	2.40	3.34	AFL46166.1	4E-105
Na_05998	Jasmonic acid 2	0.16	2.84	NP_001233972.1	6E-108
Na_05069	Jasmonic acid-amino acid-conjugating enzyme	0.49	2.67	ABC87760.1	0
Na_04090	Lipoxygenase	0.27	3.25	AAP83138.1	2E-179
Abscisic acid					
Na_02669	ABA 8'-hydroxylase CYP707A1	0.21	3.46	ABA55732.1	0
Na_24577	Abscisic acid receptor PYL2-like	3.11	4.69	XP_003545372.1	3E-65
Na_30330	homeodomain 20 transcription factor	0.01	1.60	ADI50265.2	6E-83
Na_03585	Protein phosphatase 2C ABI2 homolog	0.27	2.78	NP_001234686.1	0

[a] ir-*gla1* 1 vs. WT

[b] top NCBI hit (blastx result)

Supplemental Table S7. List of selected defense-related genes differentially regulated in Ppn-infected ir-*gla1* 1 vs. WT plants.

Gene ID	Annotation	Fold-change [a]	q-value (%)[a]	Accession No. [b]	E-value [b]
Na_06696	H+/Ca2+ exchanger 2	0.30	3.46	BAA75232.1	0
Na_03977	Na+/H+ antiporter	0.38	4.88	AAX37333.1	0
Na_23981	sodium/proton exchanger	0.16	2.87	AAK27314.2	8E-72
Na_10210	Mitogen-activated protein kinase kinase 1	0.17	2.78	ADT91696.1	0
Na_03517	Mitogen-activated protein kinase	0.42	3.34	AAQ83971.2	0
Na_08214	MAP kinase	0.33	2.79	AFP20223.1	0
Na_00928	Alpha-dioxygenase 2	0.40	2.46	ADM21465.1	0
Na_00674	Germin-like protein	0.29	2.77	AAR97545.1	2E-155
Na_30907	Hydrogen peroxide-induced 1	2.11	4.68	ACK38177.1	8E-15
Na_01233	Pathogen-inducible alpha-dioxygenase	0.15	2.99	AAG59584.1	0
Na_01376	Peroxidase	0.05	4.34	BAD98313.2	0
Na_03825	Peroxidase	0.17	2.90	NP_001234644.1	0
Na_40170	Probable phospholipid hydroperoxide glutathione peroxidase	0.16	4.88	Q9FXS3.1	1E-72
Na_11346	WRKY3	0.25	4.70	AAS13439.1	1E-943
Na_14052	WRKY6	0.10	4.82	AAS13440.1	8E-129
Na_12114	Anthocyanidin synthase 1	0.21	3.00	AFM52334.1	0
Na_03026	Caffeoyl-CoA 3-O-methyltransferase 5	0.15	4.80	AAB80931.1	2E-173
Na_00286	Cinnamyl alcohol dehydrogenase 1	0.38	2.77	AFP43763.1	0
Na_00381	Cinnamoyl-CoA hydratase-dehydrogenase	0.27	2.96	AFS41246.1	0
Na_01677	Cinnamoyl-CoA reductase	0.30	4.06	NP_001234612.1	0
Na_06408	Dihydroflavonol 4-reductase	0.12	3.47	AFD28990.1	0
Na_18171	Flavonol synthase/flavanone 3-hydroxylase	0.26	2.58	XP_002516897.1	5E-106
Na_00178	Phenylalanine ammonia-lyase 1	0.24	2.81	ABG75910.1	0
Na_00451	Putrescine n-methyltransferase 1	0.39	3.10	AAK49870.1	0
Na_03285	Threonine deaminase	0.06	2.50	AAG59585.1	8E-92
Na_04212	5-epiaristolochene 1,3-dihydroxylase	0.04	3.34	Q94FM7.2	0
Na_08733	EDS1-like protein	0.42	4.68	AAL85347.1	0
Na_11320	Phytoalexin-deficient 4-1 protein	0.19	2.87	AAW82883.1	8E-96
Na_03840	Acidic endochitinase Q	0.05	3.14	P17514.1	2E-155
Na_16045	Endochitinase 4	0.39	2.94	P52406.1	5E-70
Na_15501	Beta-1,3-galactosyltransferase 7-like	0.14	3.07	XP_003523469.1	2E-84
Na_32560	Disease resistance protein RGA2	0.35	2.79	XP_002277479.1	7E-25
Na_11290	Enhanced disease resistance 2 protein	0.23	2.66	NP_001119010.1	2E-178
Na_15078	Pathogen-related protein	0.05	2.82	XP_002285489.1	5E-125
Na_24888	Pathogenesis-related protein 1B	0.07	3.09	P07053.1	1E-104
Na_08431	Putative PR-10 type pathogenesis-related protein	3.06	2.56	BAJ25785.1	3E-59
Na_37159	Avr9/Cf-9 induced kinase 1	0.22	4.82	AAP03880.2	2E-27
Na_07538	Avr9/Cf-9 rapidly elicited protein 65	0.22	1.35	AAG43557.1	2E-27
Na_08098	Avr9/Cf-9 rapidly elicited protein 75	0.12	3.61	AAG43558.1	1E-62
Na_21463	Avr9/Cf-9 rapidly elicited protein 146	0.45	2.64	AAG43551.1	2E-110
Na_26036	Avr9/Cf-9 rapidly elicited protein 151	0.19	2.50	AAV92901.1	3E-22
Na_14933	Avr9/Cf-9 rapidly elicited protein 276	0.49	4.69	AAP03882.1	0
Na_31614	Avr9/Cf-9 rapidly elicited protein 284	0.25	3.33	AAP03883.1	5E-77

[a] ir-*gla1* 1 vs. WT

[b] top NCBI hit (blastx result)

Supplemental Table S9. List of annotated ions from Ppn-infected WT vs. ir-*gla1* 1 at 2.5 dai.

	Mass over charge m/z	Retention time [s]	Fold-change ir-*gla1* 1/WT	*P*-value (*t*-test; Tukey post-hoc test; n=5)	Ion type	Ion annotation
Alkaloid						
	377.11	291.25	0.22	0.040	$[M+K]^+$	Nicotine glucuronide
Amino acid						
	235.17	275.57	4.04	0.046	Positive dimer	Valine
	135.12	265.91	4.40	0.024	$NH4^+$ adduct	Valine
Diterpene glycosides						
	963.41	277.23	0.12	0.040	$[M-H]^-$	Dimalonylated lyciumoside II
	964.41	277.23	0.12	0.040	Monoisotopic mass	Dimalonylated lyciumoside II
	982.44	277.69	0.20	0.040	$NH4^+$ adduct	Dimalonylated lyciumoside II
	947.41	297.92	0.12	0.045	$[M-H]^-$	Nicotianoside II
	948.42	297.90	0.12	0.046	Monoisotopic mass	Nicotianoside II
	966.45	298.08	0.18	0.043	$NH4^+$ adduct	Nicotianoside II
	971.40	298.55	0.20	0.043	Na^+ adduct	Nicotianoside II
	1109.47	272.88	0.13	0.040	$[M-H]^-$	Nicotianoside VII
	1110.47	273.08	0.14	0.041	Monoisotopic mass	Nicotianoside VII
	1128.49	274.12	0.22	0.040	$NH4^+$ adduct	Nicotianoside VII
Flavonoids						
	289.07	213.60	4.24	0.011	$[M+H]^+$	Dihydrokaempferol
	611.16	148.49	4.86	0.039	$[M+H]^+$	Rutin
	319.13	133.14	12.44	0.000	$[M+H-2H2O]^+$	Trihydroxy-methyl-prenyl-flavanone
Lipid derivatives						
	614.36	266.41	4.51	0.030	$[M+K]^+$	LPC-22:2
	492.25	298.09	0.22	0.042	$[M+K]^+$	LPE-16:0
	514.23	265.04	4.21	0.037	$[M+K-2H]^-$	LPE-18:2
	123.12	266.41	4.46	0.016	$[M+H-H2O]^+$	Nonadienol/nonenal
	501.26	129.99	0.05	0.000	$[M+Na-2H]^-$	PA-(10:0/10:0)
	429.18	213.81	2.42	0.042	$[M+K-2H]^-$	PA-(16:0/0:0) [cyclic]
	435.31	263.62	4.33	0.035	$[M+H-H2O]^+$	PC-(O-14:1/0:0)
	547.25	151.62	0.14	0.042	$[M+K-2H]^-$	PG-(18:1/0:0)
	983.44	277.69	0.21	0.040	$[M+H-2H2O]^+$	PIP2-(18:3/18:1)
Organic acid						
	163.00	120.88	3.48	0.026	$[M+2Na-H]^+$	Succinic acid
Phenolics						
	139.04	443.80	2.95	0.027	$[M+H-2H2O]^+$	Shikimic acid
	139.04	419.46	4.56	0.004	$[M+H-2H2O]^+$	Shikimic acid
	341.09	291.55	0.23	0.040	$[M+H]^+$	Sinapoyl malate
Phytohormones and derivatives						
	306.18	178.47	0.23	0.042	$NH4^+$ adduct	IAA-Ile
	337.19	275.19	6.68	0.040	$[M-H]^-$	JA-Gln
	419.20	267.90	4.12	0.045	Na^+ adduct	JA-Trp
	139.04	468.10	3.88	0.040	$[M+H]^+$	Salicylic acid
	359.10	291.25	0.21	0.040	Acetate adduct	Salicylic acid-O-glucoside
	396.12	291.45	0.23	0.040	$[M+2Na-H]^+$	Zeatin-riboside
Polyamines and derivatives						
	482.22	171.14	0.23	0.040	$[M+H]^+$/ Formeate adduct	Dehydro-Caffeoylferuloylspermidine/ Dicoumaroylspermidine
	514.22	155.48	0.15	0.043	Formeate adduct	Dicaffeoylspermidine
	528.23	148.39	0.23	0.042	Acetate adduct/ Formeate adduct	Dicaffeoylspermidine/ Feruloylcaffeoylspermidine
	501.24	151.97	0.16	0.046	Monoisotopic mass	Dihydrohydroxyferuloylcaffeoylspermidine
	501.24	152.21	0.22	0.043	Monoisotopic mass	Dihydrohydroxyferuloylcaffeoylspermidine
	501.24	151.93	0.22	0.041	Monoisotopic mass	Dihydrohydroxyferuloylcaffeoylspermidine
	597.30	213.17	0.16	0.043	Monoisotopic mass/ $NH4^+$ adduct/ Monoisotopic mass	Hexanoyl-caffeoyl-sinapylspermidine/ Hexenoyl-caffeoyl-feruloylspermidine/ Hexanoyl-diferuloylspermidine
	538.23	457.72	2.81	0.040	K^+ adduct	Hydrated diferuloylspermidine
	672.30	247.44	4.01	0.041	Acetate adduct	N,N´-Biscoumaroyl-N´´-feruloylspermidine
	147.12	238.87	3.85	0.048	Acetate adduct	Putrescine

Figure legends

Figure 1. *Nicotiana attenuata* morphology during infection with *Phytophthora parasitica* var. *nicotianae*.

24 days old *N. attenuata* plants (WT and two ir-*gla1* lines) were infected with *P. parasitica* var. *nicotianae* (Ppn) and photographed at 0, 2.5 and 4 days after infection (dai). Plants treated with PDA served as medium control. White squares in the pictures of Ppn-infected plants at 4 dai indicate a plant region (5-fold magnified below) in which disease symptoms (necrosis and darkish discoloration) started to become visible.

Figure 2. Lipase activity and release of palmitoleyl-lysophospatidyl glycerol (LPG-16:1) after Ppn infection.

24 days old *N. attenuata* plants (WT and two ir-*gla1* lines) were infected with Ppn (control: PDA) and at 4 dai shoots were harvested and either extracted to measure lipase activity using ^{14}C-labeled phosphatidyl choline as substrate (**A**; two biological replicates) or to quantify LPG-16:1 levels (**B**) by LC-MS/MS. The LPG-16:1 data was analyzed using one-way-ANOVA and Tukey-post hoc test (n=3-5). Bars denote SD (**A**) or SE (**B**).

Figure 3. Differential induction of oxylipins in *ir-gla1* 1 compared to WT after Ppn.

24 days old *N. attenuata* WT and *ir-gla1* 1 plants were inoculated either with PDA as control or Ppn for 4 days and and their shoots extracted for oxylipin analysis. **A** Total ion chromatographic profiles of control and Ppn infected WT (black) and *ir-gla1* 1 (red) plant extracts analyzed by UPLC-ESI-ToF-MS in negative ionization mode. For identification, commercially available fatty acid and oxylipin standards were analyzed analogous to plant extracts. Numbers indicate oxylipins differentially regulated in *ir-gla1* 1 compared to WT after Ppn infection, letters indicate standards analyzed (**B**, see Fig. 4 for details).

Figure 4. Seven fatty acids and oxylipins differentially regulated in ir-*gla1* 1 compared to WT after Ppn infection.

A-G Oxylipins from control and Ppn-infected WT and ir-*gla1*1 were measured by UPLC-ToF-MS and seven compounds were found to be differentially induced in infected ir-*gla1* 1 plants compared to WT plants (Bars representing normalized peak areas, mean ± SE, n= 5, different letters represent statistical significance, one-way ANOVA, $p< 0.5$). For identification, compounds were compared with commonly available standards with respect to their retention times (RT) and MS/MS spectra. Chromatograms represent the extracted ion chromatogram (EI) of m/z= $[M-H]^-$ of an extract of WT infected with Ppn. MS/MS spectra were obtained at the

mean RT of each compound. If available the EI spectra of the identical standard was integrated and the structure with the fragmentation pattern is shown.

Figure 5. Microarray and Gene Ontology (GO) analysis of differentially expressed genes in Ppn-infected shoots of ir-*gla1* 1 and wild-type plants.

A. Distribution of fold-changes (FC) of genes expressed differentially in shoots of untreated (control) ir-*gla1* 1 vs. wild type plants. **B**. Distribution of FC of genes expressed differentially in shoots of Ppn-infected ir-*gla1* 1 vs. wild type plants. **C**. Venn diagram of the number of genes differentially expressed in control and Ppn-infected shoots of ir-*gla1* 1 compared to wild type. The numbers in the intersection represent the genes differentially expressed at both conditions. Downward pointing arrows indicate differential down-regulation, upwards oriented ones up-regulation. Arrows next to the numbers in the intersection indicate the differential regulation in controls (left) or Ppn-infected plants (right). **D**. Annotated genes differentially expressed in Ppn-infected shoots of ir-*gla1* 1 were categorized based on biological processes using the Blast2Go software. The summed up percentages (%) of genes from the stimuli response/signaling (RS) and from the transcription regulation (T) category are given on the right.

Figure 6. Comparison of the polar secondary metabolite profiles between Ppn-infected WT and ir-*gla1* 1 at 2.5 dai.

The pie charts show the percentage of ions belonging to a certain group of metabolites based on their annotation that are either up- (**A**) or down-regulated (**B**) in ir-*gla1* 1 vs. WT. The absolute number of differentially regulated ions belonging to a certain metabolite group are given in brackets next to the according pie chart section. For generating the pie charts, ions obtained from the negative as well as the positive mode were annotated and further analyzed together. Before the annotation process, Pareto-normalized data sets from both ion modes were analyzed individually using the MetaboAnalyst 2.0 online software tool. The Vulcano plots (**C** and **D**) show all ions differentially (FC ir-*gla1* 1 vs. WT either > 2 or < 0.5) and significantly (*t*-test; $p<0.05$) regulated in pink.

Figure 7. Model summarizing the role of GLA1 during *N. attenuata* infection with Ppn.

Infection with Ppn is perceived by the plant cell which induces *GLA1* expression. After translation, GLA1 protein is transported into the chloroplast, where it could function – either directly or indirectly – in the generation of potential signaling compounds (*e.g.* certain lysolipids, free unsaturated fatty acids and oxylipins or products derived thereof). The release of the proposed signaling molecules could then lead to further changes in gene expression in the nucleus mediating the plant's response to pathogens like Ppn.

Supplemental Figure S1. Specificity of the qPCR-primers designed for quantification of the relative *PpnEF1a* gene abundance.

A. Alignment of the *ELONGATION FACTOR 1 ALPHA* (*EF1a*) nucleotide sequences of three different Ppn isolates (Ppn_ EF418929, Ppn_GU191189 and Ppn_EU080678; GenBank accession No. EF418929, GU191189 and EU080678) with those from *Nicotiana attenuata* (Na_EF1a; sequence will be submitted to NCBI) and *Nicotiana tabacum* (Nt_D63396; GenBank accession No. D63396) using the Geneious 5.5.7 software tool using default parameters. The primer binding sites of Ppn_EF1a_fwd (5'-GGCGGTATTGGCACGGTA-3') and Ppn_EF1a_rev (5'-GCCGACGTTGTCACCAGG-3') flank a 159 bp amplified region.

B. Result of a PCR to test the Ppn_EF1a fwd/rev qPCR primers under standard PCR conditions. Lane 1: 1-kb size standard; lanes 2&3: *N. attenuata* wildtype templates + Ppn_EF1a fwd/rev; lanes 4&5: Ppn templates + Ppn_EF1a_fwd/rev; lane 6: Ppn-infected *N. attenuata* wildtype template + Ppn_EF1a_fwd/rev.

Supplemental Table S2. Applied detection parameters for lysolipid quantification.

Supplemental Figure S3. Comparison of *Nt*ACRE14 nucleotide sequence with blastn hits obtained from http://solgenomics.net/tools/blast/index.pl.

In order to identify the full length protein coding nucleotide sequence of *N. tabacum* ACRE14 (*Nt*ACRE14; Genbank: AY775029.1) it was blasted (blastn) against two different databases from

http://solgenomics.net/tools/blast/index.pl. The blast against the "*N. tabacum* Methylation Filtered Genome TGI:v.1 Contigs" resulted in "processed_tobacco_genome_sequences_ c19207 (99% identity, E-value=0) and another blast against "*N. tabacum* Methylation Filtered Genome TGI:v1 Processed Reads" gave CHO_OF4571xi05f1.ab1 (99% identity, E-value=0) and CHO_OF4768xf12r1.ab1 (99% identity, E-value=0) as best hits. All sequences were aligned using the Geneious 5.5.7 software with default parameters. Nucleotides identical between all sequences are displayed in black within the sequences and highlighted in green above the alignment.

Supplemental Figure S4. Quantification of Ppn abundance by qPCR.

Genomic DNA was extracted from shoots of 26-28 days old WT and ir-*gla1 N. attenuata* plants infected with Ppn (n=14-19) at 2.5 dai and 4 dai. Plants treated with PDA (n=3) served as control. The relative abundance of the Ppn-*EF1a* gene in 20 ng of DNA template was quantified by qPCR. ND: not detected. Bars denote ± SE.

Supplemental Figure S5. Levels of DGMG-18:3, lysolipids derived from PC, PE, PI and PG and phosphatidic acid in WT and ir-*gla1* shoots after Ppn infection.

24 day old *N. attenuata* plants (WT and two ir-*gla1* lines) were infected with *Phytophthora parasitica* var. *nicotianae* (Ppn) and shoots were harvested at 4 dai for lysolipid analysis by LC-

MS/MS. Plants treated with PDA (medium) served as control. Data was analyzed using one-way-ANOVA and Tukey-post hoc test (n=3-5). Bars represent ± SE.

Supplemental Table S6. List of selected genes involved in phytohormone signaling differentially regulated in Ppn-infected ir-*gla1* 1 vs. WT plants.

Supplemental Table S7. List of selected defense-related genes differentially regulated in Ppn-infected ir-*gla1* 1 vs. WT plants.

Supplemental Figure S8. Accumulation of abscisic and salicylic acid after Ppn infection.

Shoots of 24 days old *N. attenuata* plants (WT and two ir-*gla1* lines) infected by Ppn (control: PDA) were harvested at different time points after infection (0, 4, 24 and 96 h) and the levels of abscisic (**A**) and salicylic acid (**B**) were quantified by LC-MS/MS. ND: not detected. Bars denote ± SE (n=6-7 for 0 h, n=3-4 for 4 and 24 h and n=5-8 for 96 h after infection).

Supplemental Table S9. List of annotated ions from Ppn-infected WT vs. ir-*gla1* 1 at 2.5 dai.

Supplemental Figure S10. Comparison of *Na*GLA1 with *Nt*ACRE14 protein sequence.

The protein sequences of *N. attenuata* GLA1 (*Na*GLA1; Genbank: ACZ57767) and *N. tabacum* ACRE14 (*Nt*ACRE14; Genbank: AAV92888; full length sequence obtained by blastn against the "*N. tabacum* Methylation Filtered Genome TGI:v.1 Contigs" at http://solgenomics.net/tools/blast/index.pl; Supplemental Figure S3) were aligned using the Geneious 5.5.7 software using default parameters. Amino acids identical between both proteins are displayed in black within the sequences and highlighted in green above the sequence alignment.

Supplemental Exel File SIa. List of genes changing expression in uninfected (control) shoots of ir-*gla1* 1 compared to WT *Nicotiana attenuata* plants.

n = 3 (biological replicates per genotype)

* FC (fold-change; ir-*gla1* 1 vs. WT)

** *q*-value calculated with SAM (Statistical Analysis of Microarrays) using Multiexperiment Viewer (MeV v4.8) software (http://mev.tm4.org/)

§ Analysis performed with Blast2Go software (http://www.blast2go.com/b2glaunch)

Supplemental Exel File SIb. List of genes changing expression in *Phytophthora parasitica* var. *nicotianae*-infected shoots of ir-*gla1* 1 compared to WT *Nicotiana attenuata* plants.

n = 3 (biological replicates per genotype)

* FC (fold-change; ir-*gla1* 1 vs. WT)

** *q*-value calculated with SAM (Statistical Analysis of Microarrays) using Multiexperiment Viewer (MeV v4.8) software (http://mev.tm4.org/)

§ Analysis performed with Blast2Go software (http://www.blast2go.com/b2glaunch)

q-value > 5% and data therefore excluded from further microarray analyses

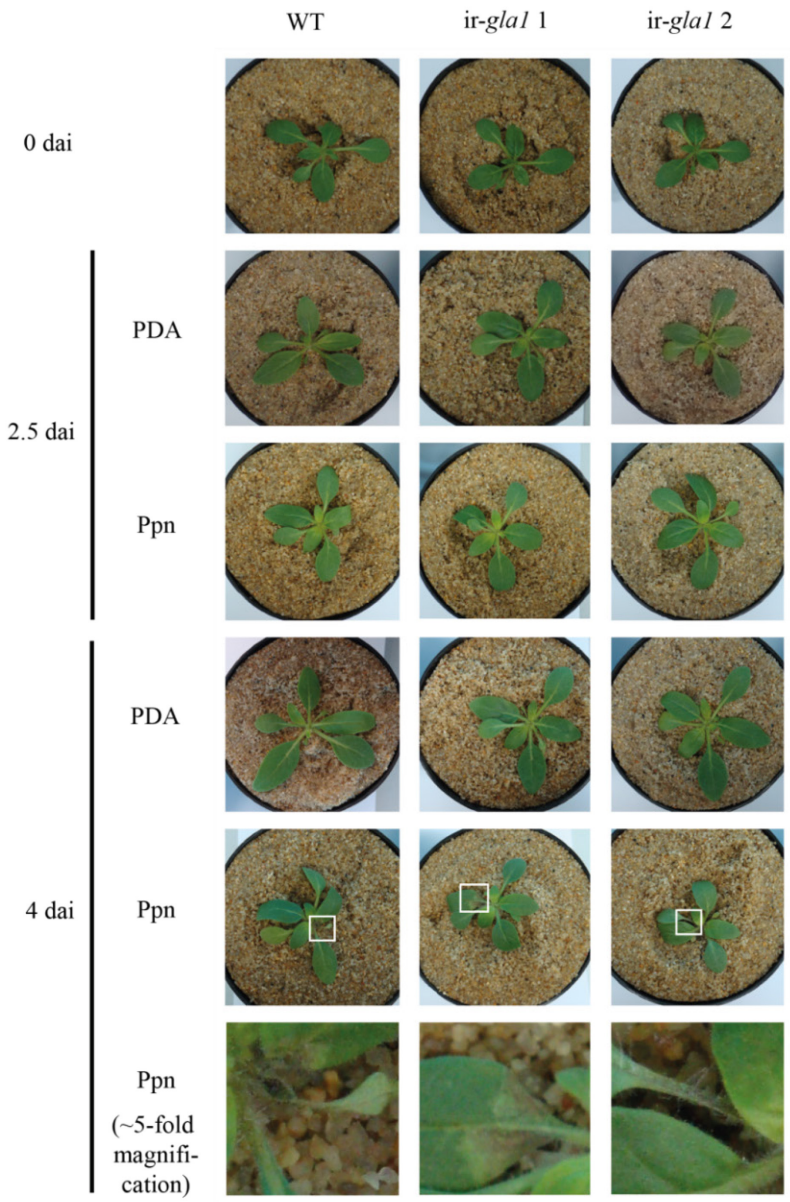

Figure 1. ***Nicotiana attenuata*** **morphology during infection with** ***Phytophthora parasitica*** **var.** ***nicotianae*****.**

24 days old *N. attenuata* plants (WT and two ir-*gla1* lines) were infected with *P. parasitica* var. *nicotianae* (Ppn) and photographed at 0, 2.5 and 4 days after infection (dai). Plants treated with PDA served as medium control. White squares in the pictures of Ppn-infected plants at 4 dai indicate a plant region (5-fold magnified below) in which disease symptoms (necrosis and darkish discoloration) started to become visible.

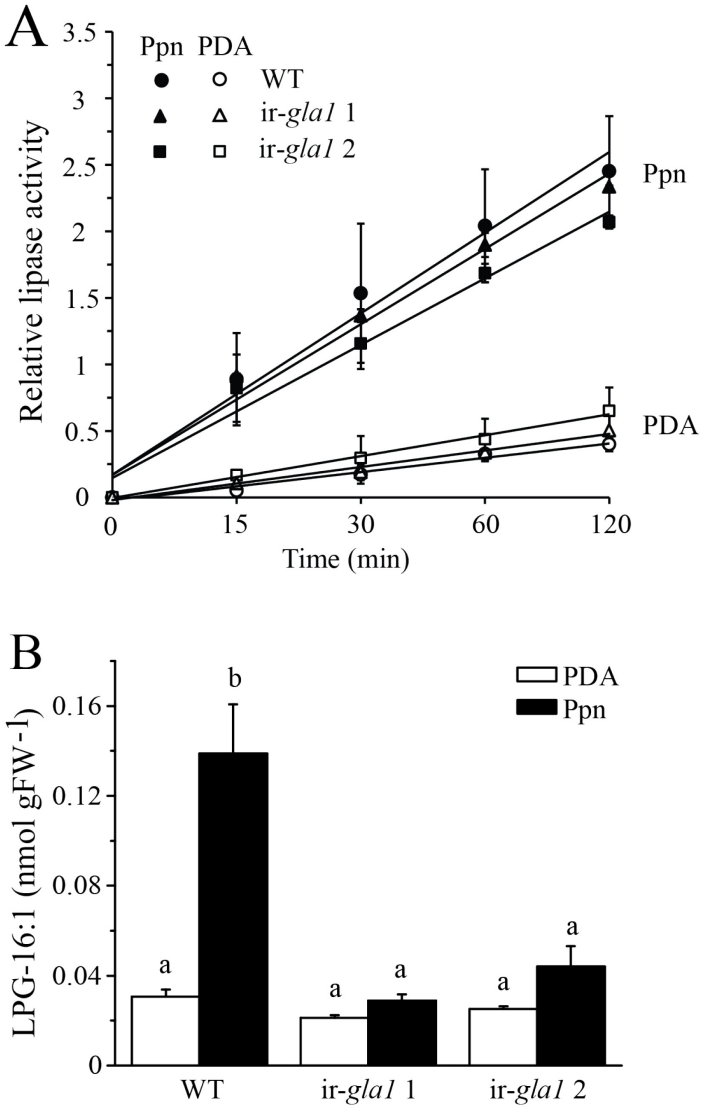

Figure 2. Lipase activity and release of palmitoleyl-lysophospatidyl glycerol (LPG-16:1) after Ppn infection.

24 days old *N. attenuata* plants (WT and two ir-*gla1* lines) were infected with Ppn (control: PDA) and at 4 dai shoots were harvested and either extracted to measure lipase activity using ^{14}C-labeled phosphatidyl choline as substrate (**A**; two biological replicates) or to quantify LPG-16:1 levels (**B**) by LC-MS/MS. The LPG-16:1 data was analyzed using one-way-ANOVA and Tukey-post hoc test (n=3-5). Bars denote SD (**A**) or SE (**B**).

A

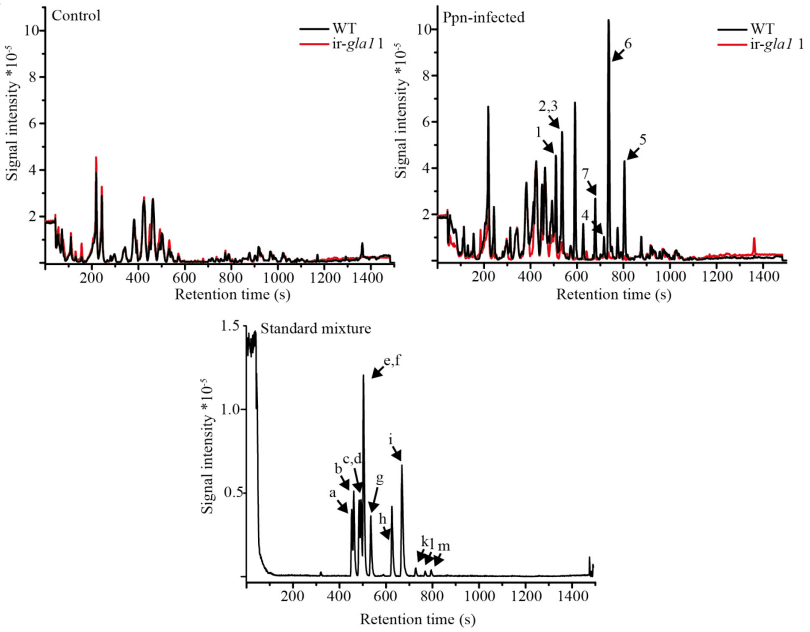

B

No.	Name	Abbreviation	Ion	m/z	RT (in s)	Sum formula
1	9-hydroxy-linoleic acid	9-OH-18:2	$[M-H]^-$	295.2277	508.94	$C_{18}H_{31}O_3$
2	Oxylipin 1	Ox 1	$[M-H]^-$	297.2428	535.54	$C_{18}H_{33}O_3$
3	Oxylipin 2	Ox 2	$[M-H]^-$	323.2222	526.82	$C_{19}H_{31}O_4$
4	Oxylipin 3	Ox 3	$[M-H]^-$	307.2276	715.77	$C_{19}H_{31}O_3$
5	Oleic acid	18:1	$[M-H]^-$	281.2483	803.40	$C_{18}H_{33}O_2$
6	Linoleic acid	18:2	$[M-H]^-$	279.2326	735.80	$C_{18}H_{31}O_2$
7	Linolenic acid	18:3	$[M-H]^-$	277.2167	677.57	$C_{18}H_{29}O_2$
a	9-hydroxy-linolenic acid	9-OH-18:3	$[M-H]^-$	293.2110	456.62	$C_{18}H_{29}O_3$
b	13-hydroxy-linolenic acid	13-OH-18:3	$[M-H]^-$	293.2110	464.73	$C_{18}H_{29}O_3$
c	9-hydroperoxy-linolenic acid	9-OOH-18:3	$[M-H]^-$	309.2051	487.81	$C_{18}H_{29}O_4$
d	13-hydroperoxy-linolenic acid	13-OOH-18:3	$[M-H]^-$	309.2051	495.84	$C_{18}H_{29}O_4$
e	9-hydroxy-linoleic acid	9-OH-18:2	$[M-H]^-$	295.2277	508.94	$C_{18}H_{31}O_3$
f	13-hydroxy-linoleic acid	13-OH-18:2	$[M-H]^-$	295.2277	514.70	$C_{18}H_{31}O_3$
g	9-oxo-linoleic acid	9-oxo-18:2	$[M-H]^-$	293.2110	538.12	$C_{18}H_{29}O_3$
h	2-hydroxy-oleic acid	2-OH-18:1	$[M-H]^-$	297.2428	629.50	$C_{18}H_{33}O_3$
i	9-oxo-stearic acid	9-oxo-18:0	$[M-H]^-$	297.2428	672.82	$C_{18}H_{33}O_3$
k	Linolenic acid	18:3	$[M-H]^-$	277.2167	677.57	$C_{18}H_{29}O_2$
l	Linoleic acid	18:2	$[M-H]^-$	279.2326	735.80	$C_{18}H_{31}O_2$
m	Oleic acid	18:1	$[M-H]^-$	281.2483	803.40	$C_{18}H_{33}O_2$

Figure 3. Differential induction of oxylipins in *ir-gla1* 1 compared to WT after Ppn.

24 days old *N. attenuata* WT and *ir-gla1* 1 plants were inoculated either with PDA as control or Ppn for 4 days and and their shoots extracted for oxylipin analysis. **A** Total ion chromatographic profiles of control and Ppn infected WT (black) and *ir-gla1* 1 (red) plant extracts analyzed by UPLC-ESI-ToF-MS in negative ionization mode. For identification, commercial available fatty acid and oxylipin standards were analyzed analogous to plant extracts. Numbers indicate oxylipins differentially regulated in *ir-gla1* 1 compared to WT after Ppn infection, letters indicate standards analyzed (**B**, see Fig. 4 for details).

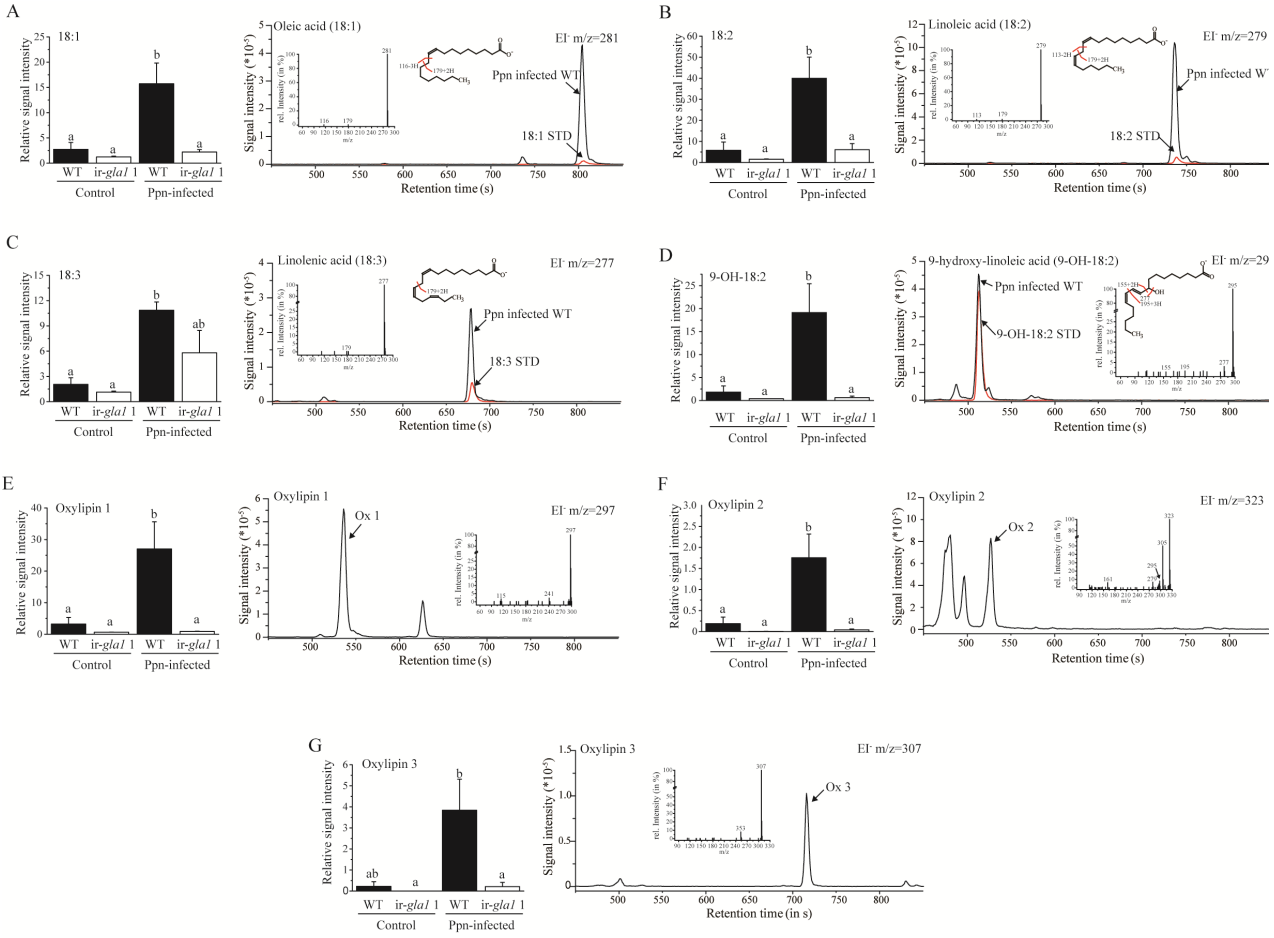

Figure 4. Seven fatty acids and oxylipins differentially regulated in ir-*gla1* 1 compared to WT after Ppn infection.

A-G Oxylipins from control and Ppn-infected WT and ir-*gla1*1 were measured by UPLC-ToF-MS and seven compounds were found to be differentially induced in infected ir-*gla1* 1 plants compared to WT plants (Bars representing normalized peak areas, mean ± SE, n= 5, different letters represent statistical significance, ANOVA, P< 0.5). For identification, compounds were compared with common available standards with respect to their retention times (RT) and MS/MS spectra. Chromatograms represent the extracted ion chromatogram (EI) of m/z= $[M-H]^-$ of an extract of WT infected with Ppn. MS/MS spectra were obtained at the mean RT of each compound. If available the EI spectra of the identical standard was integrated and the structure with the fragmentation pattern is shown.

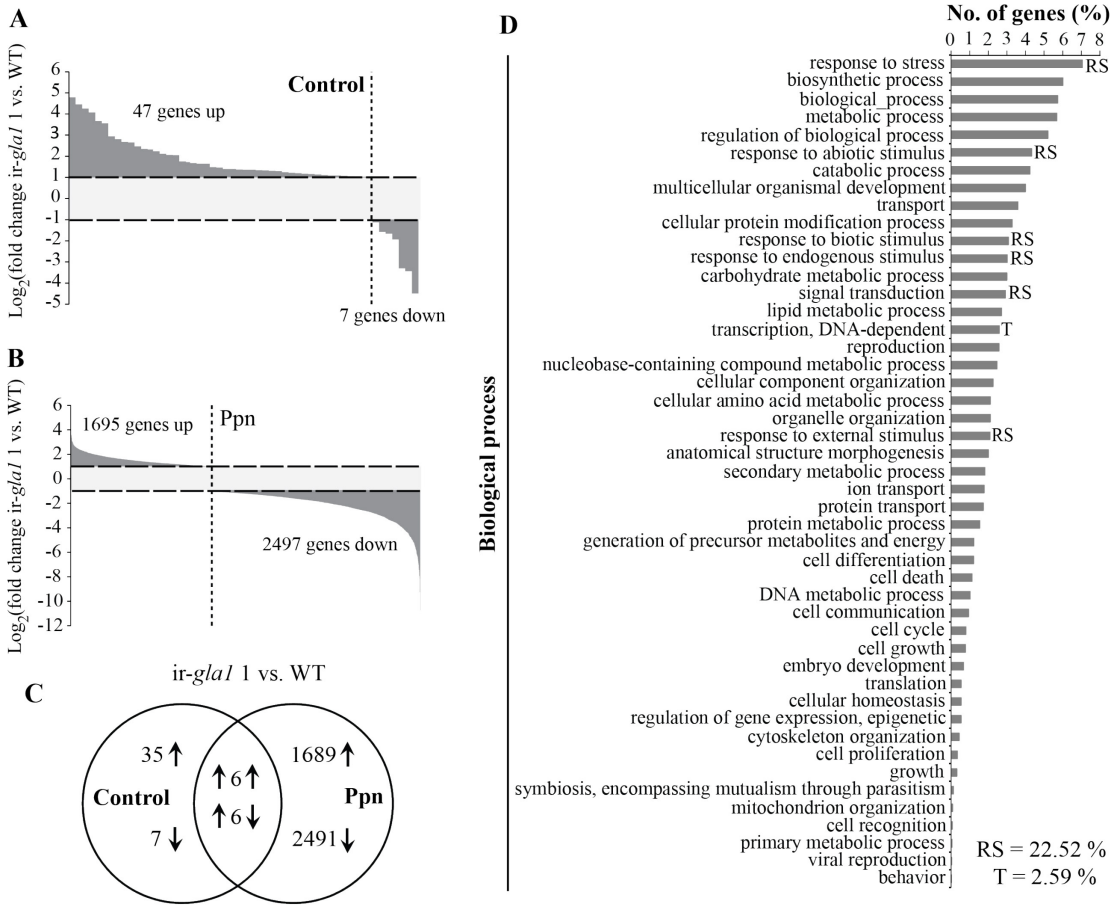

Figure 5. Microarray and Gene Ontology (GO) analysis of differentially expressed genes in Ppn-infected shoots of ir-*gla1* 1 and wild-type plants.

A. Distribution of fold-changes (FC) of genes expressed differentially in shoots of untreated (control) ir-*gla1* 1 vs. wild type plants. **B**. Distribution of FC of genes expressed differentially in shoots of Ppn-infected ir-*gla1* 1 vs. wild type plants. **C**. Venn diagram of the number of genes differentially expressed in control and Ppn-infected shoots of ir-*gla1* 1 compared to wild type. The numbers in the intersection represent the genes differentially expressed at both conditions. Downward pointing arrows indicate differential down-regulation, upwards oriented ones up-regulation. Arrows next to the numbers in the intersection indicate the differential regulation in controls (left) or Ppn-infected plants (right). **D**. Annotated genes differentially expressed in Ppn-infected shoots of ir-*gla1* 1 were categorized based on biological processes using the Blast2Go software. The summed up percentages (%) of genes from the stimuli response/signaling (RS) and from the transcription regulation (T) category are given on the right.

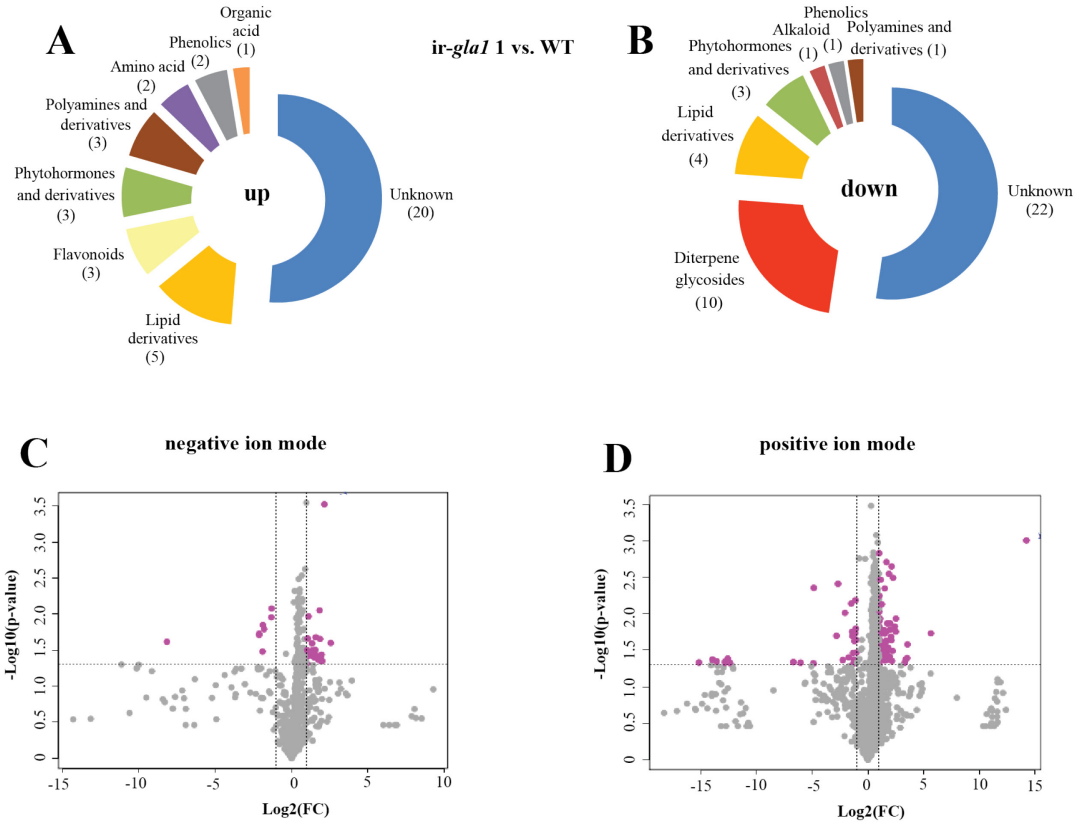

Figure 6. Comparison of the polar secondary metabolite profiles between Ppn-infected WT and ir-*gla1* 1 at 2.5 dai.

The pie charts show the percentage of ions belonging to a certain group of metabolites based on their annotation that are either up- (**A**) or downregulated (**B**) in ir-*gla1* 1 vs. WT. The absolute number of differentially regulated ions belonging to a certain metabolite group are given in brackets next to the according pie chart section. For generating the pie charts, ions obtained from the negative as well as the positive mode were annotated and further analyzed together. Before the annotation process, Pareto-normalized data sets from both ion modes were analyzed individually using the MetaboAnalyst 2.0 online software tool. The Vulcano plots (**C** and **D**) show all ions differentially (fold-change (FC) ir-*gla1* 1 vs. WT either > 2 or < 0.5) and significantly (*t*-test; $p<0.05$) regulated in pink.

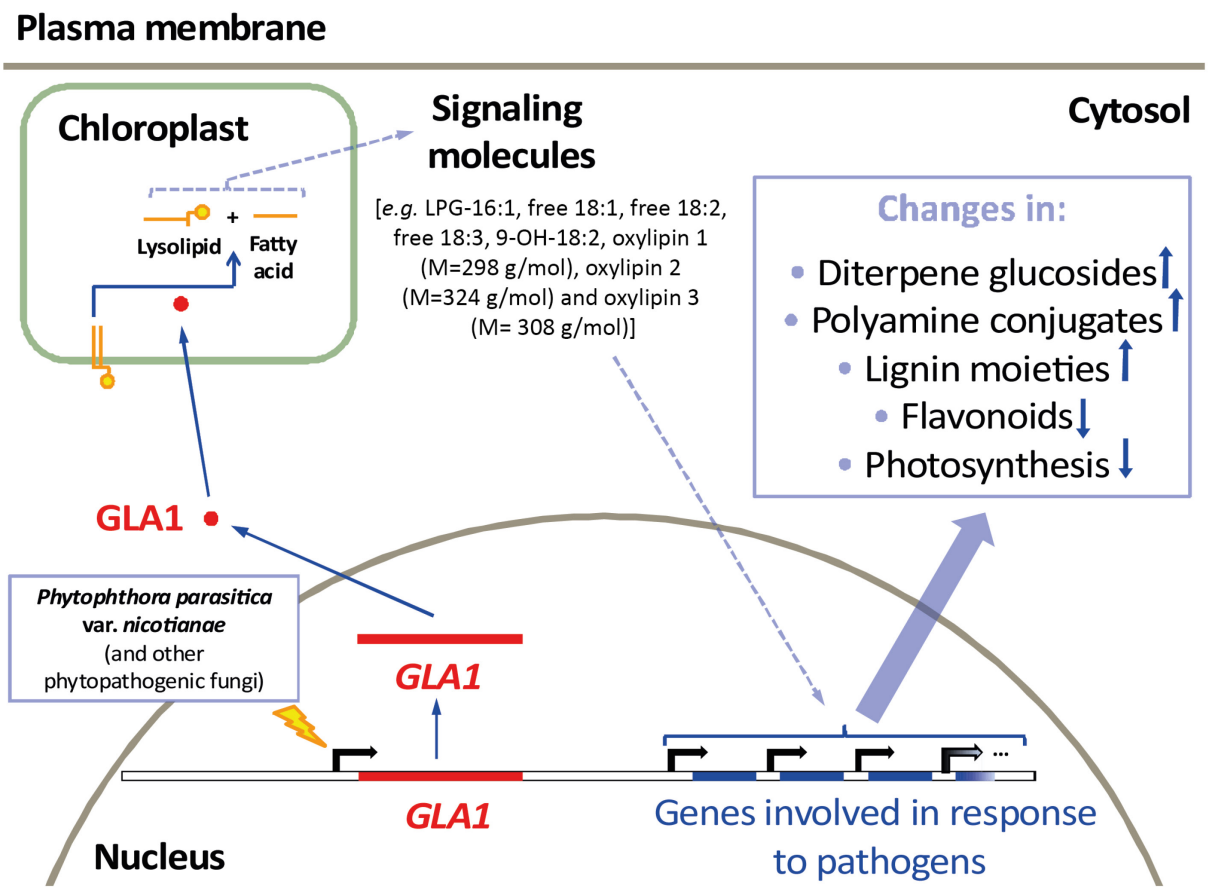

Figure 7. Model summarizing the role of GLA1 during *N. attenuata* infection with Ppn.

Infection with Ppn is perceived by the plant cell which induces *GLA1* expression. After translation, GLA1 protein is transported into the chloroplast, where it could function – either directly or indirectly – in the generation of potential signaling compounds (*e.g.* certain lysolipids, free unsaturated fatty acids and oxylipins or products derived thereof). The release of the proposed signaling molecules could then lead to further changes in gene expression in the nucleus mediating the plant's response to pathogens like Ppn.

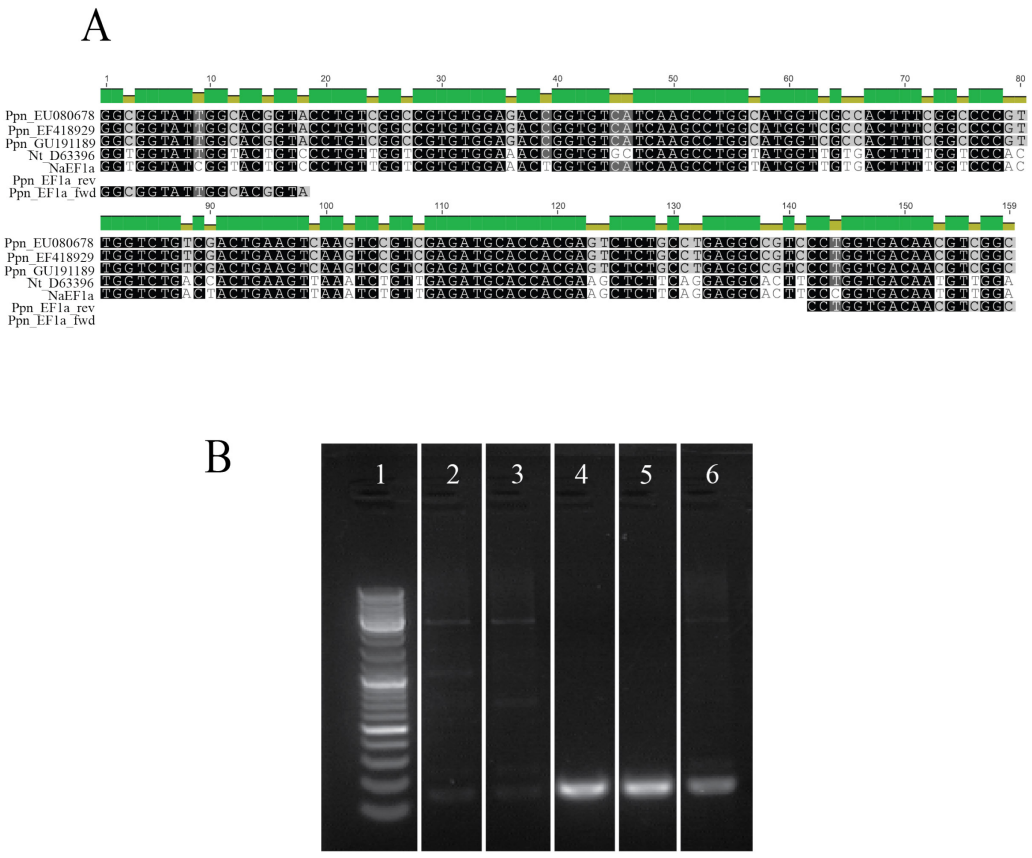

Supplemental Figure S1. Specificity of the qPCR-primers designed for quantification of the relative *PpnEF1a* gene abundance.

A. Alignment of the *ELONGATION FACTOR 1 ALPHA* (*EF1a*) nucleotide sequences of three different Ppn isolates (Ppn_ EF418929, Ppn_GU191189 and Ppn_EU080678; GenBank accession No. EF418929, GU191189 and EU080678) with those from *Nicotiana attenuata* (Na_EF1a; sequence will be submitted to NCBI) and *Nicotiana tabacum* (Nt_D63396; GenBank accession No. D63396) using the Geneious 5.5.7 software tool using default parameters. The primer binding sites of Ppn_EF1a_fwd (5'-GGCGGTATTGGCACGGTA-3') and Ppn_EF1a_rev (5'-GCCGACGTTGTCACCAGG-3') flank a 159 bp amplified region.

B. Result of a PCR to test the Ppn_EF1a fwd/rev qPCR primers under standard PCR conditions. Lane 1: 1-kb size standard; lanes 2&3: *N. attenuata* wildtype templates + Ppn_EF1a fwd/rev; lanes 4&5: Ppn templates + Ppn_EF1a_fwd/rev; lane 6: Ppn-infected *N. attenuata* wildtype template + Ppn_EF1a_fwd/rev.

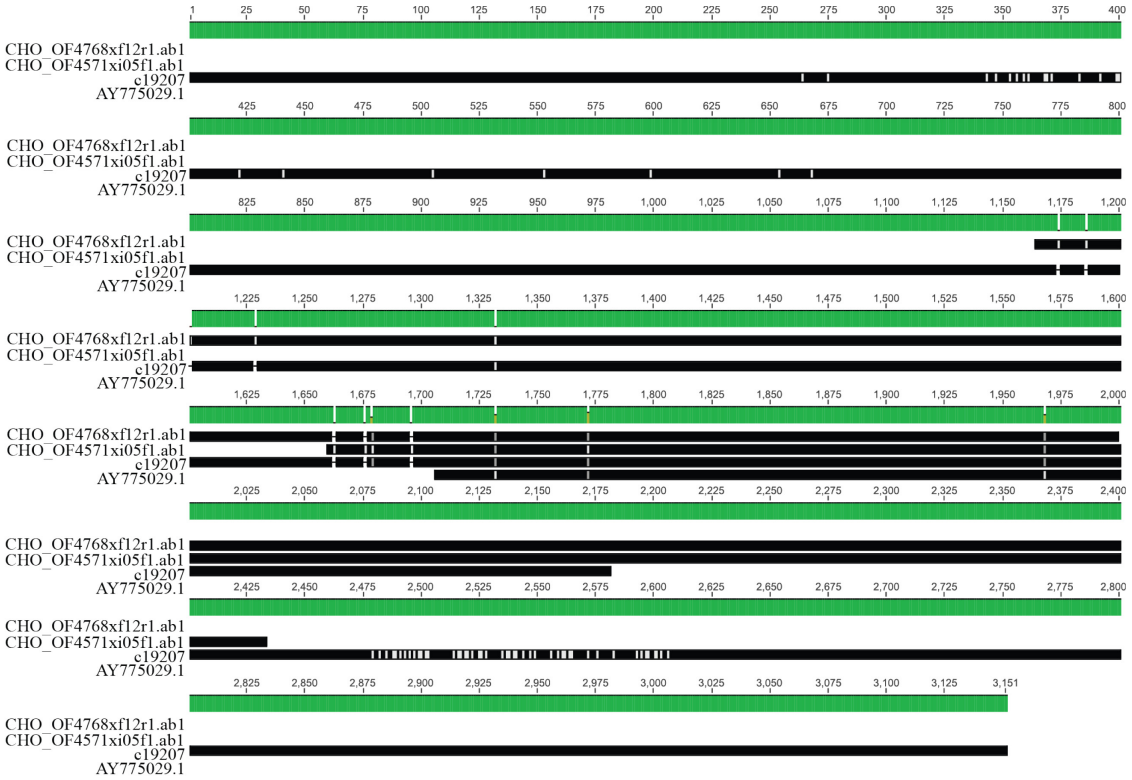

Supplemental Figure S3. Comparison of *Nt*ACRE14 nucleotide sequence with blastn hits obtained from http://solgenomics.net/tools/blast/index.pl.

In order to identify the full length protein coding nucleotide sequence of *N. tabacum* ACRE14 (*Nt*ACRE14; Genbank: AY775029.1) it was blasted (blastn) against two different databases from http://solgenomics.net/tools/blast/index.pl. The blast against the "*N. tabacum* Methylation Filtered Genome TGI:v.1 Contigs" resulted in "processed_tobacco_genome_sequences_ c19207 (99% identity, E-value=0) and another blast against "*N. tabacum* Methylation Filtered Genome TGI:v1 Processed Reads" gave CHO_OF4571xi05f1.ab1 (99% identity, E-value=0) and CHO_OF4768xf12r1.ab1 (99% identity, E-value=0) as best hits. All sequences were aligned using the Geneious 5.5.7 software with default parameters. Nucleotides identical between all sequences are displayed in black within the sequences and highlighted in green above the alignment.

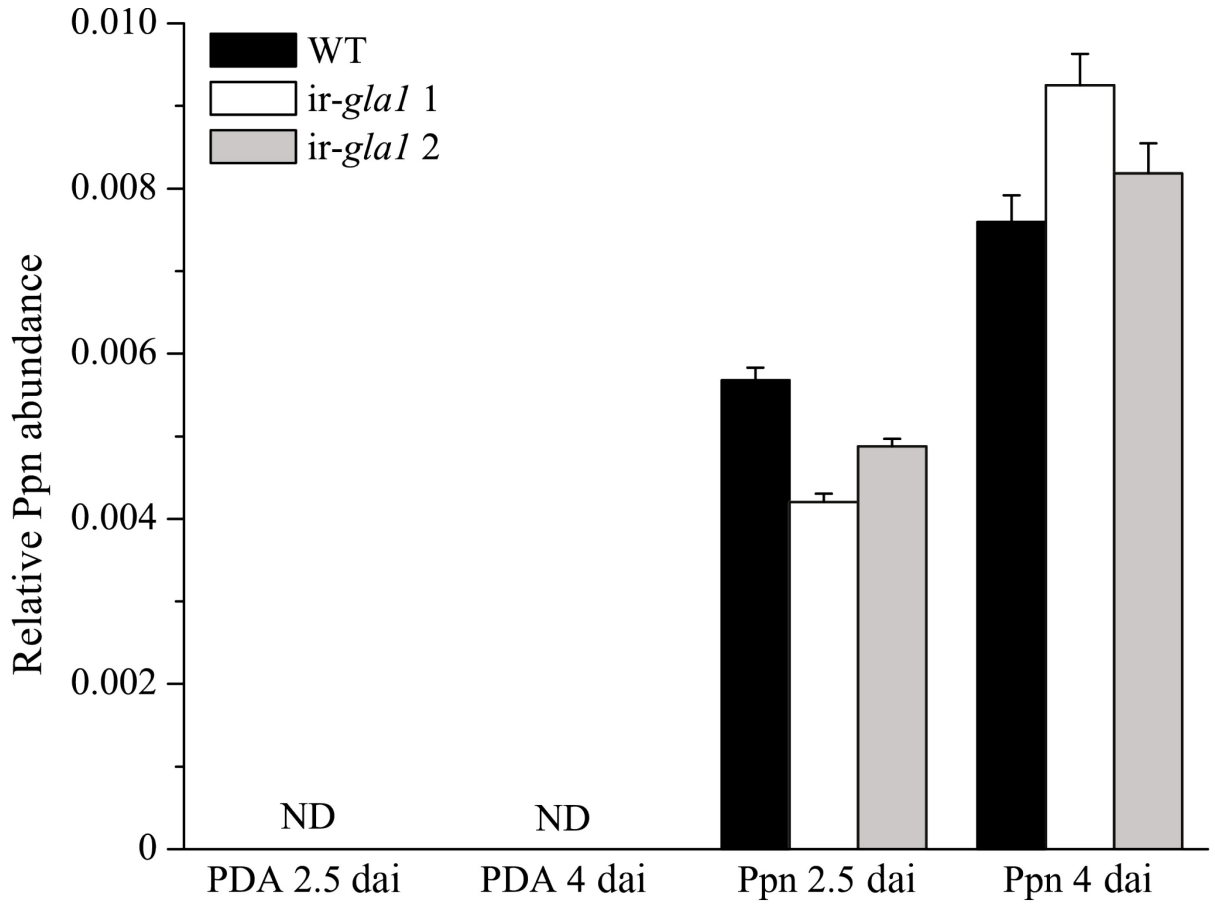

Supplemental Figure S4. Quantification of Ppn abundance by qPCR.

Genomic DNA was extracted from shoots of 26-28 days old WT and ir-*gla1 N. attenuata* plants infected with Ppn (n=14-19) at 2.5 dai and 4 dai. Plants treated with PDA (n=3) served as control. The relative abundance of the Ppn-*EF1a* gene in 20 ng of DNA template was quantified by qPCR. ND: not detected. Bars denote ± SE.

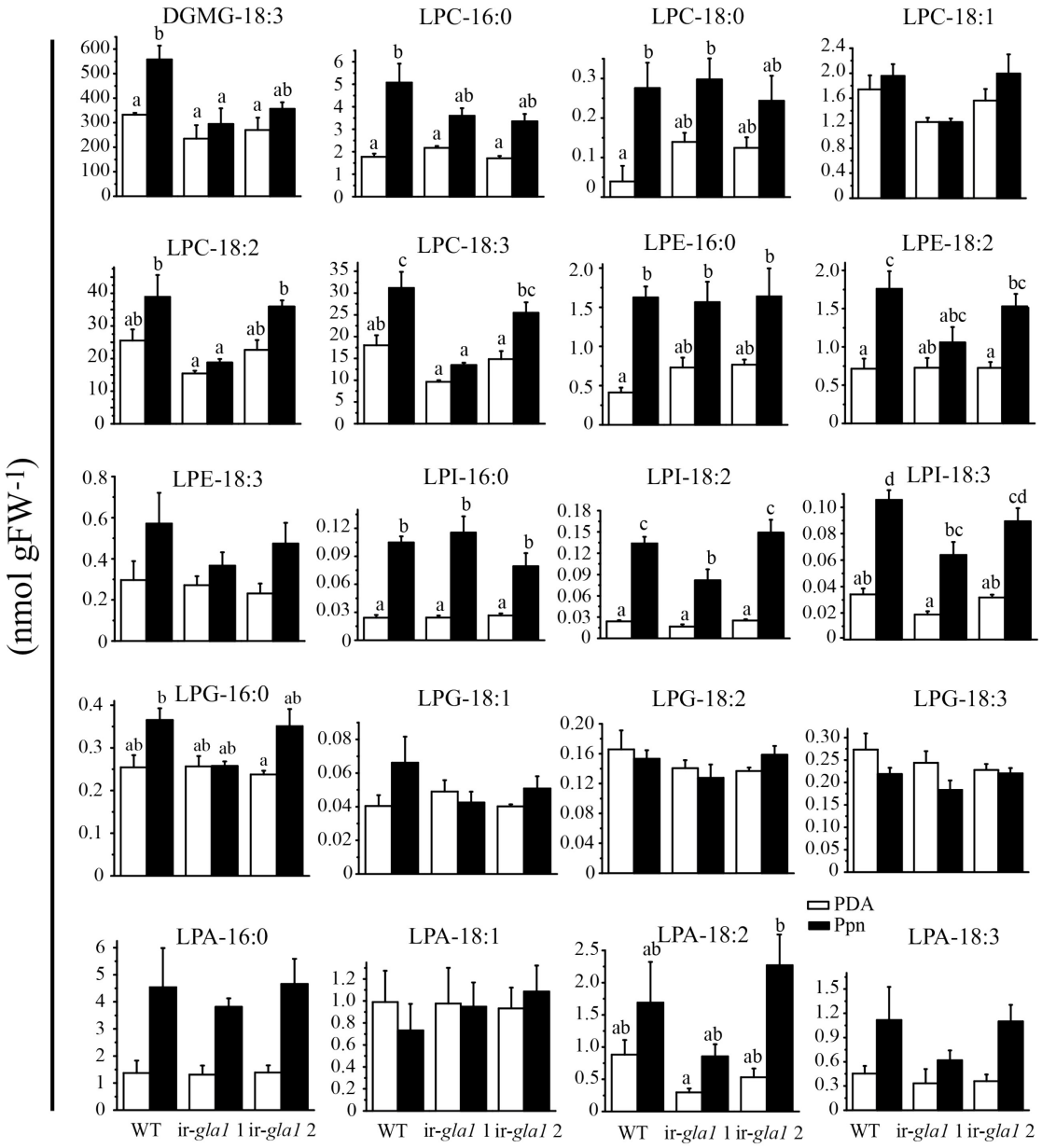

Supplemental Figure S5. Levels of DGMG-18:3, lysolipids derived from PC, PE, PI and PG and phosphatidic acid in WT and ir-*gla1* shoots after Ppn infection.

24 day old *N. attenuata* plants (WT and two ir-*gla1* lines) were infected with *Phytophthora parasitica* var. *nicotianae* (Ppn) and shoots were harvested at 4 dai for lysolipid analysis by LC-MS/MS. Plants treated with PDA (medium) served as control. Data was analyzed using one-way ANOVA and Tukey-post hoc test (n=3-5). Bars represent ± SE.

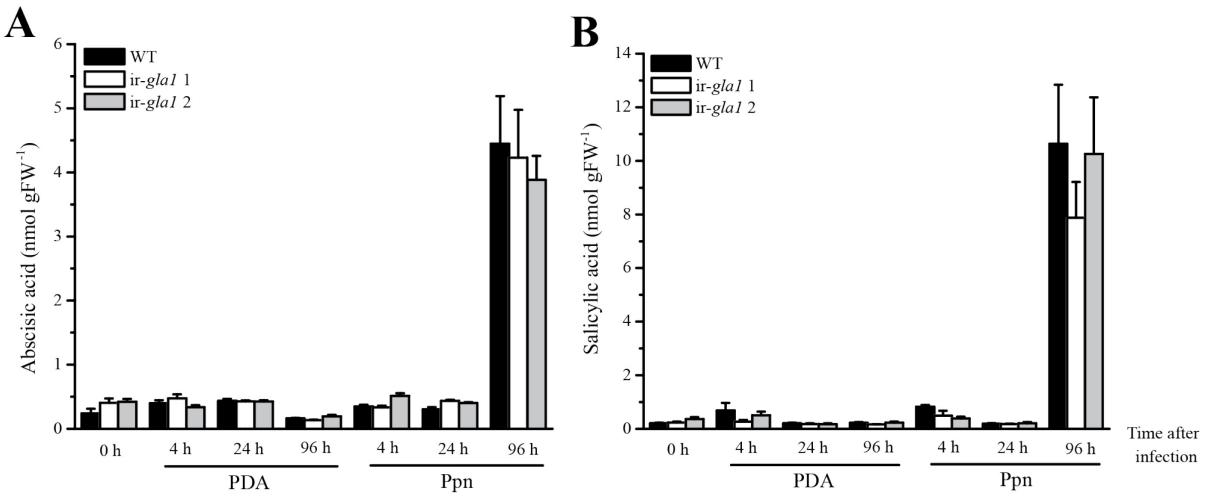

Supplemental Figure S8. Accumulation of abscisic and salicylic acid after Ppn infection.

Shoots of 24 days old *N. attenuata* plants (WT and two ir-*gla1* lines) infected by Ppn (control: PDA) were harvested at different time points after infection (0, 4, 24 and 96 h) and the levels of abscisic (**A**) and salicylic acid (**B**) were quantified by LC-MS/MS. ND: not detected. Bars denote ± SE (n=6-7 for 0 h, n=3-4 for 4 and 24 h and n=5-8 for 96 h after infection).

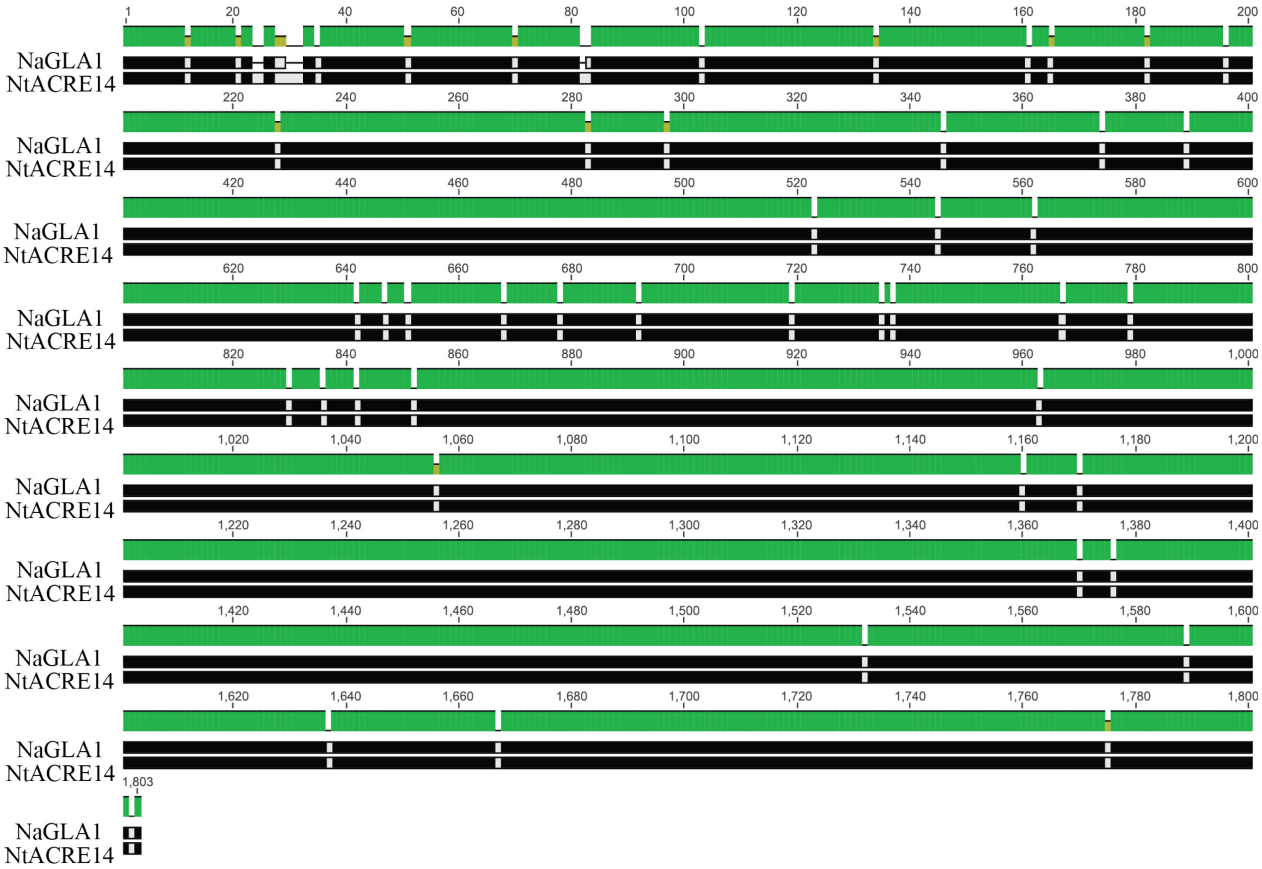

Supplemental Figure S10. Comparison of *Na*GLA1 with *Nt*ACRE14 protein sequence.

The protein sequences of *N. attenuata* GLA1 (*Na*GLA1; Genbank: ACZ57767) and *N. tabacum* ACRE14 (*Nt*ACRE14; Genbank: AAV92888; full length sequence obtained by blastn against the "*N. tabacum* Methylation Filtered Genome TGI:v.1 Contigs" at http://solgenomics.net/tools/blast/index.pl; Supplemental Figure S3) were aligned using the Geneious 5.5.7 software using default parameters. Amino acids identical between both proteins are displayed in black within the sequences and highlighted in green above the sequence alignment.

Chapter 5: Manuscript 3

HSPRO controls early *Nicotiana attenuata* seedling growth during interaction with the fungus *Piriformospora indica*

HSPRO Controls Early *Nicotiana attenuata* Seedling Growth during Interaction with the Fungus *Piriformospora indica*[1][C][W][OA]

Stefan Schuck, Iris Camehl, Paola A. Gilardoni, Ralf Oelmueller, Ian T. Baldwin, and Gustavo Bonaventure*

Department of Molecular Ecology, Max Planck Institute for Chemical Ecology, Jena 07745, Germany (S.S., P.A.G., I.T.B., G.B.); and Institute of General Botany and Plant Physiology, Friedrich-Schiller University of Jena, D–07743 Jena, Germany (I.C., R.O.)

In a previous study aimed at identifying regulators of *Nicotiana attenuata* responses against chewing insects, a 26-nucleotide tag matching the *HSPRO* (*ORTHOLOG OF SUGAR BEET Hs1^{pro-1}*) gene was found to be strongly induced after simulated herbivory (Gilardoni et al., 2010). Here we characterized the function of *HSPRO* during biotic interactions in transgenic *N. attenuata* plants silenced in its expression (ir-*hspro*). In wild-type plants, *HSPRO* expression was not only induced during simulated herbivory but also when leaves were inoculated with *Pseudomonas syringae* pv *tomato* DC3000 and roots with the growth-promoting fungus *Piriformospora indica*. Reduced *HSPRO* expression did not affect the regulation of direct defenses against *Manduca sexta* herbivory or *P. syringae* pv *tomato* DC3000 infection rates. However, reduced *HSPRO* expression positively influenced early seedling growth during interaction with *P. indica*; fungus-colonized ir-*hspro* seedlings increased their fresh biomass by 30% compared with the wild type. Grafting experiments demonstrated that reduced *HSPRO* expression in roots was sufficient to induce differential growth promotion in both roots and shoots. This effect was accompanied by changes in the expression of 417 genes in colonized roots, most of which were metabolic genes. The lack of major differences in the metabolic profiles of ir-*hspro* and wild-type colonized roots (as analyzed by liquid chromatography time-of-flight mass spectrometry) suggested that accelerated metabolic rates were involved. We conclude that *HSPRO* participates in a whole-plant change in growth physiology when seedlings interact with *P. indica*.

Nicotiana attenuata is a wild annual tobacco (*Nicotiana* spp.) plant native to the deserts of the southwestern United States and it germinates after fires from long-lived seed banks to form monocultures in post-fire nitrogen (N)-rich soils (Baldwin and Morse, 1994). As a result of its life history, *N. attenuata* grows rapidly after seed germination and the control of seedling growth is critical for plant fitness since young seedlings are more vulnerable to environmental stresses. In addition to water availability and high temperatures and light intensities, *N. attenuata* plants interact with unpredictable communities of beneficial and nonbeneficial organisms in their natural environment (Baldwin and Preston, 1999; Barazani et al., 2005; Long et al., 2010). With regard to biotic interactions, *N. attenuata* (and plants in general) readjust their metabolic and growth programs to meet the new requirements of de novo biosynthesis of direct (e.g. accumulation of toxic metabolites) and indirect (e.g. production of volatiles) defense responses as well as to induce tolerance mechanisms (e.g. carbon [C] and N bunkering in roots) or to facilitate symbiotic interactions (Rosenthal and Kotanen, 1994; Bardgett et al., 1998; Schwachtje and Baldwin, 2008). Activation of these responses requires metabolic energy and the redirection of C, N, and additional resources throughout the whole body of the plant (Schwachtje and Baldwin, 2008; Bolton, 2009). With the aim of identifying regulatory components of the pathways mediating defense and tolerance responses against lepidopteran larvae in *N. attenuata*, a serial analysis of gene expression approach was recently performed by our group to quantify the early transcriptional changes elicited by the insect elicitor *N*-linolenoyl-Glu (18:3-Glu; Gilardoni et al., 2010). The analysis targeted mRNAs encoding rare transcripts constitutively expressed and showing rapid and transient induction after 18:3-Glu elicitation. Among the approximately 500 differentially expressed transcripts, more than 25% corresponded to putative regulatory components (Gilardoni et al., 2010). One of these components was a homolog of a group of proteins denominated putative nematode resistance

[1] This work was supported by the Deutsche Forschungsgesellschaft (grant nos. BO3260/3–1 and 3–2) and the Max Planck Society.

* Corresponding author; e-mail gbonaventure@ice.mpg.de.

The author responsible for distribution of materials integral to the findings presented in this article in accordance with the policy described in the Instructions for Authors (www.plantphysiol.org) is: Gustavo Bonaventure (gbonaventure@ice.mpg.de).

[C] Some figures in this article are displayed in color online but in black and white in the print edition.

[W] The online version of this article contains Web-only data.

[OA] Open Access articles can be viewed online without a subscription.

www.plantphysiol.org/cgi/doi/10.1104/pp.112.203976

protein or ORTHOLOG OF SUGAR BEET $Hs1^{pro-1}$ (HSPRO) based on their homology to $Hs1^{pro-1}$ from sugar beet (*Beta vulgaris*; Cai et al., 1997).

To our knowledge, the study describing the role of $Hs1^{pro-1}$ was the first to provide functional information for this group of proteins, and $Hs1^{pro-1}$ was originally identified as a gene conferring resistance to the beet cyst nematode *Heterodera schachtii* (Cai et al., 1997). Subsequent studies performed in different plant species suggested however that this group of proteins has a more general role in the regulation of plant responses to biotic and abiotic stresses. For example, the Arabidopsis (*Arabidopsis thaliana*) genome encodes for two homologs of *Beta procumbens* $Hs1^{pro-1}$, *HSPRO1*, and *HSPRO2* and these two genes have been categorized as general stress signaling genes (Baena-González and Sheen, 2008). The expression of Arabidopsis *HSPRO* genes is not induced by nematode feeding (Puthoff et al., 2003) but it can be differentially induced by salicylic acid (SA), *Pseudomonas syringae* pv *tomato* (*Pst*) DC3000, and *Xanthomonas campestris* pv *campestris* infection, the bacterial elicitor flagellin22 (flg22), phosphate starvation, salt stress, drought, wounding, and UV-B (Hammond et al., 2003; Zipfel et al., 2004; Cominelli et al., 2005; Gissot et al., 2006; Fujita et al., 2007; Kudla et al., 2007; Murray et al., 2007; Walley et al., 2007). Genetic disruption of *HSPRO2* in Arabidopsis increased susceptibility to *Pst* DC3000 (Murray et al., 2007) and its ectopic expression confers increased resistance against oxidative stress (Luhua et al., 2008). The role of *HSPRO* genes in these processes is at present unknown. Interestingly, in Arabidopsis, it has been shown that HSPRO1 and HSPRO2 interact with the AKIN$\beta\gamma$ (adaptor-regulator related to the Suc NONFERMENTING1 [SNF1]/AMPK family) subunit of the SNF1-related protein kinase (SnRK1) complex (Gissot et al., 2006). This complex is a heterotrimeric protein kinase complex related to the *Saccharomyces cerevisiae* SNF1 kinase (Baena-González and Sheen, 2008). Plant SnRK1s are central regulators of metabolism via the control of gene expression and enzyme activity (Halford et al., 2003; Lovas et al., 2003; Schwachtje et al., 2006; Baena-González and Sheen, 2008).

In this study, we analyzed the role of the *HSPRO* gene in *N. attenuata* during diverse biotic interactions, including *M. sexta* herbivory, *Pst* DC3000 infection, and association with the growth-promoting fungus *Piriformospora indica*. *P. indica* is a root-colonizing basidiomycete of the order Sebacinales (Varma et al., 1999; Weiss et al., 2004) and is closely related to fungal clones isolated from soil samples collected from the rhizosphere of *N. attenuata* in its natural habitat (Barazani et al., 2005). *P. indica* has the ability to colonize roots of different plant species including *N. attenuata*, thereby initiating a mutualistic interaction resulting in plant growth promotion (Sahay and Varma, 1999; Barazani et al., 2005; Achatz et al., 2010; Fakhro et al., 2010). The results demonstrated that *HSPRO* is not involved in the regulation of traits associated with direct defense responses against *M. sexta* herbivory or performance of *Pst* DC3000 during infection, but is a negative regulator of *N. attenuata* early seedling growth stimulated by *P. indica*.

RESULTS

Sequence and Localization Analyses of *N. attenuata* HSPRO

From the serial analysis of gene expression analysis published recently by Gilardoni et al. (2010), a 26-nucleotide tag (UniTag-6205) was identified as a tag whose abundance was 18-fold enriched in leaves of *N. attenuata* plants within 30 min of elicitation with the fatty acid amino acid conjugate (FAC) 18:3-Glu. The full-length complementary DNA corresponding to UniTag-6205 was obtained by 5′ and 3′ RACE and it was found to encode for an open reading frame of 1,437 bases and for a predicted polypeptide of 478 amino acids (M_r: 54 kD). The protein presented 45% to 70% amino acid sequence identity to the sugar beet $Hs1^{pro-1}$ protein and to several homologs in other plant species including HSPRO1 and HSPRO2 from Arabidopsis (Fig. 1A; Supplemental Figs. S1 and S2). For consistency with the Arabidopsis nomenclature, we named the *N. attenuata* homolog HSPRO. The phylogenetic analysis of the 21 closest homologs of HSPRO from different plant species found in GenBank showed that amino acid similarity between paralogs was higher than between orthologs, with sequences from legumes, monocotyledonous, and Arabidopsis species clustering together (Fig. 1B). Interestingly, HSPRO sequences from monocots clustered closer to sequences from the moss *Physcomitrella patens* than did to sequences from dicots (Fig. 1B), thus not following the phylogeny of the taxa shown. In silico analysis predicted cytosolic localization for HSPRO and this prediction was confirmed by expressing an HSPRO-enhanced GFP (EGFP) C-terminal fusion protein in leaf protoplasts and analysis by fluorescence microscopy (Fig. 1C).

HSPRO Expression Is Induced by Different Biotic Stress-Associated Treatments

Analysis of *HSPRO* mRNA levels in *N. attenuata* plants showed that this gene was not only differentially induced by 18:3-Glu but also by *M. sexta* and *Spodoptera exigua* oral secretions (OS) in leaves (with *M. sexta* OS being the strongest inducer: approximately 12-fold) when compared with wounding (control treatment; Fig. 2A). FAC elicitation induces a strong jasmonic acid (JA) burst in *N. attenuata* plants (Kallenbach et al., 2010) and analysis of *HSPRO* expression in plants deficient in either JA (ir-*lox3*) and JA-Ile (ir-*jar4/6*) production or JA signaling (ir-*coi1*) showed that the induction of *HSPRO* was negatively affected by JA production (i.e. increased *HSPRO* mRNA

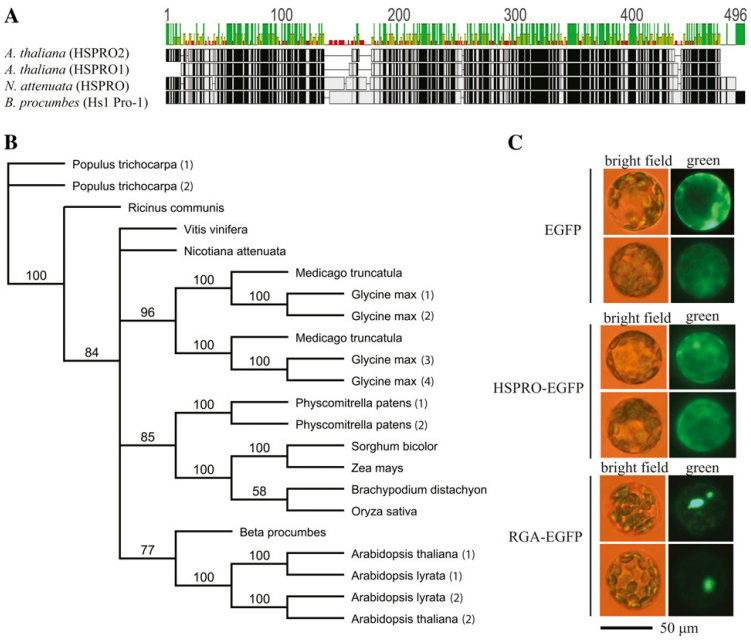

Figure 1. Analysis of HSPRO amino acid sequence and cellular localization. A, Schematic protein sequence alignment of *N. attenuata* HSPRO (JQ354963), Arabidopsis HSPRO1 (At2g4000) and HSPRO2 (At3g55840), and *B. procumbes* Hs1^{pro-1} (U79733 plus DQ148271). The cartoon above the sequences shows the percentage of similarity (green bars within the overlapping regions represent identical amino acids in the four sequences). See Supplemental Figure S2 for a detailed amino acid alignment. B, Phylogenetic analysis of HSPRO proteins from different organisms. The tree was constructed using the Geneious Pro software (5.3.4) with the Jukes-Cantor genetic distance model and the neighbor-joining tree building method with bootstrapping (602 random seed, 100 replicates, and 50% support threshold). See Supplemental Figure S1B for a reference to accession numbers. C, Arabidopsis mesophyll protoplasts were isolated and transiently transfected with vectors carrying either EGFP alone (cytosolic localization), EGFP C-terminal fusions with REPRESSOR OF ga1-3 (RGA-EGFP; nuclear localization), and EGFP C-terminal fusions with HSPRO (HSPRO-EGFP) under regulation of the cauliflower mosaic virus *35S* promoter. After transfection, protoplasts were incubated for 15 h in the dark at room temperature and images were taken with a Zeiss Axioplan fluorescence microscope with standard settings for EGFP.

accumulation in ir-*lox3* plants compared with the wild type [control]) but not affected in plants deficient in JA-Ile accumulation or *CORONATINE-INSENSITIVE1* (*COI1*) expression (Fig. 2B). Moreover, the induction of *HSPRO* expression depended on SA-induced protein kinase, a known regulator of JA-mediated responses in *N. attenuata* (Wu et al., 2007; Supplemental Fig. S3). *HSPRO* mRNA levels were induced 2.5-fold after 12 h of *Pst* DC3000 infection and 30-fold after 1 h of exogenous SA treatment (Fig. 2C; Supplemental Fig. S3) whereas they were not induced by *Agrobacterium tumefaciens* infection compared with control treatment (Fig. 2C). Thus, similar to other plant species, *HSPRO* responded to multiple biotic-stress-associated stimuli.

Analysis of tissue-specific expression showed that *HSPRO* was ubiquitously expressed with the highest levels of expression in flower parts, in particular the corolla (Fig. 2D).

Generation of *N. attenuata* Plants with Stably Reduced Levels of HSPRO Expression

To examine in further detail the function of *HSPRO*, stably transformed *N. attenuata* plants with reduced expression of this gene were generated by inverted-repeat-mediated RNA interference (see "Materials and Methods" for a detailed description of the generation of these plants). Two homozygous independently transformed lines, named ir-*hspro*1 and ir-*hspro*2, were selected and used for all the experiments described below. These lines harbored a single T-DNA insertion in their genomes (Fig. 3A) and the levels of *HSPRO* mRNA were reduced on average by 93% (ir-*hspro*1) and 95% (ir-*hspro*2) compared with wild-type plants after 18:3-Glu elicitation (a condition that maximizes *HSPRO* expression; Fig. 3B). A third line, ir-*hspro*3 harbored two T-DNA insertions in its genome (Figs. 3A) and it was used only for a selected number of

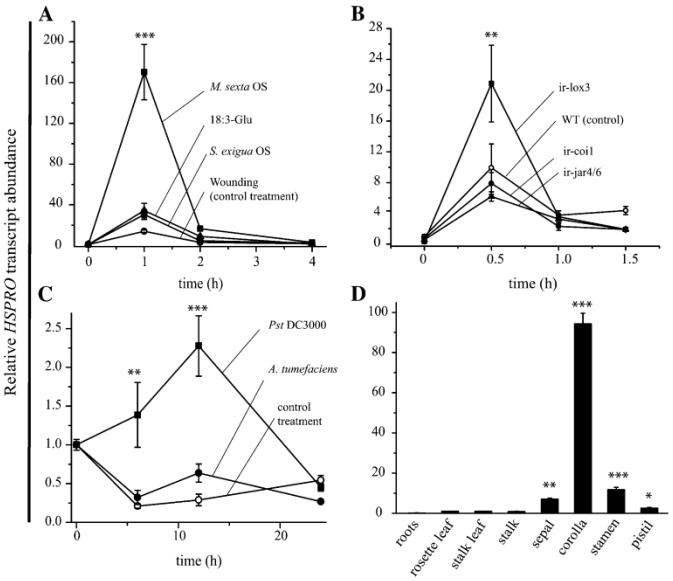

Figure 2. Analysis of *HSPRO* expression in wild-type and transgenic *N. attenuata* plants. The levels of *HSPRO* mRNA were analyzed by qPCR in leaves of wild-type and transgenic *N. attenuata* plants after different treatments and in different plant organs and tissues. mRNA levels are expressed relative to the levels of the reference gene Na-*EF1A*. Quantification was performed by the comparative cycle threshold method (n = 3–6; bars = ±SE). A, Elicitation of leaves from wild-type plants with OS from *M. sexta* and *S. exigua* larvae, synthetic 18:3-Glu, or wounding. One way-ANOVA with Tukey's post-hoc test (*M. sexta* OS versus wounding); ***, $P < 0.001$. B, Elicitation of leaves from wild-type and transgenic lines with synthetic 18:3-Glu. One way-ANOVA with Tukey's post-hoc test (ir-*lox3* versus the wild type); **, $P < 0.01$. C, Infection of leaves from wild-type plants with *Pst* DC3000 and *A. tumefaciens* (GV3101). One-way ANOVA with Tukey's post-hoc test (*Pst* DC3000 versus control); **, $P < 0.01$; ***, $P < 0.001$. D, *HSPRO* mRNA levels in different organs and tissues of wild-type *N. attenuata* plants. Relative levels of *HSPRO* mRNA in roots were set arbitrarily to 1. One-way ANOVA with Tukey's post-hoc test (roots versus other tissues); *, $P < 0.05$; **, $P < 0.01$; ***, $P < 0.001$.

experiments. The levels of *HSPRO* mRNA in this line were reduced by 91% compared with the wild type (Fig. 3B).

The growth and morphology of ir-*hspro* plants grown under standard chamber and glasshouse conditions were indistinguishable from those of the wild type at all stages of development (Fig. 3, C and D; see also below).

HSPRO Does Not Affect Defense Responses against *M. sexta* Herbivory and *Pst* DC3000 Infection

Based on the strong expression response of *HSPRO* to *M. sexta* OS and FACs (Fig. 2A), we first assessed whether ir-*hspro* plants were more susceptible to the attack of *M. sexta* larvae. The results showed that the performance of these larvae (evaluated as the gain of body mass as a function of time) was similar between ir-*hspro* and wild-type plants (Supplemental Fig. S4A). Consistently, the quantification of the JA-inducible defense metabolites nicotine, chlorogenic acid (3-*O*-caffeoylquinic acid), and rutin (quercetin-3-*O*-rutinoside) after elicitation with *M. sexta* OS showed that their amounts were similar in leaves of ir-*hspro* and wild-type plants (Supplemental Fig. S4, B–D).

Second, based on the high levels of *HSPRO* expression in flower parts and in particular the corolla (Fig. 2D), we assessed whether this gene participates in the regulation of traits (defensive and nondefensive) associated with the interaction of insects with flowers. The analyzed traits were: (1) the production of benzyl acetone in corollas, (2) the volume of nectar in flowers, (3) the amount of nicotine in nectar, (4) the amount of sugar in nectar, and (5) the level of trypsin protease inhibitor activity in ovaries and anthers. These traits were quantified in wild-type and ir-*hspro* plants grown either under control conditions or under the attack of *M. sexta* caterpillars for 15 consecutive days. All samples were collected at the end of the treatment (15 d). The results showed that the analyzed traits did not differ between ir-*hspro* and wild-type plants (Supplemental Fig. S5).

Finally, based on the induction of *HSPRO* mRNA levels by SA and *Pst* DC3000 infection (Fig. 2C), ir-*hspro* and wild-type plants were infected with this pathogen by leaf infiltration. In two independent experiments, the number of colony forming units (CFU) retrieved per area of infected leaves was similar between wild-type and ir-*hspro* plants at 24, 48, and 72 h postinfection (data not shown).

HSPRO Participates in the Mechanisms That Regulate Growth Promotion by the Fungus *P. indica*

The induction of *HSPRO* mRNA levels by diverse biotic-related stresses prompted us to investigate the interaction of ir-*hspro* plants with the growth-promoting fungus *P. indica*. This fungus has the capacity to establish symbiotic associations with roots of a broad range of plant species including *N. attenuata* (Varma et al., 1999; Barazani et al., 2005; Waller et al., 2005; Qiang et al., 2011). To study the interaction between ir-*hspro* seedlings and *P. indica*, we used a previously described plate system (Camehl et al., 2011; Fig. 4A). In this system, the hyphae reached the seedling's roots between day 4 and 5 after the start of the experiment (i.e. transfer of seedlings to plates containing *P. indica*; see "Materials and

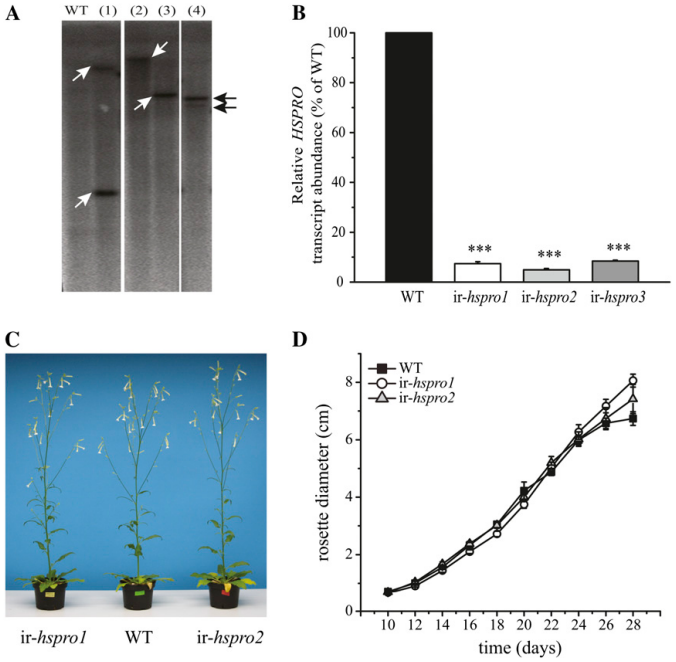

Figure 3. Characterization of ir-*hspro* plants. A, Southern-blot analysis of the ir-*hspro* transgenic lines. Genomic DNA from four independent ir-*hspro* *N. attenuata* lines (1–4) and wild-type plants was digested with *Eco*RV and resolved by agarose gel electrophoresis. A ^{32}P-labeled fragment corresponding to the hygromycin resistance gene *nptII* was used as a probe. The white arrows point to individual T-DNA insertions (lane 2: ir-*hspro1*; lane 3: ir-*hspro2*; lane 4: ir-*hspro3*). B, Analysis of *HSPRO* mRNA levels in leaves of ir-*hspro* lines at 1 h after 18:3-Glu elicitation ($n = 6$; bars = ±SE). Relative mRNA levels were quantified as detailed in caption of Figure 1. One-way ANOVA with Tukey's post-hoc test (wild type versus ir-*hspro*); ***, $P < 0.001$. C, Morphology of wild-type and ir-*hspro* plants at the late elongation stage. D, Rosette growth curve (measured as rosette diameter) of wild-type and ir-*hspro* plants (n = 8–20; bars = ±SE). [See online article for color version of this figure.]

Methods" for a detailed description of the system used). Unless noted, all the experiments were conducted with seedling tissue harvested at day 14 after the start of the experiment. In wild-type seedlings, *HSPRO* transcripts were undetected in roots of control treatment but strongly induced upon *P. indica* colonization (Fig. 4B). In colonized roots of ir-*hspro* seedlings, the level of this mRNA was also increased but it remained at less than 8% of wild-type levels (Fig. 4B).

The quantification of root, shoot, and seedling fresh biomasses showed that *P. indica*-colonized ir-*hspro* seedlings gained on average 30% more biomass than *P. indica*-colonized wild-type seedlings (Fig. 4, C–E). This experiment was repeated seven times with consistent results (Supplemental Table S1). The differential growth promotion of ir-*hspro* seedlings varied between 15% and 73% depending on the experiment and the length of the incubation period (10 or 14 d) with an average growth promotion of 32% (Supplemental Table S1). Thus, in addition to the growth promotion effect of *P. indica* observed on wild-type seedlings (Fig. 4, C–E; Supplemental Table S1), there was an enhanced differential growth promotion on ir-*hspro* seedlings. The difference in growth was maintained as the seedlings were transferred to soil and grown in the glasshouse for maturation. In this case, the rosette diameter was determined as a parameter of growth (Supplemental Fig. S6A). At the end of the rosette expansion period (i.e. start of reproductive phase [bolting]), the rosette diameter was similar between the two genotypes (Supplemental Fig. S6A). A higher percentage of ir-*hspro* plants bolted 1 d earlier than the wild type (25% and 42% of ir-*hspro1* and ir-*hspro2*, respectively) and the rate of stalk elongation and flowering time were similar between the genotypes (Supplemental Fig. S6, B–D). These results showed that the growth of *P. indica*-colonized ir-*hspro* seedlings was primarily accelerated during the early stages of seedling growth without consequences for the final plant size at the mature stage.

To analyze if the differential growth promotion of ir-*hspro* seedlings during interaction with *P. indica* was the result of a differential assimilation of CO_2 produced by the fungus, ir-*hspro* and wild-type seedlings and *P. indica* were grown together but physically separated from one another in a three-sector split-plate system (Supplemental Fig. S7A). This setting allowed for the exchange of CO_2 between organisms in the absence of physical contact. No differential growth promotion was observed between wild-type and ir-*hspro* seedlings in this experiment (Supplemental Fig. S7, B–D), indicating that physical interaction between roots and *P. indica* was required to differentially stimulate the growth of ir-*hspro* seedlings.

Analysis of *P. indica*-Root Interactions and *P. indica*-Induced Changes in Phytohormone Levels

Microscopy analysis of *P. indica*-colonized roots of wild-type and ir-*hspro* seedlings at two different times

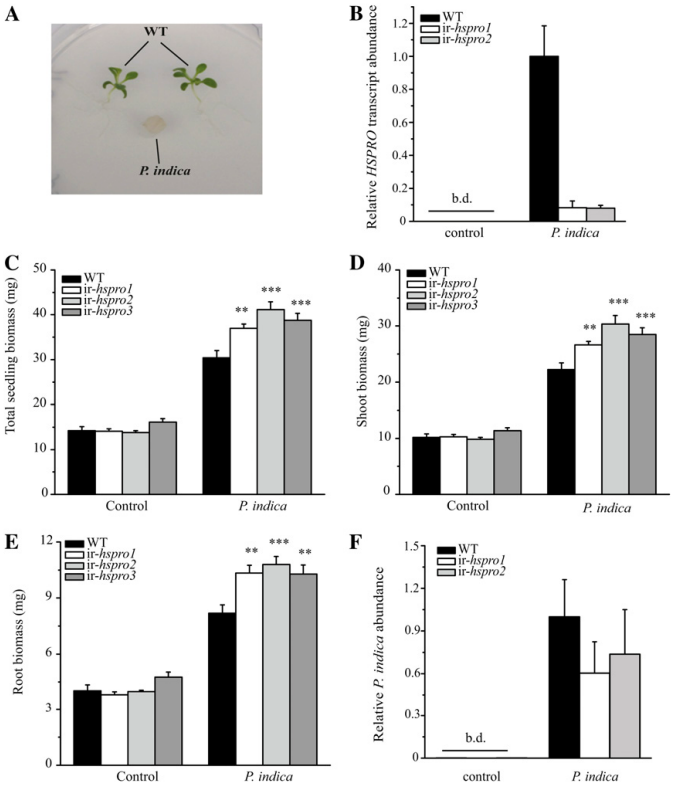

Figure 4. Induction of differential growth promotion of ir-*hspro* seedlings by *P. indica*. A, Plate system used for the experiments. Five days after germination in standard agar media, two seedlings were transferred onto a nylon mesh covering an agar plate at 1 cm distance from a plug transferred from a 2-week-old *P. indica* culture. B, Analysis of *HSPRO* mRNA levels in roots of wild-type and ir-*hspro* seedlings during interaction with *P. indica* and in control treatment (absence of *P. indica*). Root samples were harvested at day 14 ($n = 3$; bars = ±SE) and mRNA levels were quantified as detailed in caption of Figure 1. b.d., Below detection limit. C to E, Determination of the fresh biomass of total seedlings, shoots, and roots was performed with a microbalance after 14 d of seedling growth on the plate system ($n = 18$–20; bars = ±SE); one-way ANOVA with Tukey's post-hoc test (wild type versus ir-*hspro* during *P. indica* colonization); **, $P < 0.01$; ***, $P < 0.001$. F, Quantification of *P. indica* root colonization. DNA was extracted from roots of wild-type and ir-*hspro* seedlings colonized by *P. indica* at day 14 and fungal colonization was determined by qPCR based on the relative abundance of the π-*EF1a* gene compared with the Na-*EF1a* gene ($n = 16$–18; bars = ±SE). b.d., Below detection limit. [See online article for color version of this figure.]

(days 7 and 14 of the plate system) showed a close association between roots and the fungal hyphae (Supplemental Fig. S8). Similar to other plant species (Varma et al., 1999; Stein et al., 2008; Schäfer et al., 2009a; Lee et al., 2011; Zuccaro et al., 2011), the fungus colonized the maturation zone of the root without a strong association with the elongation zone and root tip (Supplemental Fig. S8). Also similar to previous observations performed with *N. attenuata* seedlings and *Sebacina vermifera* (a closely related Sebacinales species; Barazani et al., 2005), we could not detect fungal structures in the roots characteristic of endomycorrhiza (e.g. arbuscules and intracellular vesicles). Root growth and hair density after *P. indica* colonization were not different between wild-type and ir-*hspro* seedlings (Supplemental Fig. S9) and the number of secondary roots per seedling was also similar between genotypes (wild type: 5.25 ± 0.33; ir-*hspro1*: 4.50 ± 0.36; ir-*hspro2*: 4.92 ± 0.23; $n = 12$). Quantification of *P. indica* root colonization by quantitative amplification of the *P. indica EF1A* gene (Deshmukh et al., 2006) showed a lower tendency of root colonization of ir-*hspro* seedlings compared with wild-type seedlings, however the differences were not statistically significant (Fig. 4F). Hence, the differential growth promotion of ir-*hspro* seedlings was not associated with increased *P. indica* root colonization or root growth.

During colonization of Arabidopsis roots by *P. indica*, the regulation of root cell death by the fungus plays an important role (Jacobs et al., 2011; Qiang et al., 2011). When roots of *N. attenuata* wild-type and ir-*hspro* seedlings were analyzed for cell death by trypan blue staining in both the absence and presence of *P. indica* (at day 14 on the plate system), no differences in the staining pattern were observed between plant genotypes (Supplemental Fig. S10). It has been reported that the interaction of *P. indica* and closely related Sebacinales species with roots involves changes in phytohormone accumulation and signaling (Barazani et al., 2007; Stein et al., 2008; Vadassery et al., 2008; Schäfer et al., 2009b; Camehl et al., 2010). Quantification of JA, SA, abscisic acid (ABA), and ethylene (ET) levels in *P. indica*-colonized wild-type and ir-*hspro* seedlings (at day 14 on the plate system) showed that the levels of SA were reduced approximately 2-fold by root colonization but they did not differ between genotypes (Supplemental Fig. S11A). JA and ABA levels were not affected by root colonization while ET levels were induced. However, the levels of these phytohormones

were similar between genotypes (Supplemental Fig. S11B; data not shown). Interestingly, the levels of colneleic acid (CA), a divinyl-ether (DVE) derived from the action of 9-lipoxygenase (9-LOX), were strongly induced (from less than 1 nmol g fresh weight^{-1} to 40 nmol g fresh weight^{-1}) by *P. indica* in roots of both ir-*hspro* and wild-type seedlings (Supplemental Fig. S11C). These results suggested that similar to other plant species (Camehl et al., 2010; Jacobs et al., 2011; Leon-Morcillo et al., 2012), some defense-associated responses were triggered by *P. indica* in *N. attenuata* roots.

Gene Expression Profiling of ir-*hspro* Roots Reveals Significant Changes in Metabolic Processes during *P. indica* Colonization

To gain further insight into the mechanisms affected in ir-*hspro* plants, changes in gene expression in roots of ir-*hspro* and wild-type seedlings were analyzed. RNA was isolated from roots of wild-type and ir-*hspro* seedlings grown for 14 d on the plate system either in the absence or presence of *P. indica*, and changes in gene expression were evaluated with an Agilent custom array containing 43,533 *N. attenuata* probes (Gilardoni et al., 2011). This array represented approximately 70% to 80% of the *N. attenuata* transcriptome (Gase and Baldwin, 2012). Genes were considered to be differentially regulated when $\log_2$ (fold-changes [FCs]) were larger or equal to 1 or smaller or equal to −1 (ir-*hspro* versus the wild type) and *q* values were lower than 0.05 (corresponding to a false discovery rate less than 5%). Using these conditions, transcripts corresponding to 11 genes were differentially expressed in control roots of ir-*hspro* seedlings (Fig. 5A; Supplemental Table S2) while 417 genes were differentially expressed in *P. indica*-colonized roots of ir-*hspro* seedlings (Fig. 5B; Supplemental Table S2). In control roots, nine transcripts were up- and two down-regulated while in colonized roots, 293 transcripts were up-regulated and 124 were down-regulated (Fig. 5, A and B). Eight genes (all of unknown function) were differentially up-regulated in both control and *P. indica*-colonized roots (Fig. 5C; Supplemental Table S2).

In *P. indica*-colonized roots and based on the biological process, 60.6% of the annotated genes were involved in metabolic processes while 18.1% in responses to stimuli (Fig. 5D). Analysis of enzyme codes (Supplemental Tables S2 and S3), revealed that the most prevalent changes in gene expression occurred in enzymes involved in metabolic processes associated with the metabolism of starch and sugars, purines, nicotinate and nicotinamide, and membrane glycerophospholipids (Table I). Moreover, several genes involved in the transport of metabolites or ions were also affected in their expression (Table I). Gene ontology categorization by molecular function showed that genes encoding for enzymes with acyltransferase (14.2%), hydrolase (12.7%), and nucleotide binding (14.2%) activities were the most prevalent genes changing expression levels in ir-*hspro* roots (Fig. 5E; Table II). The changes in the expression of genes involved in metabolic processes were consistent with the differential growth rate of ir-*hspro* seedlings, and showed that the growth response was accompanied by significant changes in metabolic gene expression. The changes in the expression of genes involved in responses to stimuli (as the second-most prevalent group of genes; Fig. 5D) most likely reflected the processes affected in ir-*hspro* seedlings that were more directly connected with the interaction of roots with *P. indica*. The expression of several genes associated with phytohormone signaling was affected in ir-*hspro* roots and these included genes associated with JA (jasmonate zim-domain protein [JAZ], COI1), auxin (auxin response factor), and ABA (ABA INSENSITIVITY1b) signaling (Table II).

Interaction of *P. indica* with ir-*hspro* Roots Does Not Affect the Accumulation of Polar Metabolites

The changes in the expression of multiple genes involved in metabolic processes prompted us to investigate if the accumulation of primary and secondary metabolites was affected during the association of roots from ir-*hspro* seedlings with *P. indica*. For this purpose, we profiled small polar metabolites extracted from *P. indica*-colonized roots of wild-type and ir-*hspro* seedlings by liquid chromatography time-of-flight mass spectrometry. Root samples were harvested from seedlings grown for 14 d on the plate system and polar metabolites were extracted (see "Materials and Methods" for details). Ions were selected using the electrospray ionization interface in both positive and negative ion modes and those metabolites eluting from the liquid chromatography column between 125 and 550 s and having mass-to-charge ratio values ranging from 90 to 1,400 were selected for analysis. After data analysis (see "Materials and Methods" for a detailed description), no significant differences in the accumulation of ions in roots of ir-*hspro* and wild-type seedlings were detected in the negative ion mode (data not shown) and in the positive ion mode, the abundance of only three ions (out of more than 2,500 identified) changed significantly between these genotypes (Supplemental Table S4). The intensities of these ions were however low and the FCs small (between 2- and 2.8-fold down-regulated in ir-*hspro* roots).

Reduced *HSPRO* Expression in Roots Is Sufficient to Control Differential Growth Promotion in the Whole Seedling

We reasoned that if *HSPRO* had a general role associated with the control of growth instead of a more direct role in the control of the association of *P. indica* with roots, grafting experiments in which root stocks and shoot scions were reduced or not in *HSPRO* expression, could provide important information about the function of this gene. Hence, shoot scions and root stocks from either wild-type or ir-*hspro* seedlings were

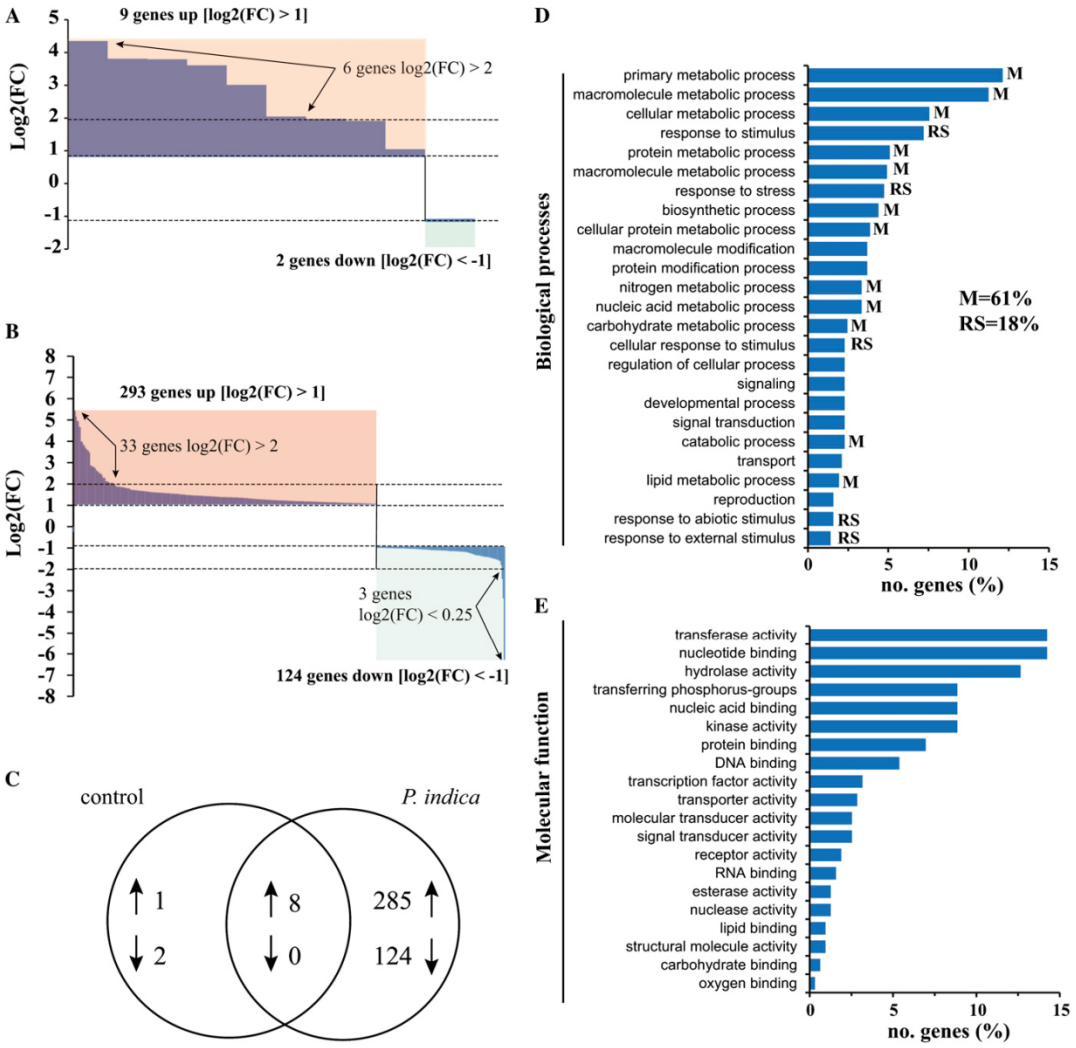

Figure 5. Microarray and Gene Ontology (GO) analysis of differentially expressed genes in *P. indica*-colonized roots of ir-*hspro* and wild-type seedlings. A, Distribution of FC of genes expressed differentially in roots of ir-*hspro* seedlings (ir-*hspro* versus the wild type). B, Distribution of FC of genes expressed differentially in roots of ir-*hspro* seedlings colonized by *P. indica* (ir-*hspro* versus the wild type). C, Venn diagram of the number of genes differentially expressed in control and colonized roots of ir-*hspro* seedlings compared with the wild type. The number in the intersection represents the genes differentially expressed in the two groups. D and E, Annotated genes differentially expressed in *P. indica*-colonized roots of ir-*hspro* seedlings were categorized based on biological processes (D) and molecular function (E), using the Blast2Go software. The numbers between brackets represent the percentage (%) of genes in the metabolism category (M) or in the stress response category (RS). [See online article for color version of this figure.]

reciprocally grafted (Fig. 6A) and the root, shoot, and seedling biomasses were quantified after 19 d of seedling growth in either the presence or absence of *P. indica*. A differential growth promotion was observed (compared with the wild type/wild-type seedlings) in all cases in which either the root stock or the shoot scion belonged to ir-*hspro* seedlings (Fig. 6, B–D). This differential growth promotion was similar to the grafted parental seedlings (ir-*hspro-1*/ir-*hspro-1* and ir-*hspro-2*/ir-*hspro-2*; Fig. 6, B–D).

Table I. *List of selected genes differentially expressed in P. indica-colonized roots of ir-hspro seedlings and involved in metabolic processes*

Gene ID	FC[a]	SD	*q* Value	Gene Description	Enzyme Codes
Starch and sugar metabolism					
Na_08858	3.4	1.1	2.8E-02	α Amylase precursor	EC:3.2.1.60; EC:3.2.1.1
Na_36852	3.0	1.0	8.7E-03	UDP-glucuronate4-epimerase3-like	EC:5.1.3.6
Na_32458	2.8	1.2	1.7E-02	Granule-bound starch synthase	EC:2.4.1.21
Na_31027	2.7	0.8	6.7E-03	β-Glucosidase41	EC:3.2.1.21
Na_36520	2.6	0.5	4.9E-03	β-Galactosidase precursor	EC:3.2.1.23
Na_16572	2.5	1.0	3.0E-02	UDP-sugar pyrophospharylase	EC:2.7.7.64
Na_33369	0.5	0.1	4.8E-03	Gal oxidase	EC:1.1.3.9
Na_42631	0.5	0.1	1.0E-02	α Glucosidase-like protein	EC:3.2.1.20
Purine metabolism					
Na_12907	3.3	1.0	1.4E-02	Nucleoside-triphosphatase	EC:3.6.1.15
Na_09592	2.8	0.2	4.0E-02	Adenosinetriphosphatase	EC:3.6.1.3
Na_26486	2.6	0.3	3.5E-02	Guanylate kinase	EC:2.7.4.8
Na_12713	2.1	0.1	1.1E-02	5′-nucleotidase	EC:3.1.3.5
Nicotinate and nicotinamide metabolism					
Na_38363	2.9	0.6	2.3E-02	Nicotinamidase	EC:3.5.1.19
Na_12713	2.1	0.2	1.1E-02	5′-nucleotidase	EC:3.1.3.5
Na_34109	2.0	0.5	2.9E-02	Aldehyde oxidase	EC:1.2.3.1
Glycerophospholipid metabolism					
Na_39990	2.1	0.3	5.7E-03	Glycerophosphodiester phosphodiesterase	EC:3.1.4.46
Na_12017	2.0	0.2	3.7E-02	Glycerol-3-phosphate dehydrogenase	EC:1.1.1.94; EC:1.1.1.8
Transport					
Na_05066	3.6	0.9	4.0E-03	Peptide transporter protein	
Na_13676	3.2	0.7	2.0E-03	Monosaccharide-sensing protein	
Na_27616	3.2	1.0	2.5E-02	Amino acid permease6	
Na_09592	2.8	0.2	4.0E-02	ATP-binding cassette transporter family protein	
Na_34386	2.3	0.3	4.9E-02	Aminophospholipid atpase	
Na_25349	2.2	0.1	1.1E-03	ATP-binding cassette transporter c family member4-like	
Na_21786	2.2	0.2	4.8E-02	Two-pore calcium channel	
Na_10110	2.1	1.1	4.9E-02	Potassium channel	
Na_27994	0.5	0.1	2.1E-03	Lipid-transfer protein	
Na_24731	0.5	0.1	7.1E-03	Bidirectional sugar transporter sweet2-like	

[a]ir-*hspro* versus the wild type.

DISCUSSION

As mentioned above, the function of $Hs1^{pro-1}$ in sugar beet was originally associated with resistance to cyst nematodes, however, several subsequent studies performed in different plant species have suggested that homologs of this gene have a more general role in the plant's response to environmental stresses (see the first section for references). Consistent with the observation that *HSPRO* homologs are induced by multiple stresses in Arabidopsis, we found that *N. attenuata HSPRO* mRNA levels were induced by multiple biotic-stress-associated stimuli including simulated lepidopteran herbivory, SA application, *Pst* DC3000 infection, and *P. indica* root colonization (Figs. 2 and 4B; Supplemental Figs. S3B and S9).

N. attenuata HSPRO Is a Negative Regulator of Seedling Growth Induced by *P. indica*

Microarray analysis of *P. indica*-colonized roots showed that silencing *HSPRO* expression brought about significant changes in gene expression and that the largest fraction (approximately 60%) of these genes were involved in metabolic processes (Fig. 5; Table I). These changes in gene expression were consistent with the accelerated growth of ir-*hspro* seedlings; increased growth rates are accompanied by increased metabolic rates to meet growth demands (e.g. cell walls and cellular membranes). Additionally, 18% of the genes affected in their expression in roots of ir-*hspro* seedlings were categorized as responses to stimuli and stresses (Fig. 5). The genes in this category probably reflected those genes having a more direct association with the interaction of roots with *P. indica* (Table II). In the absence of *P. indica* colonization, changes in gene expression in roots of ir-*hspro* plants were very small, with only 11 genes changing expression compared with wild-type seedlings (Fig. 5A). These results were consistent with a function of HSPRO in the control of metabolism during stress responses.

Similar to the interaction of roots from different plant species with arbuscular mycorrhizal fungi (Strack et al., 2003; Hause and Fester, 2005; Herrera-Medina et al., 2007), the interaction between *P. indica* and plant roots is controlled by multiple phytohomones including auxin and cytokinins (Vadassery et al., 2008), gibberellins (Schäfer et al., 2009a), ET (Barazani et al., 2007; Camehl et al., 2010), SA, and JA (Jacobs et al., 2011). Changes in

Table II. *List of selected genes differentially expressed in P. indica-colonized roots of ir-hspro seedlings and involved in regulatory processes*

Gene ID	FC[a]	SD	*q* Value	Gene Description
Transcription				
Na_10354	11.5	2.1	7.2E-05	Transcription factor Abnormal cell Lineage protein11, insulin gene enhancer protein Isl-1, Mechanosensory protein3
Na_40479	2.2	0.5	2.8E-02	No apical meristem, ATAF1 and ATAF2, CUC2 domain transcription factor
Na_31687	0.5	0.1	7.8E-03	Nuclear Protein Localization6-like
Na_26270	0.5	0.1	2.3E-02	Retinoblastoma-related protein1-like (RB1-like)
Na_06561	0.5	0.1	2.1E-02	MYB transcription factor
Na_29071	0.4	0.1	1.5E-03	MYB transcription factor
Protein kinase activity				
Na_36458	3.0	1.1	4.8E-03	Ser Thr protein kinase
Na_25553	3.0	0.6	2.3E-02	Protein kinase domain-containing protein
Na_18646	2.8	1.0	1.7E-02	Calcineurin B-Like-interacting Ser Thr-protein kinase
Na_41571	2.6	0.5	2.2E-03	Protein kinase1b
Na_18066	2.6	0.4	6.9E-03	Receptor like protein kinase-like
Na_38660	2.5	0.5	4.8E-02	Protein kinase family protein
Na_15274	2.4	0.5	1.3E-02	Tomato homolog to Arabidopsis Constitutive Triple Response2 protein
Na_26181	0.5	0.1	2.5E-02	Leu-rich repeat receptor-like protein kinase
Na_21188	0.5	0.0	4.9E-03	Leu-rich repeat protein kinase-like protein
Hormone signaling				
Na_36236	3.1	1.0	3.2E-03	Zeatin *o*-glucosyltransferase
Na_13465	2.6	1.0	4.1E-02	ABA-responsive transcription factor
Na_43242	2.5	0.6	4.1E-02	Indole-3-acetic acid-amido synthetase
Na_20394	2.3	0.7	2.2E-02	JAZ
Na_04958	2.3	0.1	2.6E-03	COI1
Na_15777	2.0	0.5	5.0E-02	Auxin response factor
Na_28242	2.0	0.5	3.0E-02	ABA INSENSITIVITY1b
Na_24453	0.5	0.0	3.6E-04	Auxin-induced saur-like protein
Na_10858	0.5	0.1	2.8E-02	ET-responsive transcription factor WIN1
Direct defense responses				
Na_00974	2.6	1.0	3.1E-02	Vicilin-like antimicrobial peptides2-1-like
Na_40698	2.0	0.4	7.2E-03	Disease resistance protein
Na_42497	0.5	0.1	6.8E-03	Callose synthase10-like

[a]ir-*hspro* versus the wild type.

the mRNA levels of auxin and ET signaling components and a cytokinin biosynthesis gene were affected in colonized roots of ir-*hspro* seedlings (Table II). Moreover, changes were also detected in the expression of COI1 and a JAZ homolog (Table II), two components of the JA-signaling pathway (Xie et al., 1998; Turner, 2007; Paschold et al., 2008). Together the results suggested that the phytohormone-signaling network was affected in ir-*hspro* plants and that these changes are probably part of the mechanisms effecting differential growth promotion of these plants during interaction with *P. indica*.

Differential expression of genes involved in ET and JA signaling in roots of wild-type and ir-*hspro* seedlings were not accompanied however by the differential accumulation of these phytohormones. The levels of JA and ABA in roots did not change during *P. indica* root colonization compared with uncolonized roots (Supplemental Fig. S11B) and although ET and SA levels were affected by *P. indica* root colonization the levels were similar between wild-type and ir-*hspro* seedlings (Supplemental Fig. S11A). The reduction in SA levels in *P. indica*-colonized roots may reflect the suppression of defense and cell death responses in *N. attenuata* seedlings. Lower SA levels in tobacco and Arabidopsis have been correlated with higher *Glomus mosseae* (Herrera Medina et al., 2003) and *P. indica* (Jacobs et al., 2011) root colonization, respectively. However, the accumulation of CA, a DVE strongly induced in leaves of Solanaceae species upon infection by *Phytophthora* spp. (Weber et al., 1999; Bonaventure et al., 2011), was also strongly induced in roots by *P. indica* in both ir-*hspro* and wild-type seedlings, indicating that oxylipin-related defense pathways were activated by this fungi (Supplemental Fig. S11C). CA is a DVE that is strongly induced in leaves of tobacco and potato (*Solanum tuberosum*) plants in response to pathogens such as *Phytophthora parasitica* and *Phytophthora infestans* (Weber et al., 1999; Göbel et al., 2002; Fammartino et al., 2007). It has been shown that DVEs have antimicrobial properties by, for example, inhibiting mycelial growth and spore germination of some

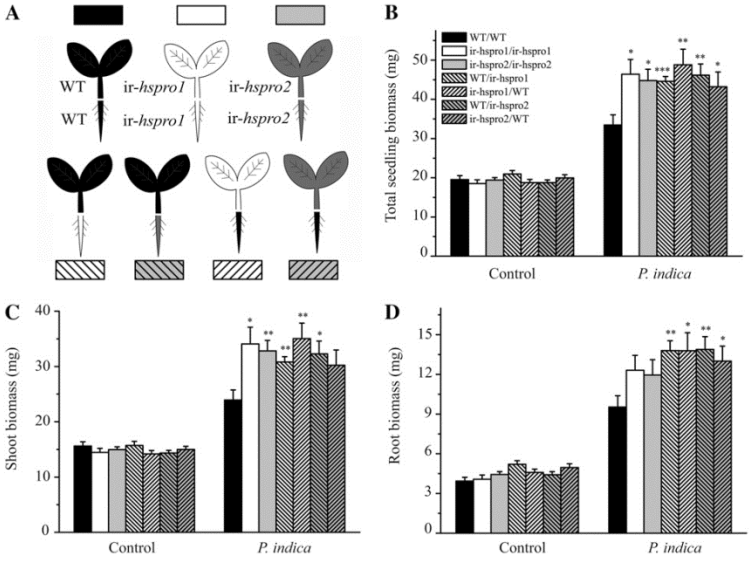

Figure 6. Reciprocal grafting of ir-*hspro* and wild-type seedlings and determination of seedling biomass during root colonization by *P. indica*. A, Scheme of the grafting combinations used. B to D, Determination of the fresh biomass of total seedlings, shoots, and roots was performed with a microbalance after 19 d of seedling growth on the plate system. One way-ANOVA with Tukey's post-hoc test (wild type versus ir-*hspro* during *P. indica* colonization); *, $P < 0.05$; **, $P < 0.01$; ***, $P < 0.001$ ($n = 18–20$; bars = ±SE).

Phytophthora species (Prost et al., 2005). Interestingly, during the interaction of *G. intraradices* with tomato (*Solanum lycopersicum*) roots, there is a strong induction of genes involved in the formation of oxylipins derived from 9-LOX activity, and it has been suggested that 9-LOX products may control arbuscular mycorrhizal fungal spread in roots (Leon-Morcillo et al., 2012).

Gene expression analysis by microarray hybridization showed only three genes directly associated with defense responses and differentially expressed in *P. indica*-colonized roots of ir-*hspro* seedlings (Supplemental Table S2). These observations were consistent with the current understanding of the mechanisms involved in the association of plant-growth-promoting rhizobacteria and fungi with roots; the activation of immune responses by plants and their suppression by microorganisms underlay the establishment of long-term mutualistic interactions (Preston, 2004; Van Wees et al., 2008; Zamioudis and Pieterse, 2012).

Grafting experiments demonstrated that the silencing of *HSPRO* expression in roots was sufficient to induce differential growth promotion in both roots and shoots of ir-*hspro* seedlings. Thus, the effect on shoot growth was dependent on the function of HSPRO in the roots. Because small-silencing RNAs generated in shoots of *N. attenuata* seedlings can be transported to roots (but not vice versa) and reduce gene expression of the targeted gene in the latter tissue (Fragoso et al., 2011), the similar effect on growth promotion observed in wild-type (shoot)/ir-*hspro* (root) and ir-*hspro* (shoot)/wild-type (root) grafted seedlings was most likely explained by shoot-induced silencing of *HSPRO* expression in roots of ir-*hspro* (shoot)/wild-type (root) grafted seedlings (Fig. 6A). Microscopy analysis of *P. indica*-colonized and uncolonized roots did not reveal morphological changes in roots of ir-*hspro* seedlings compared with the wild type, changes in the association pattern of *P. indica* with the maturation zone of the root, or differential root cell death (Supplemental Figs. S8–S10). The microbe-mediated stimulation of plant growth has been associated with improved plant nutrition via increased uptake of growth-limiting soil nutrients. Since *P. indica* root colonization and root growth was not different between ir-*hspro* and wild-type seedlings and seedlings were grown under conditions of high nutrient availability (media or soil), it is unlikely that increased uptake of growth-limiting nutrients was a main factor influencing the *P. indica*-induced differential growth promotion of ir-*hspro* seedlings. Barazani et al. (2005) showed that the nutritional status of *N. attenuata* plants colonized by *S. vermifera* and *P. indica* does not depend on N and phosphorous supply, and similar results were reported by Achatz et al. (2010) in *P. indica*-barley (*Hordeum vulgare*) symbiosis. Since growth and metabolic rates are mutually dependent, further experiments will be required to disentangle the role of *HSPRO* in the control of growth and/or metabolism. As mentioned in the introduction, the Arabidopsis HSPRO1 and HSPRO2 proteins interact with the AKIN$\beta\gamma$ subunit of the SnRK1 complex (Gissot et al., 2006). Thus, although speculative at this point, one possible scenario is that HSPRO affects *N. attenuata* seedling growth and/or metabolism via its association with SnRK1.

What's the Role of HSPRO in Responses against Insects and Pathogenic Bacteria?

Herbivore attack elicits metabolically costly defenses that can decrease plant fitness by limiting metabolic resources otherwise invested in growth and reproduction (Schwachtje and Baldwin, 2008; Bolton, 2009). The performance of *M. sexta* larvae and the *M. sexta*-OS elicited induction of the defense-associated metabolites nicotine, chlorogenic acid, and rutin were similar between ir-*hspro* and wild-type plants (Supplemental Fig. S4). Moreover, flower traits associated with the interaction of plants with insects were not affected in *M. sexta*-attacked or -unattacked ir-*hspro* plants (Supplemental Fig. S5). Thus, these results suggested that *HSPRO* was not directly involved in the regulation of induced defenses or plant-insect association traits.

Similarly, the performance of *Pst* DC3000 on leaves of ir-*hspro* plants was unaffected compared with wild-type plants. These results contrasted those made with Arabidopsis, where plants disrupted in *HSPRO2* expression supported increased *Pst* DC3000 growth in leaves (Murray et al., 2007). However, similar to *HSPRO2* expression in Arabidopsis (Murray et al., 2007), *N. attenuata HSPRO* was also induced by SA and *Pst* DC3000 infection (Fig. 2; Supplemental Fig. S3), suggesting these two genes have both overlapping and divergent functions during bacterial infection in these two plant species.

Although speculative at this point, one possible scenario is that *HSPRO* regulates plant tolerance mechanisms against insect herbivores. In *N. attenuata*, the mRNA levels of GAL83 (a β-subunit of SnRK1) are rapidly repressed upon insect herbivory and it has been shown that GAL83 is involved in the regulation of tolerance to insect herbivory via the control of resource allocation in roots (Schwachtje et al., 2006). Thus, one possibility is that the *HSPRO* gene product in *N. attenuata* participates in the regulation of tolerance mechanisms associated with the regulation of SnRK1 activity.

Plant responses to insect herbivores can also involve changes in the association of roots with belowground beneficial microorganisms such as growth-promoting fungi and rhizobacteria (Bardgett et al., 1998; Pineda et al., 2010). For example, insect herbivory can affect mycorrhizal colonization (Gehring and Whitham, 1991; Gehring and Bennett, 2009) or the composition of the root-associated microbial community (Sthultz et al., 2009). Thus, although speculative at this point, but given the results obtained with *P. indica*, an alternative (but not excluding) scenario is that *HSPRO* participates in mechanisms that control the interaction of herbivore-attacked plants with belowground microorganisms (e.g. via changes in nutrient allocation and root exudates). Plants interacting with beneficial microbes can benefit from an increase in tolerance to herbivory, for example, by affecting C and N reallocation used for tissue regrowth after herbivory (Bardgett et al., 1998). Additionally, plants can also benefit via increased resistance to plant pathogens (Pineda et al., 2010). However, association with beneficial microorganisms can also reduce plant fitness by compromising induced defense responses against insect herbivores (Barazani et al., 2005). Thus, a delicate balance of interactions between roots and microorganisms is required to optimize plant fitness in nature and *HSPRO* may play a role in this process. These hypotheses are the focus of future research.

CONCLUSION

The results presented in this study have unraveled the important role that *HSPRO* has in the control of early *N. attenuata* seedling growth stimulated by the growth-promoting fungus *P. indica*. Since the effect on growth was only observed when ir-*hspro* seedlings were colonized by this fungus, and *HSPRO* expression was induced by multiple stress-associated stimuli, the results suggested that *HSPRO* plays an important role in growth and/or metabolism readjustment during stress responses. Although speculative, the control over metabolism during insect herbivory could involve the regulation of resource partitioning between shoots and roots and its resulting consequences in the interaction of roots with soilborne microbes. The results opened new hypotheses on how this control may be achieved, and the interaction of HSPRO with components of the SnRK1 complex appears as one potential scenario. Future work will focus on the disentangling of the *HSPRO*-dependent mechanisms underlying the regulation of growth/metabolism during stress responses.

MATERIALS AND METHODS

Please refer to online Supplemental Materials and Methods S1 for additional experimental details.

Plant Growth and Treatments

Seeds of the 31st generation of an inbred genotype of *Nicotiana attenuata*, originally collected from southwestern Utah in 1988, were used for all experiments. For glasshouse experiments, seeds from wild-type and genetically transformed plants were germinated as previously described (Krügel et al., 2002). Plants were grown in the glasshouse under high-pressure sodium lamps (200–300 μmol s^{-1} m^{-2} light) with a day/night cycle of 16 h (26°C–28°C)/8 h (22°C–24°C) and 45% to 55% humidity. For plate experiments with *Piriformospora indica* see section "*P. indica* Maintenance and Inoculation of *N. attenuata* Seedlings" below. *N. attenuata* ir-*lox3* (Allmann et al., 2010), ir-*jar4/6* (Kang et al., 2006), ir-*coi1* (Paschold et al., 2008), and ir-*sipk* (Wu et al., 2007) plants have been previously described.

For wounding and elicitation treatments, leaves were wounded by rolling a fabric-pattern wheel three times on each side of the midvein and the wounds were supplemented either with 10 μL of 0.01% (v/v) Tween 20 in water (wounding treatment), 10 μL of 18:3-Glu (0.03 nmol/μL; FAC elicitation), or 10 μL of *Manduca sexta* or *Spodoptera exigua* OS (OS elicitation). For analysis of gene expression, *Pseudomonas syringae* pv *tomato* (*Pst*) DC3000 and *Agrobacterium tumefaciens* (GV3101) were grown on Luria-Bertani liquid medium containing 25 μg mL^{-1} Rifampicin until optical density at 600 nm (OD_{600}) = 0.5 to 0.6. Bacteria were pelleted and resuspended in 10 mM $MgCl_2$ to a final OD_{600} = 0.02 (10^7 CFU mL^{-1}). This suspension was syringe infiltrated into leaves (1 mL $leaf^{-1}$). As control treatment, leaves were infiltrated with an aqueous solution of 10 mM $MgCl_2$. For infection assays with *Pst* DC3000, the bacteria pellet was resuspended in 10 mM $MgCl_2$ to a final OD_{600} = 0.001 (10^5 CFU mL^{-1}) and the

suspension was syringe infiltrated into leaves (1 mL leaf^{-1}). Leaf discs of 8 mm in diameter were harvested at different times (0, 1, 2, and 3 d), ground in 0.3 mL of sterile water, and after centrifugation, one-tenth serial dilutions of the supernatant were plated out on Luria-Bertani agar plates containing 25 μg mL^{-1} Rifampicin. Plates were incubated for 2 d at 28°C and the CFU were counted. For SA treatment, a solution of 300 μM SA dissolved in 0.2% (v/v) Tween 20/water was used. The solvent alone was used as control treatment. Tissue expression profile of *HSPRO* was evaluated by collecting different plant tissues from wild-type *N. attenuata* plants; rosette leaves and roots were collected from 30-d-old (rosette stage) plants whereas stalks, stalk leaves, sepals, pistils, corolla, and stamens were collected from 50-d-old plants.

Generation of Stably Silenced Lines

A PCR fragment generated with primers ir-hspro-fwd and ir-hspro-rev (Supplemental Table S5) and *HSPRO* complementary DNA as template was subcloned using *Sac*I and *Xho*I (New England Biolabs) restriction sites into the pSOL8 transformation vector (Bubner et al., 2006) as an inverted-repeat construct. This construct was used to transform *N. attenuata* wild-type plants using *A. tumefaciens*-mediated transformation and plant regeneration as previously described (Krügel et al., 2002). T1 transformed plants were analyzed for T-DNA insertion number by DNA gel-blot hybridization (see below). Segregation analysis for hygromycin resistance in T2 seedlings was performed on agar plates supplemented with hygromycin (0.035 mg mL^{-1}). Two lines, ir-*hspro*1 and ir-*hspro*2 had a single T-DNA insertion in their genomes, and were used for most of the experiments. A third line, ir-*hspro*3 had two T-DNA insertions and was used for some experiments. Efficiency of gene silencing (*HSPRO* mRNA levels) in ir-*hspro* plants was evaluated by quantitative real-time PCR (qPCR; see below) after 1 h of 18:3-Glu elicitation using the primers listed in Supplemental Table S5. For Southern-blot analysis, genomic DNA from wild-type and ir-*hspro* plants was isolated by the cetyltrimethylammonium bromide method. DNA samples (5 μg) were digested with *Eco*RV (New England Biolabs) overnight at 37°C according to commercial instructions and separated on a 0.8% (w/v) agarose gel using standard conditions. DNA was blotted onto gene screen plus hybridization transfer membranes (Perkin Elmer Life and Analytical Sciences) using the capillary transfer method. A gene-specific probe for the hygromycin resistance gene *hptII* was generated by PCR using the primers HYG1-18 and HYG3-20 (Supplemental Table S5). The probe was labeled with [α-^{32}P]dCTP (Perkin Elmer) using the Rediprime II kit (Amersham Pharmacia) according to commercial instructions.

P. indica Maintenance and Colonization of *N. attenuata* Seedlings

P. indica was maintained on Kaefer medium (a modified *Aspergillus* spp. minimal medium; Pham et al., 2004) containing 1% (w/v) agar. For seedling colonization, 9-cm discs of polyamide mesh (pore 70 μm/thickness 80 μm; SEFAR GmbH) were placed on top of 9-cm agar plates containing modified plant nutrient culture medium [5 mM KNO_3, 2 mM $MgSO_4$, 2 mM $Ca(NO_3)_2$, 0.01 μM $FeSO_4$, 70 μM H_3BO_3, 14 μM $MnCl_2$, 0.5 μM $CuSO_4$, 1 μM $ZnSO_4$, 0.2 μM Na_2MoO_4, 0.01 μM $CoCl_2$, 10.5 g L^{-1} agar, pH 5.6, 0.6% (w/v) agar]. Two 7-d-old *N. attenuata* seedlings germinated on Gamborg's B5 medium (pH: 6.8; 0.6% [w/v] agar) were laid on the polyamide discs at a distance of 1 cm from an agar plug placed in the center of the plate and containing a 2-week-old *P. indica* culture (Fig. 4A). Agar plugs without fungus were used as control. The plates were incubated horizontally for 10 or 14 d at 21°C and light was supplied from the side for 16 h d^{-1} with a white fluorescent light source (80 μmol m^{-2} s^{-1}). The fresh biomass of total seedlings, roots, and shoots was determined with a microbalance. Seedling grafting was performed as previously described (Fragoso et al., 2011). After grafting, seedlings were first kept for 5 d on Gamborg's B5 medium containing 0.8% (w/v) agar for recovery and were then transferred to agar plates covered with polyamide mesh discs and preincubated (7 d before) with *P. indica* agar plugs. The fresh biomass of total seedlings, roots, and shoots was determined in this case 19 d after the transferring of the seedlings to the *P. indica*-containing plates (due to the slower growth of grafted seedlings compared with intact seedlings).

qPCR

Total RNA was extracted using the TRIzol reagent (Invitrogen) and 5 μg of total RNA were reverse transcribed using oligo(dT)$_{18}$ and SuperScript reverse transcriptase II (Invitrogen). qPCR was performed with a Mx3005P Multiplex qPCR system (Stratagene) and the qPCR core kit for SYBR Green I (Eurogentec). Relative quantification of *HSPRO* mRNA levels was performed by the comparative cycle threshold method using the elongation factor 1A (Na-*EF1A*) mRNA as an internal standard (Gilardoni et al., 2010). The sequences of the primers used for qPCR are listed in Supplemental Table S5. All the reactions were performed using the following qPCR conditions: initial denaturation step of 95°C for 10 min, followed by 40 cycles each of 95°C for 15 s and 60°C for 1 min, with a final extension step of 95°C for 15 s and 60°C for 30 s. All samples were obtained from at least three independent biological replicates (n = 3) for each time point, plant genotype, and treatment.

For quantification of *P. indica* colonization rates, DNA was extracted from *P. indica*-colonized roots and control roots by the cetyltrimethylammonium bromide method. qPCR was performed using SYBR Green and 20 ng of isolated DNA as template. Copy number of the *P. indica* translation elongation factor 1a (π-*EF1A*) gene (Deshmukh et al., 2006) relative to the Na-*EF1A* gene was used to quantify colonization rates of *P. indica* by the comparative cycle threshold method. The primers used are listed in Supplemental Table S5.

Statistical Analysis

Statistics were calculated using the SPSS software version 17.0. The data were subjected to one-way ANOVA (and means were compared by the Tukey's post-hoc test). For analysis of differences in bolting and flowering time the Kolmogorov-Smirnov test was used. The number of replicates (n) used in each experiment are detailed in the figures' captions.

Data from this article can be found under the following accession numbers: Na-HSPRO (JQ354963; GenBank database), Agilent Chip platform (GPL13527; National Center for Biotechnology Information Gene Expression Omnibus database), microarray data (GSE35086; National Center for Biotechnology Information Gene Expression Omnibus database).

Supplemental Data

The following materials are available in the online version of this article.

Supplemental Figure S1. Alignment of *N. attenuata* HSPRO protein sequence with close homologs in different plant and moss species.

Supplemental Figure S2. Alignment of *N. attenuata* HSPRO protein sequence with homologs in Arabidopsis and *B. procumbens*.

Supplemental Figure S3. Analysis of *HSPRO* expression in wild-type plants and in transgenic plants reduced in MAP kinase expression.

Supplemental Figure S4. Analysis of defense responses against *M. sexta* in wild-type and ir-*hspro* plants.

Supplemental Figure S5. Analysis of flower traits associated with the interactions of *N. attenuata* plants with insects.

Supplemental Figure S6. Analysis of growth and developmental parameters of *P. indica*-colonized plants grown in the glasshouse.

Supplemental Figure S7. Analysis of growth promotion of wild-type and ir-*hspro* seedlings induced by *P. indica* in a split-plate system.

Supplemental Figure S8. Laser confocal microscopy analysis of roots from *P. indica*-colonized wild-type and ir-*hspro* seedlings.

Supplemental Figure S9. Root morphology of *P. indica*-colonized wild-type and ir-*hspro* seedlings.

Supplemental Figure S10. Analysis of root cell death in wild-type and ir-*hspro* seedlings.

Supplemental Figure S11. Analysis of SA, JA, and CA levels in roots of wild-type and ir-*hspro* seedlings.

Supplemental Table S1. Analysis of wild-type and ir-*hspro* seedling's biomasses during *P. indica*-root colonization and control treatments.

Supplemental Table S2. List of genes changing expression in control and *P. indica*-colonized roots of ir-*hspro* seedlings compared with the wild type.

Supplemental Table S3. List of annotated genes involved in metabolism and with enzyme codes differentially expressed in *P.indica*-colonized roots of ir-*hspro* seedlings.

Supplemental Table S4. List of ions with differential accumulation in *P. indica*-colonized roots of ir-*hspro* seedlings compared with wild-type seedlings (positive mode of ionization).

Supplemental Table S5. List of primers.

Supplemental Materials and Methods S1.

ACKNOWLEDGMENTS

The authors would like to thank Dr. J. Wu for supplying Gateway cloning material and for his assistance during cloning and protoplast transfection, V. Fragoso for her help with seedling grafting, and A. Wissgott for her help with microarrays.

Received July 20, 2012; accepted August 14, 2012; published August 14, 2012.

LITERATURE CITED

Achatz B, Kogel KH, Franken P, Waller F (2010) Piriformospora indica mycorrhization increases grain yield by accelerating early development of barley plants. Plant Signal Behav **5:** 1685–1687

Allmann S, Halitschke R, Schuurink RC, Baldwin IT (2010) Oxylipin channelling in *Nicotiana attenuata*: lipoxygenase 2 supplies substrates for green leaf volatile production. Plant Cell Environ **33:** 2028–2040

Baena-González E, Sheen J (2008) Convergent energy and stress signaling. Trends Plant Sci **13:** 474–482

Baldwin IT, Morse L (1994) Up in smoke 2: germination of Nicotiana attenuata in response to smoke-derived cues and nutrients in burned and unburned soils. J Chem Ecol **20:** 2373–2391

Baldwin IT, Preston CA (1999) The eco-physiological complexity of plant responses to insect herbivores. Planta **208:** 137–145

Barazani O, Benderoth M, Groten K, Kuhlemeier C, Baldwin IT (2005) Piriformospora indica and Sebacina vermifera increase growth performance at the expense of herbivore resistance in Nicotiana attenuata. Oecologia **146:** 234–243

Barazani O, von Dahl CC, Baldwin IT (2007) *Sebacina vermifera* promotes the growth and fitness of *Nicotiana attenuata* by inhibiting ethylene signaling. Plant Physiol **144:** 1223–1232

Bardgett RD, Wardle DA, Yeates GW (1998) Linking above-ground and below-ground interactions: how plant responses to foliar herbivory influence soil organisms. Soil Biol Biochem **30:** 1867–1878

Bolton MD (2009) Primary metabolism and plant defense—fuel for the fire. Mol Plant Microbe Interact **22:** 487–497

Bonaventure G, Schuck S, Baldwin IT (2011) Revealing complexity and specificity in the activation of lipase-mediated oxylipin biosynthesis: a specific role of the Nicotiana attenuata GLA1 lipase in the activation of jasmonic acid biosynthesis in leaves and roots. Plant Cell Environ **34:** 1507–1520

Bubner B, Gase K, Berger B, Link D, Baldwin IT (2006) Occurrence of tetraploidy in Nicotiana attenuata plants after Agrobacterium-mediated transformation is genotype specific but independent of polysomaty of explant tissue. Plant Cell Rep **25:** 668–675

Cai D, Kleine M, Kifle S, Harloff HJ, Sandal NN, Marcker KA, Klein-Lankhorst RM, Salentijn EMJ, Lange W, Stiekema WJ, et al (1997) Positional cloning of a gene for nematode resistance in sugar beet. Science **275:** 832–834

Camehl I, Drzewiecki C, Vadassery J, Shahollari B, Sherameti I, Forzani C, Munnik T, Hirt H, Oelmüller R (2011) The OXI1 kinase pathway mediates Piriformospora indica-induced growth promotion in Arabidopsis. PLoS Pathog **7:** e1002051

Camehl I, Sherameti I, Venus Y, Bethke G, Varma A, Lee J, Oelmüller R (2010) Ethylene signalling and ethylene-targeted transcription factors are required to balance beneficial and nonbeneficial traits in the symbiosis between the endophytic fungus Piriformospora indica and Arabidopsis thaliana. New Phytol **185:** 1062–1073

Cominelli E, Galbiati M, Vavasseur A, Conti L, Sala T, Vuylsteke M, Leonhardt N, Dellaporta SL, Tonelli C (2005) A guard-cell-specific MYB transcription factor regulates stomatal movements and plant drought tolerance. Curr Biol **15:** 1196–1200

Deshmukh S, Hückelhoven R, Schäfer P, Imani J, Sharma M, Weiss M, Waller F, Kogel KH (2006) The root endophytic fungus Piriformospora indica requires host cell death for proliferation during mutualistic symbiosis with barley. Proc Natl Acad Sci USA **103:** 18450–18457

Fakhro A, Andrade-Linares DR, von Bargen S, Bandte M, Büttner C, Grosch R, Schwarz D, Franken P (2010) Impact of Piriformospora indica on tomato growth and on interaction with fungal and viral pathogens. Mycorrhiza **20:** 191–200

Fammartino A, Cardinale F, Göbel C, Mène-Saffrané L, Fournier J, Feussner I, Esquerré-Tugayé MT (2007) Characterization of a divinyl ether biosynthetic pathway specifically associated with pathogenesis in tobacco. Plant Physiol **143:** 378–388

Fragoso V, Goddard H, Baldwin IT, Kim SG (2011) A simple and efficient micrografting method for stably transformed Nicotiana attenuata plants to examine shoot-root signaling. Plant Methods **7:** 34

Fujita M, Mizukado S, Fujita Y, Ichikawa T, Nakazawa M, Seki M, Matsui M, Yamaguchi-Shinozaki K, Shinozaki K (2007) Identification of stress-tolerance-related transcription-factor genes via mini-scale full-length cDNA Over-eXpressor (FOX) gene hunting system. Biochem Biophys Res Commun **364:** 250–257

Gase K, Baldwin IT (2012) Transformational tools for next generation ecology: manipulation of gene expression remains the gold standard for the functional analyses of genes. Plant Ecol Divers (in press)

Gehring C, Bennett A (2009) Mycorrhizal fungal-plant-insect interactions: the importance of a community approach. Environ Entomol **38:** 93–102

Gehring CA, Whitham TG (1991) Herbivore-driven mycorrhizal mutualism in insect-susceptible pinyon pine. Nature **353:** 556–557

Gilardoni PA, Hettenhausen C, Baldwin IT, Bonaventure G (2011) *Nicotiana attenuata* LECTIN RECEPTOR KINASE1 suppresses the insect-mediated inhibition of induced defense responses during *Manduca sexta* herbivory. Plant Cell **23:** 3512–3532

Gilardoni PA, Schuck S, Jüngling R, Rotter B, Baldwin IT, Bonaventure G (2010) SuperSAGE analysis of the Nicotiana attenuata transcriptome after fatty acid-amino acid elicitation (FAC): identification of early mediators of insect responses. BMC Plant Biol **10:** 66

Gissot L, Polge C, Jossier M, Girin T, Bouly JP, Kreis M, Thomas M (2006) AKINbetagamma contributes to SnRK1 heterotrimeric complexes and interacts with two proteins implicated in plant pathogen resistance through its KIS/GBD sequence. Plant Physiol **142:** 931–944

Göbel C, Feussner I, Hamberg M, Rosahl S (2002) Oxylipin profiling in pathogen-infected potato leaves. Biochim Biophys Acta **1584:** 55–64

Halford NG, Hey S, Jhurreea D, Laurie S, McKibbin RS, Paul M, Zhang Y (2003) Metabolic signalling and carbon partitioning: role of Snf1-related (SnRK1) protein kinase. J Exp Bot **54:** 467–475

Hammond JP, Bennett MJ, Bowen HC, Broadley MR, Eastwood DC, May ST, Rahn C, Swarup R, Woolaway KE, White PJ (2003) Changes in gene expression in Arabidopsis shoots during phosphate starvation and the potential for developing smart plants. Plant Physiol **132:** 578–596

Hause B, Fester T (2005) Molecular and cell biology of arbuscular mycorrhizal symbiosis. Planta **221:** 184–196

Herrera Medina M, Gagnon H, Piché Y, Ocampo JA, García Garrido JM, Vierheilig H (2003) Root colonization by arbuscular mycorrhizal fungi is affected by the salicylic acid content of the plant. Plant Sci **164:** 993–998

Herrera-Medina MJ, Steinkellner S, Vierheilig H, Ocampo Bote JA, García Garrido JM (2007) Abscisic acid determines arbuscule development and functionality in the tomato arbuscular mycorrhiza. New Phytol **175:** 554–564

Jacobs S, Zechmann B, Molitor A, Trujillo M, Petutschnig E, Lipka V, Kogel KH, Schäfer P (2011) Broad-spectrum suppression of innate immunity is required for colonization of Arabidopsis roots by the fungus *Piriformospora indica*. Plant Physiol **156:** 726–740

Kallenbach M, Alagna F, Baldwin IT, Bonaventure G (2010) *Nicotiana attenuata* SIPK, WIPK, NPR1, and fatty acid-amino acid conjugates participate in the induction of jasmonic acid biosynthesis by affecting early enzymatic steps in the pathway. Plant Physiol **152:** 96–106

Kang JH, Wang L, Giri A, Baldwin IT (2006) Silencing threonine deaminase and JAR4 in *Nicotiana attenuata* impairs jasmonic acid-isoleucine-mediated defenses against *Manduca sexta*. Plant Cell **18:** 3303–3320

Krügel T, Lim M, Gase K, Halitschke R, Baldwin IT (2002) Agrobacterium-mediated transformation of Nicotiana attenuata, a model ecological expression system. Chemoecology **12:** 177–183

Kudla U, Milac AL, Qin L, Overmars H, Roze E, Holterman M, Petrescu AJ, Goverse A, Bakker J, Helder J, et al (2007) Structural and functional characterization of a novel, host penetration-related pectate lyase from

the potato cyst nematode Globodera rostochiensis. Mol Plant Pathol **8:** 293–305

Lee YC, Johnson JM, Chien CT, Sun C, Cai D, Lou B, Oelmüller R, Yeh KW (2011) Growth promotion of Chinese cabbage and Arabidopsis by Piriformospora indica is not stimulated by mycelium-synthesized auxin. Mol Plant Microbe Interact **24:** 421–431

Leon-Morcillo RJ, Angel J, Martin R, Vierheilig H, Ocampo JA, Garcia-Garrido JM (2012) Late activation of the 9-oxylipin pathway during arbuscular mycorrhiza formation in tomato and its regulation by jasmonate signalling. J Exp Bot **63:** 3545–3558

Long HH, Sonntag DG, Schmidt DD, Baldwin IT (2010) The structure of the culturable root bacterial endophyte community of Nicotiana attenuata is organized by soil composition and host plant ethylene production and perception. New Phytol **185:** 554–567

Lovas A, Bimbó A, Szabó L, Bánfalvi Z (2003) Antisense repression of StubGAL83 affects root and tuber development in potato. Plant J **33:** 139–147

Luhua S, Ciftci-Yilmaz S, Harper J, Cushman J, Mittler R (2008) Enhanced tolerance to oxidative stress in transgenic Arabidopsis plants expressing proteins of unknown function. Plant Physiol **148:** 280–292

Murray SL, Ingle RA, Petersen LN, Denby KJ (2007) Basal resistance against Pseudomonas syringae in Arabidopsis involves WRKY53 and a protein with homology to a nematode resistance protein. Mol Plant Microbe Interact **20:** 1431–1438

Paschold A, Bonaventure G, Kant MR, Baldwin IT (2008) Jasmonate perception regulates jasmonate biosynthesis and JA-Ile metabolism: the case of COI1 in Nicotiana attenuata. Plant Cell Physiol **49:** 1165–1175

Pham GH, Kumari R, Singh A, Sachdev M, Prasad R, Kaldorf M, Buscot F, Oelmüller R, Peskan T, Weiss M, Hampp R, et al (2004) Axenic cultures of *Piriformospora indica*. *In* Plant Surface Microbiology. Springer, Berlin, pp 593–616

Pineda A, Zheng SJ, van Loon JJ, Pieterse CM, Dicke M (2010) Helping plants to deal with insects: the role of beneficial soil-borne microbes. Trends Plant Sci **15:** 507–514

Preston GM (2004) Plant perceptions of plant growth-promoting Pseudomonas. Philos Trans R Soc Lond B Biol Sci **359:** 907–918

Prost I, Dhondt S, Rothe G, Vicente J, Rodriguez MJ, Kift N, Carbonne F, Griffiths G, Esquerré-Tugayé MT, Rosahl S, et al (2005) Evaluation of the antimicrobial activities of plant oxylipins supports their involvement in defense against pathogens. Plant Physiol **139:** 1902–1913

Puthoff DP, Nettleton D, Rodermel SR, Baum TJ (2003) Arabidopsis gene expression changes during cyst nematode parasitism revealed by statistical analyses of microarray expression profiles. Plant J **33:** 911–921

Qiang X, Weiss M, Kogel KH, Schafer P (2011) Piriformospora indica—a mutualistic basidiomycete with an exceptionally large plant host range. Mol Plant Pathol **13:** 508–518

Rosenthal JP, Kotanen PM (1994) Terrestrial plant tolerance to herbivory. Trends Ecol Evol **9:** 145–148

Sahay NS, Varma A (1999) Piriformospora indica: a new biological hardening tool for micropropagated plants. FEMS Microbiol Lett **181:** 297–302

Schäfer P, Pfiffi S, Voll LM, Zajic D, Chandler PM, Waller F, Scholz U, Pons-Kühnemann J, Sonnewald S, Sonnewald U, et al (2009a) Manipulation of plant innate immunity and gibberellin as factor of compatibility in the mutualistic association of barley roots with Piriformospora indica. Plant J **59:** 461–474

Schäfer P, Pfiffi S, Voll LM, Zajic D, Chandler PM, Waller F, Scholz U, Pons-Kühnemann J, Sonnewald S, Sonnewald U, et al (2009b) Phytohormones in plant root-Piriformospora indica mutualism. Plant Signal Behav **4:** 669–671

Schwachtje J, Baldwin IT (2008) Why does herbivore attack reconfigure primary metabolism? Plant Physiol **146:** 845–851

Schwachtje J, Minchin PEH, Jahnke S, van Dongen JT, Schittko U, Baldwin IT (2006) SNF1-related kinases allow plants to tolerate herbivory by allocating carbon to roots. Proc Natl Acad Sci USA **103:** 12935–12940

Stein E, Molitor A, Kogel KH, Waller F (2008) Systemic resistance in Arabidopsis conferred by the mycorrhizal fungus Piriformospora indica requires jasmonic acid signaling and the cytoplasmic function of NPR1. Plant Cell Physiol **49:** 1747–1751

Sthultz CM, Whitham TG, Kennedy K, Deckert R, Gehring CA (2009) Genetically based susceptibility to herbivory influences the ectomycorrhizal fungal communities of a foundation tree species. New Phytol **184:** 657–667

Strack D, Fester T, Hause B, Schliemann W, Walter MH (2003) Arbuscular mycorrhiza: biological, chemical, and molecular aspects. J Chem Ecol **29:** 1955–1979

Turner JG (2007) Stress responses: JAZ players deliver fusion and rhythm. Curr Biol **17:** R847–R849

Vadassery J, Ritter C, Venus Y, Camehl I, Varma A, Shahollari B, Novák O, Strnad M, Ludwig-Müller J, Oelmüller R (2008) The role of auxins and cytokinins in the mutualistic interaction between Arabidopsis and Piriformospora indica. Mol Plant Microbe Interact **21:** 1371–1383

Van Wees SCM, Van der Ent S, Pieterse CMJ (2008) Plant immune responses triggered by beneficial microbes. Curr Opin Plant Biol **11:** 443–448

Varma A, Savita Verma, Sudha , Sahay N, Butehorn B, Franken P (1999) Piriformospora indica, a cultivable plant-growth-promoting root endophyte. Appl Environ Microbiol **65:** 2741–2744

Waller F, Achatz B, Baltruschat H, Fodor J, Becker K, Fischer M, Heier T, Hückelhoven R, Neumann C, von Wettstein D, et al (2005) The endophytic fungus Piriformospora indica reprograms barley to salt-stress tolerance, disease resistance, and higher yield. Proc Natl Acad Sci USA **102:** 13386–13391

Walley JW, Coughlan S, Hudson ME, Covington MF, Kaspi R, Banu G, Harmer SL, Dehesh K (2007) Mechanical stress induces biotic and abiotic stress responses via a novel cis-element. PLoS Genet **3:** 1800–1812

Weber H, Chételat A, Caldelari D, Farmer EE (1999) Divinyl ether fatty acid synthesis in late blight-diseased potato leaves. Plant Cell **11:** 485–494

Weiss M, Selosse MA, Rexer KH, Urban A, Oberwinkler F (2004) Sebacinales: a hitherto overlooked cosm of heterobasidiomycetes with a broad mycorrhizal potential. Mycol Res **108:** 1003–1010

Wu JQ, Hettenhausen C, Meldau S, Baldwin IT (2007) Herbivory rapidly activates MAPK signaling in attacked and unattacked leaf regions but not between leaves of *Nicotiana attenuata*. Plant Cell **19:** 1096–1122

Xie DX, Feys BF, James S, Nieto-Rostro M, Turner JG (1998) COI1: an Arabidopsis gene required for jasmonate-regulated defense and fertility. Science **280:** 1091–1094

Zamioudis C, Pieterse CM (2012) Modulation of host immunity by beneficial microbes. Mol Plant Microbe Interact **25:** 139–150

Zipfel C, Robatzek S, Navarro L, Oakeley EJ, Jones JD, Felix G, Boller T (2004) Bacterial disease resistance in Arabidopsis through flagellin perception. Nature **428:** 764–767

Zuccaro A, Lahrmann U, Güldener U, Langen G, Pfiffi S, Biedenkopf D, Wong P, Samans B, Grimm C, Basiewicz M, et al (2011) Endophytic life strategies decoded by genome and transcriptome analyses of the mutualistic root symbiont Piriformospora indica. PLoS Pathog **7:** e1002290

A

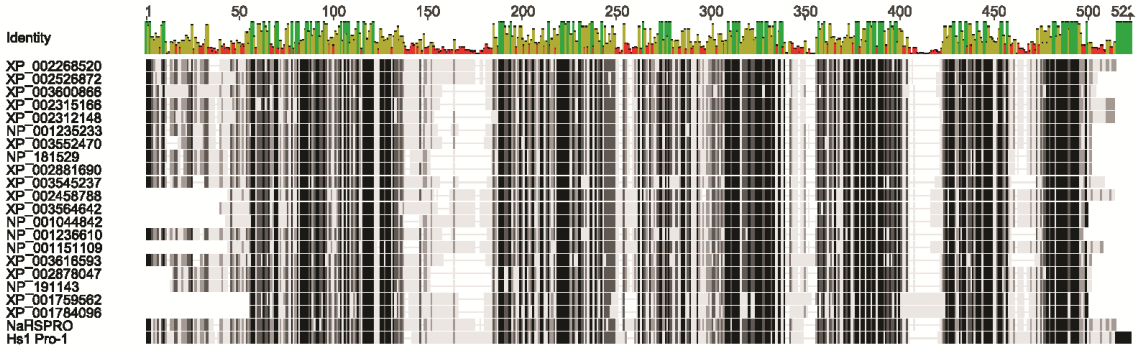

B

GenBank annotation	E-Value (blastx)	Gene ID	Organism	% Pairwise Identity
Nicotiana attenuata HSPRO	**0**	**NaHSPRO** (JQ354963)	***Nicotiana attenuata***	**100**
nematode resistance protein-like HSPRO2 isoform 1	0	XP_002268520	*Vitis vinifera*	69
conserved hypothetical protein	0	XP_002526872	*Ricinus communis*	68
predicted protein	0	XP_002315166	*Populus trichocarpa* (2)	64
Beta procumbens nematode resistance (Hs1pro-1)	0	combined AAB48305 and AAZ39087	*Beta procumbes*	63
predicted protein	0	XP_002312148	*Populus trichocarpa* (1)	61
uncharacterized protein LOC547603	0	NP_001235233	*Glycine max* (1)	58
PREDICTED: nematode resistance protein-like HSPRO2-like	0	XP_003552470	*Glycine max* (2)	58
hypothetical protein MTR_3g070230	0	XP_003600866	*Medicago truncatula*	58
PREDICTED: nematode resistance protein-like HSPRO1-like	4.14E-166	XP_003564642	*Brachypodium distachyon*	53
HS1 PRO-1 2-like protein (HSPRO2)	2.62E-175	NP_181529 (At3g55840)	*Arabidopsis thaliana* (1)	53
nematode-resistance protein	4.83E-163	NP_001151109	*Zea mays*	53
hypothetical protein ARALYDRAFT_483040	9.82E-170	XP_002881690	*Arabidopsis lyrata* (1)	53
Os01g0855600	1.01E-163	NP_001044842	*Oryza sativa*	53
hypothetical protein SORBIDRAFT_03g040300	3.51E-166	XP_002458788	*Sorghum bicolor*	53
nematode resistance HS1pro1 protein	3.66E-163	NP_001236610	*Glycine max* (4)	51
hypothetical protein ARALYDRAFT_486026	2.49E-155	XP_002878047	*Arabidopsis lyrata* (2)	51
Hs1pro-1 protein (HSPRO1)	1.69E-154	NP_191143 (At2g4000)	*Arabidopsis thaliana* (2)	50
PREDICTED: nematode resistance protein-like HSPRO2-like	7.50E-168	XP_003545237	*Glycine max* (3)	50
Nematode resistance HS1pro1 protein	1.31E-157	XP_003616593	*Medicago truncatula*	48
predicted protein	1.40E-124	XP_001759562	*Physcomitrella patens* (1)	45
predicted protein	1.28E-122	XP_001784096	*Physcomitrella patens* (2)	45

Supplemental Figure S1. Alignment of *N. attenuata* HSPRO protein sequence with close homologs in different plant species.

(a) Schematic protein sequence alignment of *N. attenuata* HSPRO (JQ354963) with the 21 closest homologs in different plant species deposited in GenBank (including *B. procumbens* $Hs1^{pro-1}$). The cartoon above the sequences shows the % of similarity (green bars within the overlapping regions represent identical amino acids). See materials and methods for alignment parameters. **(b)** Reference table for genes, accesion numbers and species used in (a) and Figure 1b.c

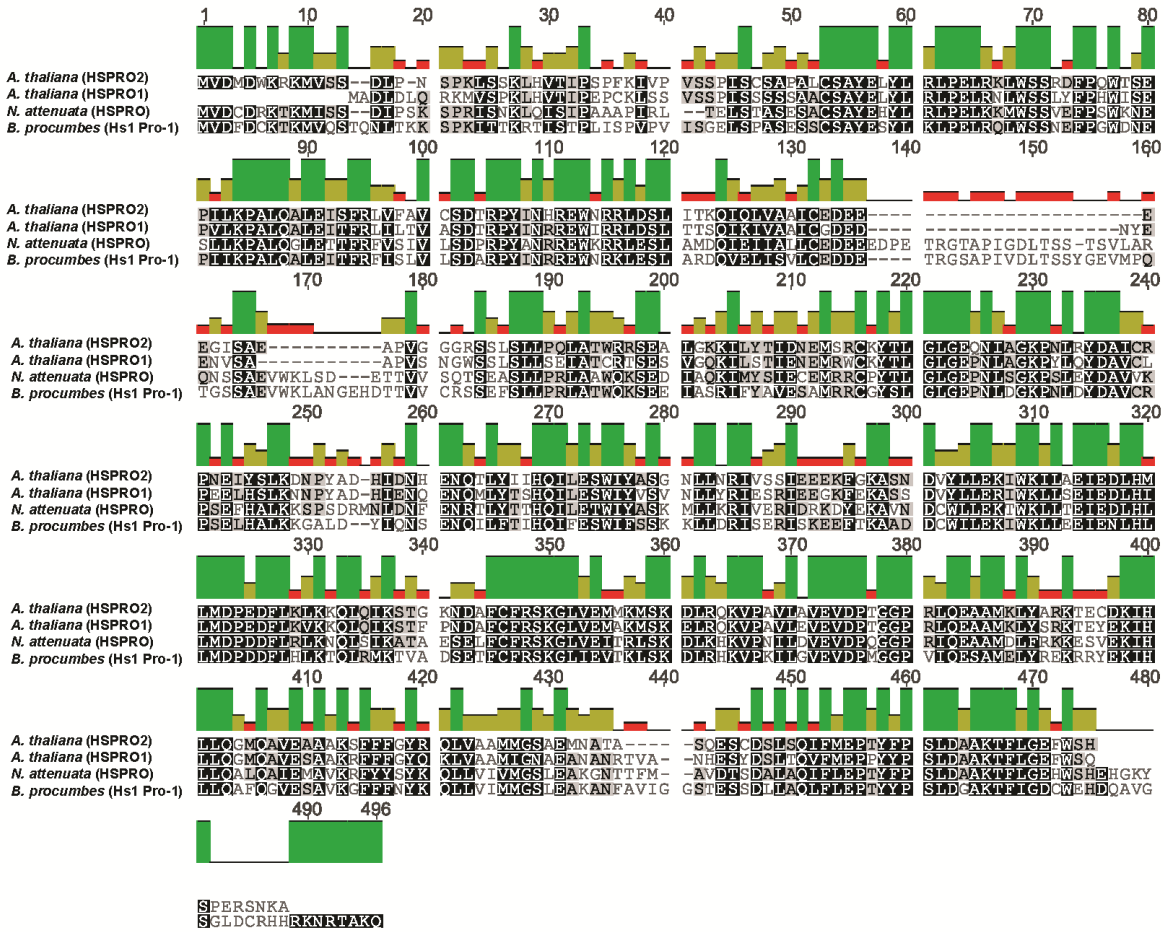

Supplemental Figure S2. Alignment of *N. attenuata* HSPRO protein sequence with homologs in *A. thaliana* and *B. procumbens*.

N. attenuata HSPRO (JQ354963); Arabidopsis HSPRO1 (NP_191143; At2g4000), Arabidopsis HSPRO2 (NP_181529; At3g55840), full lenght sugar beet (*B. procumbes)* Hs1^{pro-1} (combined AAB48305 and AAZ39087). The cartoon above the sequences represent the % of similarity (green bars within the overlapping regions shows identical amino acids in the four sequences). See materials and methods for alignment parameters.

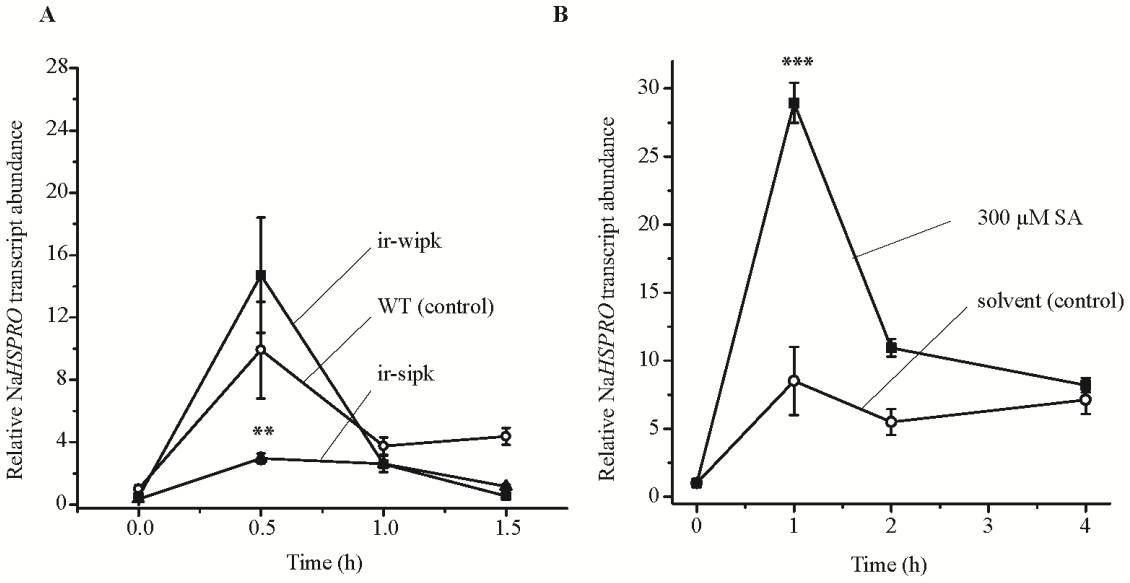

Supplemental Figure S3. Analysis of *HSPRO* expression in WT plants and in transgenic plants reduced in MAP kinase expression.

(a) Leaves of rosette-stage transgenic *N. attenuata* plants with reduced levels of SIPK (salicylic acid induced protein kinase) and WIPK (wound induced protein kinase) expression as well as control WT plants were elicited with synthetic 18:3-Glu. Total RNA was extracted from treated leaves at different times and *HSPRO* transcript levels were quantified by qPCR. *HSPRO* mRNA levels are expressed relative to the levels of the reference gene Na-*EF1A*. Quantification was performed by the ΔCt method (n=3; bars= ±S.E.). One way-ANOVA with Tukey post-hoc test (WT vs. ir-*sipk*); **: P<0.01. **(b)** Rosette stage WT plants were sprayed with 300 µM SA or control solution (see Materials and Methods for details). Leaves were harvested at different times and total RNA was extracted. *HSPRO* transcript levels were quantified as in (a) (n=3; bars= ±S.E.). Student's t-test (SA vs. control treatment); ***: P<0.001.

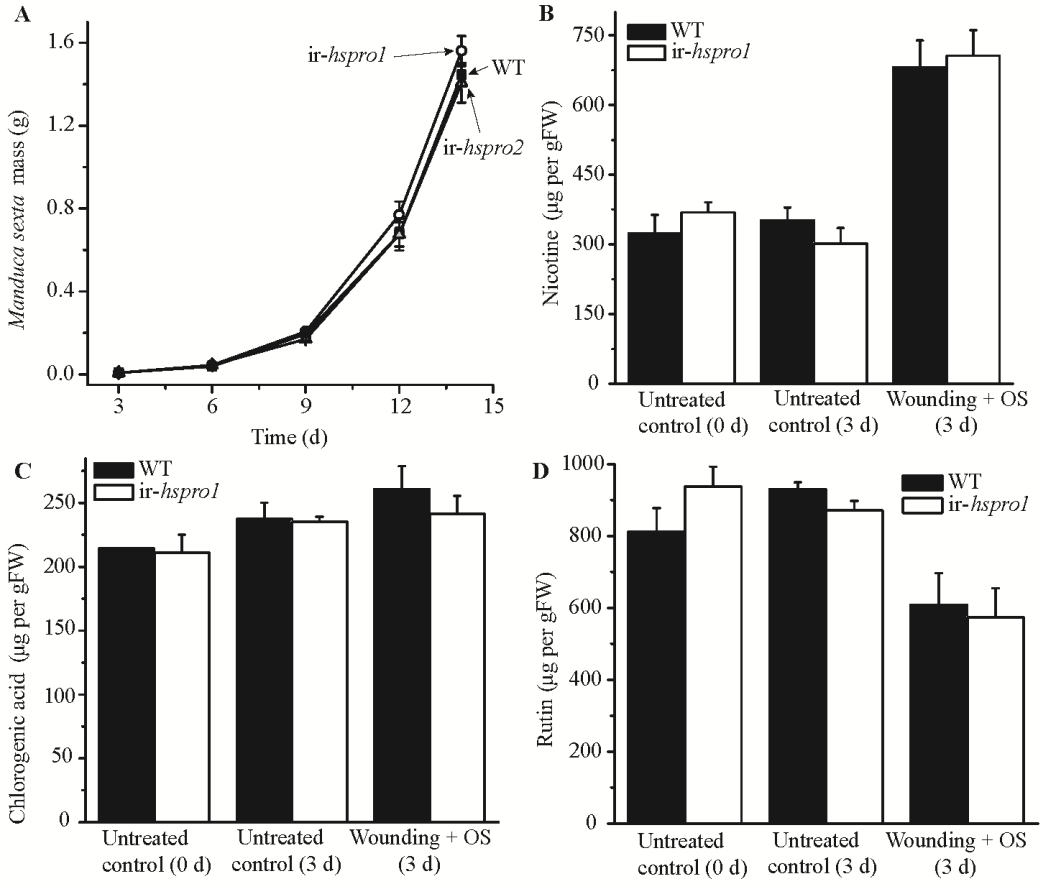

Supplemental Figure S4. Analysis of defense responses against *M. sexta* in WT and ir-*hspro* plants.

(a) Freshly hatched *M. sexta* neonates were placed on leaves of rosette stage *N. attenuata* WT and ir-*hspro* plants (one neonate per plant) and the caterpillar masses were quantified every 3 days for a period of 15 days (n=22 to 67; bars= ±S.E.). **(b,c,d)** Leaves from rosette stage WT and ir-*hspro1* plants were elicited with *M. sexta* OS once a day for three consecutive days. After three days (six days from the start of the treatment), leaves were harvested and used for quantification of defense metabolites by HPLC-UV. Control samples were leaves from untreated plants harvested either before the start of the treatment (0 days) or after three days (3 d) (n=5; bars= ±S.E.; (b) Nicotine; (c) Chlorogenic acid; (d) Rutin).

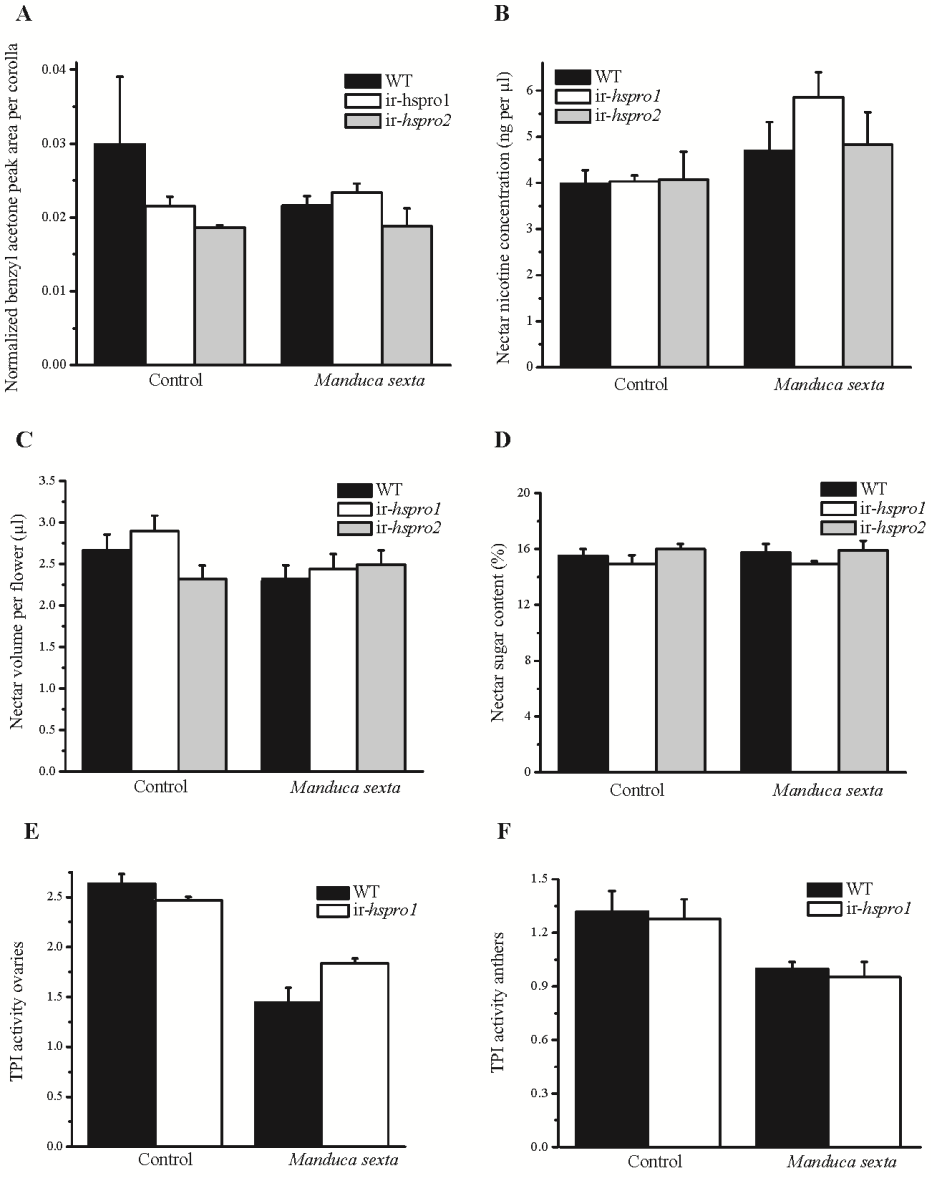

Supplemental Figure S5. Analysis of flower traits associated with the interactions of *N. attenuata* plants with insects.

N. attenuata WT and ir-*hspro* plants were challenged with *M. sexta* larvae for 15 consecutive days. Un-attacked plants were used as controls. **(a)** After removal of the caterpillars from the plants, 30 corollas from night opening flowers per genotype and treatment were collected. Samples consisting of 10 pooled corollas (n=3 per genotype per treatment) were extracted with dichloromethane and benzyl acetone levels were analyzed by GC-MS. Quantification was performed with tetraline as the internal standard. Bars denote S.E. **(b)** After removal of the caterpillars from the plants, the nectar from 10 individual flowers was pooled into a 1.5 mL tube to form one sample. The nectar volume was quantified with a glass capillary (n=3 [3x10 corollas]; bars= ±S.E.). **(c)** Nicotine levels in nectar collected in (b) were quantified by LC-MS using $^{2}H_{3}$-nicotine as internal standard (n=3; bars= ±S.E.). **(d)** Nectar collected in (b) was also used to determine sugar content with a refractometer (n=3; bars= ±S.E.). **(e,f)** After removal of the caterpillars from the plants, ovaries (e) and anthers (f) from 10 flowers were collected into a 1.5 mL tube to form one sample. Samples were used for protein extraction and measurement of trypsin proteinase inhibitor (TPI) activity (n=5; bars= ±S.E.).

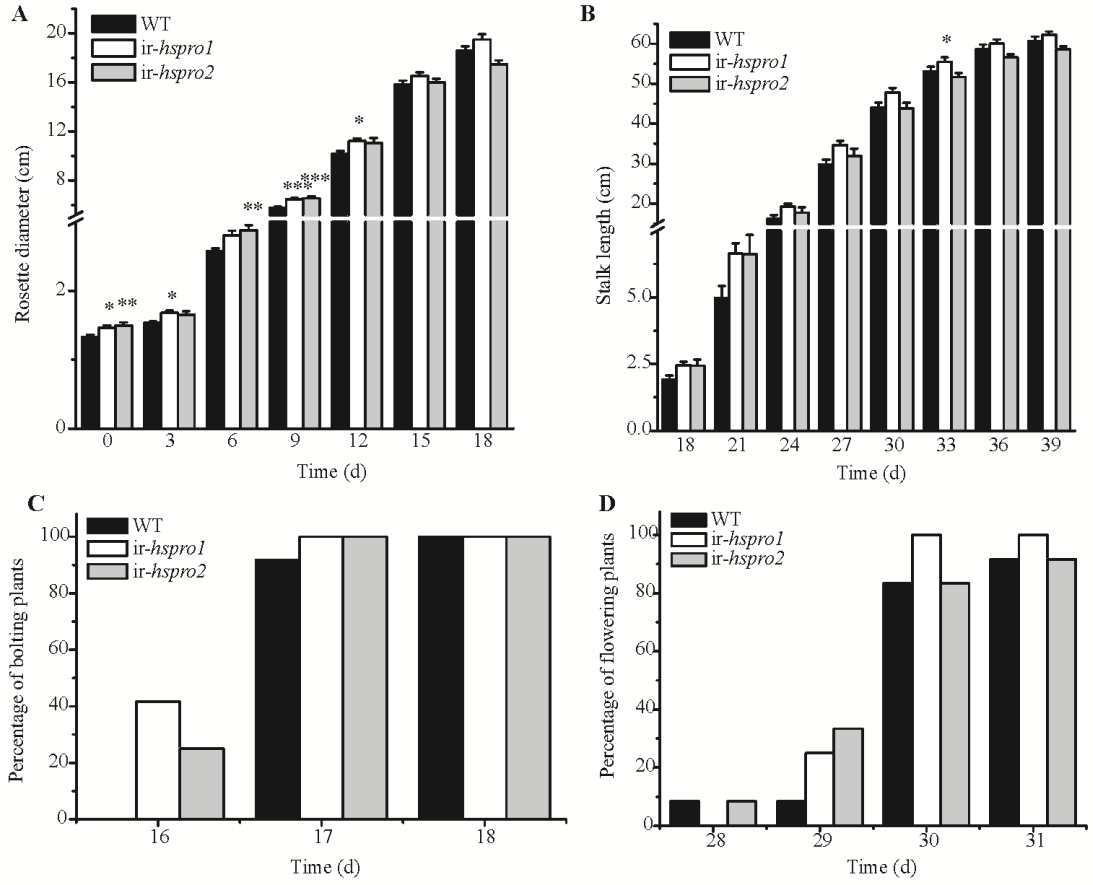

Supplemental Figure S6. Analysis of growth and developmental parameters of *P. indica*-colonized plants grown in the glasshouse.
WT and ir-*hspro* seedlings were grown on plates in the presence of *P. indica* for 14 days and the seedlings were then transferred to soil in 1L pots and grown in the glasshouse under standard growth conditions. **(a)** Rosette diameter (distance between the two longest leaves) and **(b)** stalk length were measured every three days. One way-ANOVA with Tukey post-hoc test (WT vs. ir-*hspro*); *: $P<0.05$; **: $P<0.01$; ***: $P<0.001$; $n=12$ per genotype (bars= ±S.E). **(c)** Bolting time (determined as the appearance of the reproductive meristem) and **(d)** flowering time (determined as the appearance of the first opened bud) were recorded daily ($n=12$ per genotype).

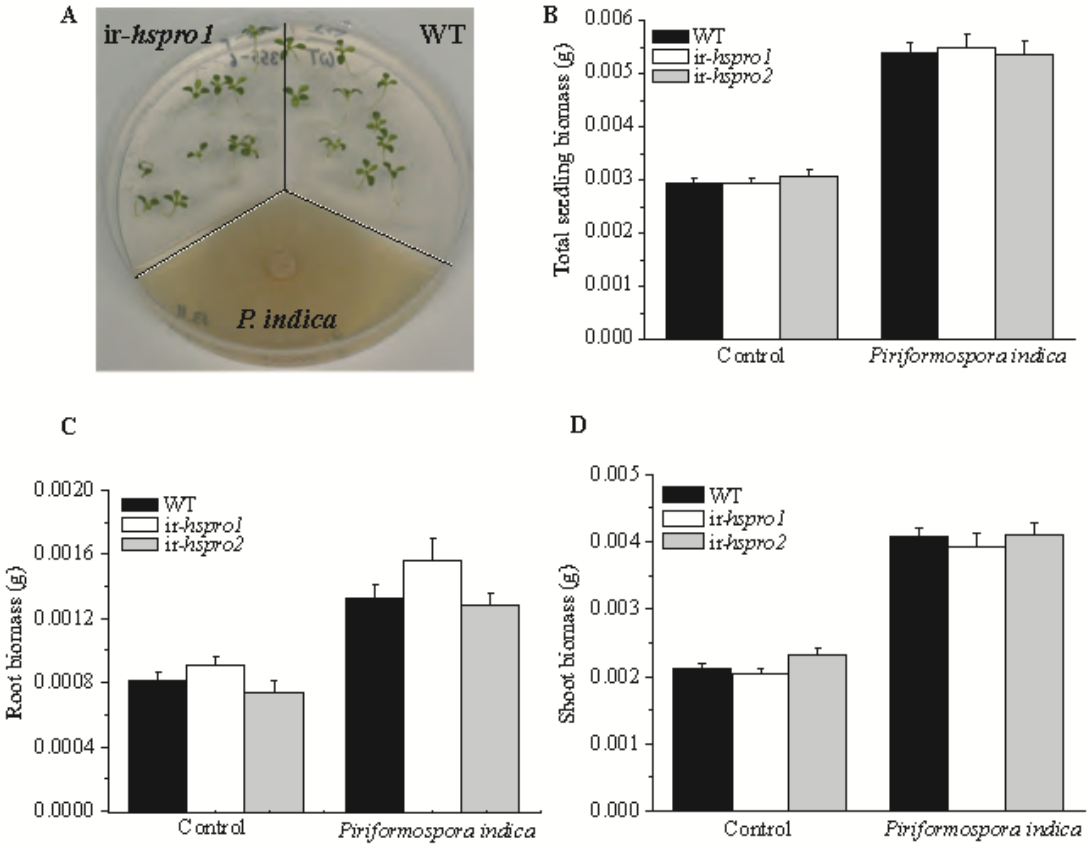

Supplemental Figure S7. Analysis of growth promotion of WT and ir-*hspro* seedlings induced by *P. indica* in a split-plate system.
(a) WT and ir-*hspro* seedlings and *P. indica* were grown in separate compartments of split Petri dishes (10 WT and 10 ir-*hspro* seedlings per plate) for 14 days. Plates without *P. indica* but with fungal media were used as controls. **(b,c,d)** Determination of fresh biomasses of total seedlings (b), shoots (c), and roots (d) was performed with a microbalance (n=26 to 29; bars= ±S.E.).

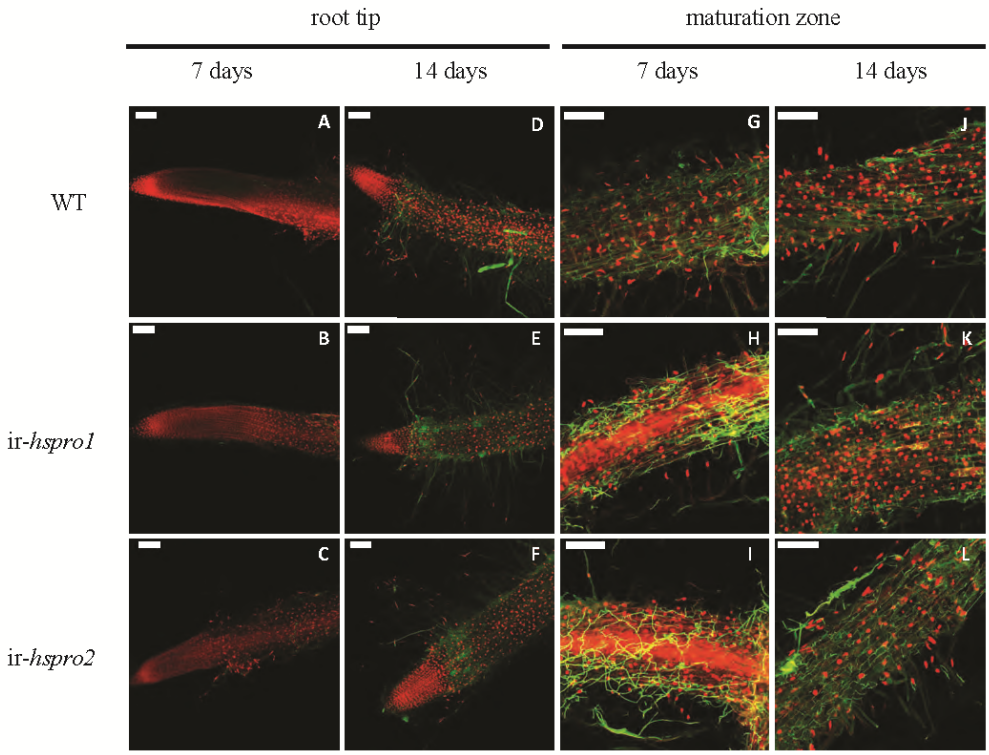

Suppl. Figure S8. Laser confocal microscopy analysis of roots from *P. indica*-colonized WT and ir-*hspro* seedlings.
(a-l) Root samples from seedlings grown in the presence of *P. indica* for 7 and 14 days were stained with WGA-AF488 (fungal structures; green) and propidium iodide (cell walls; red). Images were taken with a laser confocal microscope equipped with an argon laser. Excitation/detection was at 488/500-540 nm for WGA-AF488 and at 560/580-660 nm for propidium iodide. White bar: 100 µm.

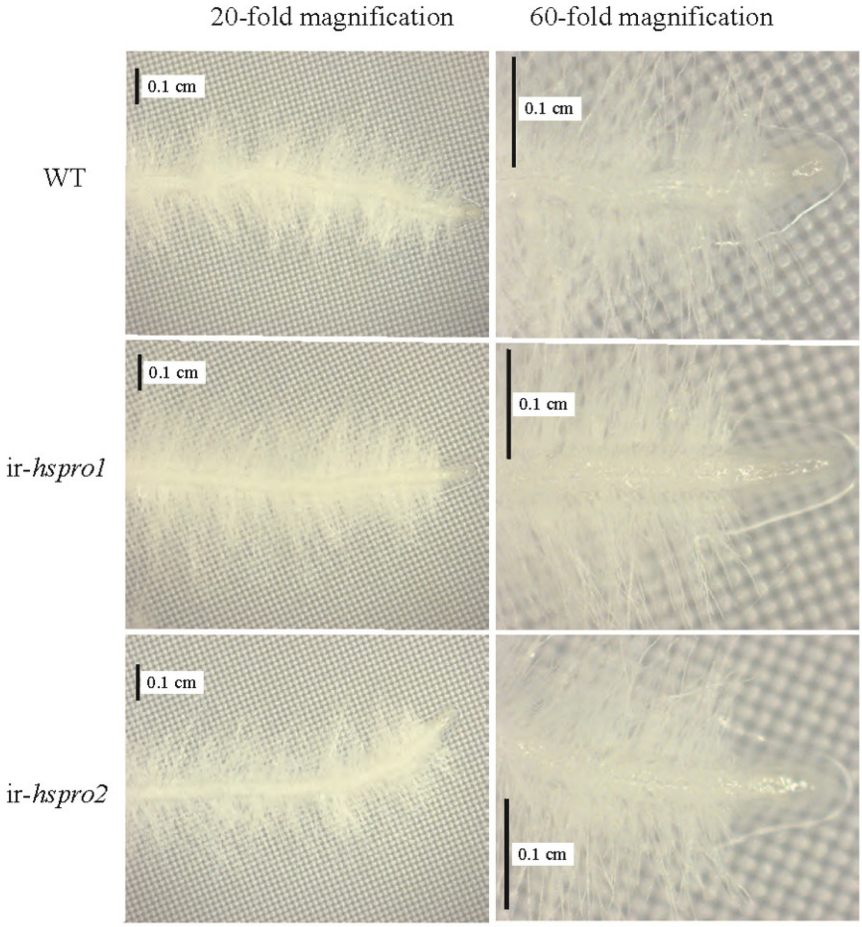

Supplemental Figure S9. Root morphology of *P. indica*-colonized WT and ir-*hspro* seedlings.
WT and ir-*hspro* seedlings were grown in the presence and absence of *P. indica* for 14 days on a plate system. Seedling roots were visualized under a stereomicroscope at 20- and 60-fold magnifications. Bars represent 0.1 cm.

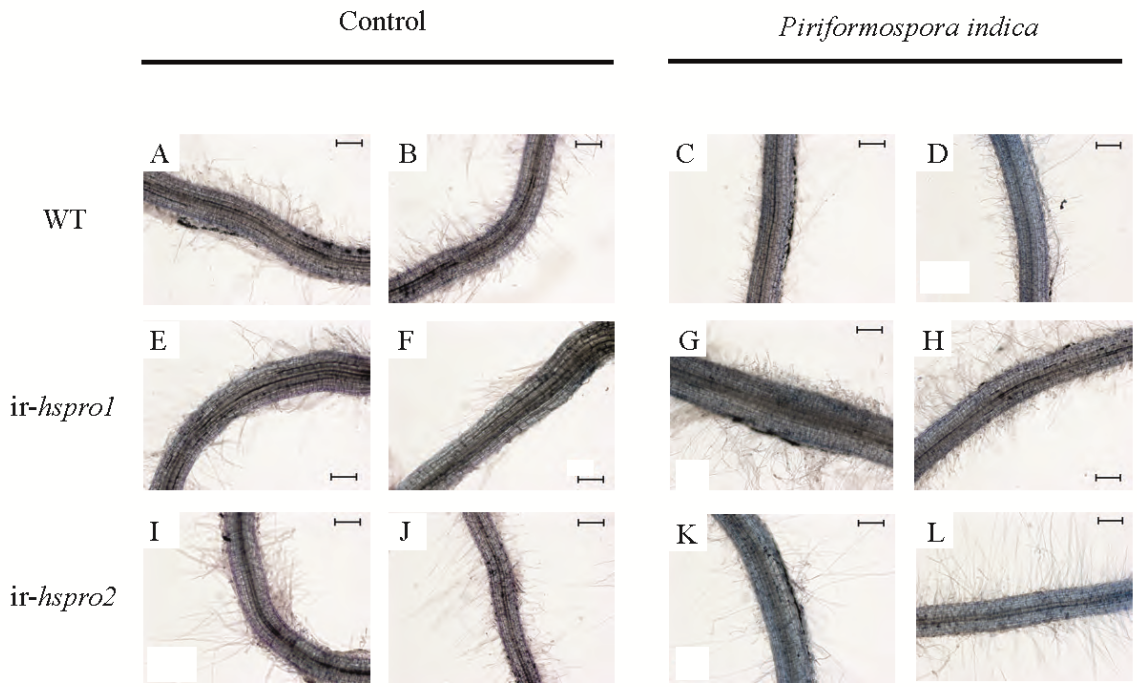

Figure S10. Analysis of root cell death in WT and ir-*hspro* seedlings.

WT and ir-*hspro* seedlings were grown in the absence (control) and presence of *P. indica* for 14 days on a plate system. Roots were excised from the seedlings and stained with trypan-blue. Images were taken with a Zeiss Imager.Z1 microscope using the AxioVision software. Bars represent 200 µm.

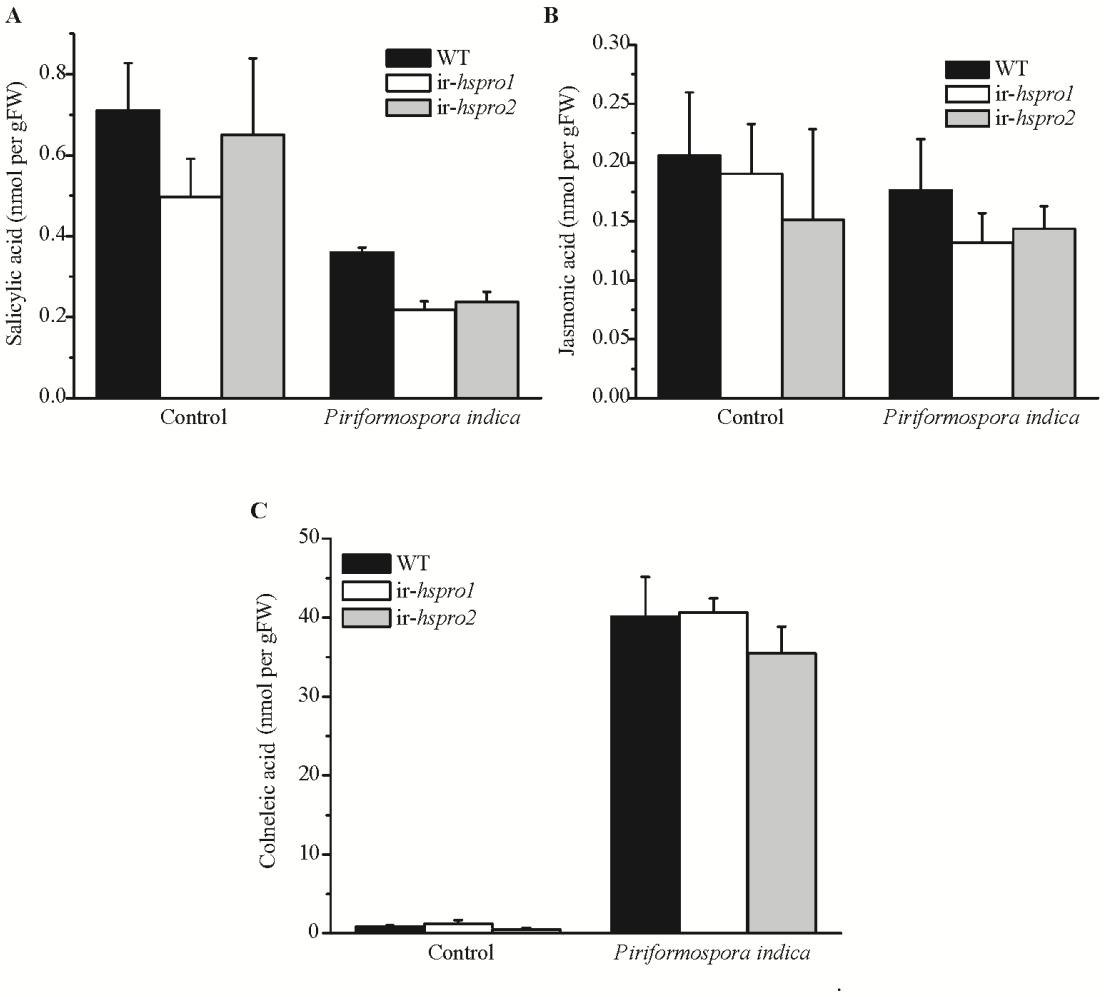

Supplemental Figure S11. Analysis of SA, JA and CA levels in roots of WT and ir-*hspro* seedlings. WT and ir-*hspro* seedlings were grown in the presence and absence of *P. indica* for 14 days on a plate system. Root samples were collected from the seedlings and the levels of **(a)** SA, **(b)** JA and **(c)** CA were quantified by LC-MS (n=3; bars= ±S.E.).

Supplemental Table SI. Analysis of WT and ir-*hspro* seedling's biomasses during *P. indica*-root colonization and control treatments.

Days of seedling growth	Genotype	Seedling weight (mg) ± SE [control]	*n*	Seedling weight (mg) ± SE [*P. indica*]	*n*	% growth promotion (*P.indica* vs. control)	% differential growth promotion (ir-hspro vs. WT)	*P*-value[1] (control vs. P. indica)	*P* value[2] (WT vs. ir-hspro)
10	WT	13.2±0.9	16	30.1±1.6	20	**114**		6.33×10^{-13}	
	ir-hspro1	13.1±0.6	17	37.3±0.9	18	**162**	**42**	6.27×10^{-13}	3.62×10^{-7}
	ir-hspro2	15.8±0.4	15	41.2±0.2	18	**198**	**73**	6.27×10^{-13}	6.72×10^{-8}
	ir-hspro3	16.1±0.8	18	38.8±1.5	20	**140**	**23**	6.27×10^{-13}	2.70×10^{-5}
10	WT	20.8±2.1	29	28.6±1.8	20	**37**		0.03	
	ir-hspro1	22.8±1.7	18	35.6±1.8	18	**56**	**51**	6.13×10^{-5}	0.08
	ir-hspro2	26.9±2.0	20	32.4±1.3	20	**55**	**48**	1.62×10^{-4}	0.64
14	WT	14.5±0.8	12	28.6±1.0	17	**97**		5.77×10^{-13}	
	ir-hspro1	14.4±0.3	9	32.1±0.7	17	**123**	**26**	5.77×10^{-13}	0.02
	ir-hspro2	15.3±0.6	12	32.6±1.0	18	**113**	**17**	5.77×10^{-13}	4.08×10^{-3}
14	WT	15.2±0.9	16	39.6±1.9	24	**200**		1.97×10^{-12}	
	ir-hspro1	14.9±0.6	19	47.7±1.7	21	**220**	**10**	5.72×10^{-12}	3.51×10^{-4}
14	WT	13.5±0.7	10	38.9±1.9	11	**189**		6.27×10^{-13}	
	ir-hspro1	14.8±0.8	11	49.0±2.4	9	**231**	**22**	6.26×10^{-13}	2.05×10^{-4}
	ir-hspro2	14.7±0.4	7	47.8±1.5	6	**223**	**18**	6.26×10^{-13}	6.31×10^{-5}
14	WT	15.5±0.4	15	52.3±1.8	26	**245**		5.94×10^{-13}	
	ir-hspro1	14.4±0.6	20	60.1±1.7	22	**302**	**23**	5.94×10^{-13}	1.99×10^{-5}
	ir-hspro2	14.1±0.3	23	59.9±2.0	24	**302**	**23**	5.94×10^{-13}	1.93×10^{-7}
14	WT	11.5±0.3	9	37.2±2.5	30	**223**		1.73×10^{-9}	
	ir-hspro1	12.0±1.0	10	53.9±3.2	30	**349**	**56**	8.50×10^{-13}	5.41×10^{-4}
	ir-hspro2	13.4±0.8	10	47.9±2.6	30	**257**	**15**	1.38×10^{-10}	0.04

[1,2] One way-ANOVA with Turkey post-hoc test (WT vs. ir-*hspro*).

Supplemental Table SIV. List of ions with differential accumulation in *P. indica*-colonized roots of ir-*hspro* compared to WT seedlings (positive mode of ionization).

Identity	log_2(FC[a])	*P*-value[b]	*m/z*	RT[s][c]	Mean peak intensity (ir-*hspro*)	S.E.	Mean peak intensity (WT)	S.E.
Unknown	-1.45	0.0348	381.789	437.273	131.929	81.947	400.507	61.602
Unknown	-1.12	0.0356	382.264	416.608	88.699	49.445	299.992	49.642
Unknown	-1.07	0.0376	450.199	165.750	77.202	43.625	272.628	50.775

[a]: FC: fold-change (ir-*hspro* vs WT)

[b]: *P*-value: Fisher's t-test (ir-*hspro* vs WT); *n*=5

[c]: RT[s]: retention time (seconds).

Supplemental Table SV. List of primers.

Gene name	template	experiment	Forward 5'—3'	Reverse 5'—3'
Na*TEF1a*/ Na*tef1a*	cDNA/ gDNA	qRT-PCR	ACACTTCCCACATTGCTGTCA	AAACGACCCAATGGAGGGTAC
Na*HSPRO*	cDNA	qRT-PCR	CTGATCCTAGACCGTATGCGAACA	CTGACAACCGTCGTCTCATCAGA
Pu*ef1a*	gDNA	qRT-PCR	TCGTCGCTGTCAACAAGATG	GGATACAACCCCAAGACGGT
Na*HSPRO* (ORF)	cDNA	HSPRO- EGFP fusion product	ATGGTTGATTGCGATAGAAAGACAAAG ATGATATC	GGCCTTGTTACTTCTCTCTGGACTATACT TG
Na*HSPRO* (ORF + partial attB sequence)	PCR product	HSPRO- EGFP fusion product	AAAAAGCAGGCTATGGTTGATTGCGAT AG	AGAAAGCTGGGTTGGCCTTGTTACTTC
Na*HSPRO* (ORF + complete attB sequence)	PCR product	HSPRO- EGFP fusion product	GGGGACAAGTTTGTACAAAAAAGCAGG CT	GGGGACCACTTTGTACAAGAAAGCTGG GT
nptII	*nptII*-contai-ning plasmic	Probe (Southern blot)	CCGGATCGGACGATTGCG	CGTCTGTCGAGAAGTTTCTG
At*RG4* (ORF + partial attB sequences)	cDNA	RGA-eGFP fusion product	AAAAAGCAGGCTTGAAGAGAGATCATC ACCAA	AGAAAGCTGGGTTGTACGCCGCCGTCG AGA
DCL2	gDNA	positiv control (diagno-stic PCR)	AAGGATGGCTCATTCCTGGTG	AGAGCTTCAACAAGCAGAGAAGG
Na*HSPRO* inverted repeat construct 5' end	gDNA	diagnostic PCR	GGAAGTTCATTTCATTTGGAG	CATACTAACTAACATCACTTAAC
Na*HSPRO* inverted repeat construct 3' end	gDNA	diagnostic PCR	GGTAACATGATAGATCCATGTC	GCGAAACCCTATAGGAACCC
Na*HSPRO*	cDNA	3'-RACE	CTGATCCTAGACCGTATGCG	According to Invitrogen Kit
Na*HSPRO*	cDNA	3'-RACE	TCGAAAACCGAACGCTGTAC	According to Invitrogen Kit
Na*HSPRO*	cDNA	3'-RACE	CGACACACCAGATCCTCGAA	According to Invitrogen Kit
Na*HSPRO*	cDNA	5'-RACE	According to Invitrogen Kit	AAGCATTTTTGACGCGTAGATCC
Na*HSPRO*	cDNA	5'-RACE	According to Invitrogen Kit	GCACAACAGAGCTATG
Na*HSPRO*	cDNA	5'-RACE	According to Invitrogen Kit	TCCATCGCCAACGATTCAAGCCTC
Na*HSPRO*	cDNA	Generation of ir-ltspro constructs	GTCGACACGACGGTTGTCAGCCAGAC	GGATCCGTAGATCCATGTTTCGAGGATC

Supplemental Experimental Procedures S1

Full length cDNA cloning, EGFP fusion protein generation, and sequence analysis

For the cloning of the full length *HSPRO* cDNA sequence, 5 µg of total RNA were isolated from leaves of *N. attenuata* plants. The 3´RACE and 5'RACE Systems for Rapid Amplification of cDNA Ends (Invitrogen, Karlsruhe, Germany) were used following the manufacturer's instructions and the primers listed in Supplemental Table SV. The PCR products were cloned into the pGEM-T easy vector (Promega, Madison, WI) and sequenced using universal primers. Sequence alignments and phylogeny analysis were performed using BLAST (http://blast.ncbi.nlm.nih.gov) and the Geneious Pro software (version 5.4; Drummond *et al.*, 2011). Phylogenetic analysis was performed with the Jukes-Cantor genetic distance model and the Neighbor Joining tree building method with bootstrapping (602 random seed, 100 replicates and 50% support threshold).

To generate C-terminal EGFP fusion proteins, the HSPRO protein coding sequence was amplified by PCR from *N. attenuata* cDNA and the nuclear localized DELLA protein RGA (Silverstone *et al.*, 2001) was amplified from Arabidopsis Col-0 cDNA (primers listed in Supplemental Table SV). PCR products were cloned into the pJET1.2 vector (Fermentas, East Lansing, MI) and transformed into *E. coli* TOP10 strain by electroporation using standard conditions. The Gateway vector pDONR221 (Invitrogen) was used as the entry vector and p2GWF7 (Karimi *et al.*, 2007) as the destination vector for C-terminal fusions to EGFP. Leaf Arabidopsis protoplasts were isolated and transformed by the polyethylene glycol (PEG) method as previously described (Yoo *et al.*, 2007). Protoplasts were incubated for 15 h in the dark at room temperature before visualization with a Zeiss Axioplan fluorescence microscope (Carl Zeiss, Jena, Germany) using standard settings for EGFP.

Genomic DNA extraction for qPCR analysis of *P. indica* root colonization

Genomic DNA from *N. attenuata* seedlings was extracted with 2 mL of extraction buffer (2 % (w/v) CTAB, 100 mM Tris-HCl pH:8.0, 20 mM EDTA, 1.4 M NaCl, 2 % (w/v) polyvinylpyrrolidone and 0.5% (v/v) 2-mercaptoethanol) pre-heated to 65ºC. Samples were kept at 65ºC for 1 h and repeatedly mixed by inverting the tube. After centrifugation (8,000 *g* for 5 min), the supernatant was collected and transferred into 50 mL plastic tubes. This initial extraction step was repeated twice. The pooled supernatants were extracted twice with 1/3 volumes (~0.6 mL) of chloroform:isoamyl alcohol (24:1) by continuously inverting the tube for 10 min and centrifugation (8,000 *g* for 10 min). 0.1 volumes (~60 µL) of 10% (w/v)

CTAB solution were added to the sample and after mixing by inverting the tube, 1.4 volumes (~1 mL) of precipitation buffer (1% (w/v) CTAB, 50 mM Tris-HCl pH=8.0, 10 mM EDTA) were added and mixed gently. After an overnight incubation, the tubes were centrifuged at 4,500 *g* for 15 min. The supernatant was removed and the pellet dissolved in 500 µL of high-salt TE (10 mM Tris-HCl pH=8.0, 0.1 mM EDTA, 1 M NaCl) containing 0.5 µg mL^{-1} RNAse-A for 20 min at 37ºC. The genomic DNA was precipitated by mixing the sample with 1 volume (500 µL) of isopropanol and incubating the mixture for 30 min. The samples were centrifuged at 16,100 *g* for 30 min and the pellet was washed with 500 µL of 70% (v/v) ethanol and finally dissolved in 5 µL of deionized water. The genomic DNA concentration was estimated by absorbance and by comparing the signal intensities on a 0.8% (w/) agarose gel to the intensities of a DNA ladder standard of known concentration.

Quantification of defense and flower-associated traits

In the morning (6 to 8 am), the nectar from 10 flowers was collected and pooled into a 1.5 mL tube to form one sample. The nectar volume per sample was determined with a graduated glass capillary. Nectar sugar content was measured with a refractometer using a sucrose standard curve. Nectar nicotine was quantified by LC-MS (liquid chromatography-mass spectrometry; Varian 1200 Triple-Quadrupole-LC-MS system; Varian, Palo Alto, CA) (see below) from samples containing 2 µL of nectar dissolved in 400 µL of deionized water spiked with 50 pg [$^2H_3$]nicotine.

For analysis of benzyl acetone (BA) in corollas, 10 corollas from recently opened (10 to 12 pm) night flowers were pooled per sample. The samples were frozen in liquid nitrogen and homogenized in 15 mL glass vials after adding 2 mL dichloromethane containing 2 µg tetraline mL^{-1}. Corolla tissue was spun down by centrifugation at 720 *g* for 10 min at room temperature. The supernatant was transferred into new glass vials with a Pasteur pipette and washed by adding 2 mL of deionized water. An aliquot from the organic phase was transferred into a glass vial and analyzed by GC-MS with a CP-3800 GC instrument (Varian 4000) equipped with a DB-Wax column (Agilent) as previously described (Re *et al.*, 2011). For identification of the benzyl acetone peak, the retention time and mass spectra were compared to a commercial standard (Sigma). Three biological replicates were used per genotype and treatment.

TPI activity from anthers and ovaries was quantified as previously described (Van Dam *et al.*, 2001). Anthers and ovaries from 10 flowers were pooled per sample and 5 samples were analyzed per genotype and treatment. Quantification of nicotine, rutin, and

chlorogenic acid after *M. sexta* OS elicitation of leaves was performed as previously described (Keinänen *et al.*, 2001). Leaves of rosette-stage plants were elicited by wounding and *M. sexta* OS elicitation once per day for three consecutive days and leaf samples were harvested at the end of the third day (six days after the start of the treatment).

Phytohormone and divinyl ether extraction and quantification

One hundred mg of *P. indica*-colonized roots (from seedlings grown for 14 days in the plate system) were homogenized to a fine powder with a Geno/Grinder 2000 (BTC and OPS Diagnostics, Bridgewater, USA) in the presence of liquid nitrogen. Each sample (biological replicate) consisted of roots pooled from 6 to 11 seedlings and 3 biological replicates per genotype per treatment were used. One mL of ethyl acetate spiked with 200 ng [$^2H_2$]JA, [$^2H_4$]SA, and [$^2H_6$]ABA as IS was used for extraction. The samples were centrifuged for 15 min at 12,000 *g* (4°C) and the upper organic phase was transferred into a fresh tube. The residual leaf material/aqueous phase was re-extracted with 0.5 mL ethyl acetate without IS. The organic phases were pooled and evaporated to dryness under reduced pressure. The dry residue was reconstituted in 0.4 mL of 70/30 (v/v) methanol/water for analysis by LC-MS (Varian 1200) as previously described (Bonaventure *et al.*, 2011).

For the analysis of ET, seedlings from WT and ir-*hspro* plants were weighed and transferred into a 250 mL glass vessel. Ten seedlings were placed in each glass vessel and a total of three glass vessels (n=3) were used per genotype. After a 5 h incubation period (glass vessels were kept in the growth chamber under the same conditions as the agar plates), the headspace of the vessels was flushed into a laser photo-acoustic spectrometer (PAS; INVIVO, Adelzhausen, Germany) for determination of ET levels (nL $h^{-1}g^{-1}$ FW) as previously described (Körner *et al.*, 2009).

Metabolic profiling of roots

P. indica-colonized roots from ir-*hspro* and WT seedlings (grown for 14 days in the plate system) were collected for metabolic profiling. Ten roots were pooled per sample and 5 samples (biological replicates) per genotype were used. Root tissue was ground with a Geno/Grinder 2000 in the presence of liquid nitrogen and thoroughly extracted with 1 mL of 40% (v/v) methanol/50 mM aqueous sodium acetate buffer (pH: 4.8) per 100 mg of root tissue. Homogenized samples were centrifuged at 12,000 *g* for 20 min at 4°C, the supernatant was transferred into a fresh 1.5 mL microcentrifuge tube and the samples were centrifuged again using the same conditions. 100 µL of the supernatant were transferred into 2 mL glass

vials for analysis by UPLC-ToF-MS (ultra-pressure-liquid-chromatography time-of-flight mass spectrometry; Bruker Daltonik GmbH, Bremen, Germany) as previously described (Gilardoni *et al.*, 2011).

Microarray analysis

P. indica-colonized roots from ir-*hspro* and WT seedlings (grown for 14 days in the plate system) were collected for microarray analysis. Ten roots were pooled per sample and 3 samples (biological replicates) per genotype were used. Total RNA was extracted as previously described (Kistner and Matamoros, 2005) and RNA quality was checked by spectrophotometry (NanoDrop, Wilmington, DE). Genomic DNA was removed by DNAse treatment following commercial instructions (Turbo DNase; Ambion, Europe), RNA was cleaned up with RNeasy MinElute columns (Qiagen, Hilden, Germany) and the RNA quality was checked with the RNA 6000 Nano kit (Agilent, Santa Clara, CA) using an Agilent 2100 Bioanalyzer. Total RNA was used to generate labeled cRNA with the Quick Amp labeling kit (Agilent) following commercial specifications and the yield of cRNA was determined spectrophotometrically (NanoDrop). Labeled cRNA was hybridized using the Gene Expression Hybridization kit (Agilent) following commercial instructions onto a 44K custom designed 60mer *N. attenuata* Agilent microarrays as previously described (Gilardoni *et al.*, 2011; Kallenbach *et al.*, 2011). Hybridization, washing and analysis were performed as previously described (Gilardoni *et al.*, 2011; Kallenbach *et al.*, 2011). Three biological replicates were used per treatment with a total of six arrays (see Accession numbers). Data was extracted using the Agilent Feature Extraction software (version 9.5) and analyzed with the SAM (Significance Analysis of Microarrays) software (Tusher *et al.*, 2001). The *q*-values for each gene corresponded to a computed false discovery rate (FDR) of less than 4%. Changes in gene expression were considered to be significant when the Log_2 of the fold change in signal intensity (ir-*hspro* versus WT) were greater than 1 or smaller than -1.

Root and fungus staining

Root samples from seedlings grown in the presence of *P. indica* for 7 and 14 days were fixed in 0.15 % (w/v) trichloroacetic acid in 4:1 (v/v) ethanol/chloroform as previously described (Deshmukh *et al.*, 2006). Samples were stained with WGA-AF488 (fungal structures; green) and propidium iodide (cell walls; red) as previously described (Zuccaro *et al.*, 2011). Confocal laser scanning microscopy was performed using a LSM 510 Meta microscope (Carl Zeiss) equipped with an argon laser. Samples were excited at 488 nm and

light emission detected at 500-540 nm for WGA-AF488. For propidium iodide, samples were excited at 560 nm and light emission detected at 580-660 nm. Macroscopic observations of WT and ir-*hspro* seedling roots grown for 14 days on the plate system in the presence or absence of *P. indica* was carried out with a stereomicroscope (Olympus SZ51). Cell death analysis in roots was performed by trypan-blue staining as previously described (Diaz-Tielas *et al.*, 2012)

M. sexta performance assays and OS collection

Larvae of the tobacco hornworm (*Manduca sexta*) were obtained from in-house colonies, generated from *M. sexta* eggs originally purchased from the Carolina Biological Supply (North Carolina, US). Eggs deposited on *N. attenuata* plants were collected and were kept in a growth chamber (Snijders Scientific) at 26°C/16 h day and 24°C/8 h night until the larvae hatched. *M. sexta* and *Spodoptera exigua* OS was collected as described by (Roda *et al.*, 2004). For *M. sexta* larval growth performance assay, freshly hatched neonates were placed carefully on leaves of rosette-stage *N. attenuata* plants (one neonate per plant). A minimum of 30 plants per genotype were used. Caterpillars were weighed every two to three days for two weeks.

References

Bonaventure G, Schuck S, Baldwin IT (2011) Revealing complexity and specificity in the activation of lipase-mediated oxylipin biosynthesis: a specific role of the Nicotiana attenuata GLA1 lipase in the activation of jasmonic acid biosynthesis in leaves and roots. Plant Cell Environ **34:** 1507-1520

Deshmukh S, Huckelhoven R, Schafer P, Imani J, Sharma M, Weiss M, Waller F, Kogel KH (2006) The root endophytic fungus Piriformospora indica requires host cell death for proliferation during mutualistic symbiosis with barley. Proc Natl Acad Sci USA **103:** 18450-18457

Diaz-Tielas C, Grana E, Sotelo T, Reigosa MJ, Sanchez-Moreiras AM (2012) The natural compound trans-chalcone induces programmed cell death in Arabidopsis thaliana roots. Plant Cell Environ

Gilardoni PA, Hettenhausen C, Baldwin IT, Bonaventure G (2011) Nicotiana attenuata LECTIN RECEPTOR KINASE1 suppresses the insect-mediated inhibition of induced defense responses during Manduca sexta herbivory. Plant Cell **23:** 3512-3532

Kallenbach M, Gilardoni PA, Allmann S, Baldwin IT, Bonaventure G (2011) C(12) derivatives of the hydroperoxide lyase pathway are produced by product recycling through lipoxygenase-2 in Nicotiana attenuata leaves. New Phytol **191:** 1054-1068

Karimi M, Depicker A, Hilson P (2007) Recombinational cloning with plant gateway vectors. Plant Physiol **145:** 1144-1154

Keinänen M, Oldham NJ, Baldwin IT (2001) Rapid HPLC screening of jasmonate-induced increases in tobacco alkaloids, phenolics, and diterpene glycosides in Nicotiana attenuata. Journal of Agricultural and Food Chemistry **49:** 3553-3558

Kistner C, Matamoros M (2005) RNA isolation using phase extraction and LiCl precipitation. *In* A Márquez, ed, Lotus japonicus Handbook. Springer Netherlands, pp 123-124

Körner E, von Dahl C, Bonaventure G, Baldwin IT (2009) Pectin methylesterase NaPME1 contributes to the emission of methanol during insect herbivory and to the elicitation of defence responses in *Nicotiana*. J Exp Bot **60:** 2631-2640

Re DA, Dezar CA, Chan RL, Baldwin IT, Bonaventure G (2011) Nicotiana attenuata NaHD20 plays a role in leaf ABA accumulation during water stress, benzylacetone emission from flowers, and the timing of bolting and flower transitions. J Exp Bot **62:** 155-166

Roda A, Halitschke R, Steppuhn A, Baldwin IT (2004) Individual variability in herbivore-specific elicitors from the plant's perspective. Mol Ecol **13:** 2421-2433

Silverstone AL, Jung HS, Dill A, Kawaide H, Kamiya Y, Sun TP (2001) Repressing a repressor: gibberellin-induced rapid reduction of the RGA protein in Arabidopsis. Plant Cell **13:** 1555-1566

Tusher VG, Tibshirani R, Chu G (2001) Significance analysis of microarrays applied to the ionizing radiation response. Proc Natl Acad Sci U S A **98:** 5116-5121

Van Dam NM, Horn M, Mares M, Baldwin IT (2001) Ontogeny constrains systemic protease inhibitor response in Nicotiana attenuata. J Chem Ecol **27:** 547-568

Yoo S-D, Cho Y-H, Sheen J (2007) Arabidopsis mesophyll protoplasts: a versatile cell system for transient gene expression analysis. Nat. Protocols **2:** 1565-1572

Zuccaro A, Lahrmann U, Guldener U, Langen G, Pfiffi S, Biedenkopf D, Wong P, Samans B, Grimm C, Basiewicz M, Murat C, Martin F, Kogel KH (2011) Endophytic life strategies decoded by genome and transcriptome analyses of the mutualistic root symbiont Piriformospora indica. PLoS Pathog **7:** e1002290

Chapter 6: Manuscript 4

HSPRO acts via SnRK1-mediated signaling in the regulation of *Nicotiana attenuata* seedling growth promoted by *Piriformospora indica*

SHORT COMMUNICATION

Plant Signaling & Behavior 8:4, e23537; April 2013; © 2013 Landes Bioscience

HSPRO acts via SnRK1-mediated signaling in the regulation of *Nicotiana attenuata* seedling growth promoted by *Piriformospora indica*

Stefan Schuck, Ian T. Baldwin and Gustavo Bonaventure*

Department of Molecular Ecology; Max Planck Institute for Chemical Ecology; Jena, Germany

Keywords: *Nicotiana attenuata*, *Piriformospora indica*, HSPRO, SnRK1, plant growth promotion, signaling

Abbreviations: Adi3, AvrPto-dependent Pto-interacting protein 3 (*Solanum lycopersicum*); AKINα10, SNF1 KINASE HOMOLOG 10, synonym: AKINα2 (*Arabidopsis thaliana*); AKINβγ, HOMOLOG OF YEAST SUCROSE NONFERMENTING 4, synonym: SNF1-related protein kinase regulatory subunit βγ (*Arabidopsis thaliana*); AKINγ1, SNF1-RELATED PROTEIN KINASE REGULATORY SUBUNIT γ 1, synonym: SNF1-related protein kinase regulatory subunit gamma-1 (*Arabidopsis thaliana*); as, antisense; GAL83, GALactose metabolism mutant 83 (*Saccharomyces cerevisiae*); HD20, homeodomain 20 transcription factor (*Nicotiana attenuata*); HSPRO, ortholog of nematode resistance protein Hs1^{pro-1} from *Beta procumbens;* ir, inverted-repeat; SNF1, sucrose non-fermenting-1 (*Saccharomyces cerevisiae*); SnRK1, SNF1-related protein kinase 1

Nicotiana attenuata HSPRO (NaHSPRO) is a negative regulator of seedling growth promoted by the fungus *Piriformospora indica*. Homologs of NaHSPRO in *Arabidopsis thaliana* (i.e., AtHSPRO1 and AtHSPRO2) are known to physically interact with the AKINβγ subunit of the SnRK1 complex.[2] To investigate whether NaHSPRO is associated with SnRK1 function during the stimulation of seedling growth by *P. indica,* we studied *N. attenuata* plants silenced in the expression of Na*GAL83* (as-*gal83* plants)—a gene that encodes for the regulatory β-subunit of SnRK1—and plants silenced in the expression of both Na*HSPRO* and Na*GAL83* (ir-*hspro*/as-*gal83* plants). The results showed that *P. indica* differentially stimulated the growth of both as-*gal83* and ir-*hspro*/as-*gal83* seedlings compared with control seedlings, with a magnitude similar to that observed in ir-*hspro* seedlings. Thus, we showed that, similar to Na*HSPRO,* Na*GAL83* is a negative regulator of seedling growth stimulated by *P. indica*. We propose that the effect of Na*HSPRO* on seedling growth is associated with SnRK1 signaling.

NaHSPRO from the wild tobacco species *Nicotiana attenuata* belongs to a group of so-called putative nematode resistance proteins named based on their homology to Hs1^{pro-1},[1] a protein from wild beet (*Beta procumbens*) that confers resistance to the beet cyst nematode *Heterodera schachtii*.[3] However, the function of Hs1^{pro-1} homologs (HSPROs) is not only restricted to nematode resistance.[3,4] In this regard, HSPROs have also been involved in the regulation of plant defense responses against the bacterial pathogen *Pseudomonas syringae*[5] and in the regulation of plant mutualistic interactions with the plant growth-promoting fungus *Piriformospora indica*.[1] *HSPRO* genes have been generically defined as stress responsive genes, and it has been suggested that they play a general role during stress responses.[6] However, the molecular function of *HSPRO* genes remains at present mostly unknown. One important step toward the unraveling of the molecular function of HSPROs has been the discovery that AtHSPRO1 and AtHSPRO2 interact with the AKINβγ regulatory subunit of SnRK1 in *Arabidopsis*.[2] Plant SnRK1s are heterotrimeric protein kinase complexes formed by one catalytic α-subunit (e.g., AKINα10 in *Arabidopsis*), one regulatory β-subunit (e.g., AKINβ1 in *Arabidopsis*, NaGAL83 in *N. attenuata*) and either one regulatory γ- or one chimeric βγ-subunit (AKINγ1 and AKINβγ in *Arabidopsis*, respectively).[2,7] It has been reported that silencing either the expression of the catalytic α-subunit or the regulatory β-subunit of plant SnRK1s leads to an inactive complex.[8] In all organisms studied thus far, SnRK1s sense the energy status of the cells, and in plants, SnRK1 represses the expression of genes involved in energy-consuming biosynthetic processes and activates the expression of catabolic genes responsible for increasing energy and nutrient availability under conditions in which those are scarce.[9] In addition to the regulation of gene expression, SnRK1 functions as a regulator of the activity of key nitrogen and carbon metabolic enzymes[6,10] and the transport of photo-assimilates from shoots to roots during tolerance responses to insect herbivory.[3] Recently, it has been shown that *Arabidopsis* and rice (*Oriza sativa*) SnRK1s

*Correspondence to: Gustavo Bonaventure; Email: gustavo.bonaventure@gmail.com
Submitted: 12/17/12; Revised: 01/08/13; Accepted: 01/08/13
http://dx.doi.org/10.4161/psb.23537
Citation: Schuck S, Baldwin IT, Bonaventure G. HSPRO acts via SnRK1-mediated signaling in the regulation of *Nicotiana attenuata* seedling growth promoted by *Piriformospora indica*. Plant Signal Behav 2013; 8: e23537

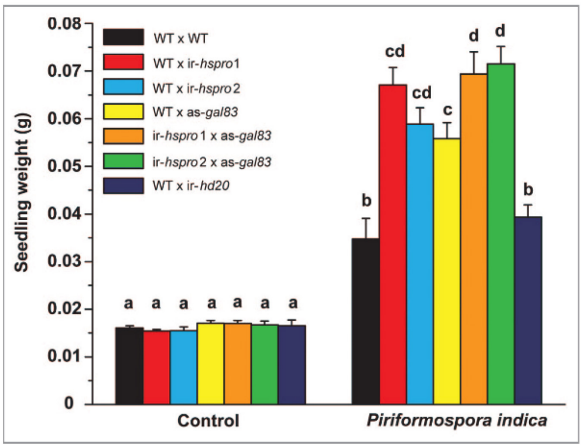

Figure 1. Differential growth promotion of *Nicotiana attenuata* seedlings mediated by *Piriformospora indica*. After seven days of germination, *N. attenuata* seedlings were transferred onto PNM (plant nutrient medium)[1] and inoculated with *P. indica* culture or a medium control. After 14 d of incubation in these conditions, the fresh biomass of seedlings was determined with a microbalance (n = 8–17; bars denote standard error of the mean). Statistical analysis was conducted using one way-ANOVA with Tuckey post-hoc test. The letters on top of the bars denote significant differences between genotypes and treatments and the *P*-values associated with the analysis are summarized in **Table 1**.

participate in stress-responsive gene regulation and in plant growth and development.[11]

Considering the previously published study on the interaction between AKINβγ and AtHSPRO1 and AtHSPRO2 in *Arabidopsis*,[2] and the fact that this interaction occurs in the cytosol (coincident with the cellular localization of NaHSPRO in *N. attenuata*),[1] we hypothesized that changes in metabolism brought about by SnRK1-mediated mechanisms underlie the differential growth promotion of ir-*hspro* seedlings during the interaction with *P. indica*.[1] To test this hypothesis, we followed a genetic approach in which we assessed seedling growth in the progeny derived from the following crosses (performed reciprocally for each genotype): WT x ir-*hspro* (two independent transgenic lines were used: ir-*hspro* 1 and ir-*hspro* 2),[1] WT x as-*gal83* (a transgenic *N. attenuata* line stably silenced in the expression of Na*GAL83* by antisense technique)[7] and ir-*hspro x* as-*gal83*. The crosses between singly silenced lines and WT plants were performed as a control for the cross between ir-*hspro* and as-*gal83* plants and therefore for hemizygosity of the transgenes. An additional cross between WT and a transgenic *N. attenuata* line stably silenced in the expression of the transcription factor HD20 (ir-*hd20*)[3] was used as a transgenic-plant control. WT plants were also manually self-crossed as a control (WT x WT). Seedling fresh weight of all genotypes used was quantified after 14 d of growth in both the presence and absence of *P. indica* and the assay was conducted in a plate system as previously described.[1] As expected, increased growth promotion (45% gain in fresh biomass) was observed in WT seedlings grown in the presence of *P. indica* as compared with WT seedlings grown in the absence of the fungus (**Fig. 1** and **Table 1**) and a stronger growth promotion (ca. 250%) was observed for WT x ir-*hspro* seedlings grown under the same conditions (**Fig. 1** and **Table 1**). WT x as-*gal83* and ir-*hspro1* as-*gal83* seedlings showed a growth promotion effect of the same magnitude as that quantified for WT x ir-*hspro* seedlings in the presence of *P. indica* (**Fig. 1** and **Table 1**). In contrast, the growth of WT x ir-*hd20* seedlings was not differentially stimulated by the fungus compared with WT seedlings (**Fig. 1** and **Table 1**). The results showed that, during interaction with *P. indica*, the silencing of Na*GAL83* expression (either alone or in combination with Na*HSPRO)* produces the same effect on seedling growth as the silencing of Na*HSPRO* alone. From a genetic perspective, these results strongly suggested that these two genes act in the same pathway and therefore that HSPRO negatively regulates WT *N. attenuata* seedling growth during interaction with *P. indica* by affecting SnRK1-mediated signaling.

SnRK1 is activated under stress conditions such as nutrient and energy deprivation, playing a central role in metabolic and transcriptional reprogramming of processes necessary for the switch in resource utilization and allocation and affecting thereby growth.[6] In cases where SnRK1 activity is inhibited (e.g., exogenous supply of sugars), plant growth is promoted. As an example, silencing the expression of AKINα10 leads to enhanced *Arabidopsis* seedling growth via a more efficient use of exogenously supplied sucrose and glucose.[9] In *N. attenuata* plants, repression of Na*GAL83* expression (and thereby

Table 1. One way-ANOVA and Tuckey post-hoc test results from the comparison of *Piriformospora indica*-colonized seedlings presented in **Figure 1**

	P-values one way-ANOVA (in the presence of *P. indica*)				
	WT x WT	**WT x ir-*hd20***	**WT x ir-*hspro* 1**	**WT x ir-*hspro* 2**	**WT x as-*gal83***
WT x WT		1.00	7.72E-10	5.06E-5	1.84E-4
WT x ir-*hd20*	1.00		9.98E-9	8.37E-4	3.19E-3
WT x ir-*hspro* 1	7.72E-10	9.98E-9		0.87	0.29
WT x ir-*hspro* 2	5.06E-5	8.37E-4	0.87		1.00
WT x as-*gal83*	1.84E-4	3.19E-3	0.29	1.00	
ir-*hspro* 1 x as-*gal83*	1.50E-12	2.91E-12	1.00	0.38	2.46E-2
ir-*hspro* 2 x as-*gal83*	1.19E-12	1.28E-12	1.00	0.14	4.14E-3

inhibition of SnRK1 activity) during insect herbivory induces an increased transport of photo-assimilates from shoots to roots (C "bunkering"), thus delaying senescence and prolonging flowering.[3]

Taking all results together, we propose two possible scenarios (non-mutually exclusive) to describe the role of HSPRO and SnRK1 in controlling WT *N. attenuata* seedling growth during *P. indica* interaction. In one scenario, activation of *HSPRO* expression by the interaction of roots with *P. indica* subsequently activates SnRK1 (by still unknown mechanisms but based on the interaction of HSPRO with the regulatory βγ-subunit of SnRK1). SnRK1 activation inhibits increased photo-assimilate transport from the shoot to the root, controlling root sugar content and the beneficial interaction with *P. indica* (i.e., stimulation of seedling growth; Fig. 2). In the cases where the activity of SnRK1 is reduced (e.g., as-*gal83* plants) or the expression of HSPRO is impaired (e.g., ir-*hspro* plants), changes in sugar content in roots affect the beneficial interaction of *P. indica* with this tissue in a manner that induces differential growth promotion of seedlings (Fig. 2). It is important to note that colonization rates of *P. indica* are similar between ir-*hspro* plants and WT,[1] and therefore the hypothetical changes in beneficial interaction are independent of higher colonization rates by the fungus. This scenario assumes that wild-type rates of C allocation in roots are an important determinant of the interaction of this tissue with *P. indica*. This assumption is consistent with previous studies showing that, in *P. indica* colonized barley roots, fungal proteins involved in carbon and nitrogen uptake and metabolism are important for the switch from a biotrophic to a necrotrophic lifestyle by the fungus.[13] Another study performed with *Arabidopsis* and tobacco (*N. tabacum*) plants showed that the expression of plant enzymes involved in starch degradation and nitrate assimilation is induced in *P. indica*-colonized roots.[14] In a second scenario, activation of *HSPRO* expression by the interaction of roots with *P. indica* activates SnRK1, and this activation leads to a more direct negative feedback control on seedling growth, for example, by repression of biosynthesis genes or deactivation of biosynthesis enzymes (Fig. 2). When either HSPRO or SnRK1 activities or expression are lower (e.g., in ir-*hspro* or as-*gal83* plants) the negative feedback on seedling growth is less restrained and seedlings increase their growth rates (Fig. 2). It is noteworthy that in tomato (*Solanum lycopersicum*), the β-subunit of SnRK1 (the ortholog of NaGAL83) is phosphorylated by the protein kinase Adi3 (AvrPto-dependent Pto-interacting protein3).[15] Thus, by associating with the βγ-subunit of SnRK1, HSPRO could interfere with the post-translation modification of, for example, NaGAL83 in *N. attenuata*.

In conclusion, the experiments presented in this study provided strong evidence for the participation of HSPRO in the regulation of SnRK1-mediated responses controlling *N. attenuata* seedling growth during interaction with *P. indica*. Interestingly, the effect of differential growth promotion of ir-*hspro* and as-*gal83* seedlings only occurs during interaction with *P. indica*, indicating that activation of HSPRO/SnRK1 by this fungus is required. New exciting hypothesis have been derived from these experiments and future studies will be focused on the understanding of the molecular connection between HSPRO and SnRK1 and on how this connection regulates metabolism to accelerate seedling growth during interaction with *P. indica* and other growth promoting microorganisms.

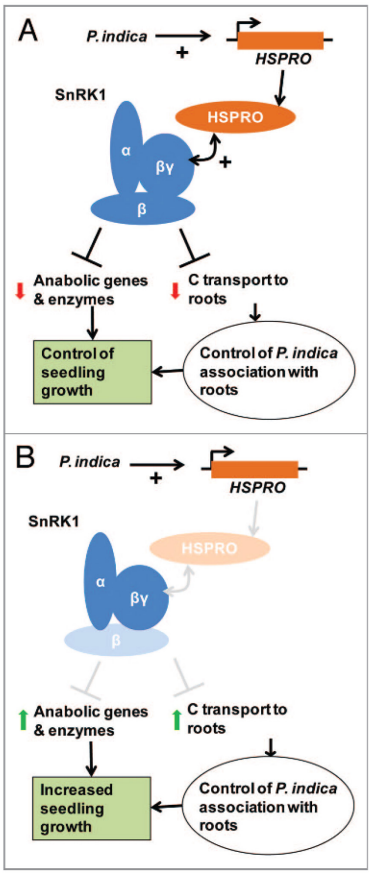

Figure 2. Hypothetical model for the role of HSPRO and SnRK1 in regulation of seedling growth during interaction of *N. attenuata* plants with the growth promoting fungus *P. indica*. (**A**) The interaction of *P. indica* with roots of *N. attenuata* seedlings induces the expression of *HSPRO* via transcriptional activation.[1] HSPRO interacts with the βγ-subunit of SnRK1[2] and this interaction activates SnRK1 by still unknown mechanisms. Activation of SnRK1 controls the allocation of carbon (**C**) from photo-assimilates to the roots[3] and negatively regulates the expression of anabolic genes and enzymes (references in text). These mechanisms either directly or indirectly affect seedling growth during interaction with *P. indica*. (**B**) In plants with reduced levels of *HSPRO* expression (e.g., triggered by gene silencing) or SnRK1 activity (e.g., triggered by silencing of the β-subunit), the negative regulation of C transport to roots, anabolic gene expression and metabolic enzyme activities by SnRK1 is lessened and seedling growth is enhanced via differential growth promotion by *P. indica*.

Disclosure of Potential Conflicts of Interest

No potential conflicts of interest were disclosed.

Acknowledgments

This study was financially supported by the Deutsche Forschungsgesellschaft (DFG; BO3260/3-1 and 3-2) and the Max Planck Society.

References

1. Schuck S, Camehl I, Gilardoni PA, Oelmueller R, Baldwin IT, Bonaventure G. HSPRO controls early Nicotiana attenuata seedling growth during interaction with the Fungus *Piriformospora indica*. Plant Physiol 2012; 160:929-43; PMID:22892352; http://dx.doi.org/10.1104/pp.112.203976.
2. Gissot L, Polge C, Jossier M, Girin T, Bouly JP, Kreis M, et al. AKINbetagamma contributes to SnRK1 heterotrimeric complexes and interacts with two proteins implicated in plant pathogen resistance through its KIS/GBD sequence. Plant Physiol 2006; 142:931-44; PMID:17028154; http://dx.doi.org/10.1104/pp.106.087718.
3. Cai D, Kleine M, Kifle S, Harloff HJ, Sandal NN, Marcker KA, et al. Positional cloning of a gene for nematode resistance in sugar beet. Science 1997; 275:832-4; PMID:9012350; http://dx.doi.org/10.1126/science.275.5301.832.
4. McLean MD, Hoover GJ, Bancroft B, Makhmoudova A, Clark SM, Welacky T, et al. Identification of the full-length $Hs1^{pro-1}$ coding sequence and preliminary evaluation of soybean cyst nematode resistance in soybean transformed with $Hs1^{pro-1}$ cDNA. Canadian Journal of Botany-Revue Canadienne De Botanique 2007; 85:437-41; http://dx.doi.org/10.1139/B07-038.
5. Murray SL, Ingle RA, Petersen LN, Denby KJ. Basal resistance against *Pseudomonas syringae* in *Arabidopsis* involves WRKY53 and a protein with homology to a nematode resistance protein. Mol Plant Microbe Interact 2007; 20:1431-8; PMID:17977154; http://dx.doi.org/10.1094/MPMI-20-11-1431.
6. Baena-González E, Sheen J. Convergent energy and stress signaling. Trends Plant Sci 2008; 13:474-82; PMID:18701338; http://dx.doi.org/10.1016/j.tplants.2008.06.006.
7. Schwachtje J, Minchin PEH, Jahnke S, van Dongen JT, Schittko U, Baldwin IT. SNF1-related kinases allow plants to tolerate herbivory by allocating carbon to roots. Proc Natl Acad Sci USA 2006; 103:12935-40; PMID:16912118; http://dx.doi.org/10.1073/pnas.0602316103.
8. Halford NG, Hey S, Jhurreea D, Laurie S, McKibbin RS, Paul M, et al. Metabolic signalling and carbon partitioning: role of Snf1-related (SnRK1) protein kinase. J Exp Bot 2003; 54:467-75; PMID:12508057; http://dx.doi.org/10.1093/jxb/erg038.
9. Baena-González E, Rolland F, Thevelein JM, Sheen J. A central integrator of transcription networks in plant stress and energy signalling. Nature 2007; 448:938-42; PMID:17671505; http://dx.doi.org/10.1038/nature06069.
10. Sugden C, Donaghy PG, Halford NG, Hardie DG. Two SNF1-related protein kinases from spinach leaf phosphorylate and inactivate 3-hydroxy-3-methylglutaryl-coenzyme A reductase, nitrate reductase, and sucrose phosphate synthase in vitro. Plant Physiol 1999; 120:257-74; PMID:10318703; http://dx.doi.org/10.1104/pp.120.1.257.
11. Cho YH, Hong JW, Kim EC, Yoo SD. Regulatory functions of SnRK1 in stress-responsive gene expression and in plant growth and development. Plant Physiol 2012; 158:1955-64; PMID:22232383; http://dx.doi.org/10.1104/pp.111.189829.
12. Ré DA, Raud B, Chan RL, Baldwin IT, Bonaventure G. RNAi-mediated silencing of the HD-Zip gene HD20 in *Nicotiana attenuata* affects benzyl acetone emission from corollas via ABA levels and the expression of metabolic genes. BMC Plant Biol 2012; 12:60; PMID:22548747; http://dx.doi.org/10.1186/1471-2229-12-60.
13. Zuccaro A, Lahrmann U, Güldener U, Langen G, Pfiffi S, Biedenkopf D, et al. Endophytic life strategies decoded by genome and transcriptome analyses of the mutualistic root symbiont *Piriformospora indica*. PLoS Pathog 2011; 7:e1002290; PMID:22022265; http://dx.doi.org/10.1371/journal.ppat.1002290.
14. Sherameti I, Shahollari B, Venus Y, Altschmied L, Varma A, Oelmüller R. The endophytic fungus *Piriformospora indica* stimulates the expression of nitrate reductase and the starch-degrading enzyme glucan-water dikinase in tobacco and Arabidopsis roots through a homeodomain transcription factor that binds to a conserved motif in their promoters. J Biol Chem 2005; 280:26241-7; PMID:15710607; http://dx.doi.org/10.1074/jbc.M500447200.
15. Avila J, Gregory OG, Su DY, Deeter TA, Chen SX, Silva-Sanchez C, et al. The β-subunit of the SnRK1 complex is phosphorylated by the plant cell death suppressor Adi3. Plant Physiol 2012; 159:1277-90; PMID:22573803; http://dx.doi.org/10.1104/pp.112.198432.

Chapter 7: Discussion

Nicotiana attenuata responds specifically to its individual attackers

As already extensively described in the introduction, *N. attenuata* plants are - as a consequence of germinating from long-lived seed banks in a post-fire environment - challenged by herbivore and pathogen communities unpredictable regarding their species composition (Baldwin & Morse, 1994; Preston & Baldwin, 1999). Therefore it is especially important for this plant species to recognize its individual attackers to react most efficiently (Diezel *et al*., 2009). At least it needs to differentiate between herbivores with different feeding modes (biting/chewing or piercing/sucking), polyphagous generalists and oligo-/monophagous specialists as well as between different pathogens with varying degrees of biotrophy/necrotrophy in their lifestyle and specialization to a certain host plant (Kirchner & Roy, 2002; Glazebrook, 2005; Ali & Agrawal, 2012). This means the reaction needs to be tailored to the attacker in a very sophisticated way that a) Darwinian fitness costs due to resource investments are minimized, b) direct (*e.g.* autotoxicity of defense chemicals) or indirect (*e.g.* damage of mutualists) detrimental side effects for the plant are avoided and c) the taken countermeasures indeed negatively affect the attacker and do not result in the opposite (*i.e*. the attacker's benefit) (Baldwin & Callahan, 1993; Euler & Baldwin, 1996; Baldwin *et al*., 1998). Ali & Agrawal (2012) proposed in their excellent review an evolutionary scenario that could explain why the plant's ability to distinguish between specialist and generalist herbivores might be of great adaptive value. According to that model there might be more selection pressure on generalist chewing herbivores compared to specialist ones to develop mechanisms which suppress elicited plant defense responses (in case of chewing herbivores typically mediated by JA signaling) because the generalists are less likely to have adapted to the JA-mediated defenses of a particular host plant during evolution (Ali & Agrawal, 2012). With respect to *N. attenuata* and its lepidopteran herbivores, this model is in full agreement with the demonstrated tolerance of the specialist *M. sexta* to the JA-inducible plant defense compound nicotine and the suppression of JA-mediated defenses by the generalist *S. exigua* (Wink & Theile, 2002; Diezel *et al*., 2009).

GLA1 is the major lipase involved in JA burst formation after wounding and *M. sexta* herbivory

After *N. attenuata* elicitation by wounding, treatment with *M. sexta* OS or with the FAC 18:3-Glu as a defined constituent of this OS, JA production is initialized within only a few minutes, leading to a peak in JA content at approximately 40-60 minutes after stimulus application which is then reduced back to basal levels within four hours after elicitation (Schittko *et al*., 2000; Halitschke *et al*., 2001; Kallenbach *et al*., 2010; manuscript 1). Additional application of *M. sexta* OS or FACs to wounding sites – to simulate *M. sexta* herbivory – leads to a drastic JA burst amplification compared to wounding alone (3-4-fold higher JA peak levels) (Schittko et al., 2000; manuscript 1). Kallenbach *et al.* (2010) demonstrated by using a transient gene silencing approach (virus-induced gene silencing) that GLA1, a chloroplastic glycerolipase A1, is the major lipase in *N. attenuata* responsible for initialization of this transient JA burst. As shown in manuscript 1, this finding could be confirmed with *N. attenuata* genotypes stably silenced in *GLA1* expression and extended to the entire JA burst duration. GLA1 catalyzes the hydrolysis of trienoic fatty acids (hexadecatrienoic or linolenic acid) from various chloroplastic lipid classes (galacto- and phospholipids) and the free fatty acid substrates are then further metabolized by several other enzymes to JA (summarized in form of a model in manuscript 1) (Schaller & Stintzi, 2009; Bonaventure *et al*., 2011). Even though this vital role of GLA1 for the JA burst was proven only for wounding and 18:3-Glu elicitation and not for the complex *M. sexta* OS, GLA1 is likely to contribute to a similar extent also to the *M. sexta* OS-induced JA burst as it does after 18:3-Glu elicitation, since it is known that FAC application is fully sufficient to obtain the full intensity of the JA response observed after *M. sexta* OS treatment (Halitschke *et al*., 2001; Kallenbach *et al*., 2010; manuscript 1). However, it remains unclear whether GLA1 retains its important role also on a larger temporal scale and throughout the entire *M. sexta* herbivory process in which JA production is repeatedly elicited (Stork *et al*., 2009). Other lipases with redundant function might get activated over time which could contribute to gradually increasing basal JA levels and compensate for – in case of any GLA1 deficiency – the function of this lipase (Stork *et al*., 2009; Ellinger *et al*., 2010). An experiment in which *M. sexta* larvae performance and plant JA contents are monitored over time on wild-type and *GLA1*-silenced *N. attenuata* plants would probably help answering the question regarding GLA1´s actual biological relevance during *M. sexta* herbivory. The additional integration of larvae from

the generalist herbivore *S. exigua* in such an experiment together with the use of transgenic *N. attenuata* crosses deficient in both, SA accumulation and *GLA1* expression, could be interesting to evaluate the Darwinian fitness benefit resulting from SA-mediated suppression of the JA burst by *S. exigua*. For sure GLA1 is essential for the JA burst formation in *N. attenuata* after single-elicitation events (manuscript 1). In contrast to DAD1 and DGL lipases from *Arabidopsis* which are highly similar to *N. attenuata* GLA1 (protein sequence identity 46% and 37%, respectively), it neither plays any role in fertility (anther dehiscence, flower opening and pollen viability) nor development of *N. attenuata* and therefore seems to be specifically relevant only for *N. attenuata* responses to distinct stress stimuli like wounding or insect herbivory (Hyun *et al*., 2008; Kallenbach *et al*., 2010; manuscript 1). *N. attenuata* infection by the phytopathogenic oomycete Ppn also leads to slight JA induction in leaves, even though the quantified JA levels are very minor compared to those observed after wounding or FAC elicitation and in view of the huge induction of other phytohormes like SA and abscisic acid (see manuscripts 1 and 2). However, there was no difference in this Ppn-induced JA levels between wild-type and GLA1-silenced *N. attenuata* plants which might be explained either by compensation via high activity of residual GLA1 protein in *GLA1*-silenced *N. attenuata* plants or the action of redundant lipases (Ellinger *et al*., 2010; manuscript 1). For the latter case being true, a GLA1 involvement in Ppn-inducible JA production can be ruled out, emphasizing the stimulus-specificity of this lipase. The rapid conversion of free fatty acid substrates provided by GLA1 into their 13-hydroperoxides by a 13-lipoxygenase (LOX3) specifically feeding the JA biosynthesis pathway suggests a tight association of both enzymes (substrate channeling) (Bonaventure & Baldwin, 2010; manuscript 1). Considering the rapid initialization of JA biosynthesis, its regulation by *de novo* GLA1 protein biosynthesis appears rather unlikely (Bonaventure & Baldwin, 2010; Kallenbach *et al*., 2010). Indeed, *GLA1* transcriptional gene expression is even down-regulated by FAC elicitation (Kallenbach *et al*., 2010). Therefore it can be concluded that the initiation of wounding- and FAC-inducible JA biosynthesis is regulated most likely by elicitor-mediated changes in GLA1 (and maybe also LOX3) protein activity *e.g*. by posttranslational modification explaining the observed rapid accumulation of 13-hydroperoxy fatty acids and the different lysolipid accumulation patterns after FAC treatment compared to wounding (Bonaventure & Baldwin, 2010; Kallenbach *et al*., 2010; manuscript 1). To test this hypothesis, changes in GLA1 or LOX3 protein masses resulting from potential posttranslational modification events could be identified

by using a 2-D gel electrophoresis and MALDI-ToF approach. The down-regulation of *GLA1* expression (lack of *de novo* GLA1 protein biosynthesis) and/or the inactivation of GLA1 protein by posttranslational modification-based mechanisms or accelerated GLA1 protein degradation could then – in addition to JA metabolism – explain the observed decline in JA levels up to basal levels within a few hours after elicitation (Stitz *et al*., 2011).

GLA1 generates potential signaling molecules in response to Ppn infection

In contrast to elicitation by wounding and 18:3-Glu treatment, *GLA1* expression is drastically up-regulated in *N. attenuata* leaves after infection by the phytopathogenic fungi Ppn and *Fusarium oxysporum* (manuscript 1), indicating a second function of GLA1 different from JA biosynthesis in *N. attenuata´*s interaction with those fungi. As shown in manuscript 1, GLA1 is also not involved in fatty acid substrate supply to a lipoxygenase (LOX1) feeding the pathway for divinyl ether (DVE) biosynthesis, since final levels of DVE after Ppn and *F. oxysporum* infection were not different between wild-type and *GLA1*-silenced *N. attenuata* leaves. However, for the early infection stage (one day after inoculation), GLA1-dependent differences in the expression of *LOX1* (after Ppn infection) and the gene encoding for divinyl ether synthase (after *F. oxysporum* infection) could be observed in *N. attenuata* leaves, as well as an accelerated initial reduction in divinyl ether levels in Ppn-infected *GLA1*-silenced *vs.* wild-type *N. attenuata* plants, giving rise to the hypothesis that GLA1 could play a role in the generation of certain signaling molecules (different from JA) affecting gene expression and early DVE metabolism (manuscript 1). This hypothesis was supported by microarray and metabolic profiling data presented in manuscript 2 revealing GLA1-dependent changes in the expression of 4192 genes after Ppn infection which are reflected in secondary metabolite levels including phenylpropanoids, polyamines and terpenoids. Both, transcriptomic as well as metabolomic data, suggest a role of GLA1during Ppn infection in regulating the flux of metabolic precursors in the phenylalanine-ammonia-lyase pathway towards the production of lignin precursors (being fungitoxic or used for cell wall enforcement) and phenolamides, whereas flavonoid and free polyamine levels decrease (La Camera *et al*., 2004; Edreva *et al*., 2007; Bassard *et al*., 2010; manuscript 2). Thereby it could influence *N. attenuata´*s polyamine homeostasis and the decision regarding plant cell fate upon Ppn infection, *i.e.* programmed cell death in form of a

hypersensitive response or induction of other defense responses (Bassard *et al*., 2010). GLA1 plays also a role in regulating the levels of dimalonylated 17-hydroxygeranyllinalool diterpene glycosides (HGL-DTGs) known to be JA-inducible anti-herbivore defense metabolites (Heiling *et al*., 2010). To my knowledge, so far no information on a potential antimicrobial function of HGL-DTGs is available in literature. Even though *in vitro* inhibition assays not necessarily reflect the *in planta* situation, a mycelial growth inhibition test with pathogenic fungi like Ppn and the application of HGL-DTGs in various concentrations could give a first impression on a potential antifungal role of these metabolites. In addition, infection assays with pathogenic fungi and transgenic *N. attenuata* plants silenced in the gene encoding for geranylgeranyl diphosphate synthase having reduced levels of HGL-DTG precursors could help answering this question (Heiling *et al*., 2010). Since JA levels during Ppn infection do not depend on *GLA1* expression, GLA1 might indirectly control the malonylation of HGL-DTGs (Heiling *et al*., 2010; manuscript 2). The analysis of lysolipid and oxidized fatty acid product (oxylipin) levels between Ppn-infected *N. attenuata* wildtype and *GLA1*-silenced leaves identified galactolipid-, phosphatidylglycerol- and phosphatidylcholine-derived lysolipids, as well as free oleic, linoleic and linolenic acid, 9-hydroxy-linoleic acid and three not further characterized oxylipins as potential candidates for the proposed signaling molecules (manuscript 2). External application of those compounds to *N. attenuata* wildtype plants and comparison of gene expression patterns and metabolic profile changes with those observed in GLA1-dependent manner during Ppn infection could be useful to test whether or not these candidates are indeed important signaling molecules regulated by GLA1. The increase of total lipase A activity occurring during Ppn infection remained unaffected by *GLA1* expression, arguing against a rather unspecific potential role of GLA1 during plant autophagy-like processes (Moreau, 1987; Roy *et al*., 1995; Hong *et al*., 2000; Scherer *et al*., 2002; Talbot and Kershaw, 2009; manuscript 2). Lysolipid data from manuscript 1 and 2 suggests that GLA1 has direct access to the outer chloroplast envelope membrane because this is the only chloroplast compartment containing phosphatidylcholine and GLA1 was shown to participate in the production of lysophosphatidylcholine after elicitation by wounding, 18:3-Glu treatment or Ppn infection (Dorne *et al*., 1985; manuscript 1 and 2). Alternatively, GLA1 could be also involved indirectly in lysophosphatidylcholine production by regulating the activity of other lipases having access to phosphatidylcholine (Cohen et al., 1993; Kachroo and Kachroo, 2009; manuscript 1 and 2). This hypothesis is supported by results from

Cho *et al.* (2012) showing that in Ppn-infected tobacco oxylipins are preferentially produced from oxidized fatty acid precursors esterified to lipids in the *sn*-2 position, and GLA1 possesses at least *in vitro sn*-1 specificity, suggesting that GLA1 might regulate the production of 9-hydroxy linoleic acid and three other oxylipins after Ppn infection via changes in activity of other lipases which are able to hydrolyze fatty acids at the *sn*-2 position (Kallenbach *et al*., 2010; manuscript 2). Lysolipid data from manuscript 1 allowing for conclusions on *sn*-1 or *sn*-2 lipase specificity of GLA1 further supports this possibility. However it cannot be excluded that GLA1 may possess *in planta* both *sn*-1 and *sn*-2 activities (manuscript 1). In contrast to the situation in leaves, *GLA1* expression is down-regulated in *N. attenuata* roots after Ppn and *F. oxysporum* infection, however relative *GLA1* transcript abundance is constitutively approximately fourtimes higher in roots compared to leaves (manuscript 1). Therefore it is tempting to speculate about contrasting functions of GLA1 in leaves and in roots during pathogen infection. Alternatively, factors resulting from pathogen infection might specifically lead to the down-regulation of *GLA1* expression in *N. attenuata* roots. The relatively higher basal *GLA1* expression in roots compared to leaves might be explained by a constitutively stronger exposure of belowground plant parts to microbial pathogens compared to aerial parts. This hypothesis is consistent with the organ-specific accumulation pattern of certain metabolites associated to plant defense response against pathogenic fungi reported in literature: relatively high basal levels in roots without inducibility of biosynthesis (constitutive protective function), while basal levels in leaves are relatively low, but biosynthesis is inducible upon elicitation (defense on demand) (Bohlmann *et al*., 2002). As an example for such tissue-specific differences in inducibility, the antimicrobial sesquiterpenoid phytoalexin capsidiol is constitutively produced in *N. attenuata* roots to protect those from pathogen attack. In shoots, capsidiol is inducible by microbial pathogens, at least in the *N. attenuata*-related plant species *Nicotiana tabacum* (Bohlmann *et al*., 2002). Interestingly, in shoots from *N. attenuata*, transcription of the capsidiol biosynthetic enzyme 5-*epi*-aristolochene synthase is induced also by insect herbivory (Bohlmann *et al*., 2002). Surprisingly all the GLA1-mediated changes induced in *N. attenuata* observed in response to Ppn infection which are listed above did not influence the symptomatic disease progression or Ppn performance, maybe a result from the chosen experimental design (see discussion section in manuscript 2 for details). Another possibility is that Ppn is so well-adapted to the defense responses of its *Nicotiana* host plant species that the GLA1-regulated changes are not effective enough against this specialized

pathogen to successfully reduce Ppn growth performance and its detrimental effects caused to the plant (Kamoun *et al*., 1994; Ponchet *et al*., 1999; Colas *et al*., 2001). However, unpublished infection assay data using another fungal pathogen, *Fusarium brachygibbosum* isolated from leaf samples of diseased *N. attenuata* plants which were collected from the natural habitat of this plant species, revealed that *GLA1*-silenced *N. attenuata* plants were far more susceptible to *F. brachygibbosum* than *N. attenuata* wildtype (unpublished data). This indicates that GLA1 may have indeed huge influence on disease progression and plant mortality in the interaction of *N. attenuata* with other pathogenic microorganisms than Ppn. The direct comparison of transcriptomic and metabolomic changes induced by Ppn and *F. brachygibbosum* (and maybe additional phytopathogen species) in *N. attenuata* wildtype and *GLA1*-silenced plants could lead to the identification of GLA-dependent responses common for *N. attenuata´*s response to both fungi (and therefore add strength to conclusions made on GLA1´s function in *N. attenuata´*s defense against phytopathogens in general).

Figure 1 summarizes changes of *GLA1* expression and GLA1 functions in *N. attenuata´*s response to wounding, *M. sexta* herbivory and Ppn function which are illustrated more detailed in figure 2 (wounding and *M. sexta* herbivory) and figure 3 (Ppn infection).

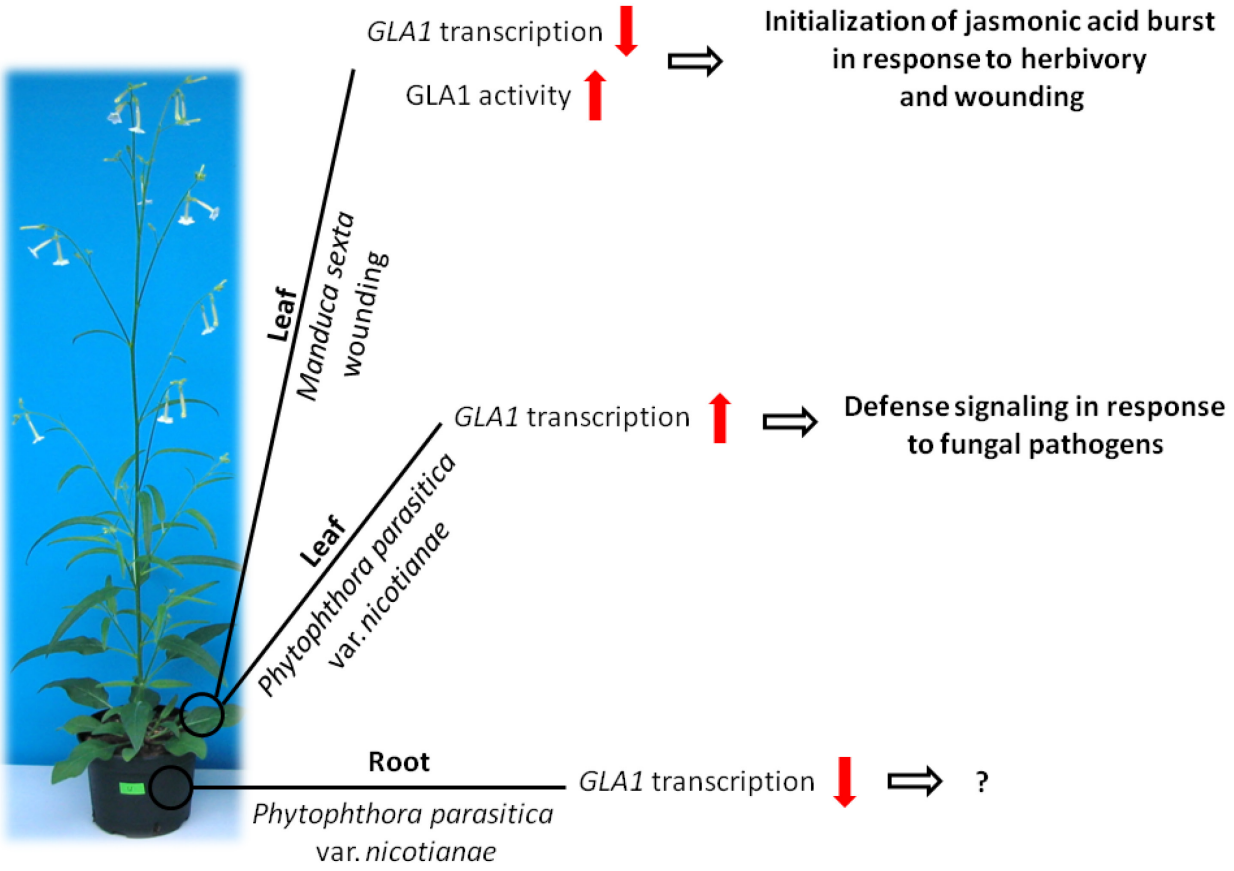

Figure 1. Organ- and stimuli-specific changes in *GLA1* transcription and GLA1 function in *N. attenuata*.

Upon elicitation of *N. attenuata* leaves by wounding or simulated herbivory by *M. sexta* (18:3-Glu treatment), GLA1 is rapidly activated and initializes the production of JA. At the same time, the transcriptional down-regulation of *GLA1* gene expression might contribute to the reduction of JA levels back to basal levels after reaching a peak, resulting in a rapid and transient JA burst. In contrast, *GLA1* transcription increases drastically in *N. attenuata* leaves during infection with the phytopathogenic oomycete Ppn and leads to big transcriptional and metabolic changes probably by the generation of signaling molecules (other than JA) by GLA1. During Ppn infection relative *GLA1* transcript abundance is reduced in *N. attenuata* roots, but it can be only speculated about GLA1´s role in this plant part.

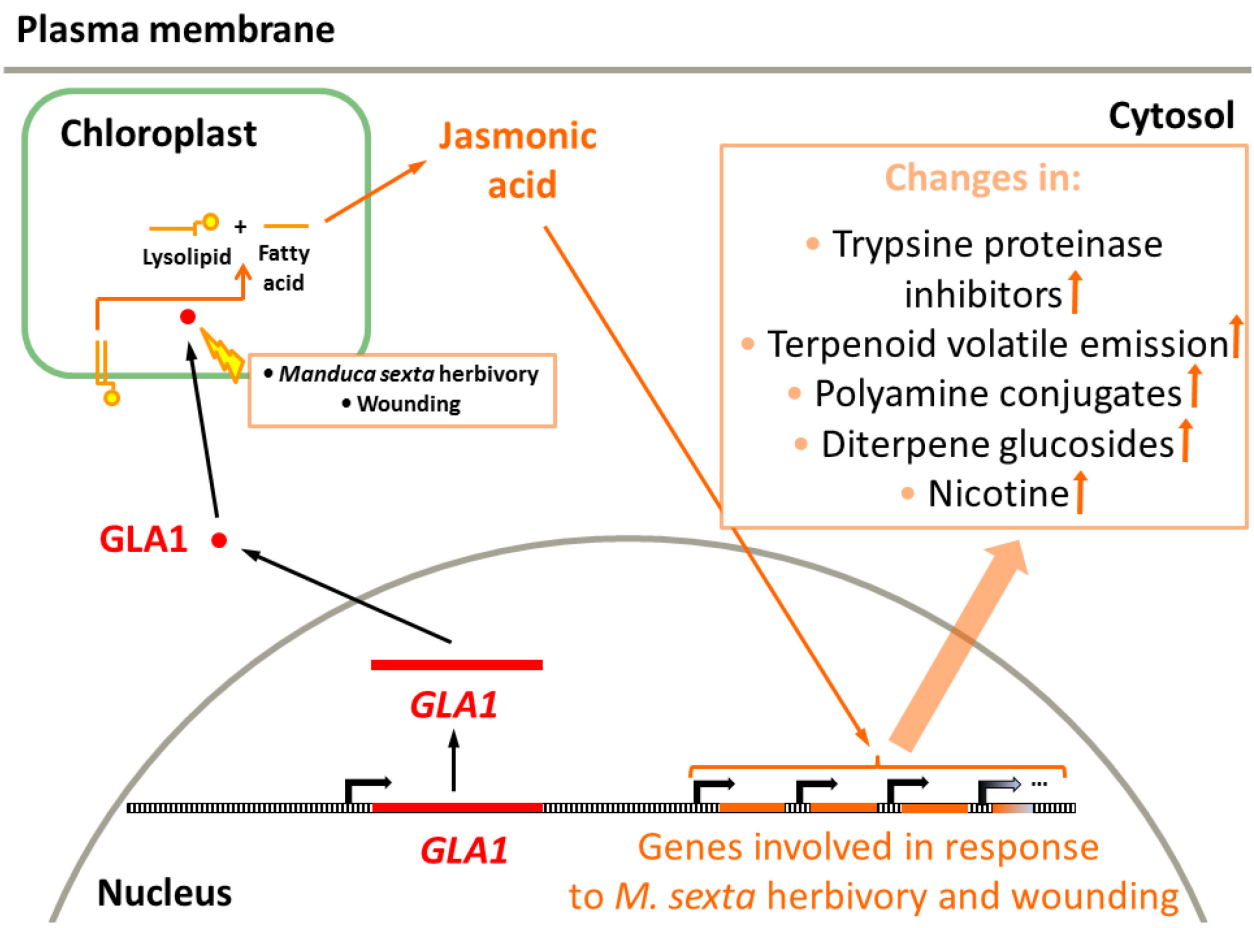

Figure 2. Function of GLA1 during wounding and *M. sexta* herbivory in *N. attenuata*.

GLA1 is constitutively expressed in leaves of *N. attenuata*. Being localized to the chloroplast, where it is rapidly activated after perception of wounding or herbivory by *M. sexta,* GLA1 hydrolizes chloroplastic membrane lipids (galactolipids, phosphatidylcholine and phosphatidylglycerol) into the respective lysolipid and trienoic fatty acids (linolenic or hexadecatrienoic acid). These fatty acids then serve as substrates for a series of other enzymes leading to the formation of JA. Activation of the JA signaling pathway then ultimately leads to changes in the expression of genes responsive to the applied stimuli (wounding or *M. sexta* herbivory) and the according (stimulus-dependent) changes in levels of JA-inducible secondary metabolites.

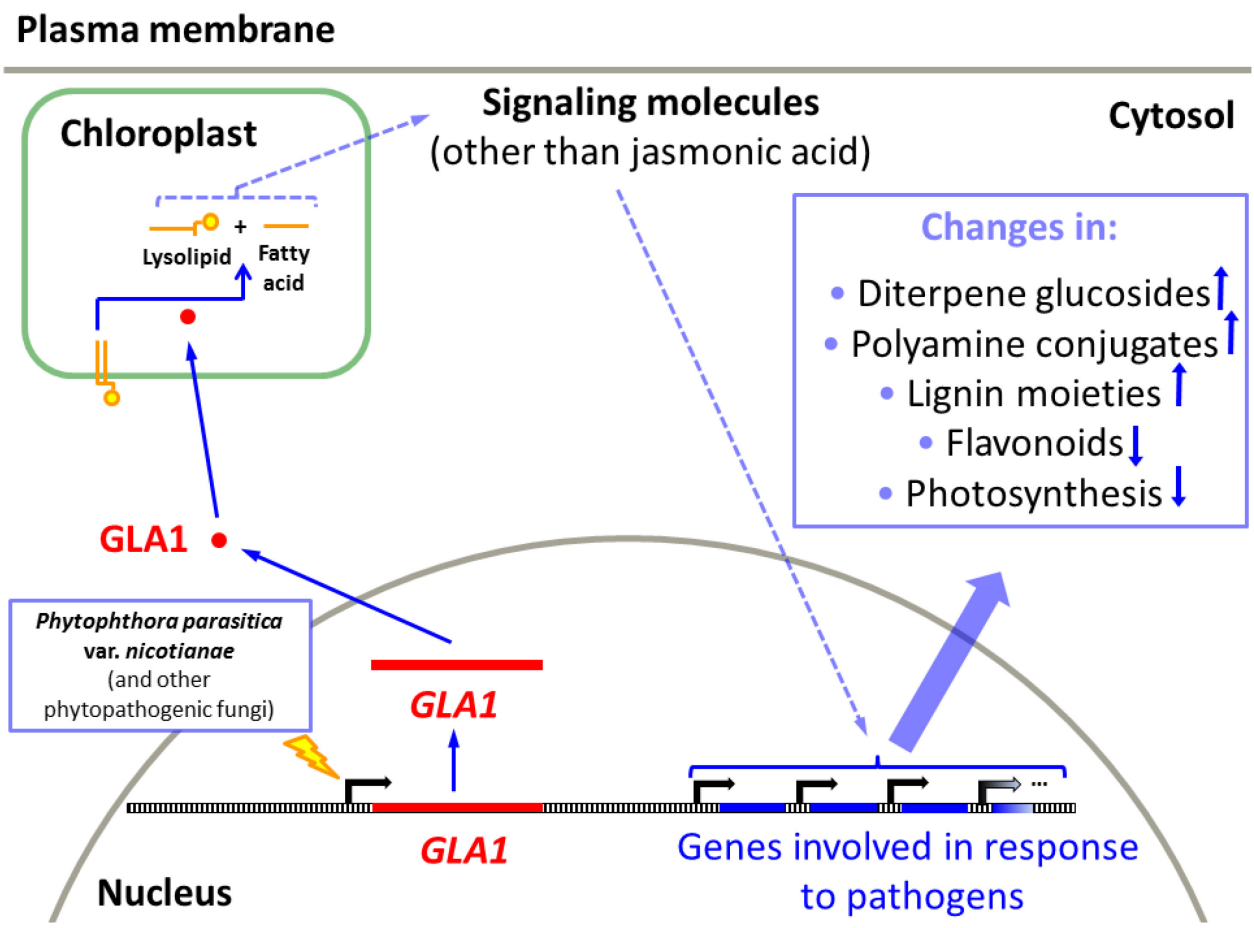

Figure 3. Function of GLA1 during infection with the phytopathogenic oomycete Ppn in *N. attenuata*.

GLA1 gene expression in *N. attenuata* leaves is induced by Ppn infection. Considering the lipase activity of GLA1, this enzyme is involved in the production of several membrane lipid-derived potential signaling molecules (lysolipids and oxylipins). Those potential signaling compounds could then affect the expression of numerous genes involved in the plant´s pathogen response which is also reflected in the levels of several secondary metabolites.

HSPRO negatively regulates *P. indica*-mediated growth promotion via SnRK1 signaling

JA not only plays an essential role in plant signaling processes related to wounding, herbivory by chewing herbivores and infection by necrotrophic phytopathogens (Glazebrook, 2005; Halim *et al*., 2006; Ali & Agrawal, 2012). It is also of immense importance for plant interactions with mutualists. One example mentioned already in the introduction is the interaction of *N. attenuata* with the root endophytic fungus *P. indica*: JA signaling pathway components are required for broad spectrum suppression of plant innate immunity necessary for successful root colonization by *P. indica* and the establishment of induced systemic resistance to pathogens, one major benefit for *P. indica*-colonized plants mediated by the fungus besides enhanced abiotic stress tolerance and plant growth promotion (Stein *et al*., 2008; Molitor & Kogel, 2009; Jacobs *et al*., 2011). In addition to JA signaling pathway components, antimicrobial divinyl ethers like colneleic acid inducible by *P. indica* in roots may also contribute to plant resistance against pathogens such as that observed for *P. indica*-colonized barley against *Fusarium graminearum* (Deshmukh & Kogel, 2007; manuscript 3). An experiment in which *P. indica*-colonized and non-colonized wild-type *N. attenuata* plants and transgenic *N. attenuata* genotypes reduced in the expression of divinyl ether biosynthetic enzymes are challenged by fungal pathogens like *Fusarium brachygibbosum* would be suitable to test this hypothesis. For *N. attenuata* it is well documented that *P. indica* and another fungus species belonging to the same family (Sebacinaceae), *Sebacina vermifera*, are both able to enhance plant growth probably independent from changes in the plant´s nutritional status but rather by impairing *N. attenuata* in its ethylene production (Barazani *et al*., 2005; Barazani *et al*., 2007). This reduced ability to biosynthesize ET results in a decreased ET burst that usually co-occurs with the JA burst elicited by chewing herbivores like *M. sexta* and, as a consequence thereof, in a impaired herbivore resistance (Barazani *et al*., 2005; Barazani *et al*., 2007; Ali & Agrawal, 2012). In other words, *P. indica*-mediated growth promotion of *N. attenuata* is caused on the expense of defensive capability (Barazani *et al*., 2005). This thesis could show that *P. indica*-mediated growth promotion of *N. attenuata* seedlings is negatively regulated – via SnRK1 signaling – by HSPRO, the *N. attenuata* ortholog of *B. procumbens* $Hs1^{pro-1}$ (manuscript 3 and 4): Stable silencing of *HSPRO* expression in *N. attenuata* even enhances *P. indica*-mediated increase in both, shoot and root fresh biomass, by approximately 30% compared to non-transformed wildtype plants (manuscript 3). A grafting experiment with *HSPRO*-silenced and wild-type *N. attenuata*

seedlings revealed further that silencing of *HSPRO* expression in roots – the interaction site with *P. indica* and plant organ in which *HSPRO* expression is induced by *P. indica* colonization – is fully sufficient to obtain the observed differential increase in growth promotion mediated by *HSPRO*-silencing throughout the entire seedling (manuscript 3). The mechanism behind the function of HSPRO as negative regulator of *P. indica*-mediated growth promotion was shown to be not related to the efficiency of *N. attenuata* to utilize carbon dioxide (or other growth-promoting volatiles released by the fungus), nor the pattern of *P. indica* root colonization, the relative *P. indica* abundance, root morphology and the extent of *P. indica*-inducible cell death reported to occur in root cortex cells of barley during *P. indica* colonization (manuscript 3; Deshmukh *et al*., 2006; Zuccaro *et al*., 2011). A microarray analysis using *P. indica*-colonized and non-colonized wild-type and *HSPRO*-silenced *N. attenuata* seedling roots revealed HSPRO-dependent changes in the expression of 417 genes during the *N. attenuata*-*P. indica* interaction (manuscript 3). Among these genes, some are involved in phytohormone (*e.g.* JA, ET, auxin and cytokinin) signaling which could possibly contribute to the regulation of *P. indica*-mediated growth promotion by HSPRO (manuscript 3). However, at least ethylene and JA levels were demonstrated not to be influenced by HSPRO during *P. indica* colonization (manuscript 3). The majority of the 417 genes (61%) turned out to be involved in metabolic processes (manuscript 3). Taken together with data from a metabolic profiling analysis of *P. indica*-colonized wild-type and *HSPRO*-silenced *N. attenuata* seedling roots showing a lack of major differences between both genotypes, this data suggests accelerated metabolic flux rates in *HSPRO*-silenced seedlings compared to WT (manuscript 3). Thus, the mechanism by which HSPRO restricts *P. indica*-mediated growth promotion of *N. attenuata* seedlings involves probably changes in metabolic fluxes (manuscript 3). To similar extent as HSPRO, plant SnRK1 signaling is involved in the negative regulation of *P. indica*-mediated seedling growth promotion in *N. attenuata* (manuscript 4). As already briefly mentioned in the introduction, SnRK1 enzymes are heteromeric protein kinase complexes and central regulators of energy metabolism, development, growth and stress tolerance able to interact via their regulatory subunit with proteins homologous to *B. procumbens* $Hs1^{pro-1}$ (Gissot *et al*., 2006; Cho *et al*., 2012). A plant growth promotion experiment with *P. indica* and crosses of transgenic *N. attenuata* genotypes stably silenced in the expression of *HSPRO*, *GAL83* (encoding for *N. attenuata* regulatory SnRK1 β-subunit) or both and *N. attenuata* wildtype could demonstrate that both proteins are indeed – from a genetic point of

view – likely to act in the same pathway (manuscript 4). Thus, the negative regulation of *P. indica*-medited growth promotion of *N. attenuata* seedlings probably occurs via changes in SnRK1 activity by protein-protein interaction with HSPRO, resulting in major metabolic flux changes and the restriction of seedling growth enhanced by *P. indica* colonization (manuscript 4; Halford *et al*., 2003; Gissot *et al*., 2006; Cho *et al*., 2012). The additional plant resources not used for enhanced growth could then be available for the plant to invest into tolerance or induced resistance mechanisms also mediated by *P. indica* to optimize the benefits resulting for the plant from this interaction on multiple levels, thereby perhaps even partially compensating for the defensive disadvantages regarding herbivore resistance caused by the fungus (Stein *et al*., 2008). In addition to metabolic flux changes, SnRK1 signaling could influence the extent of seedling growth promotion in the *N. attenuata*-*P. indica* interaction – without affecting the root colonization pattern – by controlling the availability of root carbon for the fungus (*i.e*. changes in carbon allocation), since it is known from a study on *P. indica*-colonized barley roots that *P. indica* produces proteins involved in carbon uptake and metabolism which appear relevant for a switch from a biotrophic to a necrotrophic lifestyle of *P. indica* and therefore potentially affect the extent of the beneficial outcome for *N. attenuata* in this plant-fungus mutualism (manuscript 4; Schwachtje *et al*., 2006; Zuccaro *et al*., 2011).

HSPRO might regulate the resistance *vs.* tolerance trade-off in *N. attenuata* in response to *M. sexta* herbivory and infection by *P. syringae* pv. *tomato* DC3000

The involvement of HSPRO in SnRK1 signaling provides also a plausible explanation for a potential role in *N. attenuata´*s response to *M. sexta* herbivory or *P. syringae* pv. *tomato* DC3000 infection, *i.e.* a role in tolerance to herbivores and pathogens (manuscript 3; Schwachtje *et al*., 2006; Schwachtje & Baldwin, 2008).

In the mutualistic interaction, both proteins are supposed to act together non-antagonistically to restrict *P. indica* mediated growth promotion (manuscript 4). It is known that *HSPRO* expression is induced by *P. indica* in *N. attenuata* seedling roots, and that *GAL83* expression as well as the expression of the gene encoding for the catalytic α-subunit SNF1 are constitutively relatively high in roots of flowering *N. attenuata* plants compared to other plant tissues (manuscript 3;Schwachtje *et al*., 2006). The assumption that *HSPRO*, *GAL83* and *SNF1*

are all highly expressed in *N. attenuata* roots during the interaction with *P. indica* further supports the proposed model by which HSPRO modulates SnRK1 function (manuscript 4). However, whether or not *GAL83* and *SNF1* expression change in *N. attenuata* roots during *P. indica* colonization is not known thus far. Quantification of transcript levels of *GAL83* and *SNF1* by qPCR in *P. indica*-colonized and non-colonized *N. attenuata* seedling roots could probably answer this question.

HSPRO expression is also induced in *N. attenuata* leaves by simulated *M . sexta* herbivory and *P. syringae* pv. *tomato* DC3000 infection, *GAL83* expression however is – at least after simulated *M. sexta* herbivory – down-regulated in *N. attenuata* leaves (Schwachtje *et al*., 2006; manuscript 3). Supposed both proteins interact non-antagonistically also in *N. attenuata* leaves, it might appear at first glance not reasonable that their expression is regulated differently. The reduced *GAL83* expression (resulting probably also in lower SnRK1 activity) observed in leaves after simulated *M. sexta* herbivory leads to an increase in carbon allocation to roots as tolerance response to herbivory (Schwachtje *et al*., 2006). The simultaneous increase in *HSPRO* expression could have the purpose to retain high activity of residual SnRK1 enzyme to attenuate the tolerance response to *M. sexta*. Thus, HSPRO could play an important role in a tolerance-resistance trade-off (Kessler & Baldwin, 2002; Heil, 2010; Stowe *et al*., 2000). Indeed, *M. sexta* is a well-adapted specialist herbivore and could therefore cause much bigger damage on *N. attenuata* compared to a less adapted insect herbivore species that might suffer already stronger from *e.g.* basal defense metabolite contents in *N. attenuata*. Therefore less adapted herbivores are likely to perform relatively worse on *N. attenuata* or maybe even migrate to other less defended plant species in the neighborhood, whereas the specialist *M. sexta* is restricted to host plants from the Solanaceae plant family, thus having only a limited choice to evade to neighboring plants (Schittko *et al*., 2000; del Campo *et al*., 2001; Wink & Theile, 2002; Paschold *et al*., 2007). In such a scenario the expected defoliation damage would be higher in case of herbivory by the well-adapted specialist compared to that of a less adapted generalist herbivore and compensation for herbivore-caused tissue losses (herbivore tolerance) would be more costly, making resource investment into resistance rather than tolerance mechanisms relatively more attractive to the plant. This is consistent with *HSPRO* expression data from *N. attenuata* leaves elicited with oral secretions (OS) from the specialist *M. sexta*, the generalist *S. exigua*, and the FAC elicitor 18:3-Glu found in the OS of both lepidopteran species (Diezel *et al*., 2009), or just

wounding without any additional leaf treatment (manuscript 3). Though being a rather unspecific stimulus that could result from herbivory as well as from mechanical damage, wounding alone already stimulates *HSPRO* expression (manuscript 3). FAC treatment and *S. exigua* OS induce *HSPRO* expression both to a similar, higher extent than that observed for wounding alone, which can be interpreted as the plant´s response to the definite presence of herbivores and a bigger investment in resistance compared to tolerance mechanisms in anticipation of further damage in near future (manuscript 3; Diezel *et al*., 2009). Treatment with *M. sexta* OS even amplifies the induction of *HSPRO* expression described for *S. exigua* OS and FAC treatment, supporting the hypothesis that the induction of resistance compared to tolerance mechanisms might be even more pronounced in case the plant perceives the presence of a well-adapted specialist herbivore like *M. sexta* on *N. attenuata* (manuscript 3). According to this hypothesis, the transient increase in *HSPRO* transcripts in treated *N. attenuata* leaves also appears very plausible: Systemic induction of herbivore resistance traits to protect distal tissues are induced quite rapidly after elicitation, and once the aerial plant parts have been eaten up almost completely by the herbivore, there are not too many carbon resources in form of photoassimilates left to bunker into the root (Halitschke *et al*., 2001; Schwachtje *et al*., 2006). To support the above mentioned model an experiment could be performed (using wild-type, *HSPRO*-silenced and *GAL83*-silenced *N. attenuata* plants) in which transcript levels of certain SnRK1-regulated genes (indicative for nuclear SnRK1 activity) and activities of SnRK1-regulated enzymes (indicative for cytosolic SnRK1 function) could be quantified after plant treatment with wounding or wounding plus additional *S. exigua* or *M. sexta* OS application. Such an experiment would not only be useful to figure out whether or not gradual differences in *HSPRO* expression caused by these treatments really translate into gradual differences in SnRK1 activity, but it would also allow to distinguish whether the cytosolic or nuclear function of SnRK1 is modulated by HSPRO (or maybe even both functions). This is particular interesting because Gissot *et al*. (2006) propose for the *Arabidopsis* homologs of HSPRO a cytosolic localization since an interaction of these proteins with SnRK1 could be demonstrated exclusively for this cellular compartment. Data from a transient transfection assay using *Arabidopsis* protoplasts expressing the *N. attenuata HSPRO* gene revealed a cytosolic localization also for HSPRO, however leaving the possibility open that HSPRO might be additionally localized to the nucleus (manuscript 3). Thus,

the proposed experiment could be used to further specify the modulating function of HSPRO in the fine-tuning process of SnRK1 activity on the subcellular compartment level.

Similar to herbivore damage, infection by pathogenic microbes like *P. syringae* pv. *tomato* DC3000 (Pst DC3000) could lead to a HSPRO/SnRK1-mediated redirection of *N. attenuata´*s metabolism towards defense responses at the infection site (Biemelt & Sonnewald, 2006). This hypothesis would then also explain the up-regulation of *HSPRO* expression in *N. attenuata* by Pst DC3000 and the reduced basal resistance against Pst DC3000 observed in *Arabidopsis* knockout mutants unable to express one of their *HSPRO* homologs (Murray *et al*., 2007; manuscript 3). However, performance assays with *M. sexta* larvae and *P. syringae* pv. *tomato* DC3000 on *N. attenuata* wildtype and *HSPRO*-silenced plants did not result in any HSPRO-specific difference in plant resistance (manuscript 3). Maybe these results are due to glasshouse artifacts because under the controlled conditions used in these experiments intraspecific competition and nutrient availability – in contrast to the situation in nature – did not play a major role. An experiment in which *HSPRO*-silenced and wild-type *N. attenuata* plants grown in competition and low-fertilizer conditions are challenged by *M. sexta* larvae and Pst DC3000 would probably allow to drive more solid conclusions on HSPRO´s impact on the Darwinian fitness of insect herbivores and pathogenic bacteria.

HSPRO might be involved in the control of metabolic sink/source strength and/or post-pollination senescence in flowers

The involvement of HSPRO in SnRK1 signaling could also explain the constitutively high *HSPRO, GAL83* and *SNF1* expression in *N. attenuata* flower organs compared to other plant tissues (manuscript 3; Schwachtje *et al*., 2006)). From literature it is known that SnRK1 modulates the metabolic sink/source relationship, and flowers as reproductive tissues with high Darwinian fitness value are important metabolic sink organs that require constitutively high protection (McKibbin *et al*., 2006; Jain *et al*., 2008; Meldau *et al*., 2012). It is also known that SnRK1 influences senescence processes (Cho *et al*., 2012). Therefore HSPRO could be involved in the induction of senescence of *N. attenuata* flower component (particularly the corolla) after pollination (von Dahl et al., 2007). However, no role of HSPRO in flower-associated resistance traits could be demonstrated thus far for *N. attenuata* and changes in corolla senescence were

also not observed (manuscript 3). Therefore it can be only speculated regarding HSPRO´s function in flowers. A $^{11}CO_2$–pulse feeding experiment might be used to investigate a potential role of HSPRO in the regulation of metabolic sink/source strength regulation in flowers. Another experiment using excised flowers from *N. attenuata* wildtype, *GAL83*- and *HSPRO*-silenced genotypes with and without exogenous sugar supply (causing a delay in ethylene signaling-mediated senescence processes) could contribute to elucidate a potential role of HSPRO in flower senescence via SnRK1-controlled sugar signaling (van Doorn, 2004; Rolland et al., 2006; Tripathi and Tuteja, 2007; von Dahl et al., 2007 ; Yang et al., 2008).

Figure 4 summarizes HSPRO´s function in different plant tissues with respect to its role in the interactions with *P. indica*, *M. sexta* and *P. syringae* pv. *tomato* DC3000. In figure 5, HSPRO function is illustrated on cellular level.

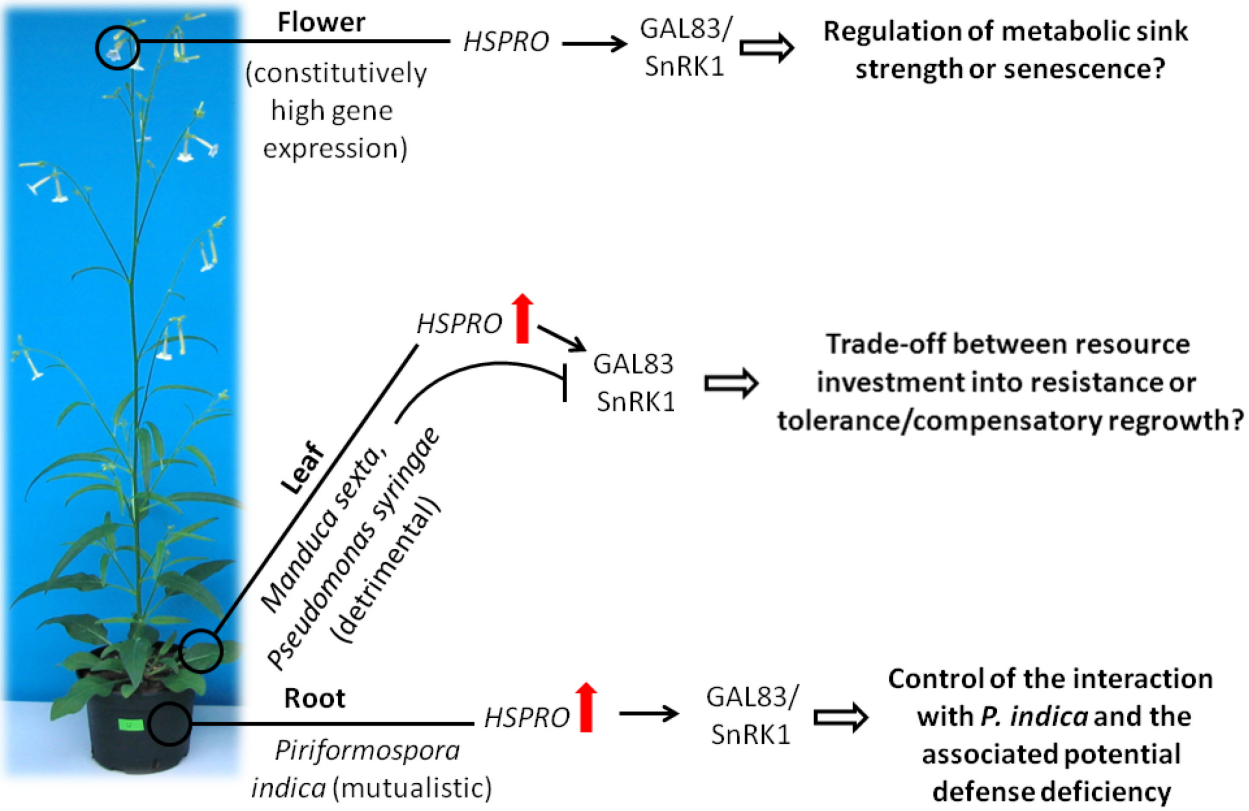

Figure 4. Organ-specific changes in *HSPRO* transcription and HSPRO function in *N. attenuata*.

Colonization of *N. attenuata* seedling roots by *P. indica* induces *HSPRO* expression. HSPRO then negatively regulates *P. indica*-mediated growth promotion via SnRK1 signaling, maybe to control the beneficial character of *N. attenuata*´s mutualism with *P. indica*. *N. attenuata* leaf elicitation by simulated *M. sexta* herbivory and *P. syringae* pv. *tomato* DC3000 infection also leads to the induction of *HSPRO* expression. In contrast, simulated *M. sexta* herbivory reduces *GAL83* transcript abundance which encodes for a regulatory SnRK1 β-subunit. HSPRO could function in the stabilization of residual SnRK1 activity in a resource investment trade-off between resistance and tolerance mechanisms. *HSPRO* expression is constitutively high in flower organs where it could be involved via SnRK1 signaling in post-pollination senescence processes and/or the modulation of metabolic source/sink strength.

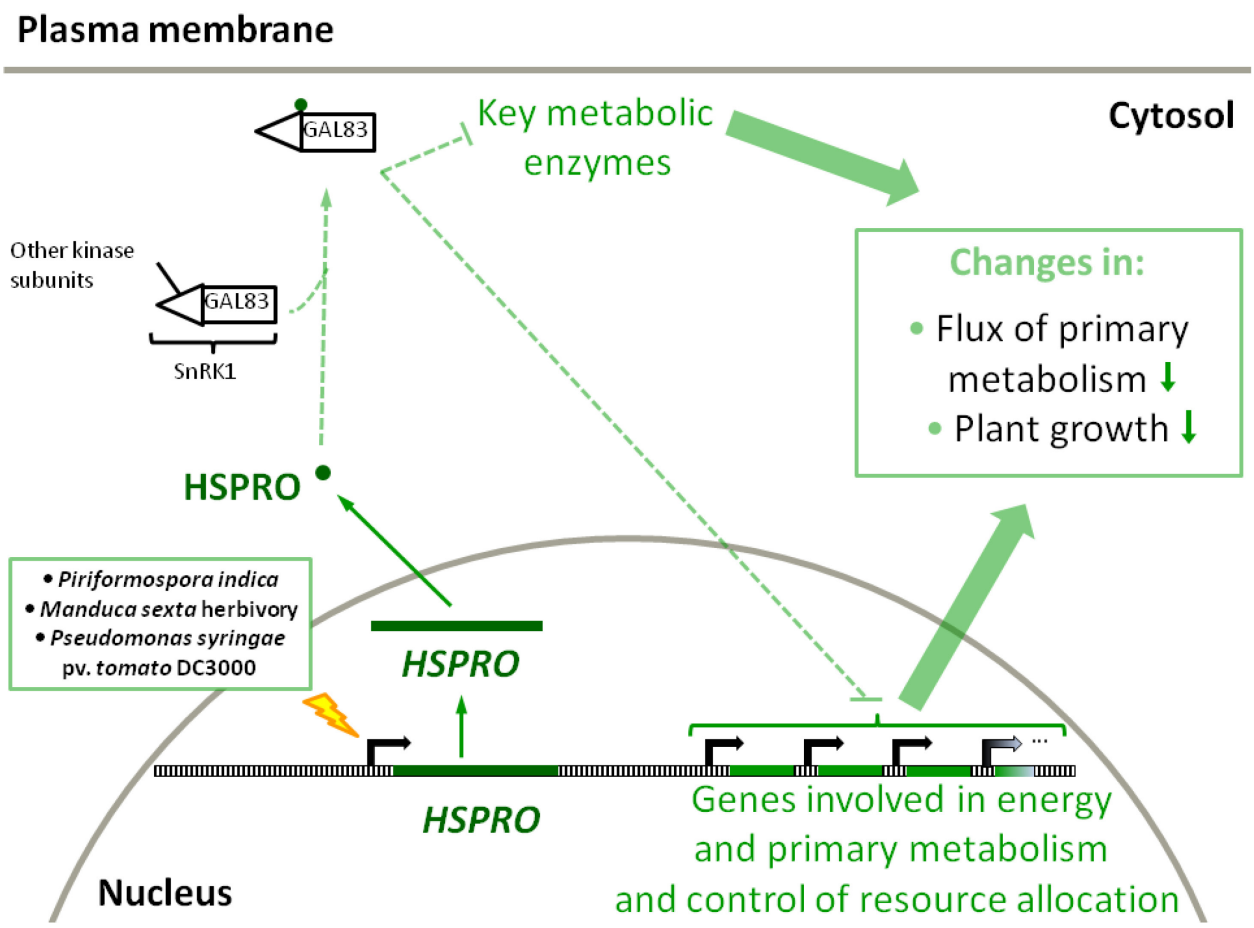

Figure 5. Function of HSPRO during *N. attenuata´*s interaction with *P. indica*, *M. sexta* and *P. syringae* pv. *tomato* DC3000.

Upon elicitation by *P. indica*, *M. sexta* or *P. syringae* pv. *tomato* DC3000 *HSPRO* transcription is induced. After being translated into protein, HSPRO interacts with a heteromeric SnRK1 kinase containing GAL83 as regulatory β-subunit. SnRK1 represses the expression of genes involved in energy and primary metabolism and the control of resource allocation and reduces the activity of key metabolic enzymes, leading to a reduced flux in primary metabolism, diminished plant growth and reduced resource investment into *M. sexta*/ *P. syringae* pv. *tomato* DC3000 tolerance (relative to resistance).

Chapter 8: Summary

The wild tobacco species *Nicotiana attenuata* germinates synchronized from long-lived seed banks in a post-fire environment and forms monoculture-like populations which are attacked by unpredictable herbivore and pathogen communities. In order to tailor its defense responses most efficiently it is particularly important for this plant species to distinguish its individual attackers and to possess a sophisticated signaling system capable of indicating the presence of their enemies accordingly.

One of these signaling components is the phytohormone jasmonic acid (JA) which is produced by *N. attenuata* in response to *e.g.* wounding or *Manduca sexta* herbivory in form of a rapid and a transient burst. This burst is initialized by the chloroplastic glycerolipase NaGLA1 which hydrolizes trienoic fatty acids (linolenic and hexadecatrienoic acid) from membrane lipids resulting in lysolipids as byproducts. The free fatty acids provided by NaGLA1 are then rapidly used as substrates by a lipoxygenase (NaLOX3) to form 13-hydroperoxy-fatty acids which are further oxidized by a series of other enzymes to finally form JA. In general, these and other oxidized fatty acid products are termed as "oxylipins", a structurally diverse group of molecules comprising not only compounds being involved in within-plant-signaling processes, but also molecules possessing a function in direct or indirect plant defense. Transgenic *N. attenuata* genotypes stably silenced in *NaGLA1* gene expression were generated by inverted-repeat technique (ir-*gla1*) to address a series of questions regarding the role of NaGLA1 during wounding, *M. sexta* herbivory and the interaction with phytopathogenic fungi such as *Phytophthora parasitica* var. *nicotianae* (Ppn). By comparing *N. attenuata* wildtype and ir-*gla1* genotypes – elicited and non-elicited by according stimuli (wounding, simulated *M. sexta* herbivory and Ppn infection) – it could be shown in this thesis work that NaGLA1 does not supply other known *N. attenuata* lipoxygenases with free fatty acid substrates and is therefore quite specific for the JA-biosynthesis pathway. Further it could be shown that NaGLA1 is the major lipase in *N. attenuata* involved in JA biosynthesis after wounding and simulated *M. sexta* herbivory, however not during Ppn infection. During Ppn infection NaGLA1 participates in the generation of potential signaling molecules (different from JA) having huge impact on *N. attenuata´*s expression of pathogen defense-associated genes which is reflected also in the plant´s metabolome.

Chapter 8: Summary

NaHSPRO, a putative nematode resistance protein, was found to be rapidly and transiently upregulated in its transcriptional expression upon simulated *M. sexta* herbivory in *N. attenuata*. Therefore it was thought to be a potential regulator of early *N. attenuata* responses to *M. sexta* herbivory. To test this hypothesis, transgenic *N. attenuata* genotypes stably silenced in *NaHSPRO* expression by inverted-repeat technique (ir-*hspro*) were generated and compared to *N. attenuata* wildtype regarding its response to simulated and real *M. sexta* herbivory. Because literature reported also a role of a NaHSPRO-homologous protein from *Arabidopsis* in resistance against *Pseudomonas syringae* pv. *tomato* DC3000, this phytopathogenic bacterium was used in experiments with *N. attenuata* wildtype and ir-*hspro* plants, too. Besides the induction of *NaHSPRO* gene expression in response to *M. sexta* and *P. syringae* pv. *tomato* DC3000 elicitation, no involvement of NaHSPRO in *N. attenuata´*s resistance to those organisms could be demonstrated. However, it is well possible that NaHSPRO plays a role in *N. attenuata* tolerance rather than resistance or in the trade-off process between these defense mechanisms. Plant tolerance is mediated by SUCROSE-NON-FERMENTING 1-RELATED PROTEIN KINASE 1 (SnRK1), a central regulator of primary and energy metabolism, growth and development. It is known from literature that NaHSPRO homologs from *Arabidopsis* are able to interact with a regulatory subunit of plant SnRK1. This thesis work could show that NaHSPRO negatively regulates growth promotion of *N. attenuata* seedlings mediated by the mutualistic fungus *Piriformospora indica* via SnRK1 signaling and this finding supports other hyptheses based also on SnRK1-involving mechanisms and dealing with a potential NaHSPRO function in plant defense against *M. sexta* and *P. syringae* pv. *tomato* DC3000.

Chapter 9: Zusammenfassung

Der wilde Tabakart *Nicotiana attenuata* formt durch das synchrone Auskeimen aus langlebigen Samenlagern in verbranntem Umfeld Monokultur-artige Populationen, die von unvorhersehbaren Herbivor- und Pathogengemeinschaften heimgesucht werden. Um sich möglichst zielgerichtet und effizient zu verteidigen ist es für diese Pflanzenart daher besonders wichtig, die einzelnen Angreifer zu unterscheiden und ein ausgeklügeltes Signaltransduktions-System zu besitzen, welches es ihnen ermöglicht, die Anwesenheit von Feinden entsprechend zu erkennen.

Eine dieser Signaltransduktions-Komponenten ist das Phytohormon Jasmonsäure (JA), welches von *N. attenuata* rasch und in explosionsartig ansteigender Menge (jedoch auf ein bestimmtes Zeitintervall beschränkt) gebildet wird, beispielsweise als Antwort auf Verwundung oder Herbivorie durch *Manduca sexta*. Dieser rapide Anstieg wird durch die in Chloroplasten lokalisierte Glycerolipase NaGLA1 eingeleitet, welche Membranlipide hydrolysiert und dabei dreifach ungesättigte Fettsäuren (Linolen- und Hexadekatriensäure) und als Nebenprodukt Lysolipide freisetzt. Die durch NaGLA1 erzeugten freien Fettsäuren werden dann rasch von einer Lipoxygenase (NaLOX3) als Substrat für die Produktion von 13-Hydroperoxiden der jeweiligen Fettsäuren genutzt, die dann von einer Reihe weiterer Enzyme letztlich zu JA weiteroxidiert werden. Allgemein werden diese und andere Fettsäure-Oxidationsprodukte als „Oxylipine“ bezeichnet, eine strukturell sehr diverse Molekülgruppe, die nicht nur Verbindungen mit einer Rolle in Signaltransduktionsprozessen innerhalb der Pflanze umfasst, sondern auch Moleküle mit einer Funktion in der direkten und indirekten pflanzlichen Abwehr. Um eine Reihe von Fragen beantworten zu können, welche sich auf die Rolle von NaGLA1 während Verwundung, *M. sexta*-Herbivorie und der Interaktion mit phytopathogenen Pilzen wie z.B. *Phytophthora parasitica* var. *nicotianae* (Ppn) beziehen, wurden stabil transformierte *N. attenuata*-Genotypen erzeugt, die mittels „inverted-repeat“-Technik eine reduzierte Expression des *NaGLA1*-Gens (ir-*gla1*) aufweisen. Durch Vergleich von *N. attenuata* Wildtyp mit ir-*gla1* Genotypen – durch entsprechende Stimuli (Verwundung, simulierte *M. sexta*-Herbivorie und Ppn-Infektion) elizitiert bzw. nicht elizitiert – konnte in dieser Doktorarbeit gezeigt werden, dass NaGLA1 keine weiteren für *N. attenuata* bekannten Lipoxygenasen mit Fettsäure-Substraten

versorgt und daher recht spezifisch für den JA-Biosyntheseweg ist. Des weiteren konnte gezeigt werden, dass NaGLA1 bei Verwundung und *M. sexta*-Herbivorie die Haupt-Lipase in der JA-Biosynthese ist, allerdings nicht während Ppn-Infektionen. Während einer Ppn-Infektion ist NaGLA1 an der Produktion potenzieller Signalmoleküle (nicht JA) beteiligt, die große Auswirkung auf die Expression Abwehr-relevanter Gene in *N. attenuata* haben, ein Sachverhalt, der sich auch im Metabolom dieser Pflanze widerspiegelt.

NaHSPRO, ein vermeintliches Nematodenresistenz-Protein, erwies sich in *N. attenuata* auf Transkriptebene als rasch und zeitlich beschränkt hochreguliert nach simulierter *M. sexta*-Herbivorie. Daher wurde angenommen, es sei ein potenzieller Regulator früher Reaktionen von *N. attenuata* auf *M. sexta*-Herbivorie. Um diese Hypothese zu testen, wurden stabil transformierte *N. attenuata*-Genotypen hergestellt, die mittels „inverted-repeat"-Technik in der Expression von *NaHSPRO* reduziert sind (ir-*hspro*), und bezüglich ihrer Reaktion auf simulierte *M. sexta*-Herbivorie mit *N. attenuata* Wildtyp verglichen. Weil laut Literatur ein zu NaHSPRO homologes *Arabidopsis*-Protein für die Resistenz gegen *Pseudomonas syringae* pv. *tomato* DC3000 eine Rolle spielt, wurde dieses bakterielle Phytopathogen ebenfalls für Experimente mit *N. attenuata* Wildtyp und ir-*hspro*-Pflanzen verwendet. Trotz der Induzierbarkeit der *NaHSPRO*-Genexpression durch Elizitierung mit *M. sexta* und *Pseudomonas syringae* pv. *tomato* DC3000 konnte keine Beteiligung von NaHSPRO an einer Resistenz von *N. attenuata* gegen diese Organismen nachgewiesen werden. Allerdings ist es sehr gut möglich, dass NaHSPRO in *N. attenuata* eher eine Rolle für die Toleranz als für die Resistenz oder in einem Abwäge-Prozess zwischen beiden Abwehrmechanismen spielt. Toleranz wird in Pflanzen vermittelt durch „SUCROSE-NON-FERMENTING 1-RELATED PROTEIN KINASE 1" (SnRK1), einem zentralen Regulator des Primär- und Energiestoffwechsels, des Wachstums und der Entwicklung. Laut Literatur können NaHSPRO-Homologe von *Arabidopsis* mit einer regulatorischen Untereinheit von pflanzlichem SnRK1 interagieren. Diese Doktorarbeit konnte zeigen, dass NaHSPRO durch SnRK1-Signaltransduktion als negativer Regulator der durch den mutualistischen Pilz *Piriformospora indica* hervorgerufenen Wachstumsförderung fungiert und dieser Sachverhalt unterstützt weitere Hypothesen, die ebenfalls auf SnRK1-Signaltransduktion basieren und sich mit einer potenziellen Funktion von NaHSPRO in der pflanzlichen Abwehr gegen *M. sexta* und *P. syringae* pv. *tomato* DC3000 befassen.

Chapter 10: References

Agrawal AA (1999) Induced plant defense: Evolution of induction and adaptive phenotypic plasticity. *In* AA Agrawal, S Tuzun, E Bent, eds, Inducible plant defenses against pathogens and herbivores: Biochemistry, ecology, and agriculture. American Phytopathological Society Press, St. Paul, MN (USA), pp 251-268

Able AJ, Guest DI, Sutherland MW (2000) Hydrogen peroxide yields during the incompatible interaction of tobacco suspension cells inoculated with *Phytophthora nicotianae*. Plant Physiology **124:** 899-910

Achatz B, Kogel KH, Franken P, Waller F (2010) *Piriformospora indica* mycorrhization increases grain yield by accelerating early development of barley plants. Plant Signaling & Behavior **5:** 1685-1687

Ali JG, Agrawal AA (2012) Specialist versus generalist insect herbivores and plant defense. Trends in Plant Science **17:** 293-302

Allmann S, Baldwin IT (2010) Insects betray themselves in nature to predators by rapid isomerization of green leaf volatiles. Science **329:** 1075-1078

Allmann S, Halitschke R, Schuurink RC, Baldwin IT (2010) Oxylipin channelling in *Nicotiana attenuata*: lipoxygenase 2 supplies substrates for green leaf volatile production. Plant, Cell and Environment **33:** 2028-2040

Amelot N, de Borne FD, Clemente HS, Mazars C, Grima-Pettenati J, Briere C (2012) Transcriptome analysis of tobacco BY-2 cells elicited by cryptogein reveals new potential actors of calcium-dependent and calcium-independent plant defense pathways. Cell Calcium **51:** 117-130

Antonovics J, Boots M, Ebert D, Koskella B, Poss M, Sadd BM (2013) The origin of specificity by means of natural selection: Evolved and nonhost resistance in host-pathogen interactions. Evolution **67:** 1-9

Atkinson NJ, Urwin PE (2012) The interaction of plant biotic and abiotic stresses: from genes to the field. Journal of Experimental Botany **63:** 3523-3543

Avila J, Gregory OG, Su DY, Deeter TA, Chen SX, Silva-Sanchez C, Xu SL, Martin GB, Devarenne TP (2012) The β-subunit of the SnRK1 complex is phosphorylated by the plant cell death suppressor Adi3. Plant Physiology **159:** 1277-1290

Avrova AO, Taleb N, Rokka VM, Heilbronn J, Campbell E, Hein I, Gilroy EM, Cardle L, Bradshaw JE, Stewart HE, Fakim YJ, Loake G, Birch PRJ (2004) Potato oxysterol binding protein and cathepsin B are rapidly up-regulated in independent defence pathways that distinguish *R* gene-mediated and field resistances to *Phytophthora infestans*. Molecular Plant Pathology **5:** 45-56

Baena-Gonzalez E, Rolland F, Thevelein JM, Sheen J (2007) A central integrator of transcription networks in plant stress and energy signalling. Nature **448:** 938-U910

Baena-Gonzalez E, Sheen J (2008) Convergent energy and stress signaling. Trends in Plant Science **13:** 474-482

Baldwin IT (1998) Jasmonate-induced responses are costly but benefit plants under attack in native populations. Proceedings of the National Academy of Sciences of the United States of America **95:** 8113-8118

Baldwin IT (1999) Inducible nicotine production in native *Nicotiana* as an example of adaptive phenotypic plasticity. Journal of Chemical Ecology **25:** 3-30

Baldwin IT (2001) An ecologically motivated analysis of plant-herbivore interactions in native tobacco. Plant Physiology **127:** 1449-1458

Baldwin IT, Callahan P (1993) Autotoxicity and chemical defense - nicotine accumulation and carbon gain in solanaceous plants. Oecologia **94:** 534-541

Baldwin IT, Gorham D, Schmelz EA, Lewandowski CA, Lynds GY (1998) Allocation of nitrogen to an inducible defense and seed production in *Nicotiana attenuata*. Oecologia **115:** 541-552

Baldwin IT, Morse L (1994) Up in Smoke: II. Germination of *Nicotiana attenuata* in response to smoke-derived cues and nutrients in burned and unburned soils. Journal of Chemical Ecology **20:** 2373-2391

Baldwin IT, Ohnmeiss TE (1993) Alkaloidal responses to damage in *Nicotiana* native to North-America. Journal of Chemical Ecology **19:** 1143-1153

Baldwin IT, Preston CA (1999) The eco-physiological complexity of plant responses to insect herbivores. Planta **208:** 137-145

Baldwin IT, Staszakkozinski L, Davidson R (1994) Up in Smoke: I. Smoke-derived germination cues for postfire annual, *Nicotiana attenuata* Torr ex Watson. Journal of Chemical Ecology **20:** 2345-2371

Barazani O, Benderoth M, Groten K, Kuhlemeier C, Baldwin IT (2005) *Piriformospora indica* and *Sebacina vermifera* increase growth performance at the expense of herbivore resistance in *Nicotiana attenuata*. Oecologia **146:** 234-243

Barazani O, Von Dahl CC, Baldwin IT (2007) *Sebacina vermifera* promotes the growth and fitness of *Nicotiana attenuata* by inhibiting ethylene signaling. Plant Physiology **144:** 1223-1232

Bardgett RD, Wardle DA, Yeates GW (1998) Linking above-ground and below-ground interactions: How plant responses to foliar herbivory influence soil organisms. Soil Biology & Biochemistry **30:** 1867-1878

Bassard JE, Ullmann P, Bernier F, Werck-Reichhart D (2010) Phenolamides: bridging polyamines to the phenolic metabolism. Phytochemistry **71:** 1808-1824

Bentz JA, Barbosa P (1992) Effects of dietary nicotine and partial starvation of tobacco hornworm, *Manduca sexta*, on the survival and development of the parasitoid *Cotesia congregata*. Entomologia Experimentalis Et Applicata **65:** 241-245

Bi JL, Felton GW, Murphy JB, Howles PA, Dixon RA, Lamb CJ (1997) Do plant phenolics confer resistance to specialist and generalist insect herbivores? Journal of Agricultural and Food Chemistry **45:** 4500-4504

Biemelt S, Sonnewald U (2006) Plant-microbe interactions to probe regulation of plant carbon metabolism. Journal of Plant Physiology **163:** 307-318

Bohlmann J, Stauber EJ, Krock B, Oldham NJ, Gershenzon J, Baldwin IT (2002) Gene expression of 5-epi-aristolochene synthase and formation of capsidiol in roots of *Nicotiana attenuata* and *N. sylvestris*. Phytochemistry **60:** 109-116

Boller T, Felix G (2009) A renaissance of elicitors: perception of microbe-associated molecular patterns and danger signals by pattern-recognition receptors. Annual Review of Plant Biology **60:** 379-406

Bolton MD (2009) Primary metabolism and plant defense-fuel for the fire. Molecular Plant-Microbe Interactions **22:** 487-497

Bonaventure G, Baldwin IT (2010) New insights into the early biochemical activation of jasmonic acid biosynthesis in leaves. Plant Signaling & Behavior **5:** 287-289

Bonaventure G, Gfeller A, Proebsting WM, Hortensteiner S, Chetelat A, Martinoia E, Farmer EE (2007) A gain-of-function allele of TPC1 activates oxylipin biogenesis after leaf wounding in Arabidopsis. Plant Journal **49:** 889-898

Bonaventure G, Schuck S, Baldwin IT (2011) Revealing complexity and specificity in the activation of lipase-mediated oxylipin biosynthesis: A specific role of the *Nicotiana attenuata* GLA1 lipase in the activation of jasmonic acid biosynthesis in leaves and roots. Plant, Cell & Environment **34:** 1507-1520

Bossart JL, Gage SH (1990) Biology and seasonal occurrence of *Manduca quinquemaculata* and *Manduca sexta* (Lepidoptera, Sphingidae) in Southwestern Michigan. Environmental Entomology **19:** 1055-1059

Böttcher C, Weiler EW (2007) cyclo-Oxylipin-galactolipids in plants: Occurrence and dynamics. Planta **226:** 629-637

Bubner B, Gase K, Berger B, Link D, Baldwin IT (2006) Occurrence of tetraploidy in *Nicotiana attenuata* plants after *Agrobacterium*-mediated transformation is genotype specific but independent of polysomaty of explant tissue. Plant Cell Reports **25:** 668-675

Burdon JJ, Thrall PH (2009) Coevolution of plants and their pathogens in natural habitats. Science **324:** 755-756

Cai D, Kleine M, Kifle S, Harloff HJ, Sandal NN, Marcker KA, Klein-Lankhorst RM, Salentijn EMJ, Lange W, Stiekema WJ (1997) Positional cloning of a gene for nematode resistance in sugar beet. Science **275:** 832-834

Camehl I, Drzewiecki C, Vadassery J, Shahollari B, Sherameti I, Forzani C, Munnik T, Hirt H, Oelmuller R (2011) The OXI1 kinase pathway mediates *Piriformospora indica*-induced growth promotion in *Arabidopsis*. PLoS Pathogens **7:** e1002051

Camehl I, Sherameti I, Venus Y, Bethke G, Varma A, Lee J, Oelmuller R (2010) Ethylene signalling and ethylene-targeted transcription factors are required to balance beneficial and nonbeneficial traits in the symbiosis between the endophytic fungus *Piriformospora indica* and *Arabidopsis thaliana*. New Phytologist **185:** 1062-1073

Canonne J, Froidure-Nicolas S, Rivas S (2011) Phospholipases in action during plant defense signaling. Plant Signaling & Behavior **6:** 13-18

Cantrell CL, Case BP, Mena EE, Kniffin TM, Duke SO, Wedge DE (2008) Isolation and identification of antifungal fatty acids from the basidiomycete *Gomphus floccosus*. Journal of Agricultural and Food Chemistry **56:** 5062-5068

Carlson SR, Wolff MF, Shew HD, Wernsman EA (1997) Inheritance of resistance to race 0 of *Phytophthora parasitica* var. *nicotianae* from the flue-cured tobacco cultivar Coker 371-Gold. Plant Disease **81:** 1269-1274

Cheng BP, Yu XL, Ma ZC, Dong SM, Dou DL, Wang YC, Zheng XB (2012) *Phytophthora sojae* effector Avh331 suppresses the plant defence response by disturbing the MAPK signalling pathway. Physiological and Molecular Plant Pathology **77:** 1-9

Cho K, Kim Y, Wi SJ, Seo JB, Kwon J, Chung JH, Park KY, Nam MH (2012) Non-targeted metabolite profiling in compatible pathogen-inoculated tobacco (*Nicotiana tabacum* L. cv Wisconsin 38) using UPLC-Q-TOF mass spectrometry. Journal of Agricultural and Food Chemistry **60**: 11015-11028

Cho YH, Hong JW, Kim EC, Yoo SD (2012) Regulatory functions of SnRK1 in stress-responsive gene expression and in plant growth and development. Plant Physiology **158:** 1955-1964

Cohen Y, Gisi U, Mosinger E (1991) Systemic resistance of potato plants against *Phytophthora infestans* induced by unsaturated fatty acids. Physiological and Molecular Plant Pathology **38:** 255-263

Colas V, Conrod S, Venard P, Keller H, Ricci P, Panabieres F (2001) Elicitin genes expressed in vitro by certain tobacco isolates of *Phytophthora parasitica* are down regulated during compatible interactions. Molecular Plant-Microbe Interactions **14:** 326-335

Colas V, Lacourt I, Ricci P, Vanlerberghe-Masutti F, Venard P, Poupet A, Panabieres F (1998) Diversity of virulence in *Phytophthora parasitica* on tobacco, as reflected by nuclear RFLPs. Phytopathology **88:** 205-212

Cominelli E, Galbiati M, Vavasseur A, Conti L, Sala T, Vuylsteke M, Leonhardt N, Dellaporta SL, Tonelli C (2005) A guard-cell-specific MYB transcription factor regulates stomatal movements and plant drought tolerance. Current Biology **15:** 1196-1200

Creelman RA, Mullet JE (1997) Biosynthesis and action of jasmonates in plants. Annual Reviews in Plant Physiology and Plant Molecular Biology **48:** 355-381

Creelman RA, Tierney ML, Mullet JE (1992) Jasmonic acid/methyl jasmonate accumulate in wounded soybean hypocotyls and modulate wound gene expression. Journal of Chemical Ecology **89:** 4938-4941

Croft K, Juttner F, Slusarenko AJ (1993) Volatile products of the lipoxygenase pathway evolved from *Phaseolus vulgaris* (L.) leaves inoculated with *Pseudomonas syringae* pv *phaseolicola*. Plant Physiology **101:** 13-24

Dangl JL, Jones JDG (2001) Plant pathogens and integrated defence responses to infection. Nature **411:** 826-833

Day B, Graham T (2007) The plant host pathogen interface: Cell wall and membrane dynamics of pathogen-induced responses. Annals of the New York Academy of Sciences **1113:** 123-134

de Jonge R, Bolton MD, Thomma BPHJ (2011) How filamentous pathogens co-opt plants: The ins and outs of fungal effectors. Current Opinion in Plant Biology **14:** 400-406

del Campo ML, Miles CI, Schroeder FC, Mueller C, Booker R, Renwick JA (2001) Host recognition by the tobacco hornworm is mediated by a host plant compound. Nature **411:** 186-189

Dellagi A, Heilbronn J, Avrova AO, Montesano M, Palva ET, Stewart HE, Toth IK, Cooke DEL, Lyon GD, Birch PRJ (2000) A potato gene encoding a WRKY-like transcription factor is induced in interactions with Erwinia carotovora subsp atroseptica and Phytophthora infestans and is coregulated with class I endochitinase expression. Molecular Plant-Microbe Interactions **13:** 1092-1101

Deshmukh S, Hueckelhoven R, Schaefer P, Imani J, Sharma M, Weiss M, Waller F, Kogel KH (2006) The root endophytic fungus *Piriformospora indica* requires host cell death for proliferation during mutualistic symbiosis with barley. Proceedings of the National Academy of Sciences of the United States of America **103:** 18450-18457

Deshmukh SD, Kogel KH (2007) *Piriformospora indica* protects barley from root rot caused by *Fusarium graminearum*. Journal of Plant Diseases and Protection **114:** 263-268

Devoto A, Ellis C, Magusin A, Chang HS, Chilcott C, Zhu T, Turner JG (2005) Expression profiling reveals COI1 to be a key regulator of genes involved in wound- and methyl

jasmonate-induced secondary metabolism, defence, and hormone interactions. Plant Molecular Biology **58:** 497-513

Diaz-Tielas C, Grana E, Sotelo T, Reigosa MJ, Sanchez-Moreiras AM (2012) The natural compound trans-chalcone induces programmed cell death in *Arabidopsis thaliana* roots. Plant, Cell and Environment **35:** 1500-1517

Diezel C, Allmann S, Baldwin IT (2011) Mechanisms of optimal defense patterns in *Nicotiana attenuata*: Flowering attenuates herbivory-elicited ethylene and jasmonate signaling. Journal of Integrated Plant Biology **53:** 971-983

Diezel C, von Dahl C, Gaquerel E, Baldwin I (2009) Different lepidopteran elicitors account for cross-talk in herbivory-induced phytohormone signaling. Plant Physiology **150:** 1576-1586

Dominguez E, Cuartero J, Heredia A (2011) An overview on plant cuticle biomechanics. Plant Science **181:** 77-84

Dorne AJ, Joyard J, Block MA, Douce R (1985) Localization of phosphatidylcholine in outer envelope membrane of spinach chloroplasts. Journal of Cell Biology **100:** 1690-1697

Edreva AM, Velikova VB, Tsonev TD (2007) Phenylamides in plants. Russian Journal of Plant Physiology **54:** 287-301

Ellinger D, Stingl N, Kubigsteltig, II, Bals T, Juenger M, Pollmann S, Berger S, Schuenemann D, Mueller MJ (2010) DONGLE and DEFECTIVE IN ANTHER DEHISCENCE1 lipases are not essential for wound- and pathogen-induced jasmonate biosynthesis: redundant lipases contribute to jasmonate formation. Plant Physiology **153:** 114-127

Ellis J, Jones D (1998) Structure and function of proteins controlling strain-specific pathogen resistance in plants. Current Opinion in Plant Biology **1:** 288-293

Ellis JG, Rafiqi M, Gan P, Chakrabarti A, Dodds PN (2009) Recent progress in discovery and functional analysis of effector proteins of fungal and oomycete plant pathogens. Current Opinion in Plant Biology **12:** 399-405

Euler M, Baldwin IT (1996) The chemistry of defense and apparency in the corollas of *Nicotiana attenuata*. Oecologia **107:** 102-112

Fakhro A, Andrade-Linares DR, von Bargen S, Bandte M, Buttner C, Grosch R, Schwarz D, Franken P (2010) Impact of *Piriformospora indica* on tomato growth and on interaction with fungal and viral pathogens. Mycorrhiza **20:** 191-200

Fammartino A, Cardinale F, Gobel C, Mene-Saffrane L, Fournier J, Feussner I, Esquerre-Tugaye MT (2007) Characterization of a divinyl ether biosynthetic pathway specifically associated with pathogenesis in tobacco. Plant Physiology **143:** 378-388

Fammartino A, Verdaguer B, Fournier J, Tamietti G, Carbonne F, Esquerre-Tugaye MT, Cardinale F (2010) Coordinated transcriptional regulation of the divinyl ether biosynthetic genes in tobacco by signal molecules related to defense. Plant Physiology and Biochemistry **48:** 225-231

Farmaki T, Sanmartin M, Jimenez P, Paneque M, Sanz C, Vancanneyt G, Leon J, Sanchez-Serrano JJ (2007) Differential distribution of the lipoxygenase pathway enzymes within potato chloroplasts. Journal of Experimental Botany **58:** 555-568

Fauconnier ML, Rojas-Beltran J, Dupuis B, Delaplace P, Frettinger P, Gosset V, du Jardin P (2008) Changes in oxylipin synthesis after *Phytophthora infestans* infection of potato leaves do not correlate with resistance. Plant Physiology and Biochemistry **46:** 823-831

Fragoso V, Goddard H, Baldwin IT, Kim SG (2011) A simple and efficient micrografting method for stably transformed *Nicotiana attenuata* plants to examine shoot-root signaling. Plant Methods **7:** 34

Fried G, Petit S, Reboud X (2010) A specialist-generalist classification of the arable flora and its response to changes in agricultural practices. BMC Ecology **10:** 20

Froehlich JE, Wilkerson CG, Ray WK, McAndrew RS, Osteryoung KW, Gage DA, Phinney BS (2003) Proteomic study of the *Arabidopsis thaliana* chloroplastic envelope membrane utilizing alternatives to traditional two-dimensional electrophoresis. Journal of Proteome Research **2:** 413-425

Fujita M, Mizukado S, Fujita Y, Ichikawa T, Nakazawa M, Seki M, Matsui M, Yamaguchi-Shinozaki K, Shinozaki K (2007) Identification of stress-tolerance-related transcription-factor genes via mini-scale Full-length cDNA Over-eXpressor (FOX) gene hunting system. Biochemical and Biophysical Research Communications **364:** 250-257

Galliard T, Phillips DR (1972) The enzymic conversion of linoleic acid into 9-(nona-1',3'-dienoxy)non-8-enoic acid, a novel unsaturated ether derivative isolated from homogenates of *Solanum tuberosum* tubers. Biochemical Journal **129:** 743-753

Gaquerel E, Heiling S, Schoettner M, Zurek G, Baldwin IT (2010) Development and validation of a liquid chromatography-electrospray ionization-time-of-flight mass spectrometry method for induced changes in *Nicotiana attenuata* leaves during simulated herbivory. Journal of Agricultural and Food Chemistry **58:** 9418-9427

Gase K, Baldwin IT (2012) Transformational tools for next-generation plant ecology: manipulation of gene expression for the functional analysis of genes. Plant Ecology and Diversity **5:** 485-490

Gehring C, Bennett A (2009) Mycorrhizal fungal-plant-insect interactions: The importance of a community approach. Environmental Entomology **38:** 93-102

Gehring CA, Whitham TG (1991) Herbivore-driven mycorrhizal mutualism in insect-susceptible Pinyon Pine. Nature **353:** 556-557

Gilardoni P, Schuck S, Jüngling R, Rotter B, Baldwin I, Bonaventure G (2010) SuperSAGE analysis of the *Nicotiana attenuata* transcriptome after fatty acid-amino acid elicitation (FAC): identification of early mediators of insect responses. BMC Plant Biology **10: 66**

Gilardoni PA, Hettenhausen C, Baldwin IT, Bonaventure G (2011) *Nicotiana attenuata* LECTIN RECEPTOR KINASE1 suppresses the insect-mediated inhibition of induced defense responses during *Manduca sexta* herbivory. Plant Cell **23:** 3512-3532

Gissot L, Polge C, Jossier M, Girin T, Bouly JP, Kreis M, Thomas M (2006) AKINβγ contributes to SnRK1 heterotrimeric complexes and interacts with two proteins implicated in plant pathogen resistance through its KIS/GBD sequence. Plant Physiology **142:** 931-944

Glauser G, Grata E, Dubugnon L, Rudaz S, Farmer EE, Wolfender JL (2008) Spatial and temporal dynamics of jasmonate synthesis and accumulation in *Arabidopsis* in response to wounding. Journal of Biological Chemistry **283:** 16400-16407

Glauser G, Grata E, Rudaz S, Wolfender JL (2008) High-resolution profiling of oxylipin-containing galactolipids in *Arabidopsis* extracts by ultra-performance liquid chromatography/time-of-flight mass spectrometry. Journal of Chemical Ecology **22:** 3154-3160

Glazebrook J (2005) Contrasting mechanisms of defense against biotrophic and necrotrophic pathogens. Annual Review of Phytopathology **43:** 205-227

Gobel C, Feussner I, Hamberg M, Rosahl S (2002) Oxylipin profiling in pathogen-infected potato leaves. Biochimica et Biophysica Acta **1584:** 55-64

Gobel C, Feussner I, Schmidt A, Scheel D, Sanchez-Serrano J, Hamberg M, Rosahl S (2001) Oxylipin profiling reveals the preferential stimulation of the 9-lipoxygenase pathway in elicitor-treated potato cells. Journal of Biological Chemistry **276:** 6267-6273

Govind G, Mittapalli O, Griebel T, Allmann S, Bocker S, Baldwin IT (2010) Unbiased transcriptional comparisons of generalist and specialist herbivores feeding on progressively defenseless *Nicotiana attenuata* plants. PLoS ONE **5:** e8735

Granke LL, Windstam ST, Hoch HC, Smart CD, Hausbeck MK (2009) Dispersal and movement mechanisms of *Phytophthora capsici* sporangia. Phytopathology **99:** 1258-1264

Grechkin AN, Hamberg M (1996) Divinyl ether synthase from garlic (*Allium sativum* L.) bulbs: Sub-cellular localization and substrate regio-and stereospecificity. FEBS Letters **388:** 112-114

Groten K, Barz W (2000) Elicitor-induced defence reactions in cell suspension cultures of soybean cultivars. Zeitschrift für Naturforschung C **55:** 718-730

Gyetvai G, Sonderkaer M, Gobel U, Basekow R, Ballvora A, Imhoff M, Kersten B, Nielsen KL, Gebhardt C (2012) The transcriptome of compatible and incompatible interactions of potato (*Solanum tuberosum*) with *Phytophthora infestans* revealed by DeepSAGE analysis. Plos One **7**

Halford NG, Hey S, Jhurreea D, Laurie S, McKibbin RS, Paul M, Zhang YH (2003) Metabolic signalling and carbon partitioning: role of Snf1-related (SnRK1) protein kinase. Journal of Experimental Botany **54:** 467-475

Halim VA, Vess A, Scheel D, Rosahl S (2006) The role of salicylic acid and jasmonic acid in pathogen defence. Plant Biology (Stuttg) **8:** 307-313

Halitschke R, Schittko U, Pohnert G, Boland W, Baldwin IT (2001) Molecular interactions between the specialist herbivore *Manduca sexta* (Lepidoptera, Sphingidae) and its natural host *Nicotiana attenuata*. III. Fatty acid-amino acid conjugates in herbivore oral

secretions are necessary and sufficient for herbivore-specific plant responses. Plant Physiology **125:** 711-717

Halitschke R, Ziegler J, Keinanen M, Baldwin IT (2004) Silencing of hydroperoxide lyase and allene oxide synthase reveals substrate and defense signaling crosstalk in *Nicotiana attenuata*. Plant Journal **40:** 35-46

Hammond JP, Bennett MJ, Bowen HC, Broadley MR, Eastwood DC, May ST, Rahn C, Swarup R, Woolaway KE, White PJ (2003) Changes in gene expression in *Arabidopsis* shoots during phosphate starvation and the potential for developing smart plants. Plant Physiology **132:** 578-596

Hause B, Fester T (2005) Molecular and cell biology of arbuscular mycorrhizal symbiosis. Planta **221:** 184-196

Heidel AJ, Baldwin IT (2004) Microarray analysis of salicylic acid- and jasmonic acid-signalling in responses of *Nicotiana attenuata* to attack by insects from multiple feeding guilds. Plant, Cell and Environment **27:** 1362-1373

Heil M (2009) Damaged-self recognition in plant herbivore defence. Trends in Plant Science **14:** 356-363

Heil M (2010) Plastic defence expression in plants. Evolutionary Ecology **24:** 555-569

Heiling S, Schuman MC, Schoettner M, Mukerjee P, Berger B, Schneider B, Jassbi AR, Baldwin IT (2010) Jasmonate and ppHsystemin regulate key malonylation steps in the biosynthesis of 17-Hydroxygeranyllinalool diterpene glycosides, an abundant and effective direct defense against herbivores in *Nicotiana attenuata*. Plant Cell **22:** 273-292

Herrera-Medina MJ, Steinkellner S, Vierheilig H, Bote JAO, Garrido JMG (2007) Abscisic acid determines arbuscule development and functionality in the tomato arbuscular mycorrhiza. New Phytologist **175:** 554-564

Hettenhausen C, Baldwin IT, Wu J (2012) Silencing MPK4 in *Nicotiana attenuata* enhances photosynthesis and seed production but compromises abscisic acid-induced stomatal closure and guard cell-mediated resistance to *Pseudomonas syringae* pv *tomato* DC3000. Plant Physiol **158:** 759-776

Hogenhout SA, Bos JIB (2011) Effector proteins that modulate plant-insect interactions. Current Opinion in Plant Biology **14:** 422-428

Hong YW, Wang TW, Hudak KA, Schade F, Froese CD, Thompson JE (2000) An ethylene-induced cDNA encoding a lipase expressed at the onset of senescence. Proceedings of the National Academy of Sciences of the United States of America **97:** 8717-8722

Hui DQ, Iqbal J, Lehmann K, Gase K, Saluz HP, Baldwin IT (2003) Molecular interactions between the specialist herbivore *Manduca sexta* (Lepidoptera, Sphingidae) and its natural host *Nicotiana attenuata*: V. Microarray analysis and further characterization of large-scale changes in herbivore-induced mRNAs. Plant Physiology **131:** 1877-1893

Hyun Y, Choi S, Hwang H-J, Yu J, Nam S-J, Ko J, Park J-Y, Seo YS, Kim EY, Ryu SB, Kim WT, Lee Y-H, Kang H, Lee I (2008) Cooperation and functional diversification of two closely related galactolipase genes for jasmonate biosynthesis. Developmental Cell **14:** 183-192

Ishiguro S, Kawai-Oda A, Ueda J, Nishida I, Okada K (2001) The *DEFECTIVE IN ANTHER DEHISCIENCE* gene encodes a novel phospholipase A1 catalyzing the initial step of jasmonic acid biosynthesis, which synchronizes pollen maturation, anther dehiscence, and flower opening in *Arabidopsis*. The Plant Cell **13:** 2191-2209

Isman MB, Duffey SS (1982) Toxicity of tomato phenolic compounds to the fruitworm, *Heliothis zea*. Entomologia Experimentalis et Applicata **31:** 370-376

Jacobs S, Zechmann B, Molitor A, Trujillo M, Petutschnig E, Likpa V, Kogel KH, Schafer P (2011) Broad-spectrum suppression of innate immunity is required for colonization of *Arabidopsis* roots by the fungus *Piriformospora indica*. Plant Physiology **156:** 726-740

Jain M, Li QB, Chourey PS (2008) Cloning and expression analyses of *sucrose non-fermenting-1-related kinase 1* (*SnRK1b*) gene during development of sorghum and maize endosperm and its implicated role in sugar-to-starch metabolic transition. Physiologia Plantarum **134:** 161-173

Jiang RHY, Tyler BM, Whisson SC, Hardham AR, Govers F (2006) Ancient origin of elicitin gene clusters in *Phytophthora* genomes. Molecular Biology and Evolution **23:** 338-351

Jones AMP, Chattopadhyay A, Shukla M, Zon J, Saxena PK (2012) Inhibition of phenylpropanoid biosynthesis increases cell wall digestibility, protoplast isolation, and facilitates sustained cell division in American elm (*Ulmus americana*). BMC Plant Biology **12**

Jones JDG, Dangl JL (2006) The plant immune system. Nature **444:** 323-329

Judelson HS, Blanco FA (2005) The spores of *Phytophthora*: Weapons of the plant destroyer. Nature Reviews Microbiology **3:** 47-58

Kachroo A, Kachroo P (2009) Fatty acid-derived signals in plant defense. Annual Review of Phytopathology **47:** 153-176

Kahl J, Siemens DH, Aerts RJ, Gabler R, Kuhnemann F, Preston CA, Baldwin IT (2000) Herbivore-induced ethylene suppresses a direct defense but not a putative indirect defense against an adapted herbivore. Planta **210:** 336-342

Kallenbach M, Alagna F, Baldwin IT, Bonaventure G (2010) *Nicotiana attenuata* SIPK, WIPK, NPR1, and fatty acid-amino acid conjugates participate in the induction of jasmonic acid biosynthesis by affecting early enzymatic steps in the pathway. Plant Physiology **152:** 96-106

Kallenbach M, Gilardoni PA, Allmann S, Baldwin IT, Bonaventure G (2011) C-12 derivatives of the hydroperoxide lyase pathway are produced by product recycling through lipoxygenase-2 in *Nicotiana attenuata* leaves. New Phytologist **191:** 1054-1068

Kamoun S (2006) A catalogue of the effector secretome of plant pathogenic oomycetes. Annual Review of Phytopathology **44:** 41-60

Kamoun S, Young M, Forster H, Coffey MD, Tyler BM (1994) Potential role of elicitins in the interaction between *Phytophthora* species and tobacco. Applied and Environmental Microbiology **60:** 1593-1598

Kang JH, Wang L, Giri A, Baldwin IT (2006) Silencing threonine deaminase and JAR4 in *Nicotiana attenuata* impairs jasmonic acid-isoleucine-mediated defenses against *Manduca sexta*. Plant Cell **18:** 3303-3320

Karimi M, Depicker A, Hilson P (2007) Recombinational cloning with plant gateway vectors. Plant Physiology **145:** 1144-1154

Kasparovsky T, Blein JP, Mikes V (2004) Ergosterol elicits oxidative burst in tobacco cells via phospholipase A2 and protein kinase C signal pathway. Plant Physiology and Biochemistry **42:** 429-435

Kasparovsky T, Milat ML, Humbert C, Blein JP, Havel L, Mikes V (2003) Elicitation of tobacco cells with ergosterol activates a signal pathway including mobilization of internal calcium. Plant Physiology and Biochemistry **41:** 495-501

Keen NT (1990) Gene-for-gene complementarity in plant-pathogen interactions. Annual Review of Genetics **24:** 447-463

Keinänen M, Oldham NJ, Baldwin IT (2001) Rapid HPLC screening of jasmonate-induced increases in tobacco alkaloids, phenolics, and diterpene glycosides in *Nicotiana attenuata*. Journal of Agricultural and Food Chemistry **49:** 3553-3558

Kemen E, Jones JDG (2012) Obligate biotroph parasitism: Can we link genomes to lifestyles? Trends in Plant Science **17:** 448-457

Kempel A, Schadler M, Chrobock T, Fischer M, van Kleunen M (2011) Tradeoffs associated with constitutive and induced plant resistance against herbivory. Proceedings of the National Academy of Sciences of the United States of America **108:** 5685-5689

Kessler A, Baldwin IT (2001) Defensive function of herbivore-induced plant volatile emissions in nature. Science **291:** 2141-2144

Kessler A, Baldwin IT (2002) Plant responses to insect herbivory: The emerging molecular analysis. Annual Review of Plant Biology **53:** 299-328

Kessler D, Baldwin IT (2007) Making sense of nectar scents: The effects of nectar secondary metabolites on floral visitors of *Nicotiana attenuata*. Plant Journal **49:** 840-854

Kessler D, Diezel C, Baldwin IT (2010) Changing pollinators as a means of escaping herbivores. Current Biology **20:** 237-242

Kirchner JW, Roy BA (2002) Evolutionary implications of host-pathogen specificity: Fitness consequences of pathogen virulence traits. Evolutionary Ecology Research **4:** 27-48

Kistner C, Matamoros M (2005) RNA isolation using phase extraction and LiCl precipitation. Springer Verlag, Dordrecht, The Netherlands

Kliebenstein DJ, Rowe HC (2008) Ecological costs of biotrophic versus necrotrophic pathogen resistance, the hypersensitive response and signal transduction. Plant Science **174:** 551-556

Koch C, Noga G, Strittmatter G (1994) Photosynthetic electron-transport is differentially affected during early stages of cultivar/race-specific interactions between potato and *Phytophthora infestans*. Planta **193:** 551-557

Körner E, von Dahl C, Bonaventure G, Baldwin IT (2009) Pectin methylesterase NaPME1 contributes to the emission of methanol during insect herbivory and to the elicitation of defence responses in *Nicotiana*. Journal of Experimental Botany **60:** 2631-2640

Krings M, Taylor TN, Dotzler N (2011) The fossil record of the Peronosporomycetes (Oomycota). Mycologia **103:** 455-457

Krings M, Taylor TN, Hass H, Kerp H, Dotzler N, Hermsen EJ (2007) Fungal endophytes in a 400-million-yr-old land plant: Infection pathways, spatial distribution, and host responses. New Phytologist **174:** 648-657

Krügel T, Lim M, Gase K, Halitschke R, Baldwin IT (2002) *Agrobacterium*-mediated transformation of *Nicotiana attenuata*, a model ecological expression system. Chemoecology **12:** 177-183

Kudla U, Milac AL, Qin L, Overmars H, Roze E, Holterman M, Petrescu AJ, Goverse A, Bakker J, Helder J, Smant G (2007) Structural and functional characterization of a novel, host penetration-related pectate lyase from the potato cyst nematode *Globodera rostochiensis*. Molecular Plant Pathology **8:** 293-305

Kunkel BN, Brooks DM (2002) Cross talk between signaling pathways in pathogen defense. Current Opinion in Plant Biology **5:** 325-331

La Camera S, Geoffroy P, Samaha H, Ndiaye A, Rahim G, Legrand M, Heitz T (2005) A pathogen-inducible patatin-like lipid acyl hydrolase facilitates fungal and bacterial host colonization in Arabidopsis. Plant Journal **44:** 810-825

La Camera S, Gouzerh G, Dhondt S, Hoffmann L, Fritig B, Legrand M, Heitz T (2004) Metabolic reprogramming in plant innate immunity: The contributions of phenylpropanoid and oxylipin pathways. Immunological Reviews **198:** 267-284

Lan HY, Tian YC, Wang CH, Liu GZ, Zhang LH, Wang LL, Chen ZH (2000) Studies of transgenic tobacco plants expressing beta-1,3-glucanase and chitinase genes and their potential for fungal resistance. Yi Chuan Xue Bao **27:** 70-77

Lebrun-Garcia A, Chiltz A, Gout E, Bligny R, Pugin A (2002) Questioning the role of salicylic acid and cytosolic acidification in mitogen-activated protein kinase activation induced by cryptogein in tobacco cells. Planta **214:** 792-797

Lee YC, Johnson JM, Chien CT, Sun C, Cai DG, Lou BG, Oelmuller R, Yeh KW (2011) Growth promotion of chinese cabbage and *Arabidopsis* by *Piriformospora indica* is not stimulated by mycelium-synthesized auxin. Molecular Plant-Microbe Interactions **24:** 421-431

Leon-Morcillo RJ, Angel J, Martin R, Vierheilig H, Ocampo JA, Garcia-Garrido JM (2012) Late activation of the 9-oxylipin pathway during arbuscular mycorrhiza formation in tomato and its regulation by jasmonate signalling. Journal of Experimental Botany **63:** 3545-3558

Lherminier J, Elmayan T, Fromentin J, Elaraqui KT, Vesa S, Morel J, Verrier JL, Cailleteau B, Blein JP, Simon-Plas F (2009) NADPH oxidase-mediated reactive oxygen species production: subcellular localization and reassessment of its role in plant defense. Molecular Plant-Microbe Interactions **22:** 868-881

Liu JJ, Ekramoddoullah AK, Zamani A (2005) A class IV chitinase is up-regulated by fungal infection and abiotic stresses and associated with slow-canker-growth resistance to *Cronartium ribicola* in Western White Pine (*Pinus monticola*). Phytopathology **95:** 284-291

Liu YD, Jin HL, Yang KY, Kim CY, Baker B, Zhang SQ (2003) Interaction between two mitogen-activated protein kinases during tobacco defense signaling. Plant Journal **34:** 149-160

Long HH, Sonntag DG, Schmidt DD, Baldwin IT (2010) The structure of the culturable root bacterial endophyte community of *Nicotiana attenuata* is organized by soil composition and host plant ethylene production and perception. New Phytologist **185:** 554-567

Lou Y, Baldwin IT (2003) *Manduca sexta* recognition and resistance among allopolyploid *Nicotiana* host plants. Proceedings of the National Academy of Sciences of the United States of America **100:** 14581-14586

Lovas A, Bimbo A, Szabo L, Banfalvi Z (2003) Antisense repression of StubGAL83 affects root and tuber development in potato. Plant Journal **33:** 139-147

Luhua S, Ciftci-Yilmaz S, Harper J, Cushman J, Mittler R (2008) Enhanced tolerance to oxidative stress in transgenic *Arabidopsis* plants expressing proteins of unknown function. Plant Physiology **148:** 280-292

Lynds GY, Baldwin IT (1998) Fire, nitrogen, and defensive plasticity in *Nicotiana attenuata*. Oecologia **115:** 531-540

Manter DK, Kelsey RG, Karchesy JJ (2007) Photosynthetic declines in *Phytophthora ramorum*-infected plants develop prior to water stress and in response to exogenous application of elicitins. Phytopathology **97:** 850-856

Mathieu Y, Lapous D, Thomine S, Lauriere C, Guern J (1996) Cytoplasmic acidification as an early phosphorylation-dependent response of tobacco cells to elicitors. Planta **199:** 416-424

McCall AC, Fordyce JA (2010) Can optimal defence theory be used to predict the distribution of plant chemical defences? Journal of Ecology **98:** 985-992

McCloud ES, Baldwin IT (1997) Herbivory and caterpillar regurgitants amplify the wound-induced increases in jasmonic acid but not nicotine in *Nicotiana sylvestris*. Planta **203:** 430-435

McKibbin RS, Muttucumaru N, Paul MJ, Powers SJ, Burrell MM, Coates S, Purcell PC, Tiessen A, Geigenberger P, Halford NG (2006) Production of high-starch, low-glucose potatoes through over-expression of the metabolic regulator SnRK1. Plant Biotechnology Journal **4:** 409-418

McLean MD, Hoover GJ, Bancroft B, Makhmoudova A, Clark SM, Welacky T, Simmonds DH, Shelp BJ (2007) Identification of the full-length *Hs1*$^{pro-1}$ coding sequence and preliminary evaluation of soybean cyst nematode resistance in soybean transformed with *Hs1*$^{pro-1}$ cDNA. Canadian Journal of Botany-Revue Canadienne De Botanique **85:** 437-441

Medina MJH, Gagnon H, Piche Y, Ocampo JA, Garrido JMG, Vierheilig H (2003) Root colonization by arbuscular mycorrhizal fungi is affected by the salicylic acid content of the plant. Plant Science **164:** 993-998

Medzhitov R, Schneider DS, Soares MP (2012) Disease tolerance as a defense strategy. Science **335:** 936-941

Meldau S, Erb M, Baldwin IT (2012) Defence on demand: mechanisms behind optimal defence patterns. Ann Bot **110:** 1503-1514

Meldau S, Ullman-Zeunert L, Govind G, Bartram S, Baldwin IT (2012) MAPK-dependent JA and SA signalling in *Nicotiana attenuata* affects plant growth and fitness during competition with conspecifics. BMC Plant Biology **12**

Mithofer A, Boland W (2008) Recognition of herbivory-associated molecular patterns. Plant Physiology **146:** 825-831

Molitor A, Kogel KH (2009) Induced resistance triggered by *Piriformospora indica*. Plant Signaling & Behavior **4:** 215-216

Moreau RA (1987) The involvement of membrane-degrading enzymes during infection of potato leaves by *Phytophthora infestans*. ACS Symposium Series **325:** 343-354

Munnik T, Testerink C (2009) Plant phospholipid signaling: "in a nutshell". Journal of Lipid Research **50:** S260-S265

Murakami N, Imamura H, Morimoto T, Ueda T, Nagai S, Sakakibara J, Yamada N (1991) Selective preparation of *sn*-1 and *sn*-2 lysogalactolipids by enzymatic hydrolysis using lipase (from *Rhizopus arrhizus*) Tetrahedron letters **32:** 1331-1334

Murray SL, Ingle RA, Petersen LN, Denby KJ (2007) Basal resistance against *Pseudomonas syringae* in *Arabidopsis* involves WRKY53 and a protein with homology to a nematode resistance protein. Molecular Plant-Microbe Interactions **20:** 1431-1438

Nakamura Y, Arimitsu H, Yamaryo Y, Awai K, Masuda T, Shimada H, Takamiya K, Ohta H (2003) Digalactosyldiacylglycerol is a major glycolipid in floral organs of *Petunia hybrida*. Lipids **38:** 1107-1112

Nifong JM, Nicholson JS, Shew HD, Lewis RS (2011) Variability for resistance to *Phytophthora nicotianae* within a collection of *Nicotiana rustica* accessions. Plant Disease **95:** 1443-1447

Nongbri PL, Johnson JM, Sherameti I, Glawischnig E, Halkier BA, Oelmuler R (2012) Indole-3-acetaldoxime-derived compounds restrict root colonization in the beneficial interaction between *Arabidopsis* roots and the endophyte *Piriformospora indica*. Molecular Plant-Microbe Interactions **25:** 1186-1197

Nowicki M, Fooled MR, Nowakowska M, Kozik EU (2012) Potato and tomato late blight caused by *Phytophthora infestans*: An overview of pathology and resistance breeding. Plant Disease **96:** 4-17

Nunez-Farfan J, Fornoni J, Valverde PL (2007) The evolution of resistance and tolerance to herbivores. Annual Review of Ecology Evolution and Systematics **38:** 541-566

Ohnmeiss TE, Baldwin IT (2000) Optimal defense theory predicts the ontogeny of an induced nicotine defense. Ecology **81:** 1765-1783

Panabieres F, Marais A, LeBerre JY, Penot I, Fournier D, Ricci P (1995) Characterization of a gene cluster of *Phytophthora cryptogea* which codes for elicitins, proteins inducing a hypersensitive-like response in tobacco. Molecular Plant-Microbe Interactions **8:** 996-1003

Panabieres F, Ponchet M, Allasia V, Cardin L, Ricci P (1997) Characterization of border species among Pythiaceae: Several Pythium isolates produce elicitins, typical proteins from *Phytophthora* spp. Mycological Research **101:** 1459-1468

Paschold A, Bonaventure G, Kant M, Baldwin IT (2008) Jasmonate perception regulates jasmonate biosynthesis and JA-Ile metabolism: The case of COI1 in *Nicotiana attenuata*. Plant and Cell Physiology **49:** 1165 -1175

Paschold A, Halitschke R, Baldwin IT (2007) Co(i)-ordinating defenses: NaCOI1 mediates herbivore- induced resistance in *Nicotiana attenuata* and reveals the role of herbivore movement in avoiding defenses. Plant Journal **51:** 79-91

Peltier JB, Cai Y, Sun Q, Zabrouskov V, Giacomelli L, Rudella A, Ytterberg AJ, Rutschow H, van Wijk KJ (2006) The oligomeric stromal proteome of *Arabidopsis thaliana* chloroplasts. Molecular and Cellular Proteomics **5:** 114-133

Pham GH KR, Singh A, Sachdev M, Prasad R, Kaldorf M, Buscot F, Oelmüller R, Peskan T, Weiss M, Hampp R, Varma A (2004) Axenic cultures of *Piriformospora indica*. *In* Plant surface microbiology. Springer, Berlin Heidelberg New York, pp 593-616

Pieterse CM, Van der Does D, Zamioudis C, Leon-Reyes A, Van Wees SC (2012) Hormonal modulation of plant immunity. Annual Review of Cell and Developmental Biology **28:** 489-521

Pineda A, Zheng SJ, van Loon JJA, Pieterse CMJ, Dicke M (2010) Helping plants to deal with insects: The role of beneficial soil-borne microbes. Trends in Plant Science **15:** 507-514

Ponchet M, Panabieres F, Milat ML, Mikes V, Montillet JL, Suty L, Triantaphylides C, Tirilly Y, Blein JP (1999) Are elicitins cryptograms in plant-Oomycete communications? Cellular and Molecular Life Sciences **56:** 1020-1047

Preston CA, Baldwin IT (1999) Positive and negative signals regulate germination in the post-fire annual, *Nicotiana attenuata*. Ecology **80:** 481-494

Preston GM (2004) Plant perceptions of plant growth-promoting *Pseudomonas*. Philosophical Transactions of the Royal Society B-Biological Sciences **359:** 907-918

Prost I, Dhondt S, Rothe G, Vicente J, Rodriguez MJ, Kift N, Carbonne F, Griffiths G, Esquerre-Tugaye MT, Rosahl S, Castresana C, Hamberg M, Fournier J (2005)

Evaluation of the antimicrobial activities of plant oxylipins supports their involvement in defense against pathogens. Plant Physiology **139:** 1902-1913

Puthoff DP, Nettleton D, Rodermel SR, Baum TJ (2003) *Arabidopsis* gene expression changes during cyst nematode parasitism revealed by statistical analyses of microarray expression profiles. Plant Journal **33:** 911-921

Qiang X, Weiss M, Kogel KH, Schafer P (2012) *Piriformospora indica* - a mutualistic basidiomycete with an exceptionally large plant host range. Molecular Plant Pathology **13:** 508-518

Rayapuram C, Baldwin IT (2008) Host-plant-mediated effects of Nadefensin on herbivore and pathogen resistance in *Nicotiana attenuata*. BMC Plant Biology **8:** 109

Rayapuram C, Wu J, Haas C, Baldwin IT (2008) PR-13/Thionin but not PR-1 mediates bacterial resistance in *Nicotiana attenuata* in nature, and neither influences herbivore resistance. Molecular Plant-Microbe Interactions **21:** 988-1000

Re DA, Dezar CA, Chan RL, Baldwin IT, Bonaventure G (2010) *Nicotiana attenuata* NaHD20 plays a role in leaf ABA accumulation during water stress, benzylacetone emission from flowers, and the timing of bolting and flower transitions. Journal of Experimental Botany **62:** 155-166

Re DA, Raud B, Chan RL, Baldwin IT, Bonaventure G (2012) RNAi-mediated silencing of the HD-Zip gene *HD20* in *Nicotiana attenuata* affects benzyl acetone emission from corollas via ABA levels and the expression of metabolic genes. BMC Plant Biology **12**

Restrepo S, Myers KL, del Pozo O, Martin GB, Hart AL, Buell CR, Fry WE, Smart CD (2005) Gene profiling of a compatible interaction between *Phytophthora infestans* and *Solanum tuberosum* suggests a role for carbonic anhydrase. Molecular Plant-Microbe Interactions **18:** 913-922

Reymond P, Weber H, Damond M, Farmer EE (2000) Differential gene expression in response to mechanical wounding and insect feeding in *Arabidopsis*. Plant Cell **12:** 707-719

Roda A, Halitschke R, Steppuhn A, Baldwin IT (2004) Individual variability in herbivore-specific elicitors from the plant's perspective. Molecular Ecology **13:** 2421-2433

Rolland F, Baena-Gonzalez E, Sheen J (2006) Sugar sensing and signaling in plants: Conserved and novel mechanisms. Annual Review of Plant Biology **57:** 675-709

Rosenthal JP, Kotanen PM (1994) Terrestrial plant tolerance to herbivory. Trends in Ecology & Evolution **9:** 145-148

Rouxel T, Balesdent M-H (2010) Avirulence Genes. *In* Encyclopedia of Life Sciences. John Wiley & Sons, Ltd, Chichester

Rowland O, Ludwig AA, Merrick CJ, Baillieul F, Tracy FE, Durrant WE, Fritz-Laylin L, Nekrasov V, Sjolander K, Yoshioka H, Jones JD (2005) Functional analysis of *Avr9/Cf-9 rapidly elicite*d genes identifies a protein kinase, ACIK1, that is essential for full Cf-9-dependent disease resistance in tomato. Plant Cell **17:** 295-310

Roy S, Pouenat ML, Caumont C, Cariven C, Prevost MC, Esquerretugaye MT (1995) Phospholipase-activity and phospholipid patterns in tobacco cells treated with fungal elicitor. Plant Science **107:** 17-25

Ryu SB (2004) Phospholipid-derived signaling mediated by phospholipase A in plants. Trends in Plant Science **9:** 229-235

Saedler R, Baldwin IT (2004) Virus-induced gene silencing of jasmonate-induced direct defences, nicotine and trypsin proteinase-inhibitors in *Nicotiana attenuata*. Journal of Experimental Botany **55:** 151-157

Sahay NS, Varma A (1999) *Piriformospora indica*: A new biological hardening tool for micropropagated plants. FEMS Microbiology Letters **181:** 297-302

Sasaki Y, Asamizu E, Shibata D, Nakamura Y, Kaneko T, Awai K, Amagai M, Kuwata C, Tsugane T, Masuda T, Shimada H, Takamiya X, Ohta H, Tabata S (2001) Monitoring of methyl jasmonate-responsive genes in *Arabidopsis* by cDNA macroarray: Self-activation of jasmonic acid biosynthesis and crosstalk with other phytohormone signaling pathways. DNA Research **8:** 153-161

Schafer P, Pfiffi S, Voll LM, Zajic D, Chandler PM, Waller F, Scholz U, Pons-Kuhnemann J, Sonnewald S, Sonnewald U, Kogel KH (2009) Manipulation of plant innate immunity and gibberellin as factor of compatibility in the mutualistic association of barley roots with *Piriformospora indica*. Plant Journal **59:** 461-474

Schafer P, Pfiffi S, Voll LM, Zajic D, Chandler PM, Waller F, Scholz U, Pons-Kuhnemann J, Sonnewald S, Sonnewald U, Kogel KH (2009) Phytohormones in plant root-*Piriformospora indica* mutualism. Plant Signaling & Behavior **4:** 669-671

Schaller A, Stintzi A (2009) Enzymes in jasmonate biosynthesis - Structure, function, regulation. Phytochemistry **70:** 1532-1538

Scherer GFE, Paul RU, Holk A, Martinec J (2002) Down-regulation by elicitors of phosphatidylcholine-hydrolyzing phospholipase C and up-regulation of phospholipase A in plant cells. Biochemical and Biophysical Research Communications **293:** 766-770

Schittko U, Preston CA, Baldwin IT (2000) Eating the evidence? *Manduca sexta* larvae can not disrupt specific jasmonate induction in *Nicotiana attenuata* by rapid consumption. Planta **210:** 343-346

Schmelz EA, Engelberth J, Alborn HT, Tumlinson JH, Teal PEA (2009) Phytohormone-based activity mapping of insect herbivore-produced elicitors. Proceedings of the National Academy of Sciences **106:** 653-657

Schmidt SM, Panstruga R (2011) Pathogenomics of fungal plant parasites: what have we learnt about pathogenesis? Current Opinion in Plant Biology **14:** 392-399

Schnabel G, Strittmatter G, Noga G (1998) Changes in photosynthetic electron transport in potato cultivars with different field resistance after infection with *Phytophthora infestans*. Journal of Phytopathology-Phytopathologische Zeitschrift **146:** 205-210

Schuck S, Camehl I, Gilardoni PA, Oelmueller R, Baldwin IT, Bonaventure G (2012) HSPRO controls early *Nicotiana attenuata* seedling growth during interaction with the fungus *Piriformospora indica*. Plant Physiology **160:** 929-943

Schulte D, Cai DG, Kleine M, Fan LJ, Wang S, Jung C (2006) A complete physical map of a wild beet (*Beta procumbens*) translocation in sugar beet. Molecular Genetics and Genomics **275:** 504-511

Schwachtje J, Baldwin IT (2008) Why does herbivore attack reconfigure primary metabolism? Plant Physiology **146:** 845-851

Schwachtje J, Minchin PEH, Jahnke S, van Dongen JT, Schittko U, Baldwin IT (2006) SNF1-related kinases allow plants to tolerate herbivory by allocating carbon to roots. Proceedings of the National Academy of Sciences of the United States of America **103:** 12935-12940

Shah J (2005) Lipids, lipases, and lipid-modifying enzymes in plant disease resistance. Annual Review of Phytopathology **43:** 229-260

Sherameti I, Shahollari B, Venus Y, Altschmied L, Varma A, Oelmuller R (2005) The endophytic fungus *Piriformospora indica* stimulates the expression of nitrate reductase and the starch-degrading enzyme glucan-water dikinase in tobacco and *Arabidopsis* roots through a homeodomain transcription factor that binds to a conserved motif in their promoters. Journal of Biological Chemistry **280:** 26241-26247

Shibata Y, Kawakita K, Takemoto D (2010) Age-related resistance of *Nicotiana benthamiana* against hemibiotrophic pathogen *Phytophthora infestans* requires both ethylene- and salicylic acid-mediated signaling pathways. Molecular Plant-Microbe Interactions **23:** 1130-1142

Silverstone AL, Jung HS, Dill A, Kawaide H, Kamiya Y, Sun TP (2001) Repressing a repressor: Gibberellin-induced rapid reduction of the RGA protein in *Arabidopsis*. Plant Cell **13:** 1555-1566

Simon-Plas F, Elmayan T, Blein JP (2002) The plasma membrane oxidase NtrbohD is responsible for AOS production in elicited tobacco cells. Plant Journal **31:** 137-147

Skibbe M, Qu N, Galis I, Baldwin IT (2008) Induced plant defenses in the natural environment: *Nicotiana attenuata* WRKY3 and WRKY6 coordinate responses to herbivory. Plant Cell **20:** 1984-2000

Stein E, Molitor A, Kogel KH, Waller F (2008) Systemic resistance in *Arabidopsis* conferred by the mycorrhizal fungus *Piriformospora indica* requires jasmonic acid signaling and the cytoplasmic function of NPR1. Plant and Cell Physiology **49:** 1747-1751

Stelmach B, Müller A, Hennig P, Gebhardt S, Schubert-Zsilavecz M, Weiler E (2001) A novel class of oxylipins, *sn1*-O-(12-oxophytodienoyl)-*sn2*-O-(hexadecatrienoyl)-monogalactosyl Diglyceride, from *Arabidopsis thaliana*. Journal of Biological Chemistry **276:** 12832-12838

Steppuhn A, Baldwin IT (2007) Resistance management in a native plant: nicotine prevents herbivores from compensating for plant protease inhibitors. Ecology Letters **10:** 499-511

Steppuhn A, Gase K, Krock B, Halitschke R, Baldwin IT (2004) Nicotine's defensive function in nature. Plos Biology **2:** 1074-1080

Stergiopoulos I, de Wit PJ (2009) Fungal effector proteins. Annual Review of Phytopathology **47:** 233-263

Sthultz CM, Whitham TG, Kennedy K, Deckert R, Gehring CA (2009) Genetically based susceptibility to herbivory influences the ectomycorrhizal fungal communities of a foundation tree species. New Phytologist **184:** 657-667

Stintzi A, Browse J (2000) The *Arabidopsis* male-sterile mutant, opr3, lacks the 12-oxophytodienoic acid reductase required for jasmonate synthesis. Proceedings of the National Academy of Sciences of the United States of America **97:** 10625-10630

Stintzi A, Weber H, Reymond P, Browse J, Farmer EE (2001) Plant defense in the absence of jasmonic acid: the role of cyclopentenones. Proceedings of the National Academy of Sciences of the United States of America **98:** 12837-12842

Stitz M, Gase K, Baldwin IT, Gaquerel E (2011) Ectopic expression of AtJMT in *Nicotiana attenuata*: Creating a metabolic sink has tissue-specific consequences for the jasmonate metabolic network and silences downstream gene expression. Plant Physiology **157:** 341-354

Stork W, Diezel C, Halitschke R, Galis I, Baldwin IT (2009) An ecological analysis of the herbivory-elicited JA burst and its metabolism: plant memory processes and predictions of the moving target model. Journal of Chemical Ecology **4:** e4697

Stork WF, Weinhold A, Baldwin IT (2011) Trichomes as dangerous lollipops: Do lizards also use caterpillar body and frass odor to optimize their foraging? Plant Signaling & Behavior **6:** 1893-1896

Stowe KA, Marquis RJ, Hochwender CG, Simms EL (2000) The evolutionary ecology of tolerance to consumer damage. Annual Review of Ecology and Systematics **31:** 565-595

Stowe MK, Turlings TC, Loughrin JH, Lewis WJ, Tumlinson JH (1995) The chemistry of eavesdropping, alarm, and deceit. Proceedings of the National Academy of Sciences of the United States of America **92:** 23-28

Strack D, Fester T, Hause B, Schliemann W, Walter MH (2003) Arbuscular mycorrhiza: Biological, chemical, and molecular aspects. Journal of Chemical Ecology **29:** 1955-1979

Strauss SY, Agrawal AA (1999) The ecology and evolution of plant tolerance to herbivory. Trends in Ecology & Evolution **14:** 179-185

Strullu-Derrien C, Kenrick P, Rioult JP, Strullu DG (2011) Evidence of parasitic Oomycetes (Peronosporomycetes) infecting the stem cortex of the Carboniferous seed fern

Lyginopteris oldhamia. Proceedings of the Royal Society B-Biological Sciences **278:** 675-680

Sugden C, Donaghy PG, Halford NG, Hardie DG (1999) Two SNF1-related protein kinases from spinach leaf phosphorylate and inactivate 3-hydroxy-3-methylglutaryl-coenzyme A reductase, nitrate reductase, and sucrose phosphate synthase in vitro. Plant Physiology **120:** 257-274

Suza WP, Rowe ML, Hamberg M, Staswick PE (2010) A tomato enzyme synthesizes (+)-7-iso-jasmonoyl-L-isoleucine in wounded leaves. Planta **231:** 717-728

Suza WP, Staswick PE (2008) The role of JAR1 in Jasmonoyl-L: -isoleucine production during *Arabidopsis* wound response. Planta **227:** 1221-1232

Takemoto D, Hardham AR, Jones DA (2005) Differences in cell death induction by *Phytophthora* elicitins are determined by signal components downstream of MAP kinase kinase in different species of *Nicotiana* and cultivars of *Brassica rapa* and *Raphanus sativus*. Plant Physiology **138:** 1491-1504

Taki N, Sasaki-Sekimoto Y, Obayashi T, Kikuta A, Kobayashi K, Ainai T, Yagi K, Sakurai N, Suzuki H, Masuda T, Takamiya K, Shibata D, Kobayashi Y, Ohta H (2005) 12-oxo-phytodienoic acid triggers expression of a distinct set of genes and plays a role in wound-induced gene expression in *Arabidopsis*. Plant Physiology **139:** 1268-1283

Talbot NJ, Kershaw MJ (2009) The emerging role of autophagy in plant pathogen attack and host defence. Current Opinion in Plant Biology **12:** 444-450

Tautenhahn R, Bottcher C, Neumann S (2008) Highly sensitive feature detection for high resolution LC/MS. BMC Bioinformatics **9:** 504

Thatcher LF, Manners JM, Kazan K (2009) *Fusarium oxysporum* hijacks COI1-mediated jasmonate signaling to promote disease development in *Arabidopsis*. Plant Journal **58:** 927-939

Thorpe KW, Barbosa P (1986) Effects of consumption of high and low nicotine tobacco by *Manduca sexta* (Lepidoptera, Sphingidae) on survival of gregarious endoparasitoid *Cotesia congregata* (Hymenoptera, Braconidae). Journal of Chemical Ecology **12:** 1329-1337

Thurau T, Kifle S, Jung C, Cai D (2003) The promoter of the nematode resistance gene

Hs1^{pro-1} activates a nematode-responsive and feeding site-specific gene expression in sugar beet (*Beta vulgaris* L.) and *Arabidopsis thaliana*. Plant Molecular Biology **52:** 643-660

Tripathi SK, Tuteja N (2007) Integrated signaling in flower senescence: An overview. Plant Signaling & Behavior **2:** 437-445

Truitt CL, Wei HX, Pare PW (2004) A plasma membrane protein from *Zea mays* binds with the herbivore elicitor volicitin. Plant Cell **16:** 523-532

Tsavkelova EA, Klimova SY, Cherdyntseva TA, Netrusov AI (2006) Hormones and hormone-like substances of microorganisms: A review. Applied Biochemistry and Microbiology **42:** 229-235

Turner JG (2007) Stress responses: JAZ players deliver fusion and rhythm. Current Biology **17:** R847-R849

Tusher VG, Tibshirani R, Chu G (2001) Significance analysis of microarrays applied to the ionizing radiation response (vol 98, pg 5116, 2001). Proceedings of the National Academy of Sciences of the United States of America **98:** 10515-10515

Vadassery J, Ritter C, Venus Y, Camehl I, Varma A, Shahollari B, Novak O, Strnad M, Ludwig-Muller J, Oelmuller R (2008) The role of auxins and cytokinins in the mutualistic interaction between *Arabidopsis* and *Piriformospora indica*. Molecular Plant-Microbe Interactions **21:** 1371-1383

van Dam NM, Baldwin IT (2001) Competition mediates costs of jasmonate-induced defences, nitrogen acquisition and transgenerational plasticity in *Nicotiana attenuata*. Functional Ecology **15:** 406-415

van Dam NM, Baldwin IT (2003) Heritability of a quantitative and qualitative protease inhibitor polymorphism in *Nicotiana attenuata*. Plant Biology **5:** 179-185

van Dam NM, Hadwich K, Baldwin IT (2000) Induced responses in *Nicotiana attenuata* affect behavior and growth of the specialist herbivore *Manduca sexta*. Oecologia **122:** 371-379

van Dam NM, Horn M, Mares M, Baldwin IT (2001) Ontogeny constrains systemic protease inhibitor response in *Nicotiana attenuata*. Journal of Chemical Ecology **27:** 547-568

Van der Biezen EA, Jones JD (1998) Plant disease-resistance proteins and the gene-for-gene concept. Trends in Biochemical Sciences **23:** 454-456

van der Does HC, Rep M (2007) Virulence genes and the evolution of host specificity in plant-pathogenic fungi. Molecular Plant-Microbe Interactions **20:** 1175-1182

van Doorn WG (2004) Is petal senescence due to sugar starvation? Plant Physiology **134:** 35-42

van Jaarsveld E, Wingfield MJ, Drenth A (2002) Evaluation of tobacco cultivars for resistance to races of *Phytophthora nicotianae* in South Africa. Journal of Phytopathology **150:** 456-462

Van Wees SCM, Van der Ent S, Pieterse CMJ (2008) Plant immune responses triggered by beneficial microbes. Current Opinion in Plant Biology **11:** 443-448

VanDoorn A, Bonaventure G, Schmidt D, Baldwin IT (2011) Regulation of jasmonate metabolism and activation of systemic signaling in *Solanum nigrum*: COI1 and JAR4 play overlapping yet distinct roles. New Phytologist **90:** 640-652

VanDoorn A, Kallenbach M, Borquez AA, Baldwin IT, Bonaventure G (2010) Rapid modification of the insect elicitor N-linolenoyl-glutamate via a lipoxygenase-mediated mechanism on *Nicotiana attenuata* leaves. BMC Plant Biology **10:** 164

Varma A, Verma S, Sudha, Sahay N, Butehorn B, Franken P (1999) *Piriformospora indica*, a cultivable plant-growth-promoting root endophyte. Applied and Environmental Microbiology **65:** 2741-2744

Vellosillo T, Martinez M, Lopez MA, Vicente J, Cascon T, Dolan L, Hamberg M, Castresana C (2007) Oxylipins produced by the 9-lipoxygenase pathway in *Arabidopsis* regulate lateral root development and defense responses through a specific signaling cascade. Plant Cell **19:** 831-846

Vick BA, Zimmerman DC (1983) The biosynthesis of jasmonic acid: a physiological role for plant lipoxygenase. Biochemical and Biophysical Research Community **111:** 470-477

Vick BA, Zimmerman DC (1984) Biosynthesis of jasmonic acid by several plant species. Plant Physiology **75:** 458-461

Viehweger K, Dordschbal B, Roos W (2002) Elicitor-activated phospholipase A(2) generates lysophosphatidylcholines that mobilize the vacuolar H^+ pool for pH signaling via the activation of Na^+-dependent proton fluxes. Plant Cell **14:** 1509-1525

Voelckel C, Baldwin IT (2004) Generalist and specialist lepidopteran larvae elicit different transcriptional responses in *Nicotiana attenuata*, which correlate with larval FAC profiles. Ecology Letters **7:** 770-775

von Dahl C, Winz R, Halitschke R, Kühnemann F, Gase K, Baldwin I (2007) Tuning the herbivore-induced ethylene burst: the role of transcript accumulation and ethylene perception in *Nicotiana attenuata*. Plant Journal **51:** 293-307

Waller F, Achatz B, Baltruschat H, Fodor J, Becker K, Fischer M, Heier T, Huckelhoven R, Neumann C, von Wettstein D, Franken P, Kogel KH (2005) The endophytic fungus *Piriformospora indica* reprograms barley to salt-stress tolerance, disease resistance, and higher yield. Proceedings of the National Academy of Sciences of the United States of America **102:** 13386-13391

Waller F, Achatz B, Deshmukh S, Baltruschat H, Kogel KH (2006) Induction of systemic resistance by the root endophytic fungus *Piriformospora indica* in barley. Plant and Cell Physiology **47:** S48-S48

Walley JW, Coughlan S, Hudson ME, Covington MF, Kaspi R, Banu G, Harmer SL, Dehesh K (2007) Mechanical stress induces biotic and abiotic stress responses via a novel cis-element. Plos Genetics **3:** 1800-1812

Walters D, Raynor L, Mitchell A, Walker R, Walker K (2004) Antifungal activities of four fatty acids against plant pathogenic fungi. Mycopathologia **157:** 87-90

Wang L, Allmann S, Wu JS, Baldwin IT (2008) Comparisons of LIPOXYGENASE3- and JASMONATE-RESISTANT4/6-silenced plants reveal that jasmonic acid and jasmonic acid-amino acid conjugates play different roles in herbivore resistance of *Nicotiana attenuata*. Plant Physiology **146:** 904-915

War AR, Paulraj MG, Ahmad T, Buhroo AA, Hussain B, Ignacimuthu S, Sharma HC (2012) Mechanisms of plant defense against insect herbivores. Plant Signaling & Behavior **7:** 1306-1320

Weber H, Chetelat A, Caldelari D, Farmer EE (1999) Divinyl ether fatty acid synthesis in late blight-diseased potato leaves. Plant Cell **11:** 485-494

Weber H, Vick BA, Farmer EE (1997) Dinor-oxo-phytodienoic acid: A new hexadecanoid signal in the jasmonate family. Proceedings of the National Academy of Sciences of the United States of America **94:** 10473-10478

Weiner J, Thomas SC (1986) Size variability and competition in plant monocultures. Oikos **47:** 211-222

Weinhold A, Baldwin IT (2011) Trichome-derived O-acyl sugars are a first meal for caterpillars that tags them for predation. Proceedings of the National Academy of Sciences of the United States of America **108:** 7855-7859

Weinhold A, Shaker K, Wenzler M, Schneider B, Baldwin IT (2011) Phaseoloidin, a homogentisic acid glucoside from *Nicotiana attenuata* trichomes, contributes to the plant's resistance against lepidopteran herbivores. Journal of Chemical Ecology **37:** 1091-1098

Weiss M, Selosse MA, Rexer KH, Urban A, Oberwinkler F (2004) Sebacinales: A hitherto overlooked cosm of heterobasidiomycetes with a broad mycorrhizal potential. Mycological Research **108:** 1003-1010

Wi SJ, Ji NR, Park KY (2012) Synergistic biosynthesis of biphasic ethylene and reactive oxygen species in response to hemibiotrophic *Phytophthora parasitica* in tobacco plants. Plant Physiology **159:** 251-265

Wink M, Theile V (2002) Alkaloid tolerance in *Manduca sexta* and phylogenetically related sphingids (Lepidoptera : Sphingidae). Chemoecology **12:** 29-46

Winz RA, Baldwin IT (2001) Molecular interactions between the specialist herbivore *Manduca sexta* (Lepidoptera, Sphingidae) and its natural host *Nicotiana attenuata*. IV. Insect-induced ethylene reduces jasmonate-induced nicotine accumulation by regulating putrescine N-methyltransferase transcripts. Plant Physiology **125:** 2189-2202

Wu J, Hettenhausen C, Meldau S, Baldwin IT (2007) Herbivory rapidly activates MAPK signaling in attacked and unattacked leaf regions but not between leaves of *Nicotiana attenuata*. Plant Cell **19:** 1096-1122

Xie DX, Feys BF, James S, Nieto-Rostro M, Turner JG (1998) *COI1*: An *Arabidopsis* gene required for jasmonate-regulated defense and fertility. Science **280:** 1091-1094

Xiong LM, Schumaker KS, Zhu JK (2002) Cell signaling during cold, drought, and salt stress. Plant Cell **14:** S165-S183

Yamamoto RT, Fraenkel GS (1960) The specificity of the tobacco hornworm, *Protoparce sexta* (Johan.) to solanaceous plants. Annals of the Entomological Society of America **53:** 503-507

Yamamoto Y, Ford RC, Barber J (1981) Relationship between thylakoid membrane fluidity and the functioning of pea-chloroplasts - effect of cholesteryl hemisuccinate. Plant Physiology **67:** 1069-1072

Yang HR, Tang K, Liu HT, Pan QH, Huang WD (2009) Jasmonic acid is induced in a biphasic manner in response of pea seedlings to wounding. Journal of Integrated Plant Biology **51:** 562-573

Yang TF, Gonzalez-Carranza ZH, Maunders MJ, Roberts JA (2008) Ethylene and the regulation of senescence processes in transgenic *Nicotiana sylvestris* plants. Annals of Botany **101:** 301-310

Yang W, Devaiah P, Pan X, Isaac G, Welti R, Wang X (2007) AtPLAl is an acyl hydrolase involved in basal jasmonic acid production and *Arabidopsis* resistance to *Botrytis cinerea*. Journal of Biological Chemistry **282:** 18116-18128

Yoo SD, Cho YH, Sheen J (2007) *Arabidopsis* mesophyll protoplasts: A versatile cell system for transient gene expression analysis. Nature Protocols **2:** 1565-1572

Yoshioka H, Numata N, Nakajima K, Katou S, Kawakita K, Rowland O, Jones JD, Doke N (2003) *Nicotiana benthamiana* gp91^{phox} homologs *NbrbohA* and *NbrbohB* participate in H_2O_2 accumulation and resistance to *Phytophthora infestans*. Plant Cell **15:** 706-718

Ytterberg AJ, Peltier JB, van Wijk KJ (2006) Protein profiling of plastoglobules in chloroplasts and chromoplasts. A surprising site for differential accumulation of metabolic enzymes. Plant Physiology **140:** 984-997

Yu LM (1995) Elicitins from *Phytophthora* and basic resistance in tobacco. Proceedings of the National Academy of Sciences of the United States of America **92:** 4088-4094

Zamioudis C, Pieterse CMJ (2012) Modulation of host immunity by beneficial microbes. Molecular Plant-Microbe Interactions **25:** 139-150

Zavala JA, Patankar AG, Gase K, Hui DQ, Baldwin IT (2004) Manipulation of endogenous trypsin proteinase inhibitor production in *Nicotiana attenuata* demonstrates their function as antiherbivore defenses. Plant Physiology **134:** 1181-1190

Zhang S, Klessig DF (2000) Pathogen-induced MAP kinases in tobacco. Results and Problems in Cell Differentiation **27:** 65-84

Zhao YF, Thilmony R, Bender CL, Schaller A, He SY, Howe GA (2003) Virulence systems of *Pseudomonas syringae* pv. *tomato* promote bacterial speck disease in tomato by targeting the jasmonate signaling pathway. Plant Journal **36:** 485-499

Ziegler J, Hamberg M, Miersch O, Parthier B (1997) Purification and characterization of allene oxide cyclase from dry corn seeds. Plant Physiology **114:** 565-573

Zipfel C, Robatzek S, Navarro L, Oakeley EJ, Jones JDG, Felix G, Boller T (2004) Bacterial disease resistance in *Arabidopsis* through flagellin perception. Nature **428:** 764-767

Zuccaro A, Lahrmann U, Guldener U, Langen G, Pfiffi S, Biedenkopf D, Wong P, Samans B, Grimm C, Basiewicz M, Murat C, Martin F, Kogel KH (2011) Endophytic life strategies decoded by genome and transcriptome analyses of the mutualistic root symbiont *Piriformospora indica*. PLoS Pathogens **7:** e1002290

Acknowledgements

I would like to thank Dr. Gustavo Bonaventure, Prof. Dr. Ian T. Baldwin and Prof. Dr. Ralf Ölmüller for their supervision, all their helpful advices and the opportunity to do my Ph.D. in their facilities dealing with such interesting projects.

Further I would like to thank the DFG and the Max Planck Society for funding my projects and making my Ph.D. projects possible.

Thanks a lot also to Prof. Dr. Jianqiang Wu for his guidance and helpful advice in the laboratory as well as his immense generosity and patience!

Special thanks also to our IMPRS coordinator Dr. Karin Groten who helped me a lot with valuable advices when they were needed most!

I would like to especially thank all my friends at work for their support, Maria Heinrich, Christian Hettenhausen, Lynn Ullmann-Zeunert, Meredith Schumann, Mario Kallenbach, Variluska Fragoso, Mariana Stanton, Younjoo Oh, Michael Stitz, Paola Gilardoni, Iris Camehl, Melkamu Woldemariam, Truong Son Dinh, Dorothea and Stefan Meldau, Felipe Yon, Van Thi Luu and Martin Schäfer and of course all other colleagues from the Baldwin department that I didn't mention here.

Thanks to Thomas Hahn, Matthias Schöttner and Alexander Weinhold for technical assistance and support!

Many thanks also to my helping students Brenda Raud, Clara Moyano and Anke Rauch!

I would like to thank Dr. Klaus Gase, Antje Wissgott, Eva Rothe, Susan Kutschbach and Wibke Kröber for plant transformation and Danny Kessler and Celia Diezel for their field work support.

Many thanks to Dr. Tamara Krügel and the gardeners, particularly to Andreas Schünzel and Elke Goschala, for excellent glasshouse and York chamber management, useful advices and their special care!

Thanks to Evelyn Clauβen for her organizational efforts!

Last but not least, I want to thank my family really a lot for all their mental and financial support, patience and love, and for trying to teach me how to bear less positive situations with Bavarian calmness and imperturbability! I promise to never forget who I always can rely on and to consider that aspect whenever it comes to putting priorities.

Curriculum vitae

Personal Information:

Name:	Stefan Schuck
Date of birth:	27. 08. 1982
Place of birth:	Sulzbach am Main
Nationality:	German
Current address:	Friedensstrasse 11, 07778 Porstendorf
E-mail:	sschuck@ice.mpg.de

Research Experience:

Since 05/2009 PhD thesis at the Max-Planck-Institute for Chemical Ecology

Dissertation on: "The control of plant defense responses and seedling growth during interactions with beneficial and non-beneficial organisms"

Main focus on:

- Molecular Biology [DNA cloning, PCR, transformation of *Escherichia coli* and *Arabidopsis* protoplasts, sequencing, RACE (rapid amplification of cDNA ends) and qRT-PCR]
- Analytical Chemistry (HPLC-UV/VIS, UPLC-microToF, LC-MS/MS, GC-MS)
- Ecology (field studies, *Manduca sexta* larvae performance assays, infection assays with *Pseudomonas syringae* and *Phytophthora parasitica* var. *nicotianae* and growth promotion assays with *Piriformospora indica* including grafting experiments, experiments using transgenic *N. attenuata* lines silenced by inverted-repeat and antisense technique and crosses thereof with wild-type *N. attenuata* plants, fluorescence microscopy)

07/2008- 4/2009	Diploma thesis at the Institute for Molecular Infection Biology, Julius-Maximilians-Universität Würzburg "Molekularbiologische Charakterisierung probiotischer Eigenschaften des *Escherichia coli*-Stammes Nissle 1917" Main focus on: • Molecular Biology (DNA cloning, PCR) • Protein Biochemistry (gel electrophoresis, protein over-expression, immunodetection) • Infection assays with *Salmonella enterica* serovar Typhimurium involving human tissue culture
10/2006- 06/2007	Student Assistant at the Julius-von-Sachs-Institute for Biosciences, Department of Ecophysiology and Vegetation Ecology, JMU Würzburg Responsibilites: • Olfactometer experiments with parasitoid wasps (*Cotesia* and *Microplitis*) and *Spodoptera* larvae feeding on corn • Plant-volatile mediated effects on mycelial growth of the phytopathogenic fungus *Setosphaeria turcica*

Education:

10/2003- 04/2009	Diploma in Biology at the JMU Würzburg; final grade: 1.3
08/2002-05/2003	Social Service at the Rohe'sche Altenheimstifung, Kleinwallstadt
09/1993- 06/2002	Abitur at the Hermann-Staudinger-Gymnasium Erlenbach am Main; final grade: 1.8
09/1989-08/1993	Elementary school at the Herigoyen-Grundschule Sulzbach am Main

Publications:

- Gilardoni, P., Schuck, S., Jüngling, R., Rotter, B., Baldwin, I. T., Bonaventure, G. (2010). SuperSAGE analysis of the *Nicotiana attenuata* transcriptome after fatty acid-amino acid elicitation (FAC): Identification of early mediators of insect responses. BMC Plant Biology 10, 66. doi: 10.1186/1471-2229-10-66.
- Bonaventure, G., Schuck, S., Baldwin, I. T. (2011). Revealing complexity and specificity in the activation of lipase-mediated oxylipin biosynthesis: A specific role of the *Nicotiana attenuata* GLA1 lipase in the activation of JA biosynthesis in leaves and roots. Plant, Cell and Environment 34, 1507–1520. doi: 10.1111/j.1365-3040.2011.02348.x.
- Gase, K., Weinhold, A., Bozorov, T. A., Schuck, S., Baldwin, I. T. (2011). Efficient screening of transgenic plant lines for ecological research. Molecular Ecology Resources 11, 890–902. doi: 10.1111/j.1755-0998.2011.03017.x.
- Schuck, S., Camehl, I., Gilardoni, Paola A., Oelmueller, R., Baldwin, I. T., Bonaventure, G. (2012). HSPRO controls early *Nicotiana attenuata* seedling growth during interaction with the fungus *Piriformospora indica*. Plant Physiology 160: 929-943. doi: 10.1104/pp.112.203976.
- Schuck, S., Baldwin, I. T., Bonaventure, G. (2013) HSPRO acts via SnRK1-mediated signaling in the regulation of *Nicotiana attenuata* seedling growth promoted by *Piriformospora indica.* Plant Signaling & Behavior 8, e23537. doi: http://dx.doi.org/10.4161/psb.23537
- Schuck, S., Kallenbach, M., Baldwin, I. T., Bonaventure, G. NaGLA1´s role in *Nicotiana attenuata´*s defense against *Phytophthora parasitica* var. *nicotianae* (will be submitted to Plant, Cell and Environment).
- Luu, T. V., Schuck, S., Weinhold, A., Baldwin, I.T. The impact of jasmonic and salicylic acid signaling on disease progression in *Nicotiana attenuata* infected with two native fungal pathogens, *Fusarium brachygibbosum* and *Alternaria alternata* (will be probably submittedto Phytopathology).

Oral presentations:

- Schuck S. NaHSPRO affects growth promotion during the interaction of *Nicotiana attenuata* with the fungus *Piriformospora indica*. 11th IMPRS Symposium, MPI for Chemical Ecology, Dornburg, DE, Feb 2012
- Schuck S. Elucidating the role of PNRP, AEP150 and AEP65 in plant defense against herbivores and pathogens. 9th IMPRS Symposium, MPI for Chemical Ecology, Dornburg, DE, Feb 2010
- Schuck S. Chemische Ökologie. Schülervortrag, Hermann-Staudinger Gymnasium, Erlenbach am Main, DE, Nov 2009

Poster presentations:

- Schuck S., Bonaventure, G., Baldwin, I. T. NaGLA1 – a lipase specific for the jasmonic acid biosynthesis pathway in *Nicotiana attenuata*. 10th IMPRS Symposium, MPI for Chemical Ecology, Dornburg, DE, Feb 2011
- Weinhold A., Meldau, D., Santhanam, R., Schuck, S., Luu, T. V., Groten, K., Baldwin, I. T. Microbial Interactions with *Nicotiana attenuata*. SAB Meeting 2012, MPI for Chemical Ecology, Jena, DE, Oct 2012

Selbstständigkeitserklärung

Entsprechend der geltenden, mir bekannten Promotionsordnung der Biologisch-Pharmazeutischen Fakultät der Friedrich-Schiller-Universität Jena erkläre ich, dass ich die vorliegende Dissertation eigenständig angefertigt und alle von mir benutzten Hilfsmittel und Quellen angegeben habe. Personen, die mich bei der Auswahl und Auswertung des Materials sowie bei der Fertigstellung der Manuskripte unterstützt haben, sind am Beginn eines jeden Kapitels genannt. Es wurde weder die Hilfe eines Promotionsberaters in Anspruch genommen, noch haben Dritte für Arbeiten, welche im Zusammenhang mit dem Inhalt der vorliegenden Dissertation stehen, geldwerte Leistungen erhalten. Die vorgelegte Dissertation wurde außerdem weder als Prüfungsarbeit für eine staatliche oder andere wissenschaftliche Prüfung noch als Dissertation an einer anderen Hochschule eingereicht.

_____

Stefan Schuck

Jena, den